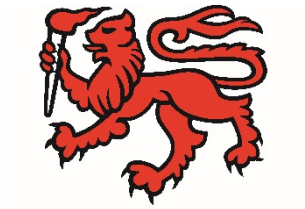

Understanding the role of stomatal traits and tissue-tolerance mechanisms in salinity stress responses in quinoa and wild barley

by

Ali Kiani-Pouya

B. of Agronomy and Plant Breeding and MS in Agronomy

Ferdowsi University, Mashhad, Iran

Submitted in fulfilment of the requirements for the degree of

Doctor of Philosophy

University of Tasmania

October 2019

Statements and Declarations

Declarations of Originality

This thesis contains no material which has been accepted for a degree or diploma by the University or any other institution, except by way of background information and duly acknowledged in the thesis, and to the best of my knowledge and belief no material previously published or written by another person except where due acknowledgement is made in the text of the thesis, nor does the thesis contain any material that infringes copyright.

Authority of Access

This thesis is not to be made available for loan or copying for two years following the date this statement was signed. Following that time, the thesis may be made available for loan and limited copying and communication in accordance with the Copyright Act 1968.

Statement Regarding Published Work Contained in Thesis

The publishers of the papers comprising Chapter 2, 4, 5 and 6 hold copyright for that content and access to the material should be sought from the respective publisher and journals. The remaining non published contents of the thesis may be made available for loan and limited copying and communication in accordance with the Copyright Act 1968.

Student Signature

Primary Supervisor Signature

Statement of Co-Authorship

This thesis was completed during the course of my enrolment in a PhD degree in the Tasmanian Institute of Agriculture at the University of Tasmania. This thesis contains no experimental results that have previously presented for any degree at this or other institution.

This thesis contains one literature review chapter, one general discussion chapter and five main research chapters. Results described in the two research chapters (Chapters 2 and 4) have been published in two different journals. Results described in Chapters 5 and 6 have been submitted for publication.

The following people and institutions contributed to the publication of work undertaken as part of this thesis:

Author	Name	Institution
Candidate	Ali Kiani-Pouya	Tasmanian Institute of Agriculture University of Tasmania
Author 1	Sergey Shabala	Tasmanian Institute of Agriculture University of Tasmania
Author 2	Meixue Zhou	Tasmanian Institute of Agriculture University of Tasmania
Author 3	Heng Zhang	Shanghai Centre for Plant Stress Biology Chinese Academy of Sciences
Author 4	Rainer Hedrich	Institute for Molecular Plant Physiology and Biophysics, University of Wuerzburg
Author 5	Fatemeh Rasouli	Tasmanian Institute of Agriculture University of Tasmania
Author 6	Lana Shabala	Tasmanian Institute of Agriculture University of Tasmania
Author 7	Ute Roessner	School of BioSciences University of Melbourne
Author 8	Nirupama Jayasinghe	School of BioSciences University of Melbourne
Author 9	Adrian Lutz	School of BioSciences University of Melbourne

Author	Name	Institution
Author 10	Thusitha Rupasinghe	School of BioSciences University of Melbourne
Author 11	Nadia Bazihizina	Tasmanian Institute of Agriculture University of Tasmania
Author 12	Jennifer Bohm	Tasmanian Institute of Agriculture University of Tasmania
Author 13	Sulaiman Alharbi	Zoology Department, College of Science King Saud University
Author 14	Barkat Rabbi	School of Science and Health Western Sydney University
Author 15	Zhinous Falakboland	Tasmanian Institute of Agriculture University of Tasmania
Author 16	Zhong-Hua Chen	School of Science and Health Western Sydney University
Author 17	Miing Yong	School of Science and Health Western Sydney University
Author 18	Ayesha T.Tahir	Department of Biosciences COMSATS University Islamabad

Author details and their roles:

Paper 1, **Kiani-Pouya A.**, Roessner U., Jayasinghe,N.S., Lutz A., Rupasinghe T., Bazihizina N., Bohm J., Alharbi S., Hedrich R., Shabala S. 2017. Epidermal bladder cells confer salinity stress tolerance in the halophyte quinoa and Atriplex species. Plant, Cell & Environment 40, 1900–1915. **Located in chapter 2**

Candidate was the primary author and contributed 70% of the experimental work and wrote the paper. Author 1 contributed to the designs the experiments, data interception and took the leading role in writing. Authors 7, 8, 9 and 10 contributed to the metabolomics analysis and interpretation of the results. Authors 11 and 12 contributed to MIFE experiment. Authors 4 and 13 reviewed the paper.

Paper 2, **Kiani-Pouya A.,** Rasouli F., Bazihizina N., Zhang H., Shabala S. 2019. A large-scale screening of quinoa accessions reveals an important role of epidermal bladder cells and stomatal patterning in salinity tolerance. Environ Exp Bot. 168, 103885. **Located in chapter 4**

Candidate was the primary author and contributed 80% to the planning, execution and preparation of the work for the paper. Author 1 contributed to the conception and design of the project and the analysis and interpretation of the research data. Author 5 contributed to elements analysis and taking the image using ESEM. Author 11 contributed to image analyses. Authors 3 and 4 contributed to analysing the data and reviewed the paper.

Paper 3, **Kiani-Pouya A.,** Rasouli F., Shabala L., T.Tahir A, Zhou M., Shabala S. 2019. Understanding the role of root-related traits in salinity tolerance of quinoa accessions with contrasting epidermal bladder cells patterning. Under review in Planta. **Located in chapter 5.**

Candidate was the primary author and contributed 80% to conduct the research, data analysis and wrote the paper. Author 1 designed the experiment and wrote the paper. Authors 5 and 6 contributed to elements and MIFE analysis. Authors 2 and 18 reviewed the paper.

Paper 4, **Kiani-Pouya A.,** Rasouli F., Rabbi B., Falakboland Z., Yong M., Chen Z., Zhou M., Shabala S. 2019. Stomatal traits as a determinant of superior salinity tolerance in wild barley. Under review in J Plant Physiol. **Located in chapter 6.**

Candidate was the primary author and contributed 80% to conduct the research, data analysis and wrote the paper. Author 1 designed the experiment and wrote the paper. Authors 5, 14, 15 and 17 contributed to elements and data analysis. Authors 2 and 16 reviewed the paper.

We the undersigned agree with the above stated "proportion of work undertaken" for each of the above published (or submitted) peer-reviewed manuscripts contributing to this thesis:

Signed:

	Ali Kiani-Pouya Tasmanian Institute of Agriculture, University of Tasmania	Prof Sergey Shabala Tasmanian Institute of Agriculture, University of Tasmania	Prof Holger Meinke Tasmanian Institute of Agriculture, University of Tasmania
Date:	8 October 2019	8 October 2019	8 October 2019

Publications Arising from this Thesis

Kiani-Pouya A., Roessner U., Jayasinghe N.S., Lutz A., Rupasinghe T., Bazihizina N., Bohm J., Alharbi S., Hedrich R., Shabala S. 2017. Epidermal bladder cells confer salinity stress tolerance in the halophyte quinoa and Atriplex species. Plant Cell Environ 40 (9):1900-1915.

Kiani-Pouya A., Rasouli F., Bazihizina N., Zhang H., Hedrich R., Shabala S. 2019. A large-scale screening of quinoa accessions reveals an important role of epidermal bladder cells and stomatal patterning in salinity tolerance. Environ Exp Bot. 168, 103885.

Kiani-Pouya A., Rasouli F., Rabbi B., Falakboland Z., Yong M., Chen Z., Zhou M., Shabala S. 2019. Stomatal traits as a determinant of superior salinity tolerance in wild barley. Under review in J Plant Physiol.

Kiani-Pouya A., Rasouli F., Shabala L., T.Tahir A, Zhou M., Shabala S. 2019. Understanding the role of root-related traits in salinity tolerance of quinoa accessions with contrasting epidermal bladder cells patterning. Under review in Planta.

Acknowledgements

I would like to express my sincere gratitude to my supervisory team, Professor Sergey Shabala, Professor Meixue Zhou, Professor Heng Zhang and Professor Rainer Hedrich for their supervision and guidance throughout my PhD study. Their expertise and advice have been critical elements in the accomplishment of this work. I would like to specially thank Professor Sergey Shabala and Professor Heng Zhang for providing the opportunity to continue this research in a new omics area, to gain a blend of various skills and for all of the valuable insight I have gained as a result of our collaboration.

I really thank Sue Webster and Fatemeh Rasouli for their special support and generosity during this difficult time. You have been extremely supportive and I could not have gotten through this thesis without you.

I also thank the University of Tasmania for providing the scholarship Tasmania Graduate Research Scholarship. Tasmanian Institute of Agriculture provided me all the required facilities to carry out the proposed projects for my PhD. I also would like to thank the numerous people from the Tasmanian Institute of Agriculture for their valuable contributions and assistance with logistics and lab works. I thank Associate Professor Lana Shabala for her assistance and contribution to the lab works. I am grateful for Mr. Phil Andrew's assistance with glasshouse facility and his assistance to the experimental issues. I also extend thanks for the help rendered at the Core Facility for Genomics at the Shanghai Plant Stress Biology Centre particularly my supervisor Professor Heng Zhang. I am also appreciative for help from CSL at the University of Tasmania, particularly Dr Richard Wilson at the Proteomics facility, Dr Adam Smolenski and Ms. Sharee McCammon at the Molecular Genetics lab.

Finally, I thank all my friends at the Plant Stress Physiology Group, Tasmanian Institute of Agriculture, University of Tasmania for their support and friendship with whom I share great memories and had many conversations about my research and enjoying Tasmania.

Table of Contents

List of Figures

List of Supplementary Figures

List of Tables

List of Supplementary Tables

List of Abbreviations

ANK, ankyrin repeat family proteins

ANOVA, analysis of variance

ATP, adenosine triphosphate

BD, bladder density

BDM, bladder diameter

bHLH, basic helix loop helix

BI, bladder index

BSM, basal salt medium

BV, bladder volume

CaM, calmodulins

CAM, crassulacean acid metabolism

CaML, CaM-like

CB, cultivated barley

CBL, calcineurin B-like

CDK, Cyclin-dependent kinase

CDPK, Ca^{2+} dependent protein kinases

CPC: caprice

CYC, cyclin

DEGs, differently expressed genes

DTX, detoxification

DW, dry weight

EBC, epidermal bladder cell

ECA, epidermal cell area

EF, elongation factor

EPF, epidermal patterning factors

EST, expressed sequence tag

ETC2: enhancer of triptychon and caprice2

FDR, false discovery rate

FW, fresh weight,

GABA, gamma-aminobutyric acid

GC-MS, gas chromatography-mass spectrometry

GIPC, glycosyl inositol phosphorylceramide

GL: glabra

GLR, glutamate receptor

GO, gene ontology

GORK, Gated outward rectifying K^+ channel

Gs, stomatal conductance

GsSRK, G-type lectin S-receptor-like serine/threonine protein kinase

HAK, high affinity K^+ transporter

HCA, hierarchical cluster analysis

KEGG, Kyoto Encyclopedia of Genes and Genomes

LRR-RK, leucine-rich repeat receptor kinase

LSD, least significant difference

MAPK, mitogen-activated protein kinase

MATE, multidrug and toxic compound extrusion or multi-antimicrobial extrusion

MCM, minichromosome maintenance

MIFE, microelectrode ion flux estimation system

MYB, *my*elo*b*lastosis

NBr, non-brushed

NBr-Br, non-brushed brushed

NHX, Na^+/H^+ exchanger

PCD, plant cell death

PLSDA, partial least square discriminant analysis

Pn, net photosynthesis

ROS, reactive oxygen species

SCRM, scream

SD, stomatal density

SE, standard error

SEM, scanning electron microscope

S(HBV), salt-sensitive with high EBC volume

SIM, siamese

SKOR, Stelar K^+ outward rectifier

SL, stomatal length

S(LBV), salt-sensitive with low EBC volume

SOS, salt overly sensitive

SPAD, soil plant analysis development

SPCH, speechless

SSD, stomatal density and distribution

STI, salinity tolerance index

TCA, tricarboxylic acid

T(HBV), salt-tolerant with high EBC volume

TIA, Tasmanian Institute of Agriculture

T(LBV), salt-tolerant with low EBC volume

TRY: triptychon

TTG, thioglucoside glucohydrolase

WB, wild barley

WUE, water use efficiency

Abstract

Agricultural production needs to be doubled by year 2050; this task is complicated by various abiotic stresses severely affecting crop production. Salinity stress is among major environmental stresses that influences crop production globally and it is estimated that around 950 million hectares of arable land is affected by this environmental stress. Considering this fact, it is necessary to introduce new approaches to manage this main challenge. One of them is breeding for enhanced salinity tolerance. An alternative solution may be the use of halophyte relatives.

Despite having high tolerance to salt stress, halophytic plants have not been extensively used to study salinity tolerance mechanisms. Also, studies investigating the salinity tolerance mechanism in halophytes have concentrated on physiological or anatomical aspects with relatively little focus being given to the omics-based studies such as metabolomics and transcriptome analysis.

Epidermal bladder cells (EBCs) are specialized structures in some of halophytic plants that provide external store for toxic ions such as Na^+ and Cl^-, and hence understanding the function of EBCs may eventually play an important role in transferring this ability to crop plants.

Stomata also being another focus of this study. Although there have been significant advances of understanding mechanisms that controlling stomatal development and also the signalling pathways that regulate guard cells function in glycophytes, much less is known about stomata development and operation in halophytes. In light with this fact a question on how environmental variables and in particular salinity stress change the basal stomatal development pathway requires more studies. Given the fact that osmotic stress and toxic Na^+ level negatively affect stomatal parameters under saline conditions the question is that why are halophytes capable to optimise their stomata performance? Do halophytic plants possess unique stomata operation mechanisms? How does salinity stress affect epidermal cell differentiation which leads to either an increase or decrease in stomatal density? Hence, the major aim of this PhD project was to fill some of above discussed gaps in our knowledge by addressing the following specific objectives: (i) investigate the role of EBC in salinity tolerance in quinoa; (ii) identifying key genes related to salt sequestration into EBCs by transcriptome analysis of EBC through comparing bladder-bearing quinoa plants with those that EBCs were mechanically removed;

(iii) evaluate the effects of salinity on EBC patterning in quinoa and correlate the extent of variability in this trait with the genetic variation in salinity stress tolerance; (iv) investigate stomata patterning and development and associate the extent of variability in stomata characteristics with genetic variation in salinity stress tolerance; (v) comparing stomatal traits as a component of the tolerant mechanism between halophytic crops and their wild relatives (using cultivated and wild barley as a case study).

To provide direct supporting evidence for the role of EBCs that have been postulated to assist halophytes to cope with saline environment, *Chenopodium quinoa* plants were grown under saline conditions for 5 weeks. One day prior to commencement of salinity stress EBC from all leaves and petioles were gently removed using soft cosmetic brush. Physiological, ionic and metabolic changes in brushed and non-brushed leaves were compared. Gentle removal of EBC did neither initiate wound metabolism nor affected physiology and biochemistry of control-grown plants but had a pronounced effect on salt-grown plants resulting in a salt-sensitive phenotype. Of 91 detected metabolites, more than half (50) were significantly affected by salinity. Removal of EBC has dramatically modified these metabolic changes, with the biggest differences reported for gamma-aminobutyric acid (GABA), proline, sucrose and inositol, affecting ion transport across cellular membranes (as shown in electrophysiological experiments). This work provides the first direct evidence for the role of EBC in salt tolerance in halophytes and attributes this role to (1) key role of EBC as a salt dumper to externally sequester salt load; (2) improved K^+ retention in leaf mesophyll and (3) storage space for several metabolites known to modulate plant ionic relations.

To identify key genes related to salt sequestration abilities in EBCs, a transcriptome study was conducted with bladder-bearing and bladderless plants similar to above experiment. Comparing differently expressed genes (DEGs) of brushed and non-brushed leaves grown under 400 mM NaCl using a p-value < 0.05 and fold change > 2 as the significance cut-offs, indicated that 2015 genes were differently expressed where 1399 genes were up-regulated and 616 genes were down-regulated in bladder-bearing leaves. Significant alterations of genes related to ion transport, DNA replication, and genes related to stress signalling in response to salinity stress were determined. Altogether, the finding that the transcriptome of bladder-bearing leaves differed from those of bladderless leaves suggests that

EBCs do not function as a passive external store place for salt as it was perceived before but play active metabolic role in quinoa plant.

Varietal differences in salinity tolerance of quinoa was explored by evaluation of 114 accessions grown under control and 400 mM NaCl conditions, and different physiological and anatomical characteristics were measured. Accessions were grouped to sensitive, intermediate and tolerant classes based on relative dry weight defined as salinity tolerance index (STI). Results showed a large variability for fresh and dry weights indicating a strong genetic variation for salinity tolerance in quinoa. Bladder density increased in majority of accessions under saline condition while bladder diameter remained unchanged; this resulted in a large variability in a bladder volume as a dependant variable. Stomata density remained unchanged between saline and non-saline conditions while stomata length declined between 3% to 43% among accessions. Correlation analysis indicated a significant positive association between EBC diameter and STI on one hand and EBC volume and STI on the other hand, in a salt-tolerant group. A negative association between STI and stomata length was also found in a salt-tolerant group, suggesting that these plants were able to efficiently regulate stomatal patterning to efficiently balance water loss and CO_2 assimilation under saline condition. Both salt-sensitive and salt-tolerant groups had the same Na^+ content under saline condition; however, a negative association between leaf Na^+ concentration and STI in salt-sensitive plants indicated an efficient Na^+ sequestration into the EBCs in salt-tolerant plants.

While sequestration of toxic ions into EBCs is an efficient mechanism contributing to salinity tolerance in quinoa, many halophytes do not utilize EBCs to modulate their tissue ion concentrations but still possess superior salinity tolerance ability. To elucidate possible compensation mechanism(s) underlying superior salinity tolerance in the absence of external salt storage capacity, we have selected four accessions from our previous experiment to address this issue. Whole-plant physiological and electrophysiological characteristics were assessed after 2 days and 3 weeks of 400 mM NaCl stress. The results showed that accession Q21 that had low EBC volume had superior photosynthetic rate and stomatal conductance at both 2 days and 3 weeks of salt stress than the counterpart Q68 with high EBC volume. Both accessions with low EBC volume (Q21 and Q30) utilised Na^+ exclusion at the root level and were capable to maintain low Na^+ concentration

in leaves, to compensate for inability to sequester Na^+ load in EBC. These conclusions were further confirmed by electrophysiological experiments showing higher Na^+ efflux from Q21 and Q30 roots as compared with 195 and Q68 as accessions with high EBC volume. Furthermore, accessions with low EBC volume had significantly higher K^+ concentration in their leaves at long-term salinity stress compared to plants with high EBC sequestration ability suggesting that the ability to maintain high K^+ content in mesophyll was as another key compensation mechanism.

In the light of importance of stomatal traits as a determinant of salinity tolerance in quinoa, we have extrapolated this work to cereal plants, comparing cultivated (CB; *Hordeum vulgare*) and wild (WB; *Hordeum spontaneum*) barley. Twenty-six genotypes of WB and CB were grown under control and saline conditions and stomatal characteristics, leaf ion content and epidermal strips response to Na^+ and K^+ were measured. WB had higher relative biomass than CB when exposed to salinity stress. Under saline conditions, WB plants were able to keep constant stomata density (SD) while SD significantly decreased in CB. The higher SD in WB also resulted in higher stomatal conductance (g_s) under saline conditions, with g_s reduction being 51% and 72% in WB and CB, respectively. Furthermore, WB showed faster stomatal response to light, indicating their better ability to adapt to changing environmental conditions. Experiments with isolated epidermal strips indicated that CB genotypes have the higher stomatal aperture when incubated in 80 mM KCl solution, and its aperture declined when KCl was substituted by NaCl, indicating strong preference to KCl for stomatal operation in CB. On the contrary, WB genotype had the highest stomata aperture being exposed to 80 mM NaCl suggesting that WB plants may use Na^+ instead of K^+ for stomata movements. *Our* data suggest that CB employ a stress-escaping strategy by reducing stomata density, in an attempt to conserve water when grown under salinity conditions. WB, on the contrary, is capable to utilize Na^+ as a cheap osmoticum for stomatal operation.

In conclusion, this work has demonstrated that stomatal traits and tissue-tolerance mechanisms represent critical traits enabling plants adaptation to saline environment. These traits should become a focus of future breeding programs aimed to improve salinity tolerance in traditional crops.

Chapter 1: Literature Review

1.1 Salinity

It is predicted that the world population will increase in excess of 9 billion by 2050; thus, world food production has to be doubled by this year (Lal, 2010). While agricultural production needs to be increased, various abiotic stresses affect crop production. Salinity stress is among major environmental stresses that affects crop production globally and it is estimated that around 950 million hectares of arable land is affected by salt stress (Ruan et al., 2010). Considering this fact, it is necessary to introduce new approaches to manage this main challenge (Hanin et al., 2016). The increasing trend of Na^+ affected lands can be decreased by reclamation of saline lands and farm management practices. However, reclaiming saline soils by engineering projects is not a cheap option and thus would not feasible. On the other hand, improving salinity tolerance of crop plants, appears a more possible approach (Bressan et al., 2013; Zorb et al., 2019). Designing plant breeding program to enhance salinity tolerance in crops has great environmental and economic advantages. Another potential strategy to cope with increased salinity problem is to cultivate halophyte crops, which can resistant severe salinity stress (Koyro et al., 2008).

1.2 Halophytes

Halophytes are small group of plants from different families that constitute 0.4% of the total plants in the world. They are able to survive and complete their life cycle under saline condition of more than 200 mM salt (Santos et al., 2016; Shabala, 2013).

Salinity tolerance mechanisms have extensively been studied in halophytes during the past years (Bose et al., 2014; Flowers and Colmer, 2008, 2015; Shabala, 2013; Shabala et al., 2016; Shabala and Mackay, 2011). The results of these studies have indicated there are various morphological, anatomical and physiological differences between halophytes and glycophytes however, the primary characteristic which differentiates halophytes from their counterpart is the ability of halophytes to efficiently take away salt from active metabolic tissues. This effective compartmentalisation ability is achieved through either an internal mechanism (sequestration of salt into large vacuoles) (Bonales-Alatorre et al.,

2013)or by secretion of excessive salt into external store such as epidermal bladder cells (EBCs) or salt glands (Barkla et al., 2018; Dassanayake and Larkin, 2017).

1.3: What makes halophytes tolerant to salinity stress

Halophytes indicating complex responses to environmental stresses such as salinity by employing a variety of tolerance mechanisms which includes biochemical, physiological, and anatomical processes at both cell and whole plant levels (Fig. 1.1). Plant growth reduction under saline conditions is mainly due to osmotic and ionic factors (Munns and Tester, 2008), and hence some of the most important salinity tolerance mechanisms in halophytes to a large extent are based on ion homeostasis. Given this fact, the salinity tolerance in plants is mostly associated with the plant's ability in minimizing Na^+ content in the shoot or to deal with higher concentration of Na^+ once it has been accumulated in plant tissues. While the physiological processes of salinity tolerance in traditional plants have been well-studied, our knowledge of the underlying physiological and anatomical mechanisms in halophytes is poor. Thus, much more research is required to fully elucidate the salinity tolerance bases in halophytes.

1.4: Physiological mechanisms of salinity tolerance in halophytes

1.4.1: Osmotic adjustment

To maintain growth and produce new tissues, plants need positive turgor pressure that is gained through osmotic adjustment. In this context Na^+ concentration that is below the toxic level can be beneficiary to the plant growth through a positive role in osmotic adjustment by acting as a cheap osmoticum. It is well-known that halophytes heavily rely on inorganic ions as cheap osmolytes to keep their cell osmotic adjustment under salinity stress (Flowers and Colmer, 2015; Munns and Tester, 2008; Shabala and Mackay, 2011). For example, the growth of quinoa stimulated under 100 mM NaCl stress compared to the non-saline conditions (Hariadi et al., 2011). Also, it has reported that quinoa uses Na^+ as a cheap osmolyte (Santa-Cruz et al., 1999; Shabala and Mackay, 2011) and 80-85% of osmotic adjustment in young leaves in quinoa is achieved by means of accumulation of inorganic ions (Na^+, K^+ and Cl^-) under saline conditions (Hariadi et al., 2011).

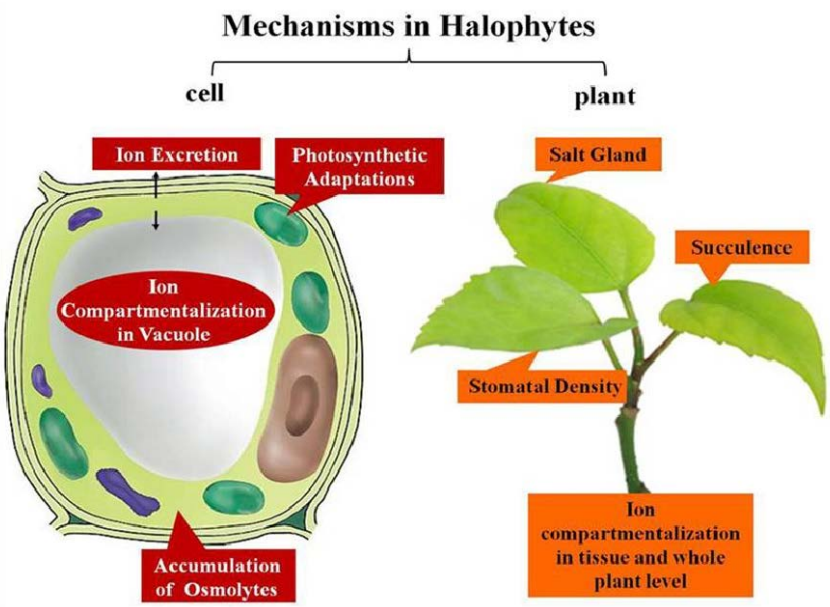

Fig. 1.1 The mechanisms of salinity tolerance in halophytes from cells to whole plant level (Xu et al., 2016)

At the root level, to overcome high osmotic pressure resulted from excess Na^+ and Cl^- ions in the root zone, they need to increase osmotic potential either through synthesis of compatible organic solutes or by accumulating of inorganic ions. Given the fact that de novo synthesis of organic compounds requires high carbon cost (Raven, 1985), it is remarkedly beneficial to roots to adopt Na^+ as a metabolically cheap osmolyte for osmotic adjustment. To prevent this toxic effect on root cells would be is to excrete these toxic ions and particularly Na^+ into the vacuoles of mesophyll cells (Shabala, 2013).

1.4.2: Vacuole sequestration

While prevention of Na^+ from entry via limited root uptake is mostly represented in glycophtes, Na^+ exclusion from metabolic pathways and sequestration of substantial amounts of this ion into the vacuole has been known as a primary salinity tolerance strategy in halophytes (Flowers and Colmer, 2008; Munns and Tester, 2008). The rationale behind this strategy is that halophytes species achieve osmotic adjustment primarily by the accumulation of inorganic ions which are energetically cheap rather than organic solutes which require high amount of energy to be synthesised (Hariadi et al., 2011). Several plant membrane transporters have primary roles in tolerance mechanisms to abiotic stress, and in this respect

Na^+ and K^+ transporters have a vital role for tolerance to salinity (Schroeder et al., 2013; Shabala et al., 2016). Plants are able to reduce the amount of Na^+ content through sequestration of Na^+ out of cytoplasm via different ion transporters such as tonoplast-localized Na^+/H^+ exchanger 1 (NHX1) (Blumwald and Poole, 1985). The majority of NHXs are required for Na^+ detoxification through compartmentalisation of this ion into the vacuole (Deinlein et al., 2014).

NHXs genes which encode cation/H^+ antiporters have important roles in mediating sequestration of K^+ and Na^+ ions into the vacuole (Bassil et al., 2011). It has been recently shown in Arabidopsis that NHX1 and NHX2 ion transporters have comparatively greater role in K^+ homeostasis than in sequestration of Na^+, and thus it has been argued that other ion transporters than NHX1 and NHX2 control the translocation of Na^+ into the vacuole in this plant (Barragan et al., 2012). In halophytic species, *Suaeda salsa*, it has been shown that SsNHX1 gene was up-regulated under 500 mM NaCl in leaves and thus it was proposed that this Na^+/H^+ antiporter has an important role in conferring salinity tolerance in this species (Ma et al., 2004).

The information on the role of NHXs transporters in quinoa is very scarce. In this plant it is reported that CqNHX transcript level was significantly induced under 300 mM salinity stress in both shoot and root tissues (Ruiz-Carrasco et al., 2011). Over-expression of CqNHX was observed in all the studied accessions except in one that the authors concluded that was because of the origin of that accession and the fact it was considered as the most salt-sensitive accession.

1.4.3: Na^+ exclusion from uptake

It is argued that neither halophytes nor glycophytes are able to tolerant high concentrations of salt in their cytoplasm, due to ion toxicity and therefore, to deal with high Na^+ concentration plants have developed tolerance strategies (Munns and Tester, 2008; Neumann, 1997; Tester and Davenport, 2003). In general, plants can cope with high content of cytosolic Na^+ by different means at root or shoot levels. At root level, they can limit Na^+ entry either through restricting Na^+ uptake or reducing Na^+ loading into xylem and at shoot level plants are able to re-translocate Na^+ from the shoot or sequester this toxic ion into vacuoles (Munns and Tester, 2008). Given the fact that the unidirectional influx of Na^+ is thermodynamically passive and hence is not well regulated, the primary strategy for Na^+ exclusion

appears to be the prevention of Na^+ loading into the xylem (Tester and Davenport, 2003). Sodium extrusion from the cytosol is achieved by plasma membrane Na^+/H^+ antiporter. It has been reported that in Arabidopsis SOS1 transporters are over-expressed in xylem parenchyma tissue (Shi et al., 2000; Shi et al., 2002) and accordingly suggested that Na^+ loading to the xylem in halophytic species is an active process that needed over-expression of SOS1 Na^+/H^+ antiporters at the xylem parenchyma tissue (Shabala and Mackay, 2011). Also, rapid Na^+ loading into the xylem at the early growth stages may be adopted strategy to deal with saline conditions (Flowers and Colmer, 2015; Hariadi et al., 2011). Given the fact that water uptake from saline root zone needed higher energy, rapid loading and uptake of Na^+ at the initial phases of growth may be beneficial for shoot osmotic adjustment. It has been shown that transgenic barley plants with up-regulated HvHKT2;1 gene had higher Na^+ levels in the xylem and superior salinity tolerance compared to wild type counterpart (Mian et al., 2011). It was suggested that the capacity to translocate Na^+ to the shoot was more limiting than accumulating and sequestration of this ion in leaf tissue and therefore is a factor that limit salinity tolerance in this crop (Mian et al., 2011). This finding also suggests the importance of Na^+ exclusion at the root level and also shows the vital role of SOS1 as a transporter. In addition to the role of Na^+ extrusion from the roots, SOS1 transporters also play an important role in long-distance Na^+ transport through regulation of Na^+ loading into the xylem and Na^+ retrieval from the xylem (Shabala and Mackay, 2011; Shi et al., 2002).

1.4.4: ROS detoxification

Plants have developed defence systems against damaging effects of increased level of ROS resulted from stressful conditions such as salinity by enzymatic and non-enzymatic antioxidant compounds (Munns and Tester, 2008). The increased activity of enzymes such as glutathione peroxidases, superoxide dismutase, glutathione, catalase and non-enzymatic antioxidants such as α-tocopherols, ascorbic acid, and glutathione have been reported under saline conditions (Gill and Tuteja, 2010). Also, other non-enzymatic antioxidants compound such as carotenoids, polyols, soluble sugars, trehalose, and polyamines have been reported that play a role in ROS regulation with more accumulation in halophytes (Bose et al., 2014).

Given the fact that halophytic plants have strategies to restrict the build-up of toxic level of oxidative damage either through reducing ROS production or by overexpression of enzymatic and non-enzymatic means, they experience less damage resulted from ROS than crop plants (Bose et al., 2014; Gill and Tuteja, 2010). To this reason, the threshold of salt concentration needed to impose oxidative damage appears to be higher in halophytes than glycophytes. The first symptom of lipid peroxidation was observed in halophytes at salt concentration higher than 150 mM where this salt stress level severally damages the majority of glycophytes (Ozgur et al., 2013).

Halophytes are able to reduce the potential damage of oxidative stress through synthesising protective compounds (e.g. proteins such as CP24 protein and modification in fatty acid profile) which can stabilize the photosystems I and II and as a result reduce the production of ROS (Peng et al., 2009; Sengupta and Majumder, 2010). Such protective mechanisms have not been observed in crop plants (Bose et al., 2014). As another defence line against oxidative damage, halophytic plants are able to switch between various carbon fixation pathways, and particularly switch to C4 and crassulacean acid metabolism (CAM) after being imposed by salinity stress which enable them to reduce the production of ROS (Bose et al., 2014). For instance, C3 halophyte species *Portulacaria afra* and *Mesembryanthemum crystallinum* are able to alter their photosynthesis system to CAM during salinity stress (Cushman and Bohnert, 1999).

1.5: Stomata as gatekeepers for gaseous exchange in plant

Plants need to efficiently balance gaseous exchange of leaf to maximize CO_2 uptake for photo-assimilation and to minimize water loss through transpiration. Although the stomatal pores only represent less than 3% of total leaf surface (Chaves et al., 2016; Hetherington and Woodward, 2003), they are responsible for about 95% of total water loss in plants (Hedrich and Shabala, 2018).

Salinity stress severely impacts water balance in plants and stomata are the "gatekeepers" responsible for all gaseous diffusion and thus show the ultimate boundary line for regulating water relation in plants under saline condition. To this fact, understanding the drivers of stomatal dynamics has a key role in predicting plant responses under saline condition. Also, the fact that stomata play a major role in plant water use efficiency (WUE), makes stomata a potential target for its

alteration to enhance photosynthesis and transpiration (Chaves et al., 2016; Hetherington and Woodward, 2003).

Stomata show a diverse range of morphological and anatomical differences including shapes, sizes, and numbers across different plant species which in turn have the potential to influence stomatal movement and, consequently, plant photosynthesis capacity, stomatal conductance and WUE (Bertolino et al., 2019; Chen et al., 2017). Although different stomatal properties such as behaviour, patterning and morphology have an important influence on plant performance (Bertolino et al., 2019; Lawson and Vialet-Chabrand, 2019), there is little information about how targeted alteration of stomatal characteristics affect physiological responses in crop plants (Chaves et al., 2016) with no information on halophytes. The question in this area that needs to be answered is that is there a potential for manipulating stomatal properties of crop species to enhance WUE and consequently crop productivity without a significant change in assimilation capacity? Although stomata are not the only limiting factor for water loss by the crop plants but they have a main role in this process and hence needs appropriate considerations in this context. In respect to this fact, several approaches have been attempted to improve photosynthesis rate and WUE with the focus on stomata.

1.5.1: Developmental stomata responses

Arguably, alteration of stomatal density could be a primary strategy by which plant can control WUE. Alteration of stomatal density in crop plants with the aim of improving WUE was first analysed decades ago in different breeding programs which had a limited success (Casson and Hetherington, 2010; Shabala, 2013). The hypothesis of those studies was that decreasing or increasing stomatal density would, respectively, decrease or increase stomatal conductance. However, several investigations have shown that this is a very complex approach. For instance, stomatal density and distribution (*sdd1-1*) mutants in Arabidopsis resulted in plants with a 250% higher stomatal density compared with wild-type counterpart (Berger and Altmann, 2000). On the other hand, transgenic Arabidopsis plants overexpressing SDD1 gene have a 40% less stomatal numbers compared with the wild type (Von Groll et al., 2002). A comparative study of above Arabidopsis plants revealed no difference in photosynthesis rate or stomatal conductance between the *sdd1-1* mutants, overexpressing SDD1 plants, and wild-type plants (Büssis et al.,

2006) indicating that the lower stomatal density in the SDD1 plants was compensated with increased aperture of stomata while in sdd1-1 plants the higher stomata density was resulted in lower aperture. This result shows a negative association between stomatal density and size (Hetherington and Woodward, 2003) suggesting a plastic developmental response to changes in environmental conditions (de Boer et al., 2016; Sun et al., 2014). It is noteworthy to mention that the relation between stomatal density and size and the impact of these traits on stomatal functions have recently received much attention (Franks and Farquhar, 2007). However, stomata size and density can be influenced by the growth environment (Drake et al., 2013), thus the manipulation of stomatal density and size studies should be with consideration of understanding the interactions between stomatal density and size and the influence they can have on speed of stomatal opening and closing.

Another important aspect of stomatal density and size alterations that needs to be taken in consideration is that these characteristics may change due to genetic factors or different environmental conditions. For instance, stomata density is changed by different environmental factors such as light (Gay and Hurd, 1975) and CO_2 concentration (Gray et al., 2000).

1.5.2: Impact of stomatal patterning on gas exchange

In addition to investigations that have concentrated on the stomata density and size on gas exchange, some studies have established the physiological importance of stomatal patterning on water loss and CO_2 uptake (Casson and Hetherington, 2010; Hetherington and Woodward, 2003). There is advance understanding of molecular mechanisms controlling stomatal patterning that provide the opportunity to investigate the physiological impacts of stomatal parameters alterations on plant performance. In the absence of studies on quinoa, stomatal development investigations in Arabidopsis have been shown that this process is regulated by a complex genetic network. It has been shown that bHLH (Basic Helix Loop Helix) transcription factors such as FAMA, SPEECHLESS (SPCH), and MUTE together with SCRM (SCREAM) or SCRM2 regulate the cell fate differentiation (Zoulias et al., 2018). The activity of the bHLH transcription factors is controlled by an intercellular signalling network including leucine-rich repeat receptor kinases (LRR-RKs), peptide ligands, and a mitogen-activated protein kinase (MAPK)

cascade (Vaten and Bergmann, 2012). Additionally, the aforementioned signalling pathway includes the secretory peptides epidermal patterning factors such as epidermal patterning factor1 (EPF1), EPF2, and EPF-like 9 where EPF1 and EPF2 negatively control stoatal density (Hara et al., 2009). It has been indicated that while EPF1 prevents stomatal clustering, EPFL9 promotes stomatal development (Hunt et al., 2010; Lee et al., 2015). Understanding of these molecular mechanisms provided an opportunity to generate many mutants e.g. *mute*, *tmm*, *fama* and *spch* in which specific gene mutation has resulted in cell division and differentiation alteration. These mutations resulting in stomatal pairing or clustering that in turn changes the stomata and epidermal cells patterns (Lau and Bergmann, 2012). For example, changes in the expression of the various epidermal patterning factor family members influenced division and differentiation of stomatal and epidermal cells as well as the spacing of cells (Doheny-Adams et al., 2012). In this regard, double mutants of *epf1* and *epf2*, indicated increases in stomatal density in plants.

1.5.3: Impact of stomatal anatomy on gas exchange

Besides physiological drivers that influence stomatal responses, their function is also determined by anatomical traits. Theoretically, anatomical features of stomata determine the maximum conductance (Dow et al., 2014) and these characteristics also affect the speed of response.

Several investigations have argued that smaller stomata respond faster than larger ones due to the fact that they have higher surface-to-volume ratios that allows faster solute transport, results to faster guard cell turgor changes and a more rapid movement (Chaves et al., 2016; Drake et al., 2013). However, it has also been argued that stomatal movement is a mechanical process with a requirement of guard cells to overcome the osmotic pressure imposed by the subsidiary cells. Hence, stomatal opening is possible with a considerable decrease in turgor pressure of surrounding subsidiary cells (Franks and Farquhar, 2007).

In addition to stomata size, the shape of guard cells and the presence of subsidiary cells are other anatomical characteristics that influence stomatal responsiveness of movement (Franks and Farquhar, 2007). For instance, on the contrary to two kidney-shaped guard cells that have been identified in many plants, grass species develop dumbbell-shaped guard cells that has been argued to have successfully contributed to various environmental conditions and in particular in

regions with variable water availability (Chen et al., 2017). Evidence of some investigations have indicated that stomatal opening and closing in grasses is faster than species with kidney-shaped stomata suggesting efficient stomatal regulation in grasses (Haworth et al., 2018; McAusland et al., 2016; Vico et al., 2011). The rationale behind this characteristic is that the dumbbell-shaped guard cells in grass species needed small volume alteration to achieve stomatal opening (Hetherington and Woodward, 2003) which eventually resulted in fast and efficient stomatal movement. Furthermore, slow stomatal movement has negative consequences on stomatal gas exchange where it leads to inefficient CO_2 uptake when stomata are open and also result in unnecessary water loss during closure of stomata (McAusland et al., 2016). Based on this discussion, plant species with high stomata response might gain higher WUE under fluctuating environmental conditions.

1.6: Anatomical mechanisms of salinity tolerance in halophytes

1.6.1: Succulency

Salinity tolerance in halophytes requires high tissue osmolality to overcome the high osmotic pressure caused by salt in the root zone. To this reason, the majority of halophytic plants avoid physiological drought caused by salinity stress through the absorption of ionic solutes (Flowers and Colmer, 2015) to maintain a favourable water potential gradient between the soil solution and the plant (McNulty, 1985).

In halophytic plants, succulency is an adaptive mechanism that has contribution to the regulation of internal ion concentrations (Pessarakli, 2016). It has been argued that succulency moderates the toxic effects of ions (Zeng et al., 2018) that could be achieved by diluting of potentially lethal levels Na^+ and Cl^- in plant tissues (Glenn and O'Leary, 1984). For example, it has reported that the exposure of halophyte species such as *Sarcocornia natalensis* and *Halosarcia pergranulata* to high concentrations of salt resulted in increased succulency of these plants (Naidoo and Rughunanan, 1990; Short and Colmer, 1999).

Succulent halophytic species need salt for optimal growth and accumulate ions such as Na^+ and Cl^- in their tissues for osmotic adjustment (Neumann, 1997; Wang et al., 2009). For example, *Arthrocnemum macrostachyum* as a coastal habitat succulent halophyte from the Chenopodiaceae family, had high ion contents of 455 mmol kg^{-1} Na^+ and 490 mmol kg^{-1} Cl^- (Winter et al., 1976). Also, it is reported that the stem-succulent halophyte, *Haloxylon stocksii*, had high shoot ion

concentration which varied from 278 to 528 mmol Na^+ kg^{-1} dry mass and 215 to 488 mmol Cl^- kg^{-1} during the growing season. These high shoot ion contents may serve as a strategy for osmoregulation. The role of increased ion contents is well-represented in ash content in halophytes. In an investigation with *A. macrostachyum* it was shown that the ash content of plants increased from 35% under the non-saline conditions to about 60% under 200 mM of salt stress (Khan et al., 2005). As additional example, in *Suaeda maritima*, ion contents of plants constituted of 27% and 45% of dry weight under non-saline and saline conditions, respectively (Yeo and Flowers, 1980). In this regard, it has been argued that the high content of ash which is resulted from the accumulation of ions is considered as a major adaptive mechanism for osmotic adjustment in the Chenopodiaceae family (Pessarakli, 2016).

Another advantage of succulency in halophytes is a greater water content in these species where it has been shown that the water content of halophytic plants is much higher than glycophyte species (Flowers and Colmer, 2008). The shoot water content in *A. macrostachyum* was significantly higher under high salt stress condition (200 to 600 mM NaCl) than under control condition, suggesting that succulency was increased with an increase in salinity (Pessarakli, 2016).

Moreover, it has been hypothesised that the increase in succulency induced by salinity stress also result in higher CO_2 uptake of leaves due to the greater internal surface area of the mesophyll relative to organ surface area (Zheng et al., 2009). It was argued that the increased mesophyll area and succulence may play a role in maintaining of high photosynthesis rates at moderate salinity levels (Moir-Barnetson et al., 2016).

1.6.2: Salt glands as external salt sequestration structure in halophytes

A significant proportion of halophytes are able to sequester salt from their leaves into the external store cells. This external anatomical feature called salt glands (Dassanayake and Larkin, 2017; Liphschitz et al., 1974; Shabala et al., 2014). Halophytic plants with this external secretion ability also called recreto-halophytes which approximately including 370 species all over the world (Flowers and Colmer, 2008, 2015). In terms of structural perspective, salt glands originated from epidermal cells and thus considered as specialized trichomes (Esau, 1965). From functional perspective, salt glands have been categorised as exo-recretohalophytes

which directly secrete salts to the surface of the leaf and endo-recretohalophytes as plants that sequester salt into the vacuole of a specialized bladder cell (Ding et al., 2010).

Based on the similarities among salt glands they have been categorised into four groups (Dassanayake and Larkin, 2017). First group are salt bladders (also called epidermal bladder cells) consisting of a large vacuolated cell without any stalk cell or they may have one or two stalk cells. This kind of external salt store are found only in Aizoaceae and Amaranthaceae plant families. The second type of salt glands consisting multicellular structure ranging from 4 to 40 cells, with cells commonly differentiated into collecting and secretory cells in a cuticle lined structure. This group widely distributed among eudicots halophytic plants from various families. The third group of salt glands are bicellular secretory hair-like features with a basal cell and a cap cell that are present in chloridoid grasses. The fourth structural type of salt glands are unicellular highly vacuolated secretory hairs that are formed in Porteresia.

1.6.3: The role of epidermal bladder cells and in salinity tolerance of halophytic plants

Epidermal bladder cells (EBC) is a unique structure that directly sequester toxic ions such as Na^+ and Cl^- out of the plant and are present on stem and both abaxial and adaxial leaf surfaces (Dassanayake and Larkin, 2017; Shabala et al., 2014). EBC is composed of one bladder cell, without or with one or more stalk cells (Fig. 1.2).

The presence of EBC improves salinity tolerance in halophytes and this is mainly due to the fact that EBCs volume has a significant proportion of total leaf volume. It has been indicated in *Mesembryanthemum crystallinum* that Na^+ concentration can reach to 0.4 – 1.2 M in EBCs under salinity stress (Barkla et al., 2002; Oh et al., 2015) with similar amount for other halophyte plants. For instance, it is reported that Na^+ concentration in young leaves of *Atriplex gmelini* may reach 500 mM, with 80% of all accumulated Na^+ stored in EBC (Tsutsumi et al., 2015). This high role of contribution in Na^+ dumping may come from the higher volume of EBCs. For example, in *M. crystallinum* EBCs comprise up to 25% of the total aerial volume under saline conditions (Barkla et al., 2002).

Current study on EBCs of *M. crystallinum* has been indicated that EBCs do not function as a passive external store place for salt as it was perceived before, instead they have active metabolism in plant. It has been revealed that EBCs play

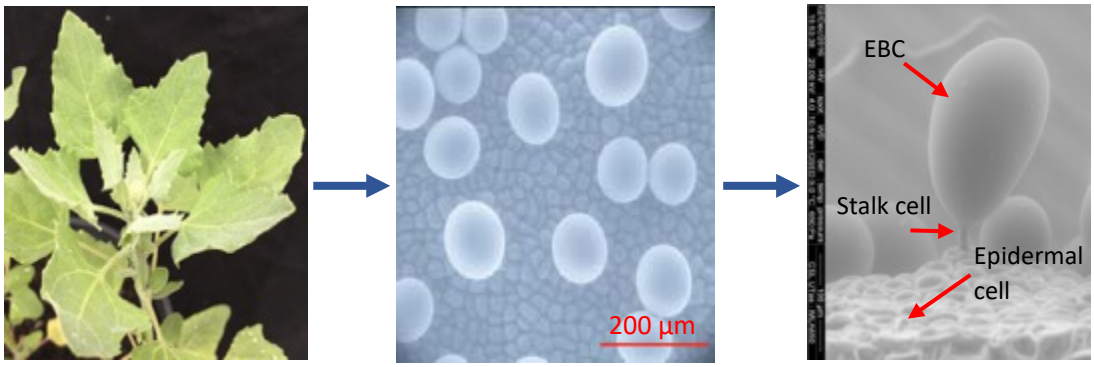

Fig. 1.2 The structure of an epidermal bladder cell. The large balloon-like object shows the typical structure of the salt bladder in quinoa. Na^+ can be sequestered from mesophyll into the EBC by stalk cell.

roles in accumulation of organic osmolytes, providing a secondary epidermal layer to protect against water loss, protection of leaves against UV and also have a role in energy generation, and stress signalling (Adolf et al., 2013; Barkla and Vera-Estrella, 2015; Barkla et al., 2012; Jou et al., 2007; Oh et al., 2015). Comparison of metabolic profile of salt-grown *M. crystallinum* plants with their control counterparts revealed that 352 metabolites were differently expressed in EBCs (Barkla and Vera-Estrella, 2015). Transcriptomic analysis of EBCs of *M. crystallinum* also indicated EBC-specific salt adaptive responses under saline conditions (Oh et al., 2015).

It has been argued that EBC function may change with leaf development. For halophytic plants Aizoaceae and Amaranthaceae it is proposed that salt compartmentalisation capacity of EBCs may be more critical function for young leaves (Barkla and Vera-Estrella, 2015; Bonales-Alatorre et al., 2013), but as the leaf matures and the EBC reaches its final volume, salt secretion content required to be paused (Jou et al., 2007; Oh et al., 2015). Under this circumstance, the aforementioned functions of EBCs may contribute more to plant survival under stressful conditions such as salinity stress (Barkla and Vera-Estrella, 2015).

1.6.3.1 Development of EBC

There is little information on molecular mechanisms of EBC or salt glands formation and patterning in halophytes. The existing knowledge in Arabidopsis indicates that trichome formation is the result of an interaction between neighbouring epidermal cells which is controlled by a number of positive and negative regulators (Pesch and Hulskamp, 2009; Shabala et al., 2014). Trichome formation in Arabidopsis occurs initially in all leaf epidermal cells (Martin and Glover, 2007) and is triggered by a transcription factor complex including Glabera1 (GL1), GL3, and THIOGLUCOSIDE GLUCOHYDROLASE (TTG) (Larkin et al., 2003). This complex directly activates transcription of its inhibitors such as Enhancer of triptychon and caprice2 (ETC2), Caprice (CPC), Triptychon (TRY), and single-repeat R3 *MY*ELO*B*LASTOSIS (MYB) transcription factor that is subjected to protein movement to neighboring cells (Grebe, 2012) which result in inactivating TTG1, GL3, GL1 complex there (Martin and Glover, 2007). This process eventually prevents trichome formation in neighboring cells. The activator transcription factor complex is also playing a role in directly activating of transcription of GL2 which function as a downstream regulator of trichome differentiation (Grebe, 2012). It also activates transcription of the mitosis inhibitor SIAMESE (SIM) that is needed for endoreplication process. Based on the traveling distance of the negative regulator, some epidermal cells will form trichomes, while the remaining cell do not and thus a trichome pattern is generated. In Arabidopsis it has been indicated by forward genetics studies that around 40 genes are involved in cell differentiation and trichome formation (Martin and Glover, 2007; Pesch and Hulskamp, 2009).

As in Arabidopsis the number of trichomes branches associated with the ploidy level (Passardi et al., 2007), it has also been shown in *M. crystallinum* that salinity stress induced endopolyploidy in EBCs with one or two additional rounds of endoreduplication under saline condition (Barkla et al., 2018). It has been suggested that this increase in cell size may contribute to salinity tolerance through increasing the external store volume for Na^+ sequestration. Thus, a similar mechanism may be involved in quinoa where endoreduplication plays a key role in EBC size in this plant.

1.6.3.2 How is salt transported into the EBCs?

EBCs are external structure which act as an extra reservoir for toxic ions and they required to have all the necessary metabolic pathways in place e.g. they need a source of energy for their activities (Shabala et al., 2014). Current study of comparison between salt responsiveness of transcriptomes from bladder bearing leaves with bladderless leaves showed a low expression of genes related to photosystem II in EBCs. It has also indicated that there were relatively few chloroplasts in EBCs (Bohm et al., 2018) and therefore, they need external energy source which is provided from leaf.

The simplified working model identified key transporters that play a role in delivery of Na^+ and Cl^- to EBCs is shown in Figure 1.3 and details of the involved transporters are discussed below (Brownlee, 2018). Based on the working model, vacuole of EBC is the final destination of salt. To make this happen, salt has to be transported from root to leaf and then be stored in EBC vacuole (Fig. 1.3). For Na^+ and Cl^- to be entered and accumulated in the vacuole of EBC, they need to pass through plasma membranes and to be transported to the bladder cytoplasm. Large vacuole of EBC is considered as a final destination of taken away salt from photosynthetically active tissue of leaf and therefore, certain vacuolar membrane transporters are needed for this function. To cross the plasma membrane, EBCs need membrane transporters and there is sufficient information confirming that SOS1 and HKT1 genes are primary players in Na^+ transport across the plasma membrane in plant (Shi et al., 2002; Waters et al., 2013). SOS1 is a Na^+/H^+-antiporter that utilizes the proton-motive-force to transport Na^+ out of the cell (Qiu et al., 2002; Shi et al., 2000), and as a result the cytoplasm to be prevented from reaching the toxic concentration of Na^+. In quinoa, EBCs had a quite low level of SOS1 transcripts compared to leaf whereas there was found high expression levels of the sodium-permeable ion channel HKT1 in EBCs (Bohm et al., 2018; Brownlee, 2018). HKT-type channels have been found to mediate Na^+-selective or a combined K^+/Na^+ transport across the plasma membrane (Platten et al., 2006; Waters et al., 2013). In case with EBC in quinoa, two co-orthologs of AtHKT1 namely CqHKT1.1 and CqHKT1.2 were found in both leaves and EBCs (Bohm et al., 2018). With the presence of Na^+ and hyperpolarization of membrane, CqHKT1.2 mediated inward Na^+ currents and the voltage-dependent Na^+ channel is responsible for loading this ion into the EBC. Some transporters such as NHX1 and ClC-c

quinoa orthologs, which are characterised as vacuolar proton-coupled Na^+ and anion exchangers were highly up-regulated in EBCs and therefore, it has been proposed that CqClC-c acts as a Cl^-/H^+ antiporter and uses the proton-motive-force to compartmentalise Cl^- into the EBC vacuole (Bohm et al., 2018; Brownlee, 2018).

1.6.3.3: Responsive genes for balancing the osmotic pressure in EBCs

As it has been mentioned above, under salinity stress NaCl content of EBCs can reach up to 1 M and therefore, salt gradient must be balanced between the bladder apoplast and cytoplasm on one side and cytoplasm and vacuole on the other

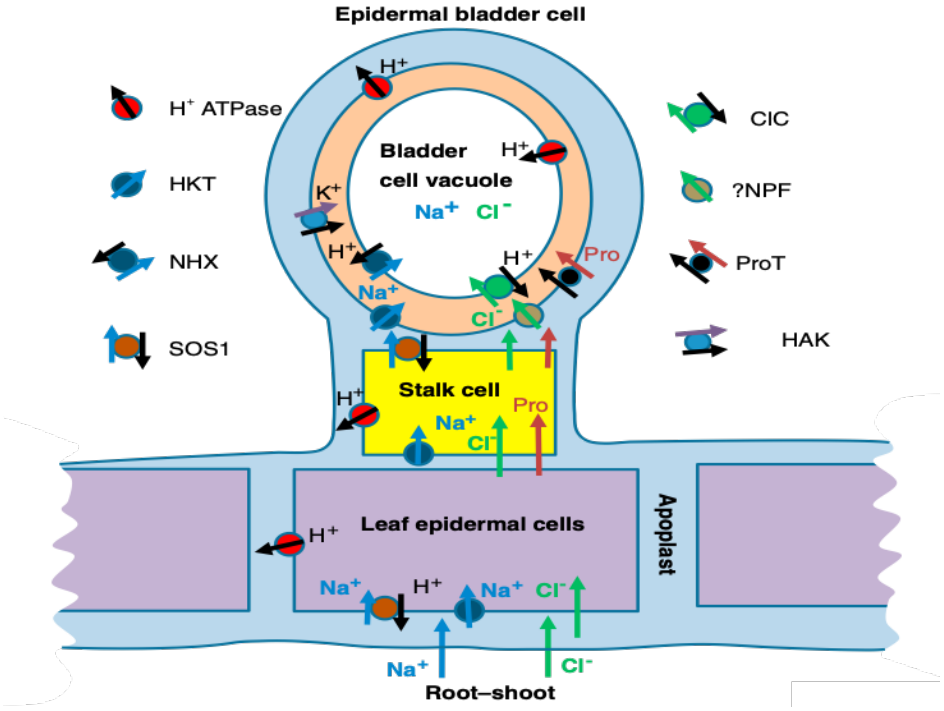

Fig. 1.3 Suggested roles of key identified ion and solute transporters responsible for transportation of ions and compatible osmolytes from leaves to epidermal bladder cell (EBC). Leaf epidermal cells move Na^+, Cl^- and compatible osmolytes via the stalk cell to the EBC through co-ordinated action of different cation, anion and solute transporters (Brownlee, 2018).

(Barkla et al., 2002; Shabala et al., 2014). Transportation of ions such as Na^+ and Cl^- across the cytoplasmic layer of the EBC into the vacuole is most probably buffered by the synthesis or uptake of osmo-protectant. These compatible osmolytes play an important role to protect the cytoplasmic metabolism from the toxic effects of toxic ions (Shabala and Mackay, 2011). It has already been revealed that proline as a major organic osmolyte has a crucial role in balancing the osmotic

adjustment and also providing shield against the toxic effects of toxic ions (Daum et al., 2010). Furthermore, in a current study the role of proline in EBCs is further investigated in quinoa and it has been indicated up-regulation of a ProT-type proline transporter which mediates a proton-driven proline uptake. This indicates that proline is transported from surrounding leaf cells into EBCs. This observation has been further confirmed through over-expression of proline synthesis-related genes in leaves under saline conditions (Bohm et al., 2018; Brownlee, 2018). Additionally, CqProT transporter also has a role in transportation of GABA, which is stress-related and have effects on plant channel activity (Shabala et al., 2014). It was also reported higher content of GABA in EBCs could facilitate the rate of salt loading into EBC and thus it could be suggested that CqProT has dual role of providing proline as an osmolyte and regulating ion transport through GABA (Ramesh et al., 2015)

In addition to proline as an organic osmolyte, K^+ is the primary inorganic osmolyte in the cytoplasm of plant species and it has a vital role in many metabolic functions such as cytoplasmic homeostasis, maintaining membrane potential and cell turgor and as a result plants need to take up K^+ under saline conditions (Tada et al., 2014). In the case with EBC of quinoa, it has been shown that two genes of the high affinity plasma membrane high affinity K^+ transporter (HAK/KUP/KT family) up-regulated EBC (Bohm et al., 2018).

1.7: Salinity stress studies using omics technologies

Environmental stresses such as salinity and drought are largely affecting plant growth and hence understanding plant responses to these stresses are very important to enhance plant's productivity under unfavourable condition (Munns and Tester, 2008; Neumann, 1997; Pessarakli, 2016; Ruan et al., 2010; Shabala, 2013; Turkan, 2011; Zorb et al., 2019). Plant adaptation to these stresses occurs at different biochemical, physiological, molecular and cellular levels (Yamaguchi-Shinozaki and Shinozaki, 2006). In the post-genomics era, studies on environmental stresses such as salinity has been developed with a diverse range of omics sciences. Using functional genomics technologies such as metabolomics and transcriptomics, comprehensive analyses have been conducted and our knowledge of the complicated regulatory networks of plants under these stresses have increased (Urano et al., 2010).

Salinity stress responses in quinoa occur at different tissues among which the EBCs specific processes are of particular importance because of the ability of these cells to take out the salt from metabolically active leaf tissue. Previous studies have been revealed that salinity stress alter various aspect of EBC such as modification of metabolism and plasma membrane characteristics (Barkla et al., 2012; Oh et al., 2015; Oh et al., 2010). It has also been shown that these alterations are not caused by a single phenomenon but rather are generated by a combination effects of various salt stress related pathway networks. These changes can also be best analysed at the comprehensive levels through applying high-throughput technologies such as transcriptome investigation (Petricka et al., 2012).

1.7.1: Metabolomics

It is estimated that there are around 200,000 metabolites within the plant kingdom (Fiehn, 2002), however it should be taken into consideration that due to reasons such as species-specific metabolites, rapid metabolite turnover, various metabolite distribution between tissues and spatiotemporal determinants, it is difficult to detect all the metabolites in a specific plant at any one time (Barkla and Vera-Estrella, 2015). Thus, using multiple analytical methods enable us to detect more metabolites. Metabolomics approaches which have been combined with other tools such as proteomics, genomics and transcriptomics provide this ability to understand the association between phenotype and genome in an organism. This understanding then can be associated with crop plants growing in adverse growth conditions to produce genotypes of crops with capability of efficiently coping with unfavourable environmental conditions such as salinity stress (Barkla and Vera-Estrella, 2015; Benjamin et al., 2019).

Metabolomics is a fast-developing technology that has been extensively used in plant stress studies. Depending on the questions need to be answered, specific metabolomics approach such as metabolite profiling and targeted analysis or a combination of these methods might be used (Kumari et al., 2015). For instance, metabolomics approach has been applied to investigate oxidative (Zhou et al., 2011), temperature (Kaplan et al., 2007), salinity (Kumari et al., 2015), and water (Akashi et al., 2011) stresses or it has been used to study a combination of these environmental stresses in plants (Cramer et al., 2007).

Salinity stress results in severe osmotic and ion toxic disbalance which cause detrimental alterations at different physiological and molecular levels in cellular components (Munns and Tester, 2008; Neumann, 1997). Plants response to these conditions through up and down regulation of a diverse metabolic components that protect plants from detrimental effects of salt stress (Benjamin et al., 2019; Shiri et al., 2015).

A broad-spectrum metabolite in response to salt stress has been determined in various halophytes (Barkla and Vera-Estrella, 2015; Kumari et al., 2015). For example, mono-, di-, oligo-, and polysaccharides such as glucose, fructose, sucrose, trehalose, raffinose, and fructans; polyol compounds such as sorbitol, mannitol, glycerol, inositol have been identified. Also, in amino acid group metabolites such as proline and in methylated proline-related group, compounds such as methyl-proline, proline betaine, and hydroxyproline betaine pipecolic acid have been determined (Kumari et al., 2015).

Benjamin et al. (2019) investigated the metabolomic profile of three halophytic plants namely *Salicornia brachiata, Suaeda maritima* and *Sesuvium portulacastrum,* under saline conditions. Metabolomics analysis of these plants indicated that the species-specific salinity tolerance mechanism in each of these species in adoption to saline conditions. It has been shown that several compounds of well-known or novel metabolites have been determined as critical players in mitigation to salinity stress across halophytic plants (Benjamin et al., 2019; Kumari et al., 2015; Shiri et al., 2015).

In a combination study of applying GC-MS profiling with microarray analysis, metabolic profile of Arabidopsis was compared with its halophytic counterpart, *Thellungiella halophila,* and significant differences revealed in metabolic contents of these plants (Gong et al., 2005). In general, Thellungiella had a higher metabolite levels than Arabidopsis under both saline and non-saline conditions. The results of this study also indicated that although Arabidopsis had an increase in sucrose, proline content in under 150 mM NaC however, the response of Thellungiella, was more complicated than Arabidopsis. In addition to having higher levels of many metabolites under non-saline condition, Thellungiella also showed alterations in other compounds such as sugars, sugar alcohols and organic acids under saline condition (Gong et al., 2005; Lugan et al., 2010; Shiri et al., 2015).

Barkla and Vera-Estrella (2015) conducted a comprehensive global analysis of the metabolites present in the EBC extract of facultative halophytic species *M. crystallinum* through non-targeted metabolite profiling under saline conditions. The results of this study determined 194 known and 722 total molecular features by which 352 metabolites were significantly changed between saline and non-saline conditions. Biochemical pathway enrichment analysis indicated that 13 biochemical pathways significantly enriched as defined in Kyoto Encyclopedia of Genes and Genomes (KEGG). Further analysis revealed that a significant proportion of the metabolites (more than 50%) that significantly changed in the EBC, were categorised as compatible solutes including sugars, sugar alcohols, protein and non-protein amino acids, and organic acids. This finding suggests that EBC requires these metabolites for maintaining osmotic adjustment to balance the accumulated salt. Altogether, by comparing the metabolic alteration in saline and non-saline conditions the result of this metabolomics study confirmed large changes in the EBCs of *M. crystallinum*.

1.7.2: Transcriptomic analysis

The perception of environmental stress and adaptive response induction has vital importance in halophytes (Chantre Nongpiur et al., 2016; Deinlein et al., 2014; Flowers and Colmer, 2015; Gong et al., 2005; Munns and Tester, 2008; Nikalje et al., 2017). Adaptive responses in halophytes are modulated through well-coordinated signalling pathway networks such as calcium signalling, ROS and plant hormones (Nikalje et al., 2017). A transcriptome study which uses currently developed sequencing technologies, represents a complete set of transcripts in given tissue or specific cell, under certain physiological condition or in a specific developmental stage. This kind of investigations provide information to interpret the function of genes and indicates the molecular components of cells (Oh et al., 2015; Oh et al., 2010; Wang et al., 2009). Additionally, transcriptomic studies recognise different types of transcripts such as mRNAs and small RNAs which in turn facilitate the identification of genes structure, post-transcriptional modifications and splicing patterns as well as expression level quantification under specific condition. Due to sensitivity and high-throughput of mRNA sequencing technology, this is a method of choice for gene expression profiling and its

instrumental capability in transcript abundance and discovery has been confirmed (Trapnell et al., 2010; Wang et al., 2009).

Advances in sequencing technologies has provided this capability to move to non-model plants to study molecular mechanisms of salinity tolerance (Turkan, 2011) thus, there is a possibility to address biological questions under unfavourable conditions for many crop plants (Jha et al., 2019; Nikalje et al., 2017). This advancement resulted in a significant progress in salinity stress information in recent years using mRNA sequencing technology and many salt-stress responses genes have been identified (Hanin et al., 2016; Wang et al., 2009).

Using transcriptome characterization and sequencing technology, (Huang et al., 2012) argued that in terms of expressed genes under saline condition there is a similarity among a variety of plants although they emphasised that there are species-specific salt-responsive genes also existed. Several investigations have been conducted to characterize the responsive genes in halophytes under saline conditions and transcriptome analyses have revealed a number of pathways associated with the salinity stress (Bressan et al., 2013; Joshi et al., 2019; Oh et al., 2010). Also, a number of comparative genomics studies have been done between halophytes and glycophytes and our understanding of Na transport and of salinity tolerance mechanism has been increased (Nah et al., 2009; Oh et al., 2010; Taji et al., 2004). Using deep sequencing technology, the genes regulatory network in ice plant has been characterized under saline condition (Tsukagoshi et al., 2015). Using mRNA database, the aforementioned study compared the gene expression of Arabidopsis and ice plant and identified novel patterns of transcriptional responses under high-saline condition. The critical finding of comparative investigations between glycophytes and halophytes is that while most of the salt-responsive genes are constitutively expressed in halophytes, they are salt inducible in glycophyte plants (Nikalje et al., 2017).

An expressed sequence tags (ESTs) study has been conducted on EBCs to compare the transcriptome profile under different treatments including developmental states, diurnal cycles and stress intensity in *M. crystallinum* (Cushman et al., 2008). In another RNA-seq study on this plant, significant alterations have been identified in biological process such as signal transduction, ion transport and also changes in carbon metabolism and metabolism related to osmolyte accumulation (Oh et al., 2015). It was shown that there were specific

transcriptomes related to EBC which in a number of precisely defined pathways responded to salt, differing from canonical salt-stress responses. They argued that this alterations in signalling and organelle functions likely resulted from accumulation of osmolytes induced by salinity stress and significant anatomical modification in EBCs (Oh et al., 2015).

Altogether, omics-based investigations suggest that EBCs have highly active metabolism (Barkla and Vera-Estrella, 2015; Bohm et al., 2018; Brownlee, 2018; Oh et al., 2015; Shabala et al., 2014) and this is in contrary to the previous views that EBCs as mere metabolically passive and considered these cells as a place to keep components such as salt, and water (Lüttge et al., 1978).

1.8: Quinoa

Quinoa is a cultivated species of most economic importance of the family Amaranthaceae (well-known for having the highest proportion of halophytes). This plant is a facultative halophyte that shows remarkable durability under various environmental stresses such as salt and drought (Adolf et al., 2013; Agarie et al., 2007; Jacobsen, 2003) which allows its cultivation in a wide range of environmental conditions. It has a very high tolerance to salinity stress well above tolerance threshold of any glycophyte so that some accessions of this species can tolerate salt concentrations identical to sea water (Jacobsen, 2003). Quinoa cultivation has been reported that started for over 7000 years ago in the Andean regions, which is known for its extreme conditions such as infertile soil and harsh climatic conditions (Adolf et al., 2013; Jacobsen, 2003). In addition to its outstanding ability to cope with various environmental stresses, quinoa is also considered a super-food due to its nutritious values. The physiological and molecular basis behind this significant salinity tolerance is not fully understood however, it has been argued that quinoa may use several unique mechanisms in order to acclimate to a saline environment (Wilson et al., 2002). Therefore, it has been suggested that it is an interesting model plant for the identification of specific ion transport processes mechanisms in halophytes under saline conditions.

Recognising the importance of quinoa, the genome of this plant has recently been released (Jarvis et al., 2017; Zou et al., 2017) and it provides the possibility to conduct more detailed studies of the molecular mechanisms underlying salinity tolerance and identification of salt-responsive genes in this plant species.

1.9: Research aims

Plants ability to grow under saline conditions depends on their tolerance to deal with various osmotic, oxidative and ionic hurdles resulted from salt stress. It has been shown that a high concentration of Na^+ in the cytosol of both traditional plants and halophytes is equally detrimental to their metabolism (Flowers and Colmer, 2008). Therefore, employing different strategies to tackle excess Na^+ concentration could be considered as the hallmark of salinity tolerance in plants and hence, it requires understanding of salinity adaptation mechanisms.

Despite having high tolerance to salt stress, halophytic plants have not been extensively used to study salinity tolerance mechanisms (reviewed in (Shabala, 2013). Also, studies investigating the salinity tolerance mechanism in halophytes have concentrated on physiological or anatomical aspects with little focus being given to the omics-based studies such as metabolomics, proteomics and transcriptome.

EBCs are specialized structures in some of halophytic plants that provide external store for toxic ions such as Na^+ and Cl^-, and hence understanding the function of EBCs may eventually play an important role in transferring this ability to crop plants. While there are limited studies focusing EBCs, it is argued that this scarcity may have arisen from their occurrence on diverse taxa in ecologically important plant families, but not economically valued as crop plants. Also, it is suggested that this lack of information could be due to the difficulty in studying EBCs as isolated cells in a low density in the leaf epidermis (Dassanayake and Larkin, 2017).

Stomata also being another focus of this study. Although there have been significant advances of understanding mechanisms that controlling stomatal development and also the signalling pathways that regulate guard cells function in glycophytes (Casson and Hetherington, 2010), much less is known in stomata in halophytes (Hedrich and Shabala, 2018). In light with this fact a question on how environmental variables and in particular salinity stress changes the basal stomatal development pathway requires more studies. There are many questions related to the stomata patterning as a component of the salt tolerance mechanism that have not been answered. Given the fact that osmotic stress and toxic Na^+ level negatively affect stomatal parameters under saline conditions (Tavakkoli et al., 2012) the question is that why are halophytes capable to optimise their stomata performance?

Do halophytic plants have special stomata operation mechanisms that utilise under saline conditions to cope with salt stress? How does salinity stress affect epidermal cell differentiation which leads to either an increase or decrease in stomatal density?

To fill some of above discussed gaps in our knowledge, the current study aimed to:

- Investigate the role of EBC in salinity tolerance in quinoa and provide the direct evidence by comparing the bladder-less quinoa with that of bladder-bearing plants
- Conducting RNA-sequencing analysis of EBC through comparing bladder-bearing quinoa plants with those that EBCs were gently brushed under saline and non-saline conditions. By doing this we focused on understanding salt-induced transcriptome changes in EBC and leaf lamina, as well as looking for proteins and ion transporters that likely are involved in ion sequestration.
- Evaluate the effects of salinity on EBC patterning in quinoa and correlate the extent of variability in this trait with genetic variation in salinity stress tolerance amongst the large number of accessions.
- Investigate stomata patterning and development in a large number of quinoa accessions and associate the extent of variability in stomata characteristics with genetic variation in salinity stress tolerance.
- Additionally, we aimed to investigate the difference in stomata operation and patterning in barley as a glycophyte and to compare these traits between wild and cultivated barley under saline condition. Understanding of these mechanisms in barley as a salt-tolerant crop plant and in a halophytic species would be beneficial to breeding programs through introducing desirable physiological traits for screening for salinity tolerance.

1.10: References

Adolf, V.I., Jacobsen, S.-E., Shabala, S., 2013. Salt tolerance mechanisms in quinoa (*Chenopodium quinoa*). Environ Exp Bot 92, 43-54.

Agarie, S., Shimoda, T., Shimizu, Y., Baumann, K., Sunagawa, H., Kondo, A., Ueno, O., Nakahara, T., Nose, A., Cushman, J.C., 2007. Salt tolerance, salt accumulation, and ionic homeostasis in an epidermal bladder-cell-less mutant

of the common ice plant *Mesembryanthemum crystallinum*. J Exp Bot 58, 1957-1967.

Akashi, K., Yoshida, K., Kuwano, M., Kajikawa, M., Yoshimura, K., Hoshiyasu, S., Inagaki, N., Yokota, A., 2011. Dynamic changes in the leaf proteome of a C3 xerophyte, *Citrullus lanatus* (wild watermelon), in response to water deficit. Planta 233, 947-960.

Barkla, B.J., Rhodes, T., Tran, K.T., Wijesinghege, C., Larkin, J.C., Dassanayake, M., 2018. Making Epidermal Bladder Cells Bigger: Developmental- and salinity-induced endopolyploidy in a model halophyte. Plant Physiol 177, 615-632.

Barkla, B.J., Vera-Estrella, R., 2015. Single cell-type comparative metabolomics of epidermal bladder cells from the halophyte *Mesembryanthemum crystallinum.* Front Plant Sci 6, 435.

Barkla, B.J., Vera-Estrella, R., Camacho-Emiterio, J., Pantoja, O., 2002. Na^+/H^+ exchange in the halophyte *Mesembryanthemum crystallinum* is associated with cellular sites of Na^+ storage. Funct Plant Biol 29, 1017-1024.

Barkla, B.J., Vera-Estrella, R., Pantoja, O., 2012. Protein profiling of epidermal bladder cells from the halophyte *Mesembryanthemum crystallinum.* Proteomics 12, 2862-2865.

Barragan, V., Leidi, E.O., Andres, Z., Rubio, L., De Luca, A., Fernandez, J.A., Cubero, B., Pardo, J.M., 2012. Ion exchangers NHX1 and NHX2 mediate active potassium uptake into vacuoles to regulate cell turgor and stomatal function in Arabidopsis. Plant Cell 24, 1127-1142.

Bassil, E., Tajima, H., Liang, Y.C., Ohto, M.A., Ushijima, K., Nakano, R., Esumi, T., Coku, A., Belmonte, M., Blumwald, E., 2011. The Arabidopsis Na^+/H^+ antiporters NHX1 and NHX2 control vacuolar pH and K^+ homeostasis to regulate growth, flower development, and reproduction. Plant Cell 23, 3482-3497.

Benjamin, J.J., Lucini, L., Jothiramshekar, S., Parida, A., 2019. Metabolomic insights into the mechanisms underlying tolerance to salinity in different halophytes. Plant Physiol Biochem 135, 528-545.

Berger, D., Altmann, T., 2000. A subtilisin-like serine protease involved in the regulation of stomatal density and distribution in *Arabidopsis thaliana*. Genes Dev 14, 1119-1131.

Bertolino, L.T., Caine, R.S., Gray, J.E., 2019. Impact of stomatal density and morphology on water-use efficiency in a changing world. Front Plant Sci 10, 225.

Blumwald, E., Poole, R.J., 1985. Na^+/H^+ antiport in isolated tonoplast vesicles from storage tissue of *Beta vulgaris*. Plant Physiol 78, 163-167.

Bohm, J., Messerer, M., Muller, H.M., Scholz-Starke, J., Gradogna, A., Scherzer, S., Maierhofer, T., Bazihizina, N., Zhang, H., Stigloher, C., Ache, P., Al-Rasheid, K.A.S., Mayer, K.F.X., Shabala, S., Carpaneto, A., Haberer, G., Zhu, J.K., Hedrich, R., 2018. Understanding the molecular basis of salt sequestration in epidermal bladder cells of *Chenopodium quinoa*. Curr Biol 28, 3075-3085.

Bonales-Alatorre, E., Pottosin, I., Shabala, L., Chen, Z.H., Zeng, F., Jacobsen, S.E., Shabala, S., 2013. Differential activity of plasma and vacuolar membrane transporters contributes to genotypic differences in salinity tolerance in a halophyte species, *Chenopodium quinoa*. Int J Mol Sci 14, 9267-9285.

Bose, J., Shabala, L., Pottosin, I., Zeng, F., Velarde-Buendia, A.M., Massart, A., Poschenrieder, C., Hariadi, Y., Shabala, S., 2014. Kinetics of xylem loading, membrane potential maintenance, and sensitivity of K^+-permeable channels to reactive oxygen species: physiological traits that differentiate salinity tolerance between pea and barley. Plant Cell Environ 37, 589-600.

Bressan, R.A., Park, H.C., Orsini, F., Oh, D.-h., Dassanayake, M., Inan, G., Yun, D.-J., Bohnert, H.J., Maggio, A., 2013. Biotechnology for mechanisms that counteract salt stress in extremophile species: a genome-based view. Plant Biotechnol Rep 7, 27-37.

Brownlee, C., 2018. Plant physiology: One way to dump salt. Curr Biol 28, R1145-R1147.

Büssis, D., von Groll, U., Fisahn, J., Altmann, T., 2006. Stomatal aperture can compensate altered stomatal density in *Arabidopsis thaliana* at growth light conditions. Funct Plant Biol 33, 1037-1043.

Casson, S.A., Hetherington, A.M., 2010. Environmental regulation of stomatal development. Curr Opin Plant Biol 13, 90-95.

Chantre Nongpiur, R., Lata Singla-Pareek, S., Pareek, A., 2016. Genomics approaches for improving salinity stress tolerance in crop plants. Curr genomics 17, 343-357.

Chaves, M., Costa, J., Zarrouk, O., Pinheiro, C., Lopes, C., Pereira, J., 2016. Controlling stomatal aperture in semi-arid regions—The dilemma of saving water or being cool? Plant Sci 251, 54-64.

Chen, Z.H., Chen, G., Dai, F., Wang, Y., Hills, A., Ruan, Y.L., Zhang, G., Franks, P.J., Nevo, E., Blatt, M.R., 2017. Molecular evolution of grass stomata. Trends Plant Sci 22, 124-139.

Cramer, G.R., Ergul, A., Grimplet, J., Tillett, R.L., Tattersall, E.A., Bohlman, M.C., Vincent, D., Sonderegger, J., Evans, J., Osborne, C., Quilici, D., Schlauch, K.A., Schooley, D.A., Cushman, J.C., 2007. Water and salinity stress in grapevines: early and late changes in transcript and metabolite profiles. Funct Integr Genomics 7, 111-134.

Cushman, J.C., Bohnert, H.J., 1999. Crassulacean acid metabolism: molecular genetics. Annu Rev Plant Physiol Plant Mol Biol 50, 305-332.

Cushman, J.C., Tillett, R.L., Wood, J.A., Branco, J.M., Schlauch, K.A., 2008. Large-scale mRNA expression profiling in the common ice plant, *Mesembryanthemum crystallinum*, performing C3 photosynthesis and crassulacean acid metabolism (CAM). J Exp Bot 59, 1875-1894.

Dassanayake, M., Larkin, J.C., 2017. Making plants break a sweat: the structure, function, and evolution of plant salt glands. Front Plant Sci 8, 406.

Daum, B., Nicastro, D., Austin, J., 2nd, McIntosh, J.R., Kuhlbrandt, W., 2010. Arrangement of photosystem II and ATP synthase in chloroplast membranes of spinach and pea. Plant Cell 22, 1299-1312.

de Boer, H.J., Price, C.A., Wagner-Cremer, F., Dekker, S.C., Franks, P.J., Veneklaas, E.J., 2016. Optimal allocation of leaf epidermal area for gas exchange. New Phytol 210, 1219-1228.

Deinlein, U., Stephan, A.B., Horie, T., Luo, W., Xu, G., Schroeder, J.I., 2014. Plant salt-tolerance mechanisms. Trends Plant Sci 19, 371-379.

Ding, F., Yang, J.-C., Yuan, F., Wang, B.-S., 2010. Progress in mechanism of salt excretion in recretohalopytes. Front Biol 5, 164-170.

Doheny-Adams, T., Hunt, L., Franks, P.J., Beerling, D.J., Gray, J.E., 2012. Genetic manipulation of stomatal density influences stomatal size, plant growth and tolerance to restricted water supply across a growth carbon dioxide gradient. Philos Trans R Soc Lond B Biol Sci 367, 547-555.

Dow, G.J., Berry, J.A., Bergmann, D.C., 2014. The physiological importance of developmental mechanisms that enforce proper stomatal spacing in *Arabidopsis thaliana*. New Phytol 201, 1205-1217.

Drake, P.L., Froend, R.H., Franks, P.J., 2013. Smaller, faster stomata: scaling of stomatal size, rate of response, and stomatal conductance. J Exp Bot 64, 495-505.

Esau, K., 1965. Plant anatomy 2nd Ed John Wiley & Sons. Inc New York, NY.

Fiehn, O., 2002. Metabolomics—the link between genotypes and phenotypes, Functional genomics. Springer, pp 155-171.

Flowers, T.J., Colmer, T.D., 2008. Salinity tolerance in halophytes. New Phytol 179, 945-963.

Flowers, T.J., Colmer, T.D., 2015. Plant salt tolerance: adaptations in halophytes. Ann Bot 115, 327-331.

Franks, P.J., Farquhar, G.D., 2007. The mechanical diversity of stomata and its significance in gas-exchange control. Plant Physiol 143, 78-87.

Gay, A., Hurd, R., 1975. The influence of light on stomatal density in the tomato. New Phytol 75, 37-46.

Gill, S.S., Tuteja, N., 2010. Reactive oxygen species and antioxidant machinery in abiotic stress tolerance in crop plants. Plant Physiol Biochem 48, 909-930.

Glenn, E.P., O'Leary, J.W., 1984. Relationship between salt accumulation and water content of dicotyledonous halophytes. Plant Cell Environ 7, 253-261.

Gong, Q., Li, P., Ma, S., Indu Rupassara, S., Bohnert, H.J., 2005. Salinity stress adaptation competence in the extremophile *Thellungiella halophila* in comparison with its relative *Arabidopsis thaliana*. Plant J 44, 826-839.

Gray, J.E., Holroyd, G.H., Van Der Lee, F.M., Bahrami, A.R., Sijmons, P.C., Woodward, F.I., Schuch, W., Hetherington, A.M., 2000. The HIC signalling pathway links CO_2 perception to stomatal development. Nature 408, 713.

Grebe, M., 2012. The patterning of epidermal hairs in Arabidopsis—updated. Curr Opin Plant Biol 15, 31-37.

Hanin, M., Ebel, C., Ngom, M., Laplaze, L., Masmoudi, K., 2016. New insights on plant salt tolerance mechanisms and their potential use for breeding. Front Plant Sci 7, 1787.

Hara, K., Yokoo, T., Kajita, R., Onishi, T., Yahata, S., Peterson, K.M., Torii, K.U., Kakimoto, T., 2009. Epidermal cell density is autoregulated via a secretory

peptide, EPIDERMAL PATTERNING FACTOR 2 in Arabidopsis leaves. Plant Cell Physiol. 50, 1019-1031.

Hariadi, Y., Marandon, K., Tian, Y., Jacobsen, S.E., Shabala, S., 2011. Ionic and osmotic relations in quinoa (*Chenopodium quinoa*) plants grown at various salinity levels. J Exp Bot 62, 185-193.

Haworth, M., Marino, G., Cosentino, S.L., Brunetti, C., De Carlo, A., Avola, G., Riggi, E., Loreto, F., Centritto, M., 2018. Increased free abscisic acid during drought enhances stomatal sensitivity and modifies stomatal behaviour in fast growing giant reed (*Arundo donax*). Environ Exp Bot 147, 116-124.

Hedrich, R., Shabala, S., 2018. Stomata in a saline world. Curr Opin Plant Biol 46, 87-95.

Hetherington, A.M., Woodward, F.I., 2003. The role of stomata in sensing and driving environmental change. Nature 424, 901-908.

Huang, J., Lu, X., Yan, H., Chen, S., Zhang, W., Huang, R., Zheng, Y., 2012. Transcriptome characterization and sequencing-based identification of salt-responsive genes in *Millettia pinnata*, a semi-mangrove plant. DNA Res 19, 195-207.

Hunt, L., Bailey, K.J., Gray, J.E., 2010. The signalling peptide EPFL9 is a positive regulator of stomatal development. New Phytol 186, 609-614.

Jacobsen, S.-E., 2003. The worldwide potential for quinoa (*Chenopodium quinoa*). Food Rev. Int. 19, 167-177.

Jarvis, D.E., Ho, Y.S., Lightfoot, D.J., Schmöckel, S.M., Li, B., Borm, T.J., Ohyanagi, H., Mineta, K., Michell, C.T., Saber, N., 2017. The genome of *Chenopodium quinoa*. Nature 542, 307.

Jha, U.C., Bohra, A., Jha, R., Parida, S.K., 2019. Salinity stress response and 'omics' approaches for improving salinity stress tolerance in major grain legumes. Plant Cell Rep 38, 255-277.

Joshi, R., Gupta, B.K., Pareek, A., Singh, M.B., Singla-Pareek, S.L., 2019. Functional Genomics Approach Towards Dissecting Out Abiotic Stress Tolerance Trait in Plants, Genetic Enhancement of Crops for Tolerance to Abiotic Stress: Mechanisms and Approaches, Vol. I. Springer, pp 1-24.

Jou, Y., Wang, Y.-L., Yen, H.E., 2007. Vacuolar acidity, protein profile, and crystal composition of epidermal bladder cells of the halophyte *Mesembryanthemum crystallinum*. Funct Plant Biol 34, 353-359.

Kaplan, F., Kopka, J., Sung, D.Y., Zhao, W., Popp, M., Porat, R., Guy, C.L., 2007. Transcript and metabolite profiling during cold acclimation of Arabidopsis reveals an intricate relationship of cold-regulated gene expression with modifications in metabolite content. Plant J 50, 967-981.

Khan, M.A., Ungar, I.A., Showalter, A.M., 2005. Salt stimulation and tolerance in an intertidal stem-succulent halophyte. J Plant Nutr 28, 1365-1374.

Koyro, H.-W., Geißler, N., Hussin, S., Huchzermeyer, B., 2008. Survival at extreme locations: life strategies of halophytes-the long way from system ecology, whole plant physiology, cell biochemistry and molecular aspects back to sustainable utilization at field sites, Biosaline Agriculture and High Salinity Tolerance. Springer, pp 1-20.

Kumari, A., Das, P., Parida, A.K., Agarwal, P.K., 2015. Proteomics, metabolomics, and ionomics perspectives of salinity tolerance in halophytes. Front Plant Sci 6, 537.

Lal, R., 2010. Managing soils and ecosystems for mitigating anthropogenic carbon emissions and advancing global food security. BioScience 60, 708-721.

Larkin, J.C., Brown, M.L., Schiefelbein, J., 2003. How do cells know what they want to be when they grow up? Lessons from epidermal patterning in Arabidopsis. Annu Rev Plant Biol 54, 403-430.

Lau, O.S., Bergmann, D.C., 2012. Stomatal development: a plant's perspective on cell polarity, cell fate transitions and intercellular communication. Development 139, 3683-3692.

Lawson, T., Vialet-Chabrand, S., 2019. Speedy stomata, photosynthesis and plant water use efficiency. New Phytol 221, 93-98.

Lee, J.S., Hnilova, M., Maes, M., Lin, Y.C., Putarjunan, A., Han, S.K., Avila, J., Torii, K.U., 2015. Competitive binding of antagonistic peptides fine-tunes stomatal patterning. Nature 522, 439-443.

Liphschitz, N., Eshel, A., Waisel, Y., 1974. Salt glands on leaves of Rhodes grass (*Chloris gayana*). Ann Bot 38, 459-462.

Lugan, R., Niogret, M.F., Leport, L., Guégan, J.P., Larher, F.R., Savouré, A., Kopka, J., Bouchereau, A., 2010. Metabolome and water homeostasis analysis of *Thellungiella salsuginea* suggests that dehydration tolerance is a key response to osmotic stress in this halophyte. Plant J 64, 215-229.

Lüttge, U., Fischer, E., Steudle, E., 1978. Membrane potentials and salt distribution in epidermal bladders and photosynthetic tissue of *Mesembryanthemum crystallinum*. Plant Cell Environ 1, 121-129.

Ma, X.-L., Zhang, Q., Shi, H.-Z., Zhu, J.-K., Zhao, Y.-X., Ma, C.-L., Zhang, H., 2004. Molecular cloning and different expression of a vacuolar Na^+/H^+ antiporter gene in Suaeda salsa under salt stress. Biol Plant 48, 219-225.

Martin, C., Glover, B.J., 2007. Functional aspects of cell patterning in aerial epidermis. Curr Opin Plant Biol 10, 70-82.

McAusland, L., Vialet-Chabrand, S., Davey, P., Baker, N.R., Brendel, O., Lawson, T., 2016. Effects of kinetics of light-induced stomatal responses on photosynthesis and water-use efficiency. New Phytol 211, 1209-1220.

McNulty, I.B., 1985. Rapid osmotic adjustment by a succulent halophyte to saline shock. Plant Physiol 78, 100-103.

Mian, A., Oomen, R.J., Isayenkov, S., Sentenac, H., Maathuis, F.J., Very, A.A., 2011. Over-expression of an Na^+-and K^+-permeable HKT transporter in barley improves salt tolerance. Plant J 68, 468-479.

Moir-Barnetson, L., Veneklaas, E.J., Colmer, T.D., 2016. Salinity tolerances of three succulent halophytes (*Tecticornia spp.*) differentially distributed along a salinity gradient. Funct Plant Biol 43, 739-750.

Munns, R., Tester, M., 2008. Mechanisms of salinity tolerance. Annu Rev Plant Biol 59, 651-681.

Nah, G., Pagliarulo, C.L., Mohr, P.G., Luo, M., Sisneros, N., Yu, Y., Collura, K., Currie, J., Goicoechea, J.L., Wing, R.A., Schumaker, K.S., 2009. Comparative sequence analysis of the SALT OVERLY SENSITIVE1 orthologous region in *Thellungiella halophila* and *Arabidopsis thaliana*. Genomics 94, 196-203.

Naidoo, G., Rughunanan, R., 1990. Salt tolerance in the succulent, coastal halophyte, *Sarcocornia natalensis*. J Exp Bot 41, 497-502.

Neumann, P., 1997. Salinity resistance and plant growth revisited. Plant Cell Environ 20, 1193-1198.

Nikalje, G., D Nikam, T., Suprasanna, P., 2017. Looking at halophytic adaptation to high salinity through genomics landscape. Curr genomics 18, 542-552.

Oh, D.H., Barkla, B.J., Vera-Estrella, R., Pantoja, O., Lee, S.Y., Bohnert, H.J., Dassanayake, M., 2015. Cell type-specific responses to salinity - the epidermal

bladder cell transcriptome of *Mesembryanthemum crystallinum*. New Phytol 207, 627-644.

Oh, D.H., Dassanayake, M., Haas, J.S., Kropornika, A., Wright, C., d'Urzo, M.P., Hong, H., Ali, S., Hernandez, A., Lambert, G.M., Inan, G., Galbraith, D.W., Bressan, R.A., Yun, D.J., Zhu, J.K., Cheeseman, J.M., Bohnert, H.J., 2010. Genome structures and halophyte-specific gene expression of the extremophile *Thellungiella parvula* in comparison with *Thellungiella salsuginea* (*Thellungiella halophila*) and Arabidopsis. Plant Physiol 154, 1040-1052.

Ozgur, R., Uzilday, B., Sekmen, A.H., Turkan, I., 2013. Reactive oxygen species regulation and antioxidant defence in halophytes. Funct Plant Biol 40, 832-847.

Passardi, F., Dobias, J., Valerio, L., Guimil, S., Penel, C., Dunand, C., 2007. Morphological and physiological traits of three major *Arabidopsis thaliana* accessions. J Plant Physiol 164, 980-992.

Peng, X., Li, F., Li, S., Zhu, Y., 2009. Expression of a mitochondrial gene orfH79 from the CMS-HongLian rice inhibits *Saccharomyces cerevisiae* growth and causes excessive ROS accumulation and decrease in ATP. Biotechnol Lett 31, 409-414.

Pesch, M., Hulskamp, M., 2009. One, two, three...models for trichome patterning in Arabidopsis? Curr Opin Plant Biol 12, 587-592.

Pessarakli, M., 2016. Handbook of Plant and Crop Stress. CRC press.

Petricka, J.J., Schauer, M.A., Megraw, M., Breakfield, N.W., Thompson, J.W., Georgiev, S., Soderblom, E.J., Ohler, U., Moseley, M.A., Grossniklaus, U., Benfey, P.N., 2012. The protein expression landscape of the Arabidopsis root. Proc Natl Acad Sci U S A 109, 6811-6818.

Platten, J.D., Cotsaftis, O., Berthomieu, P., Bohnert, H., Davenport, R.J., Fairbairn, D.J., Horie, T., Leigh, R.A., Lin, H.X., Luan, S., Maser, P., Pantoja, O., Rodriguez-Navarro, A., Schachtman, D.P., Schroeder, J.I., Sentenac, H., Uozumi, N., Very, A.A., Zhu, J.K., Dennis, E.S., Tester, M., 2006. Nomenclature for HKT transporters, key determinants of plant salinity tolerance. Trends Plant Sci 11, 372-374.

Qiu, Q.S., Guo, Y., Dietrich, M.A., Schumaker, K.S., Zhu, J.K., 2002. Regulation of SOS1, a plasma membrane Na^+/H^+ exchanger in *Arabidopsis thaliana*, by SOS2 and SOS3. Proc Natl Acad Sci U S A 99, 8436-8441.

Ramesh, S.A., Tyerman, S.D., Xu, B., Bose, J., Kaur, S., Conn, V., Domingos, P., Ullah, S., Wege, S., Shabala, S., Feijo, J.A., Ryan, P.R., Gilliham, M., 2015. GABA signalling modulates plant growth by directly regulating the activity of plant-specific anion transporters. Nat Commun 6, 7879.

Raven, J.A., 1985. Regulation of pH and generation of osmolarity in vascular plants: a cost-benefit analysis in relation to efficiency of use of energy, nitrogen and water. New Phytol, 25-77.

Ruan, C.-J., da Silva, J.A.T., Mopper, S., Qin, P., Lutts, S., 2010. Halophyte improvement for a salinized world. Crit Rev Plant Sci 29, 329-359.

Ruiz-Carrasco, K., Antognoni, F., Coulibaly, A.K., Lizardi, S., Covarrubias, A., Martinez, E.A., Molina-Montenegro, M.A., Biondi, S., Zurita-Silva, A., 2011. Variation in salinity tolerance of four lowland genotypes of quinoa (*Chenopodium quinoa*) as assessed by growth, physiological traits, and sodium transporter gene expression. Plant Physiol Biochem 49, 1333-1341.

Santa-Cruz, A., Acosta, M., Rus, A., Bolarin, M.C., 1999. Short-term salt tolerance mechanisms in differentially salt tolerant tomato species. Plant Physiol Biochem 37, 65-71.

Santos, J., Al-Azzawi, M., Aronson, J., Flowers, T.J., 2016. eHALOPH a database of salt-tolerant plants: helping put halophytes to work. Plant Cell Physiol 57, e10.

Schroeder, J.I., Delhaize, E., Frommer, W.B., Guerinot, M.L., Harrison, M.J., Herrera-Estrella, L., Horie, T., Kochian, L.V., Munns, R., Nishizawa, N.K., Tsay, Y.F., Sanders, D., 2013. Using membrane transporters to improve crops for sustainable food production. Nature 497, 60-66.

Sengupta, S., Majumder, A.L., 2010. *Porteresia coarctata* (Roxb.) Tateoka, a wild rice: a potential model for studying salt-stress biology in rice. Plant Cell Environ 33, 526-542.

Shabala, S., 2013. Learning from halophytes: physiological basis and strategies to improve abiotic stress tolerance in crops. Ann Bot 112, 1209-1221.

Shabala, S., Bose, J., Fuglsang, A.T., Pottosin, I., 2016. On a quest for stress tolerance genes: membrane transporters in sensing and adapting to hostile soils. J Exp Bot 67, 1015-1031.

Shabala, S., Bose, J., Hedrich, R., 2014. Salt bladders: do they matter? Trends Plant Sci 19, 687-691.

Shabala, S., Mackay, A., 2011. Ion Transport in Halophytes, in: Turkan, I. (Ed.), Plant Responses to Drought and Salinity Stress - Developments in a Post-Genomic Era. Academic Press, pp 151-199.

Shi, H., Ishitani, M., Kim, C., Zhu, J.K., 2000. The *Arabidopsis thaliana* salt tolerance gene SOS1 encodes a putative Na^+/H^+ antiporter. Proc Natl Acad Sci U S A 97, 6896-6901.

Shi, H., Quintero, F.J., Pardo, J.M., Zhu, J.K., 2002. The putative plasma membrane Na^+/H^+ antiporter SOS1 controls long-distance Na^+ transport in plants. Plant Cell 14, 465-477.

Shiri, M., Rabhi, M., El Amrani, A., Abdelly, C., 2015. Cross-tolerance to abiotic stresses in halophytes: application for phytoremediation of organic pollutants. Acta Physiol Plant 37, 209.

Short, D.C., Colmer, T.D., 1999. Salt Tolerance in the halophyte *Halosarcia pergranulatasub* sp. pergranulata. Ann Bot 83, 207-213.

Sun, Y., Yan, F., Cui, X., Liu, F., 2014. Plasticity in stomatal size and density of potato leaves under different irrigation and phosphorus regimes. J Plant Physiol 171, 1248-1255.

Tada, Y., Komatsubara, S., Kurusu, T., 2014. Growth and physiological adaptation of whole plants and cultured cells from a halophyte turf grass under salt stress. AoB PLANTS 6.

Taji, T., Seki, M., Satou, M., Sakurai, T., Kobayashi, M., Ishiyama, K., Narusaka, Y., Narusaka, M., Zhu, J.-K., Shinozaki, K., 2004. Comparative genomics in salt tolerance between Arabidopsis and Arabidopsis-related halophyte salt cress using Arabidopsis microarray. Plant Physiol 135, 1697-1709.

Tavakkoli, E., Fatehi, F., Rengasamy, P., McDonald, G.K., 2012. A comparison of hydroponic and soil-based screening methods to identify salt tolerance in the field in barley. J Exp Bot 63, 3853-3867.

Tester, M., Davenport, R., 2003. Na^+ tolerance and Na^+ transport in higher plants. Ann Bot 91, 503-527.

Trapnell, C., Williams, B.A., Pertea, G., Mortazavi, A., Kwan, G., van Baren, M.J., Salzberg, S.L., Wold, B.J., Pachter, L., 2010. Transcript assembly and quantification by RNA-Seq reveals unannotated transcripts and isoform switching during cell differentiation. Nat Biotechnol 28, 511-515.

Tsukagoshi, H., Suzuki, T., Nishikawa, K., Agarie, S., Ishiguro, S., Higashiyama, T., 2015. RNA-seq analysis of the response of the halophyte, *Mesembryanthemum crystallinum* (ice plant) to high salinity. PLoS One 10, e0118339.

Tsutsumi, K., Yamada, N., Chaum, S., Tanaka, Y., Takabe, T., 2015. Differential accumulation of glycinebetaine and choline monooxygenase in bladder hairs and lamina leaves of *Atriplex gmelini* under high salinity. J Plant Physiol 176, 101-107.

Turkan, I., 2011. Plant Responses To Drought And Salinity Stress: Developments In A Post-Genomic Era. Academic Press.

Urano, K., Kurihara, Y., Seki, M., Shinozaki, K., 2010. 'Omics' analyses of regulatory networks in plant abiotic stress responses. Curr Opin Plant Biol 13, 132-138.

Vaten, A., Bergmann, D.C., 2012. Mechanisms of stomatal development: an evolutionary view. Evo Devo 3, 11.

Vico, G., Manzoni, S., Palmroth, S., Katul, G., 2011. Effects of stomatal delays on the economics of leaf gas exchange under intermittent light regimes. New Phytol 192, 640-652.

Von Groll, U., Berger, D., Altmann, T., 2002. The subtilisin-like serine protease SDD1 mediates cell-to-cell signaling during Arabidopsis stomatal development. Plant Cell 14, 1527-1539.

Wang, Z., Gerstein, M., Snyder, M., 2009. RNA-Seq: a revolutionary tool for transcriptomics. Nat Rev Genet 10, 57-63.

Waters, S., Gilliham, M., Hrmova, M., 2013. Plant High-Affinity Potassium (HKT) transporters involved in salinity tolerance: structural insights to probe differences in ion selectivity. Int J Mol Sci 14, 7660-7680.

Wilson, C., Read, J.J., Abo-Kassem, E., 2002. Effect of mixed-salt salinity on growth and ion relations of a quinoa and a wheat variety. J Plant Nutr 25, 2689-2704.

Winter, K., Troughton, J.H., Evenari, M., Lauchli, A., Luttge, U., 1976. Mineral ion composition and occurrence of CAM-like diurnal malate fluctuations in plants of coastal and desert habitats of israel and the Sinai. Oecologia 25, 125-143.

Yamaguchi-Shinozaki, K., Shinozaki, K., 2006. Transcriptional regulatory networks in cellular responses and tolerance to dehydration and cold stresses. Annu Rev Plant Biol 57, 781-803.

Yeo, A., Flowers, T., 1980. Salt tolerance in the halophyte *Suaeda maritima*: evaluation of the effect of salinity upon growth. J Exp Bot 31, 1171-1183.

Zeng, F., Shabala, S., Maksimovic, J.D., Maksimovic, V., Bonales-Alatorre, E., Shabala, L., Yu, M., Zhang, G., Zivanovic, B.D., 2018. Revealing mechanisms of salinity tissue tolerance in succulent halophytes: a case study for *Carpobrotus rossi*. Plant Cell Environ 41, 2654-2667.

Zheng, Q., Liu, L., Liu, Z., Chen, J., Zhao, G., 2009. Comparison of the response of ion distribution in the tissues and cells of the succulent plants *Aloe vera* and *Salicornia europaea* to saline stress. J Plant Nutr Soil Sci 172, 875-883.

Zhou, S., Sauvé, R.J., Liu, Z., Reddy, S., Bhatti, S., Hucko, S.D., Fish, T., Thannhauser, T.W., 2011. Identification of salt-induced changes in leaf and root proteomes of the wild tomato, *Solanum chilense*. J Am Soc Hortic Sci 136, 288-302.

Zorb, C., Geilfus, C.M., Dietz, K.J., 2019. Salinity and crop yield. Plant Biol 21 Suppl 1, 31-38.

Zou, C., Chen, A., Xiao, L., Muller, H.M., Ache, P., Haberer, G., Zhang, M., Jia, W., Deng, P., Huang, R., 2017. A high-quality genome assembly of quinoa provides insights into the molecular basis of salt bladder-based salinity tolerance and the exceptional nutritional value. Cell research 27, 1327.

Zoulias, N., Harrison, E.L., Casson, S.A., Gray, J.E., 2018. Molecular control of stomatal development. Biochem J 475, 441-454.

Chapter 2: Epidermal bladder cells confer salinity stress tolerance in the halophyte quinoa and Atriplex species[1]

Abstract

Epidermal bladder cells (EBCs) have been postulated to assist halophytes in coping with saline environments. However, little direct supporting evidence is available. Here, *Chenopodium quinoa* plants were grown under saline conditions for 5 weeks. One day prior to salinity treatment, EBCs from all leaves and petioles were gently removed by using a soft cosmetic brush and physiological, ionic and metabolic changes in brushed and non-brushed leaves were compared. Gentle removal of EBC neither initiated wound metabolism nor affected the physiology and biochemistry of control-grown plants but did have a pronounced effect on salt-grown plants, resulting in a salt-sensitive phenotype. Of 91 detected metabolites, more than half were significantly affected by salinity. Removal of EBC dramatically modified these metabolic changes, with the biggest differences reported for gamma-aminobutyric acid (GABA), proline, sucrose and inositol, affecting ion transport across cellular membranes (as shown in electrophysiological experiments). This work provides the first direct evidence for a role of EBC in salt tolerance in halophytes and attributes this to (1) a key role of EBC as a salt dump for external sequestration of sodium; (2) improved K^+ retention in leaf mesophyll and (3) EBC as a storage space for several metabolites known to modulate plant ionic relations.

2.1 Introduction

Halophytes constitute less than 0.4% of all land plants (Yuan et al., 2016). While the precise definition of the term halophyte is still a matter of debate (e.g. (Flowers and Colmer, 2008), in a broad sense, it defines plant species that naturally inhabit saline environments and benefit from having substantial amounts of salt in the growth media(Shabala, 2013). Consequently, in lay terms, they are often referred to as ‘salt-loving plants’. Halophytes flourish under conditions that would kill 99%

[1] This chapter has been published as: **Kiani-Pouya A,** Roessner U, Jayasinghe NS, Lutz A, Rupasinghe T, Bazihizina N, Bohm J, Alharbi S, Hedrich R, Shabala S (2017) Epidermal bladder cells confer salinity stress tolerance in the halophyte quinoa and Atriplex species. Plant Cell Environ 40 (9):1900-1915.

of crop species, so are considered a viable alternative to conventional agriculture in saline areas (Glenn et al., 2010; Panta et al., 2014; Ruan et al., 2010; Ventura et al., 2015).

The superior salinity tolerance in halophytes is achieved via an orchestrated performance of a large number of physiological mechanisms and anatomical and morphological features(Adolf et al., 2013; Barkla and Pantoja, 1996; Bohnert et al., 1995; Bressan, 2001; Flowers and Colmer, 2008; Ozgur et al., 2013; Shabala and Mackay, 2011). Amongst the latter, the ability to secrete salt through specialized leaf structures termed salt glands is arguably one of the most remarkable features of halophytes, which is found in a large number of species from different families (Flowers et al., 2015; Yuan et al., 2016). One type of salt gland is the epidermal bladder cells (EBCs), which are modified trichomes (Shabala et al., 2014) of a spherical shape, typically with an average diameter of 1 mm and a cell volume of about 500 nL (Adams et al., 1998).

EBCs have long been suggested to play an important role in plant performance under saline conditions. Some suggested roles include (i) sequestration sites for excessive salt load; (ii) storage of metabolites; (iii) a secondary epidermis for protection against UV radiation; (iv) external water reservoirs and (v) a reservoir for reactive oxygen species (ROS)-scavenging metabolites and organic osmoprotectants (Adams et al., 1998; Adams et al., 1992; Agarie et al., 2007; Barkla and Vera-Estrella, 2015; Ibdah et al., 2002; Jou et al., 2007; Oh et al., 2015; Rygol et al., 1989; Steudle et al., 1975). However, most of these roles are postulations based solely on circumstantial evidence; they lack direct experimental evidence. Hence, the question as to whether EBCs are essential for salinity stress tolerance is not yet unequivocally answered.

To date, most studies on salt bladders were conducted on the inducible crassulacean acid metabolism (CAM) plant *Mesembryanthemum crystallinum*. The classical CAM physio-logical studies by Winter and co-authors in 1970s (e.g. (Winter, 1973) and the subsequent research have provided a significant conceptual advance in our understanding of various aspect of cell-specific regulation under saline conditions (Barkla and Vera-Estrella, 2015; Barkla et al., 2012; Oh et al., 2015). However, from both a physiological and biochemical point of view, *M. crystallinum* plants are unique and have some features (e.g. a transition from C3 to CAM metabolism under stress conditions and a pronounced succulency; (Adams

et al., 1998; Adams et al., 1992) that are rarely found in any crop species. When wild-type and *M. crystallinum* mutants lacking EBCs were confronted with salinity stress, the EBC mutant showed a significant impairment in seed yield. However, this impairment was not due to an inability of the bladderless mutant to sequester salt in EBC as, contrary to expectations, shoots of wild-type plants had approximately 1.5-fold higher Na^+ and Cl^- content than the mutant under saline conditions (Agarie et al., 2007). De facto, these findings questioned the role of EBC as an external storage space for the excess salt load. Thus, although extremely interesting, these observations do not prove a direct role for salt bladders as a component of the plant's salt tolerance mechanism. Moreover, given the previously mentioned unique physiological and anatomical features of *M. crystallinum*, it is rather difficult to translate these findings into breeding concepts for salt tolerance in traditional crops.

Over the last decade, our research has focused on *Chenopodium quinoa*. This recretohalophyte C3 species has become a pseudo-cereal plant of a high economic value. It possesses a combination of highly orchestrated physiological traits that confer its superior salinity stress tolerance (Adolf et al., 2013; Hariadi et al., 2010; Jacobsen, 2003; Shabala et al., 2014; Shabala et al., 2013). Moreover, the simple anatomy of the *C. quinoa* EBC complex makes it an ideal model for studying mechanism of salt sequestration in salt bladders (Shabala et al., 2014). Early studies have shown that quinoa plants rely on both external (salt bladders) and internal (mesophyll cell vacuoles) Na^+ sequestrations (Bonales-Alatorre et al., 2013). Younger plants with higher EBC density and underdeveloped vacuoles in mesophyll cells rely predominantly on bladder-based sequestration mechanisms, while old leaves retain Na^+ in the leaf cell vacuoles (Bonales-Alatorre et al., 2013). In this study, we used *C. quinoa* plants to provide direct evidence for a role of EBC in salinity stress tolerance. Our underlying working hypothesis was 2-fold. Firstly, we assumed that EBC operate as external Na^+ storage and their removal should increase the salt load in the leaf lamina, so affecting plant performance under saline conditions. Secondly, we hypothesized that EBC may preferentially accumulate certain metabolites that are known for their ability to modulate plant ionic relations. Indeed, it was shown earlier that some of so-called 'compatible solutes' could possess a strong ability to block ion channels mediating plant ionic homeostasis (e.g. the role of choline in vacuolar Na^+ sequestration, which originates from its

ability to block slow vacuolar channels; Pottosin et al. 2014, or improved K^+ retention in plant tissues treated with exogenous glycine betaine; Cuin and Shabala 2005). In addition, some compatible solutes also act as scavengers of reactive oxygen species (ROS; (Peshev et al., 2013; Smirnoff and Cumbes, 1989), so if accumulated in high concentrations, may potentially prevent ROS-induced changes in the activation of a broad range of Na^+, K^+ and Ca^{2+} permeable ion channels (see (Demidchik and Maathuis, 2007) for a review).

Here, we show that the removal of EBC results in a salt-sensitive growth phenotype. We also demonstrate that when exposed to salinity stress, *C. quinoa* undergoes a significant shift in its metabolite profile and that EBC removal impacts upon metabolite homeostasis in the leaf lamina. Comparing salt-induced metabolic and ionic changes, we discuss the transporters likely involved in ion sequestration in the EBC.

2.2 Materials and Methods

2.2.1 Plant materials and growth conditions

Three plant species, quinoa (*Chenopodium quinoa*), its close relative *Chenopodium album* and *Atriplex lentiformis* were used in this study. The quinoa seeds were a gift from Prof SE Jacobsen (University of Copenhagen, Denmark). Atriplex seeds were obtained from Wildseed Tasmania (Sorrel, Australia), and *C. album* seeds were obtained from Rühlemann's Kräuter & Duftpflanzen (Horstedt, Germany). Plants were grown from seed in 20 cm diameter pots filled with standard potting mix (Chen et al., 2007), under temperature-controlled glasshouse conditions (mean day/night temperatures 26/20 °C; humidity 65%; day length 15 h) at the University of Tasmania in Hobart, Australia, between November 2015 and March 2016. Ten seeds were sown in each pot and later thinned to leave four uniform plants per pot. Experiments were organized in a completely randomized design, with each treatment including at least four pots (with four plants in each). Of these six to eight uniform plants were later selected for sampling. All experiments were replicated three times and showed consistent results.

2.2.2 Experiments with intact plants (experiment 1)

Quinoa plants were grown for 5 weeks under control conditions. One day prior to the commencement of salinity stress, EBCs of all leaves were gently removed from

both sides of the leaf by using a soft cosmetic brush (Fig. 2.1A,B). In addition, all the EBCs were removed on the stem and petioles. Plants were then irrigated with 400 mM NaCl for 5 weeks (Fig. 2.1D). As new leaves emerged, EBCs were removed from the leaf surface and petioles on a regular basis (3–4 times per week) until the experiment was stopped and plants harvested for analysis (Fig. 2.1D). All lateral buds were also removed on a regular basis. Three types of measurements were conducted for both control and salt-treated plants: (1) non-brushed (intact) leaves (abbreviated here as NBr); (2) leaves that were brushed shortly before commencing the salt stress (abbreviated as Br) and (3) leaves that were not brushed during the salt exposure but from which EBCs were removed prior to elemental analysis (abbreviated as NBr-Br) (Fig. 2.1D).

2.2.3 Experiment with decapitated plants (experiment 2)

Plants were grown until seven-leaf stage under control conditions prior to commencement of treatments (~5 weeks for *C. quinoa* and *C. album* and ~8 weeks for *A. lentiformis*). At the seven-leaf stage, the shoot apex was excised (chopped off), leaving six leaves remaining on the plant's shoot (Fig. 2.1C). Then, the EBCs of all the remaining leaves were gently brushed from both the upper and lower surfaces of leaves by using a soft cosmetic brush (Fig. 2.1B). Salinity stress was then imposed as described in the earlier section, and all the emerging lateral buds were removed on a regular basis, keeping the number of leaves constant during the entire experiment.

2.2.4 Physiological assessment

The fresh weight (FW) of the shoot biomass was determined immediately after harvest. Dry weights (DW) of the plants were measured after drying the plants in an oven at 65 °C for 72 h. Leaf chlorophyll content was measured (in arbitrary units) by the Minolta Special Products Analysis Division (SPAD)-502 meter (Konica Minolta Sensing, Tokyo, Japan). Net CO_2 assimilation (Pn) and stomatal conductance (Gs) were measured by using the LiCor 6400 gas exchange system (Lincoln, NE, USA) under full sunlight (around mid-day) under glasshouse conditions. All measurements were carried out on the mid-portion part of the topmost leaves in chopped plants and on the young fully expanded leaves in non-chopped plants. For plant nutrient analysis, two types of measurements were

conducted. In the first, approximately 0.1 g of dry matter was added to 7 mL of nitric acid and microwave-digested for 40 min. The digested material was diluted to a final volume of 15 mL, and leaf Na^+ and K^+ content was measured by using Flame Photometer (PFP7, Jenway, UK). In the second set of measurements, a freeze–thaw method (Cuin et al., 2009) was used. Appropriate leaves were collected, placed in Eppendorf tubes and immediately placed in a -18°C freezer. Before measurement, the samples were thawed and hand-squeezed to extract all the sap. The collected sample was thoroughly mix and measured for its K^+ and Na^+ concentration (in mM per water basis) by using flame photometry as described earlier. Chloride concentration in the squeezed samples was measured by using Cl^- selective microelectrodes using the Microelectrode Ion Flux Estimation (MIFE) system (see details in the succeeding texts).

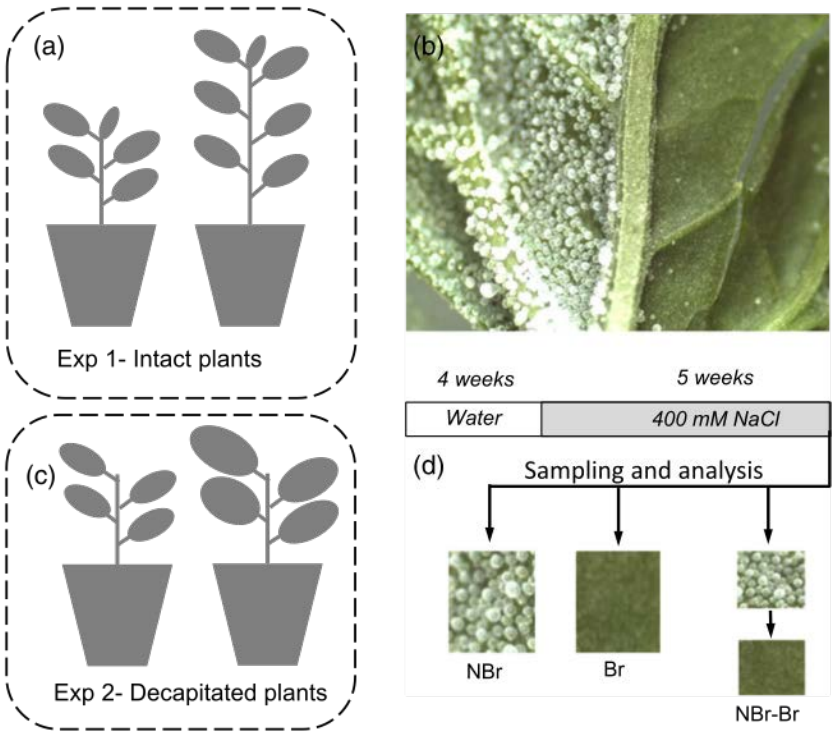

Fig. 2.1 Details of experimental design used in this study. Br – brushed leaves; NBr – non-brushed leaves; NBr-Br – leaves that were non-brushed during salt exposure but from which EBCs were removed prior to elemental analysis. (a and c) Cartoons illustrating two types of experiments conducted (on intact and decapitated plants, accordingly). (b) *Chenopodium quinoa* leaf with EBC removed from one half of the leaf. (d) A summary of treatment and sampling protocols. The scale bar in is 1 mm.

To determine the variability of physiological measurements, the experimental data were subjected to analysis of variance (SAS Institute, Cary, NC, USA). The least significant difference (LSD) at P = 0.05 probability level was used to compare means between the treatments.

2.2.5 Metabolite extraction

For each sample, approximately 100 mg of leaf was harvested and immediately frozen in liquid nitrogen and stored at 80°C until freeze-drying, which was carried out using Alpha 1–2 LD plus (Martin Christ, Osterode, Germany). Aliquots(10 mg) of homogenized, freeze-dried leaf material were transferred to Eppendorf tubes and accurate weights were recorded. Methanol (MeOH, 500 µL) containing the internal standards (D-Sorbitol-13C6 (0.02 mg/mL) and L-Valine-13C5,15 N (0.02 mg/mL), Sigma Aldrich (Australia)] was added to the sample tubes. The samples were vortexed, then incubated in a Thermomixer at 70°C with a mixing speed of 850 rpm for 15 min, followed by a 15 min centrifugation at 13,000 rpm (15, 900 x g). The MeOH supernatant was transferred into a 1.5 mL Eppendorf tube and set aside. Water (500 µL, Milli Q grade) was added to the remaining sample pellet and vortexed before being centrifuged for 15 min at 13,000 rpm (15, 900 g). The supernatant was removed and combined with the MeOH supernatant (supernatant 'A'). This supernatant was used for gas chromatography–mass spectrometry (GC–MS) untargeted and targeted analysis.

2.2.6 Derivatization for GC–MS analysis

Derivatization for GC–MS analysis was carried out as described in Dias et al. (Dias et al., 2015). The derived sample was then left for 1 h before 1 µL was injected onto the GC column using a hot needle technique. Splitless and split (1:10) injections were performed for each sample.

2.2.7 Untargeted GC–MS analysis

Untargeted GC–MS analysis and data analysis were carried out as described in Hill et al. (2015).

2.2.8 Quantification of sucrose and inositol using GC–MS

An aliquot of supernatant 'A' was further diluted 10-fold with 50% MeOH, and aliquots of 100 µL from the 10-fold diluted supernatant were transferred to clean

Eppendorf tubes and dried under vacuum by using a Rotational Vacuum Concentrator (RVC 2-33 CD plus, John Morris Scientific, Pty Ltd, Melbourne, Australia). Sucrose and inositol were quantified as described in Dias et al. (2015). Calculated concentrations (concentrations based on response of standards and their expected concentrations) were exported, and the final concentrations were expressed in mM on a FW basis.

2.2.9 Quantification of gamma-aminobutyric acid and proline using liquid chromatography–mass spectrometry

Quantification of gamma-aminobutyric acid (GABA) and proline was performed as described in Boughton et al. (Boughton et al., 2011). Calculated concentrations (concentrations based on response of standards and their expected concentrations) were exported, and the final concentrations were expressed in mM on a FW basis.

2.2.10 Statistical and further data analysis

Statistical analysis (Student's t-test including Benjamini–Hochberg False Discovery Rate correction, Partial Least Square Discriminant Analysis (PLSDA) and heat map in combination with hierarchical cluster analysis) of untargeted GC–MS was generated through the web-based, open-source metabolomic data analysis tool Metabo Analyst version 3.0. To generate PLSDA score plots, area responses for all features detected are normalized to the FW and internal standard before uploading into Metabo Analyst. Normalized responses were log10 transformed to achieve normal distribution. The 2-D PLSDA scores plot (Fig. 2.7A) were performed based on the sample group information provided and selected PC component 1 and component 2. Heat maps were generated from GC–MS data (Fig. 2.7B).

GC–MS untargeted data were mapped on an author-created metabolite network of the primary metabolism via the built-in graph editor in VANTED (http://vanted.ipk-gatersleben.de/) (Junker et al., 2006). The bar charts indicate relative response per metabolite from control non-brushed and salt-treated non-brushed leaves (Fig. 2.6).

2.2.11 MIFE electrophysiology

Net ion fluxes were measured from quinoa leaf mesophyll and stalk cells by using the Microelectrode Ion Flux Estimation (MIFE, University of Tasmania, Hobart,

Australia) technique. The full details on the principles and methods of this technique are available in our previous publications (Chen et al., 2007; Shabala et al., 2006). Commercially available liquid ion exchangers K^+, Na^+ and Cl^- cocktails were used (catalogue numbers 60031, 71747 and 24902, respectively, all from Sigma-Aldrich, St Louis, MO, USA). Youngest fully mature quinoa leaves were harvested from 5-week-old plants, grown under ambient light in a temperature-controlled glasshouse (between 19°C and 26°C and average humidity of approximately 65%) at the University of Tasmania. Seeds were sown in 2 L plastic pots filled with standard potting mix and irrigated with either water (for mesophyll measurements) or 100 mM NaCl (for stalk cell measurements).

For K^+ flux measurements in the mesophyll, the abaxial epidermis of youngest fully mature quinoa leaves was removed by using fine tweezers, and leaf segments of ~5–8 mm were cut and left floating (peeled side down) overnight in buffered Tris/MES basal salt medium (BSM: 0.5 mM KCl, 0.1 mM $CaCl_2$, pH 5.5) solution to eliminate possible confounding wounding effects. The following day, leaf segments were immobilized in the measuring chamber containing either 4 mL of buffered Tris/MES BSM or 4 mL of buffered Tris/MES BSM with the addition of 8 mM sucrose for 1.5 h prior to the measurements. Ion fluxes were measured under control conditions for 5 min, and then the hydroxyl-radical generating (Demidchik, 2003) Cu/ascorbate mixture (0.1/0.3 mM) was applied by pipetting and mixing the required volume of stock solutions into the bathing solution.

For Cl^- and Na^+ flux measurements in stalk cells, the petioles of youngest fully mature quinoa leaves were excised and immobilized in the measuring chamber containing 4 mL of BSM (0.5 mM KCl, 0.1 mM $CaCl_2$, pH 5.5) for 1.5 h prior to measurement. Ion fluxes were then measured under control conditions for 5 min, then 5 mM GABA was applied by pipetting and mixing the required volume of stock solutions into the bathing solution. For mock controls, the same amount of BSM solution was added to the chamber.

2.3 Results

Gentle removal of EBC does not affect the physiology and biochemistry of quinoa plants.

To study the role of epidermal bladder cells in salt tolerance of *C. quinoa* plants, these trichome-like structures were removed with a soft cosmetic brush.

Such a mechanical disturbance to plant tissues could activate a broad array of mechano-sensing channels (Monshausen and Haswell, 2013), thus potentially result in significant changes in the growth patterns of plant organs by the process termed thigmo-morphogenesis (Coutand, 2010).

Nonetheless, in our hands and in the absence of salt stress, removal of EBC by a gentle brushing did not result in any obvious growth phenotype (Fig. 2.2A,B). Both brushed and non-brushed plants had the same FW and dry weight (DW) (Fig. 2.2C). While non-brushed plants had slightly a greener appearance to the naked eye (Fig. 2.2B), there was no significant (at $P < 0.05$) difference in the leaf chlorophyll content between treatments (measured as SPAD value; Fig. 2.2D). In addition, similar between brushed and non-brushed leaves ($P > 0.05$) were net CO_2 assimilation rates (Pn; Fig. 2.2F) and stomatal conductance (Gs; Fig. 2.2G). Thus, the previously mentioned visual difference is most likely explained by different light reflective properties of the leaf surface (albedo effect) due solely to the presence or absence of bladder cells. We also compared leaf K^+ content between treatments. No statistically significant difference in leaf content was found between brushed and non-brushed leaves (Fig. 2.2E) for this major cationic osmolyte. To study brushing effects on the leaf metabolism, we monitored the metabolic profiles by using GC–MS (Table S2.1 in the Supporting Information) but did not find significantly ($P < 0.05$) altered levels of amino acids, sugars or sugar alcohols. Thus, the unique anatomy of the epidermis–stalk cell–EBC complex (Fig. S2.1 in the Supporting Information) of predetermined breaking zone/junction allows EBC to be removed without the bulk of leaf being disturbed. Therefore, under control conditions, the removal of salt bladders by gentle brushing of the leaf surface seems not to induce any damage or cause thigmo-morphogenetic effects.

As a ‘negative control’ and in order to ensure sensitivity of the metabolite profiling method, we also removed EBC in more ‘cruel ways’ by rubbing the leaf surface with fingers. Such removal does result in an altered plant phenotype (Fig. S2.2), with brushed plants being more stunted and having (Fig. S2.2A) smaller leaves (Fig. S2.2B). None of these plants were used in further studies.

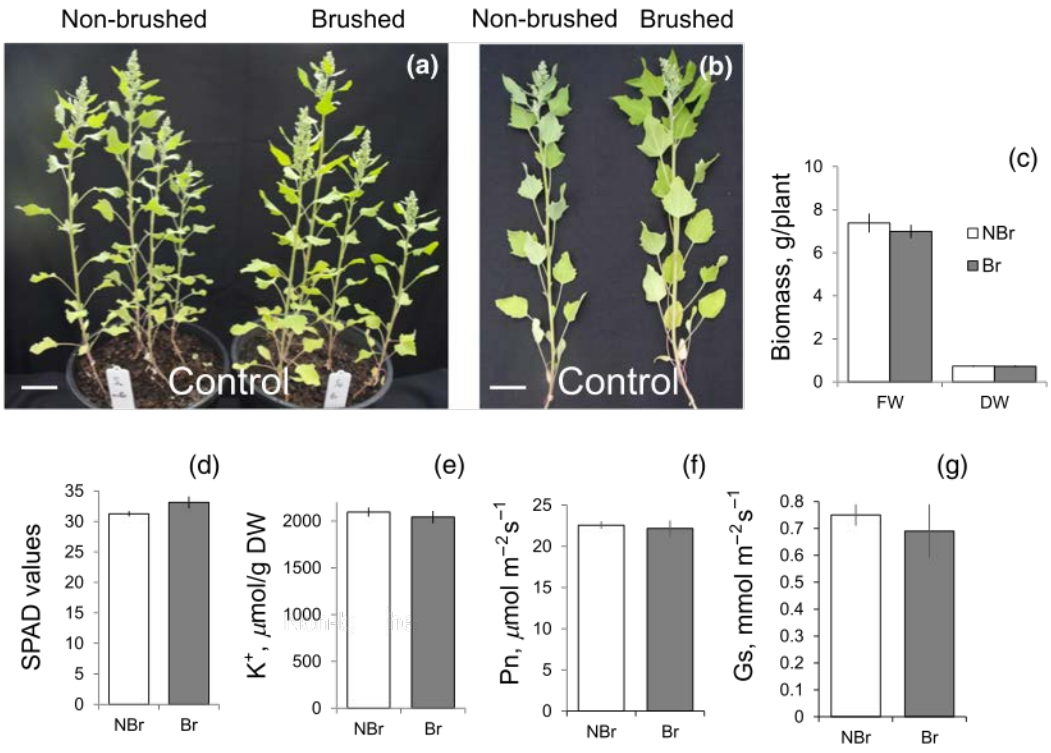

Fig. 2.2 The gentle removal of EBC does not alter plant phenotype (a and b) or have any significant impact on its agronomical or physiological characteristics in *Chenopodium quinoa* plants grown under control conditions. (c) Shoot fresh (FW) and dry (DW) weigh; (d) chlorophyll content (SPAD readings); (e) leaf K^+ content; (f) net CO_2 assimilation, Pn; and (g) stomatal conductance, Gs. Data are mean ± SE (n = 5 to 8). The scale bar is 5 cm.

2.3.1 Removal of EBC results in a salt-sensitive phenotype

The effect of gentle brushing became visible, however, for plants grown under saline (400 mM NaCl for 5 weeks) conditions (Fig. 2.3), showing significantly ($P < 0.05$) smaller biomass (Fig. 2.3C).

We then looked at how the presence of EBC affects the accumulation of Na^+, K^+ and Cl^- in the leaf lamina. To do this, we brushed EBC (containing accumulated salt) off salt-grown plants immediately prior to analysis (abbreviated as NBr-Br in Fig. 2.3) and compared Na^+, K^+ and Cl^- contents in the leaf lamina with those where EBCs were removed prior to the imposition of salinity stress (Br treatment). Our working hypothesis was that NBr-Br leaves should have less Na^+ and Cl^- (the two components of salt) accumulated in leaf lamina as they possessed the capability to sequester a large part of the salt load into EBC during plant growth. Indeed, this appeared to be true; plants that had EBC during exposure to salinity

accumulated only ~60% of both Na^+ and Cl^- in their leaf lamina compared with plants from which EBC were removed before NaCl treatment (Fig. 2.3D,E). Brushed plants also had nearly 50% lower potassium content in leaves compared with non-brushed counterparts (Fig. 2.3F). This suggests that about 50% of the total K^+ and 40% Na^+ and Cl^- taken up by leaves are stored in EBC.

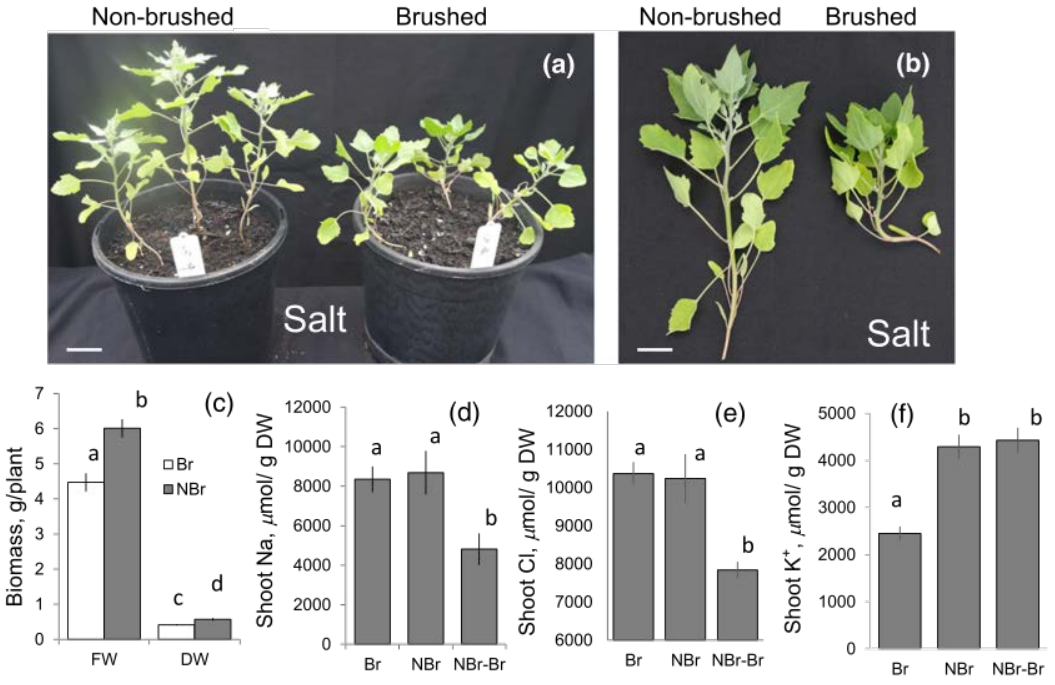

Fig. 2.3 Removal of EBC from salt-grown *Chenopodium quinoa* plants results in a salt-sensitive phenotype (a–c) and has a major impact on ionic relations in leaf lamina. (a and b) Typical images of brushed (Br; with EBC removed prior to salt stress onset) and intact (non-brushed; NBr) quinoa plants grown for 5 weeks at 400 mM NaCl. (c) Shoot fresh (FW) and dry (DW) weight, (d) leaf Na^+ content and (e) leaf sap K^+ concentration. Data are mean ± SE (n = 5 to 8). Data labelled with different lowercase letters are significantly different at $P < 0.05$. The scale bar is 5 cm.

Next, we tested how does the plant responds when either the bladders were removed from developing leaves or when we prevented the generation of new, growing young leaves. The rationale behind this study was that in intact plants, the removal of EBC might potentially impact upon formation and development of new leaves; in decapitated plants, this developmental aspect was eliminated. To answer this question, the shoot apex from 4-week-old plants was removed to have just a fixed number of leaves (Fig. 2.2C). Brushing of EBC under saline conditions again

resulted in a salt-sensitive phenotype (Fig. 2.4A), with both FW and DW and leaf surface area being significantly bigger in non-brushed plants (Fig. 2.4B-D). Similar to the trend with plants possessing an apex, we found that bladder-free individuals accumulated ~410 mM Na^+ in the leaf lamina compared with only 270 mM in those allowed to have EBC operating as salt dumps (e.g. 30% increase; Fig. 2.4E).

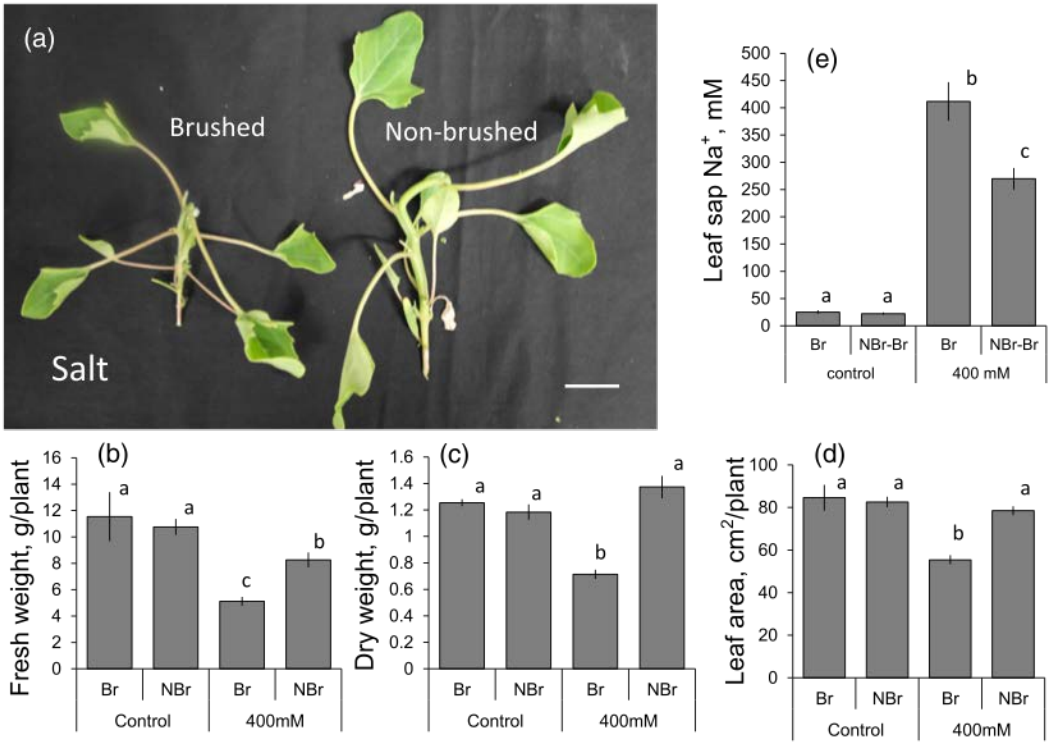

Fig. 2.4 Salt-sensitive phenotype resulting from the gentle removal of EBC from leaves of decapitated *Chenopodium quinoa* plants (in which shoot apex was removed to have just a fixed number of leaves). (a) Typical images of brushed and non-brushed plants, shoot fresh (b) and dry (c) weight of control and salt-grown plants, (d) leaf surface area and (e) leaf sap Na^+ content. Data are mean ± SE (n = 5 to 8). Data labelled with different lowercase letters are significantly different at $P < 0.05$. The scale bar is 5 cm.

To confirm the role of bladders, we performed brushing experiments with another halophyte species that has rather dense EBC (Fig. S2.3), *Atriplex lentiformis*. As with *C. quinoa* observations, removal of EBC resulted in a salt-sensitive phenotype in *A. lentiformis* (Fig. 2.5A-C), with brushed plants accumulating more Na^+ (Fig. 2.5E) and having reduced biomass under saline conditions (Fig. 2.5D). As a negative bladder control, we used *C. album*, a close relative of *C. quinoa*. The ecotype we selected had very few EBC on the leaf surface

(and only in very young leaves; Fig. S2.3), thus cannot rely on Na^+ sequestration in EBC as a dominant tolerance mechanism. As expected, brushing of the leaf surface of bladderless *C. album* did not result in a salt-sensitive phenotype (Fig. S2.4A,B), and no significant (at $P < 0.05$) difference in leaf Na^+ content was observed between brushed and non-brushed plants (Fig. S2.4C).

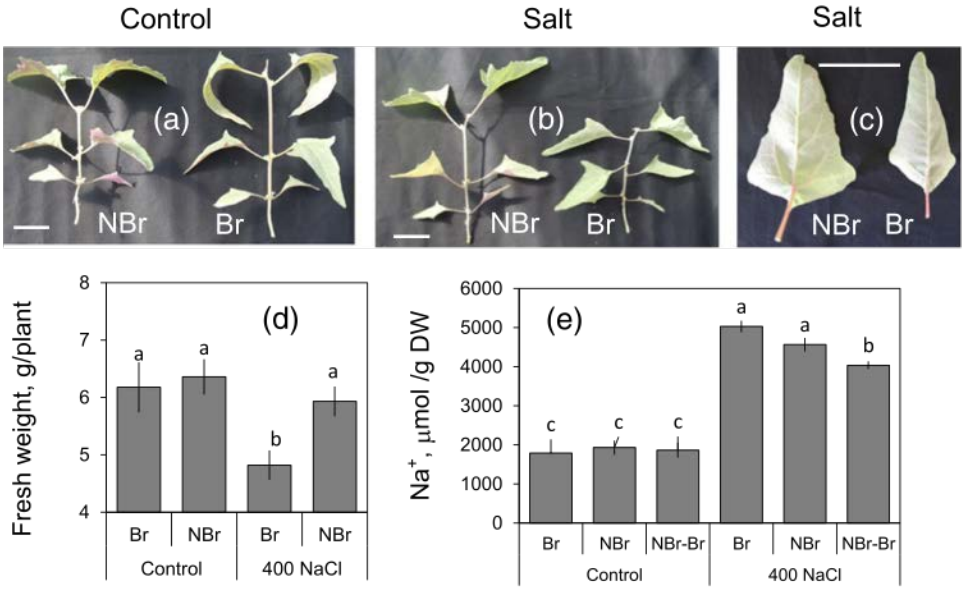

Fig. 2.5 Effect of EBC removal on growth and physiological characteristics of *Atriplex lentiformis* plants. (a–c) Typical images of brushed and non-brushed plants grown under control and salt conditions. (d) Shoot fresh weight; (e) leaf Na^+ content. Br – brushed leaves; NBr – non-brushed leaves; NBr-Br – leaves that were non-brushed during the salt exposure but from which EBC were removed prior to elemental analysis. Data are mean ± SE (n = 5 to 8). Data labelled with different lowercase letters are significantly different at $P < 0.05$.

2.3.2 Salinity induces pronounced changes in leaf metabolic profile

Salt-grown plants need to adjust osmotically to hyperosmotic conditions. Under such a scenario, salt tolerant plants take up salt and store it in the vacuole. Thus, we hypothesized that they will also need to synthesize metabolites to serve as compatible solutes that would compensate in the cytoplasm for the rise in vacuole osmolality due to the increased Na^+ and Cl^-. Using GC–MS, we analysed the salt and bladder-dependent change in *C. quinoa* leaves. We detected 91 metabolites in leaves with EBC, grown in control and salt treatments (Table 2.1; Fig. 2.6). Of these, more than half of the metabolites (50) were statistically significantly affected

upon salt treatment (based on Student's t-test $P < 0.05$), while 46 remained significant following False Discovery Rate correction using the Benjamin–Hochberg method (Chong et al., 2015). Among them, six amino acids, 11 organic acids, 13 sugars and sugar alcohols and 17 unidentified metabolites were significantly changed. Most amino acids such as proline (16.79-fold), glycine (8.38-fold), phenylalanine (4.09-fold), serine (3.51-fold) and glutamate (1.59-fold) were significantly increased. Aspartate was the only amino acid that decreased (8.26-fold). Interestingly, apart from succinate and nicotinate, which did not significantly change, 10 organic acids significantly decreased (between 32.78-fold and 1.71-fold) and with only one (mucic/saccharate) being increased (1.99-fold). Three sugars increased, threitol (2.36-fold), rhamnose (1.52-fold) and inositol (1.61-fold). Three sugar acids and one sugar alcohol decreased, erythronate (1.67-fold), threonate (4.13-fold), galactonate (2.54-fold) and arabitol (1.65-fold). Two sugar phosphates decreased, glucose-6-phosphate (5.34-fold) and fructose-6-phosphate (3.59-fold). There were also significant decrease in primary sugars including xylose (3.60-fold), maltose (6.37-fold), glucose (13.80-fold) and sucrose (1.93-fold). In addition, monomethylphosphate (7.76-fold) and cytosine (1.74-fold) significantly decreased (Table 2.1).

2.3.3 Removal of EBC affects plant metabolic adaptation to salinity

Removal of EBC of plants grown in control conditions did not alter the metabolite profile (Table S2.1). When the metabolic profile of salt-grown bladderless leaves was compared with their bladder-bearing counterparts, pronounced differences were observed (Table S2.2 and Fig. 2.7A,B). Using GC–MS, we identified 11 known and 5 unknown metabolites, which were significantly different in salt-treated leaves with EBC removed (Table S2.2) compared with salt-treated intact leaves. Interestingly, all significantly changed metabolites decreased in leaves with EBC removed, which we confirmed with quantitative GC–MS and liquid chromatography (LC)–MS assays: GABA content dropped from 1.5 ± 0.199 to 0.5 ± 0.17 mM (–3-fold), proline and inositol from 2.75 ± 0.13 to 1.3 ± 0.26 mM (–2.12-fold) and from 0.31 ± 0.3 to 0.25 ± 0.05 mM (–1.24-fold), respectively.

Table 2.1 Comparison of GC–MS untargeted metabolite profiles of non-brushed leaves with and without salinity treatment

	Control NBr		Salt NBr	
Organic acids	x-fold	SEM	x-fold	SEM
4_hydroxy cinnamic acid	1.000	±0.183	**−3.404**	**±0.201**
Ascorbic acid/Iso ascorbic	1.000	±0.240	**−4.637**	**±0.172**
Benzoate	1.000	±0.141	**−1.708**	**±0.061**
Citrate	1.000	±0.266	**−3.626**	**±0.235**
Glycerate	1.000	±0.097	**−2.010**	**±0.022**
Fumarate	1.000	±0.152	**−4.915**	**±0.248**
Malate	1.000	±0.142	**−3.147**	**±0.176**
Mucic/saccharic	1.000	±0.142	**1.998**	**±0.118**
Nicotinic acid	1.000	±0.185	−1.675	±0.195
Oxalate	1.000	±0.567	**−32.783**	**±0.271**
Pantothenic acid	1.000	±0.134	**−7.667**	**±0.044**
Pyroglutamate	1.000	±0.317	1.459	±0.178
Succinate	1.000	±0.152	−1.895	±0.245
Threonate-1,4-lactone	1.000	±0.178	**−2.299**	**±0.144**
Sugars and sugar alcohols	x-fold	SEM	x-fold	SEM
Arabinose	1.000	±0.078	1.015	±0.361
Arabitol	1.000	±0.140	**−1.650**	**±0.127**
Erythronate	1.000	±0.066	**−1.665**	**±0.048**
Fructose	1.000	±0.165	1.772	±0.482
Fructose-6-P	1.000	±0.190	**−3.587**	**±0.258**
Galactitol	1.000	±0.138	1.042	±0.084
Galactonate	1.000	±0.177	**−2.539**	**±0.070**
Galactose	1.000	±0.122	1.409	±0.548
Glucose	1.000	±0.313	**−13.796**	**±0.442**
Glycerol-3-P	1.000	±0.139	−1.819	±0.277
Glucose-6-P	1.000	±0.197	**−5.336**	**±0.100**
Inositol	1.000	±0.043	**1.605**	**±0.066**
Inositol	1.000	±0.036	**1.611**	**±0.064**
Maltose	1.000	±0.124	**−6.374**	**±0.169**
Rhamnose	1.000	±0.097	**1.519**	**±0.067**
Ribonate	1.000	±0.371	−1.456	±0.168
Ribose	1.000	±0.072	2.000	±0.431
Sucrose	1.000	±0.035	**−1.927**	**±0.147**
Threitol	1.000	±0.184	**2.366**	**±0.082**
Threonate	1.000	±0.193	**−4.137**	**±0.180**
Trehalose	1.000	±0.220	−1.347	±0.079
Xylose	1.000	±0.156	**−3.602**	**±0.093**
Others	x-fold	SEM	x-fold	SEM
Monomethylphosphate	1.000	±0.259	**−7.757**	**±0.350**
Cytosine	1.000	±0.177	**−1.742**	**±0.047**
Diethylene_glycol	1.000	±0.313	−1.559	±0.165
Phosphate	1.000	±0.199	−1.297	±0.144
Amino acids and amines	x-fold	SEM	x-fold	SEM
Aspartate	1.000	±0.154	**−8.260**	**±0.158**
Ethanolamine	1.000	±0.212	2.567	±0.329
GABA	1.000	±0.378	−1.523	±0.335
Glutamate	1.000	±0.226	**1.588**	**±0.105**
Glycine	1.000	±0.117	**8.283**	**±0.085**
Isoleucine	1.000	±0.295	−1.254	±0.243
Phenylalanine	1.000	±0.329	**4.098**	**±0.276**
Proline	1.000	±0.261	**16.792**	**±0.185**
Serine	1.000	±0.160	**3.511**	**±0.081**
Threonine	1.000	±0.322	2.002	±0.168
Tyrosine	1.000	±0.433	1.643	±0.220
Valine	1.000	±0.239	−1.249	±0.425
UNKNOWNS	x-fold	SEM	x-fold	SEM
UN_2_276_13.279	1.000	±0.229	−1.657	±0.102
UN_3_205_13.816	1.000	±0.382	−2.702	±0.158

(*Continues*)

Table 2.1 continued

	Control NBr		Salt NBr	
Organic acids	x-fold	SEM	x-fold	SEM
UN_4_262_14.466	1.000	±0.050	−1.026	±0.353
UN_6_306_16.105	1.000	±0.095	**1.728**	**±0.055**
UN_7_306_16.255	1.000	±0.092	1.113	±0.038
UN_8_292_16.499?	1.000	±0.151	**−9.271**	**±0.101**
UN_9_204_18.259	1.000	±0.136	**−2.080**	**±0.230**
UN_10_217_18.860	1.000	±0.403	**−3.342**	**±0.196**
UN_11_292_19.232	1.000	±0.125	**−1.767**	**±0.144**
UN_12_275_20.337	1.000	±0.086	**−1.898**	**±0.023**
UN_13_285_20.524	1.000	±0.367	−1.635	±0.211
UN_14_275_20.752	1.000	±0.161	1.287	±0.091
UN_15_273_21.216	1.000	±0.095	**−14.250**	**±0.331**
UN_16_361_21.963	1.000	±0.433	**−15.054**	**±0.404**
UN_17_174_23.147	1.000	±0.181	**−2.802**	**±0.109**
UN_18_319_23.921	1.000	±0.074	**−9.420**	**±0.041**
UN_19_445_25.068	1.000	±0.166	**−3.338**	**±0.114**
UN_20_204_25.590	1.000	±0.214	**−4.366**	**±0.148**
UN_21_290_26.044	1.000	±0.088	**−4.665**	**±0.064**
UN_22_318_27.667	1.000	±0.174	1.389	±0.297
UN_23_321_28.613	1.000	±0.073	**−1.508**	**±0.023**
UN_24_191_29.266	1.000	±0.211	1.157	±0.078
UN_25_204_30.286	1.000	±0.056	−1.048	±0.048
UN_26_328_31.254	1.000	±0.122	**−6.257**	**±0.126**
UN_27_318_31.709	1.000	±0.159	**−2.158**	**±0.057**
UN_31_297_33.138	1.000	±0.158	1.387	±0.123
UN_32_327_33.739	1.000	±0.197	−1.613	±0.180
UN_33_647_35.483	1.000	±0.284	**−4.125**	**±0.307**
UN_154_7.967	1.000	±0.418	−1.548	±0.255
UN_14_275_20.752	1.000	±0.134	1.418	±0.086
UN_18.033	1.000	±0.118	1.083	±0.047

CNB = control non-brushed; TNB = treated non-brushed. Data are presented as x-fold with CNB set to 1 (n = 5). The blue cells indicate statistical significance determined with Student's t-test (P > 0.05), and the green cells indicate statistical significance following Benjamin– Hochberg False Discovery Rate correction.

At the same time, the sucrose content increased from 0.27 ± 0.01 mM in samples with EBC to 0.86 ± 0.27 mM (3.19-fold). Besides the latter metabolites, GC–MS analysis revealed relative changes for another amino acid; aspartate (–2.82-fold), four organic acids; citrate (–2.59-fold), glycolate (–1.72-fold), oxalate (–6.25- fold) and threonate (–3.68-fold). Only two sugar phosphates decreased; glycerol-3-phosphate (–2.28-fold) and inositol-1- phosphate (–2.17-fold). Threitol was the only sugar that increased in salt-treated leaves with EBC removed compared with intact salt-treated leaves (1.77-fold). There was also a decrease of kampferol (0.33-fold) and uracil (0.29-fold).

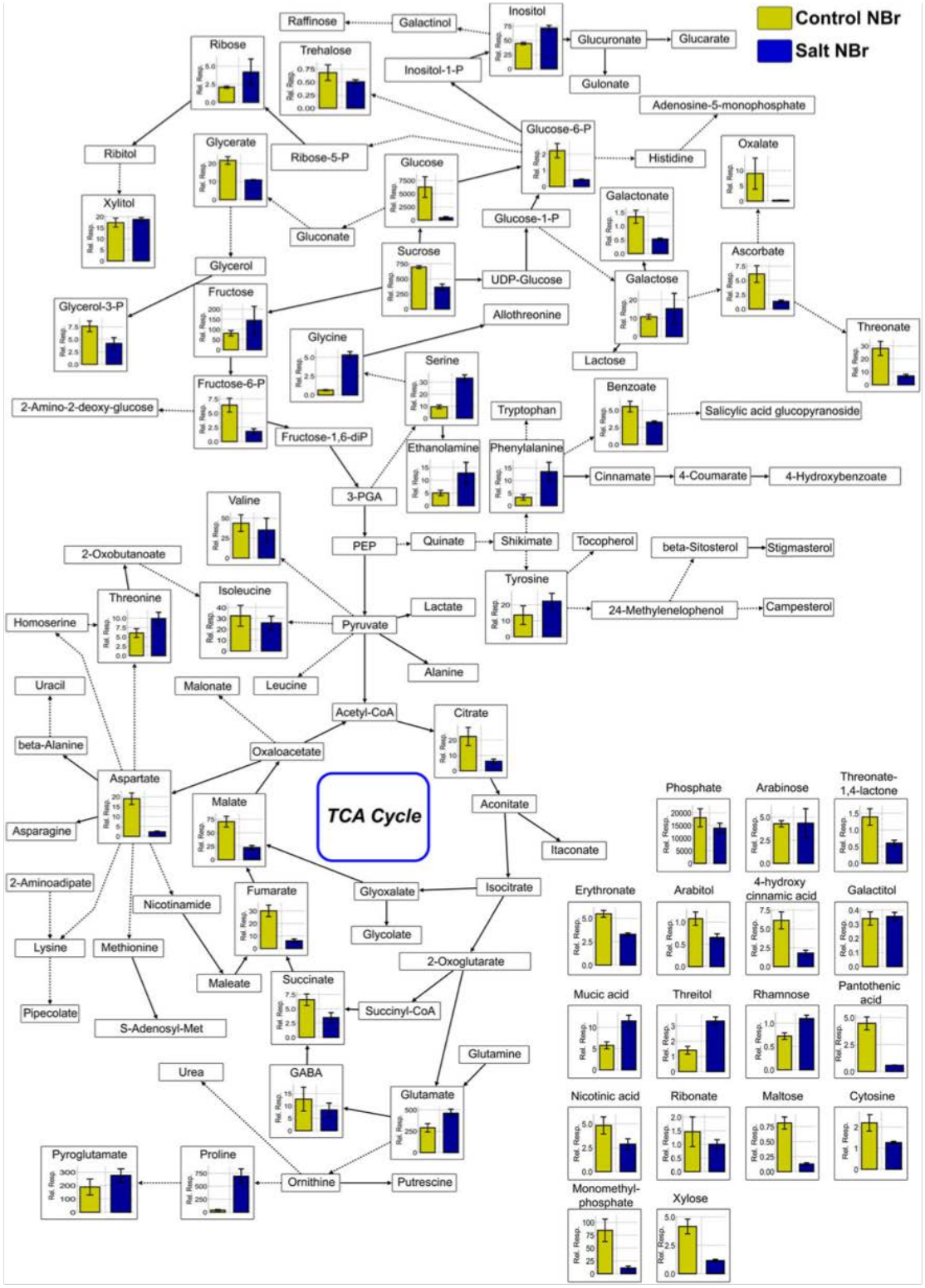

Fig. 2.6 Pathway map of metabolite differences between control and salt-treated intact quinoa leaves (with EBC present). Metabolic pathway and graphs were created using VANTED (Junker et al., 2006). The bars represent control (green) and salt treated (blue) (n = 5).

PLSDA and unsupervised Hierarchical Cluster Analysis (HCA) combined with Heat Map Analysis are routinely used methods for visualization of metabolite profiling data and were applied to our samples to ascertain the overall patterns of metabolite profiles as determined with untargeted GC–MS (Fig. 2.7A,B). An analysis of GC–MS data revealed a clear separation between intact salt-treated leaves and salt-treated leaves with EBC removed. The score plots (Fig. 2.7A) also demonstrate that following the removal of EBC, the biological variation of metabolite levels is much higher, indicated by a larger distribution of samples within the PLSDA plot, while the biological variation of metabolite levels of intact leaves is relatively smaller, as demonstrated by a more stringent clustering. HCA combined with Heat Map Analysis also revealed a clear separation between salt-treated intact leaves and salt-treated leaves with EBC removed (Fig. 2.7A).

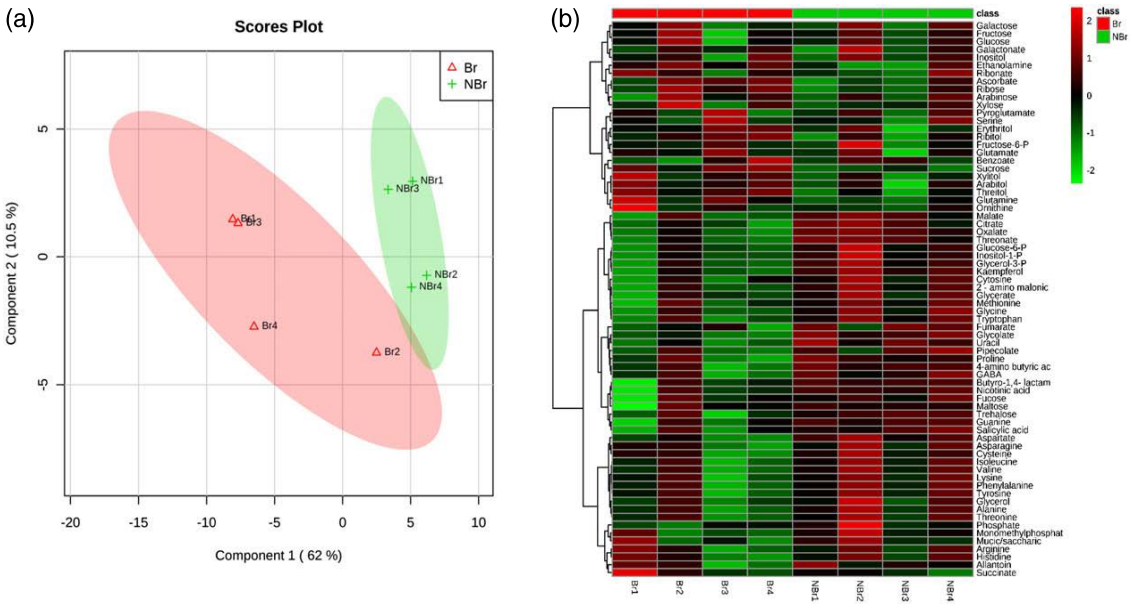

Fig. 2.7 Partial Least Square Discriminant Analysis (a) and Hierarchical Cluster Analysis combined with heatmap analysis (b) of untargeted GC–MS of salt-treated quinoa leaves with EBC present (non-brushed) and EBC removed (brushed). The shaded circles in Panel A indicate a 95% confidence level.

2.3.4 GABA and sucrose modulate ion transport across mesophyll and stalk cell plasma membrane

We next attempted to establish a causal relationship between the observed changes in a leaf metabolic profile and the plant ionic relations. Accordingly, we

hypothesized that changes in some of the previously mentioned metabolite concentrations caused by brushing may be essential for controlling transport of ions across the cellular membranes of the leaf mesophyll and thus in the maintenance of cytosolic K^+/Na^+ homeostasis. We tested this hypothesis by measuring the ability of mesophyll cells to retain K^+ upon exposure to oxidative stress (associated with salinity – in both glycophytes (Mittler et al., 2011) and halophytes (Bose et al., 2014). The addition of the hydroxyl radical-generating Cu/ascorbate mix to the leaf mesophyll resulted in a massive K^+ efflux across the plasma membrane (Fig. 2.8A, open symbols). Pre-treating leaves with exogenously applied 8 mM sucrose (mimicking the increase in sucrose levels in brushed cells) completely mitigated this ROS-induced K^+ efflux (Fig. 2.8A,B) so potentially improving the cytosolic K^+/Na^+ ratio.

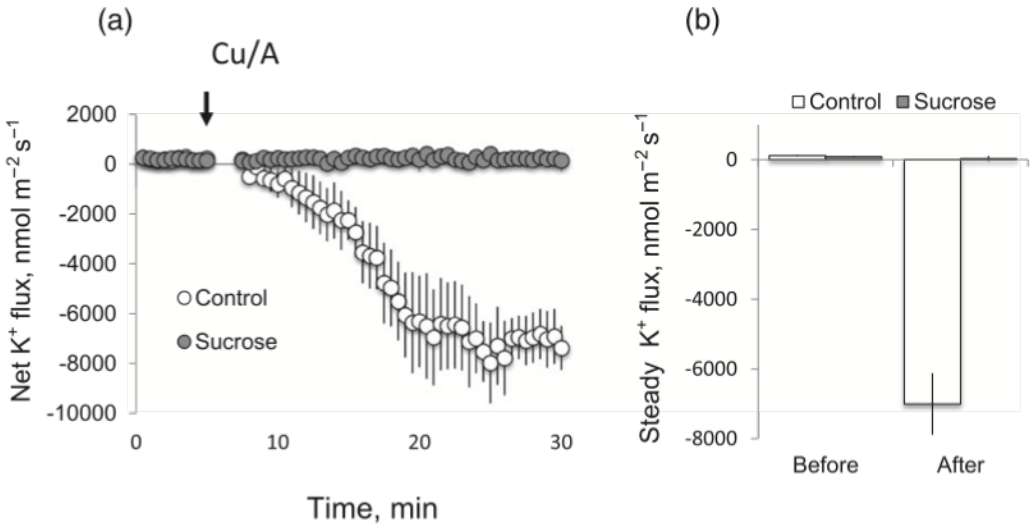

Fig. 2.8 Effect of sucrose on K^+ retention in quinoa leaf mesophyll exposed to ROS. (a) Hydroxyl radical-induced transient net K^+ flux kinetics measured from mesophyll cells pre-treated with 8 mM of sucrose for 1.5 h prior to onset of oxidative stress. Hydroxyl radicals were generated by applying 0.1/0.3 mM Cu/ascorbate mix (see Demidchik et al. 2003 for details). The sign convention is 'efflux negative'. Values are mean ± SE (n = 10). (b) Steady state K^+ fluxes in mesophyll tissues of quinoa leaves before and after (30 min) the addition of Cu/ascorbate mix. Values are mean ± SE (n = 10). *Significant at $P < 0.001$.

We then studied the effect of GABA on ion loading into EBC by looking at its impact on Na^+ and Cl^- transport from the stalk cells (Fig. 2.9). In salt-grown

plants, a substantial Na^+ and Cl^- efflux (of about 700 and 1500 nmol m^{-2} s^{-1}, respectively) was measured from the stalk cell under steady conditions before GABA treatment (Fig. 2.9A,C). Application of 5 mM GABA significantly reduced this efflux by about 25% for Na^+ and 50% for Cl^- (Fig. 2.9B,D; both significant at $P < 0.05$). No such changes were measured in mock controls when the equivalent amount of BSM solution was added to the bath instead of GABA (Fig. 2.9).

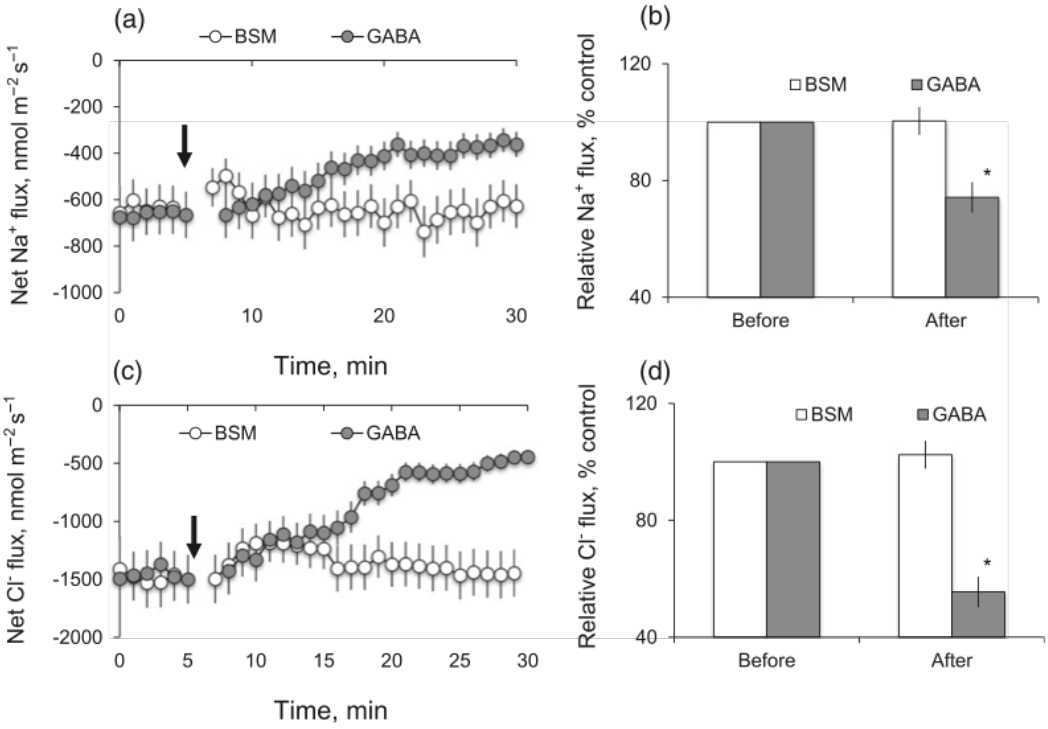

Fig. 2.9 Effect of GABA on Na^+ and Cl^- efflux from the stalk cells in quinoa. (a) A representative transient net Na^+ flux from the stalk cells from plants germinated and grown in the presence of 100 mM NaCl. (b) Relative Na^+ fluxes from stalk cells (% of initial values) after the addition of 5 mM GABA to the bath. Values are mean ± SE (n = 5). (c) A representative transient net Cl^- flux from the stalk cells from plants germinated and grown in the presence of 100 mM NaCl. (d) Relative Cl^- fluxes from stalk cells (% of initial values) after the addition of 5 mM GABA to the bath. Values are mean ± SE (n = 5). In controls, the appropriate amounts of BSM solution was added instead of GABA. For all MIFE data, the sign convention is 'efflux negative'. *Significant at $P < 0.05$.

2.4 Discussion

The physiological role of EBC in plant adaptive responses to salinity has been a matter of numerous experimental and review papers (see the Introduction section), but the reported evidence is mostly circumstantial. Here we show that the gentle removal of EBC, which did not cause any thigmo-morphogenic response (Kamano et al., 2015; Moulia et al., 2015), results in a salt-sensitive phenotype. This provides the first direct evidence for a role of EBC in salt tolerance in halophytes.

2.4.1 EBC act as major Na^+ and Cl^- store, rescuing growth under salinity stress

Removal of EBC and preventing the ability of halophyte plants to sequester Na^+ and Cl^- in external structures results in a salt-sensitive phenotype in both *C. quinoa* (Figs 2.3 and 2.4) and *A. lentiformis* (Fig. 2.5) plants. At the same time, brushing *C. album* leaves with very few or no bladder cells present (Fig. S2.3) did not alter the plant's responses to salinity stress (Fig. S2.4). This indicates that the presence of EBC increases chenopod salinity stress tolerance.

The CAM plant *M. crystallinum* accumulates up to 0.4 – 1.2 M Na^+ in EBC when grown under saline conditions (Adams et al., 1992; Barkla et al., 2002; Oh et al., 2015). Similar numbers were reported for other halophyte species. For example, in *Atriplex gmelini*, 80% of all Na^+ accumulated in young leaves were located in EBC (Tsutsumi et al., 2015), reaching concentrations close to 500 mM.

In *M. crystallinum*, EBCs remain compressed to the epidermal surface in unstressed plants but expand to comprise up to 25% of the total aerial volume once the plants have responded to stress (Barkla et al., 2002; Steudle et al., 1975). The same is true for quinoa (Fig. S2.5). The typical cell diameter of EBC in the young leaves used in our study was ~80 μm, the density was about 85 cells per mm^2 (Fig. S2.5) and the overall volume of all EBC on one side of the leaf was ~0.02 μL^3, or 0.04 μL^3, assuming that EBCs are distributed uniformly on both sides. The leaf lamina thickness is ~120 μm, making the corresponding volume of the leaf lamina 0.12 μL^3. Thus, the ratio between the volume of EBC and the volume of the leaf lamina in quinoa leaves reaches one-third, with EBC representing about 25% of the total aerial volume. At the same time, the difference in Na^+ sap concentration in the leaf lamina between brushed and non-brushed leaves is about 150 mM (Fig. 2.4E). Thus, we estimate the Na^+ concentration of quinoa EBC to be around 850 mM. A

similar calculation for chloride results in an estimated Cl^- concentration in EBC of about 1 M (Fig. 2.3E).

2.4.2 Salt dumping in EBC may cost plants less compared with intracellular sequestration

In mechanistic terms, EBC may be considered as 'inverted vacuoles' (Shabala et al., 2014). Nonetheless, the carbon cost of internal and external sequestration mechanisms may be different and should be considered. As the cell volume is proportional to the third power of the diameter while the surface area is to the second power, the volume to area ratio increases with increased cell diameter (Table S2.3). This implies that the carbon cost related to the formation of the cell wall decreases as the cells become bigger (a 10-fold increase in efficiency for a 10-fold increase in diameter). Thus, assuming both epidermal and mesophyll cells possess the same set of transporters for Na^+ sequestration, the carbon cost will be an order of magnitude lower in EBC. Given that plants need to allocate a substantial amount of carbon for de novo synthesis of compatible solutes for osmotic adjustment under saline conditions (Flowers and Colmer, 2015; Flowers et al., 2015), the ability to reduce the amount of carbon for cell wall deposits may be a critical factor conferring salinity stress tolerance at the whole-plant level. This suggestion is fully consistent with the generalized energy balanced model proposed by (Munns and Gilliham, 2015) showing that stress tolerance mechanisms represent additional costs to a plant required to deal with the salt load in the soil, so at high salinity, there may be zero growth, the total costs to the plant will equal any energy gain.

2.4.3 Removing EBC compromises leaf K^+ retention ability

Over the last decade, the ability of cells to maintain cytosolic K^+ homeostasis and retain K^+ under saline conditions has emerged as one of the critical mechanisms conferring salinity tissue tolerance in both root and shoot tissues (Anschütz et al., 2014; Shabala et al., 2016; Wu et al., 2015). In this work, we have shown that brushed quinoa plants accumulated much less K^+ in leaf lamina, with leaf sap K^+ concentration being nearly 2-fold lower in plants with EBC removed prior to salinity exposure (Fig. 2.3E). It remains to be answered as to whether such better K^+ retention is associated with better control of membrane potential in mesophyll

cells of non-brushed plants or is related to the prevention of ROS accumulation in these cells under saline conditions. Both voltage and ROS-inducible pathways of K^+ leak operate in plant cells under saline conditions (reviewed in (Shabala et al., 2016; Shabala and Pottosin, 2014), and follow-up experiments are required to reveal which of these pathways was affected by brushing.

The loss of the mesophyll K^+ retention ability may be also causally related to changes in the leaf metabolic profile (discussed in the succeeding texts) and specifically, the difference in oxalate content (6-fold lower in brushed leaves compared with intact counterparts; Table 2.1). Earlier, (Jou et al., 2007) suggested that in *M. crystallinum* plants, calcium oxalate crystals present in EBC can serve as a regulatory site for intracellular K^+. According to this suggestion, K^+ is remobilized from the crystals to increase the cytosolic K^+ concentration in nearby leaf mesophyll cells under conditions of reduced K^+ uptake and compromised leaf K^+ retention (such as under saline conditions).

2.4.4 Effect of salinity on metabolic profile in quinoa leaves

Salt treatment of intact leaves induced a strong shift in the metabolite profile when compared with untreated intact leaves (Table 2.1 and Fig. 2.6), which aligns well with reported metabolite changes upon salinity in halophytes (Kumari et al., 2015). As described before, major changes also found in quinoa leaves were an increase of proline and inositol (and other polyols) accompanied by a decrease in organic acids, including tricarboxylic acid (TCA) cycle intermediates (Kumari et al., 2015). Contrary to reported metabolite effects, we found a decrease in sucrose and glucose in salt-treated intact quinoa leaves compared with untreated leaves. However, the reported changes did not include any reference to the involvement of bladders towards the metabolite changes. Only one study reported metabolic changes upon salinity in EBC specifically prepared from *M. crystallinum*, which under salt stress, also showed a decrease in most organic acids and an increase in proline and fructose (Barkla and Vera-Estrella, 2015).

Proline, a known osmolyte involved in salt responses in plants (Szabados and Savouré, 2010) increased more than 16-fold, which has been previously observed in salt-treated quinoa cotyledons (Ruffino et al., 2009). Proline accumulates in several plant species under stressful environmental conditions including salt, drought, heat and cold, where it mitigates the adverse effects of stress

in multiple ways including protecting cell structures, protein integrity and enhancing enzyme activities (Szabados and Savouré, 2010). Most of the organic acids decreased, a metabolic phenotype previously observed in salt- treated barley, rice, Arabidopsis and grapevine (Cramer et al., 2006; Gong et al., 2005; Widodo et al., 2009; Zuther et al., 2007). The halophyte Thellungiella showed a similar reduction in organic acids to that seen in our experiments (Gong et al., 2005). Reduction of organic acids, and in particular TCA cycle intermediates, has been correlated with both decreased TCA cycle activity and an increased drawing on carbon structures for the synthesis of compounds required for coping with stress (Sanchez et al., 2007; Widodo et al., 2009). For instance, the precursor for proline synthesis is glutamate, which also decreased significantly. Glutamate is derived from 2-oxoglutarate, a TCA cycle intermediate.

Increased sugars have also been associated with osmotic stresses such as salinity, providing an increase in cellular osmolarity and providing energy and building blocks for osmoprotectants, such as inositol, and for scavenging ROS (Kumari et al., 2015; Sanchez et al., 2007; Widodo et al., 2009). In most reports, sucrose, fructose and glucose have all increased after salt stress in plants. However, in quinoa, glucose, as well as glucose-6-phosphate, decreased massively under salt treatment, down to 7% of the levels in control leaves. This may indicate an increased consumption of glucose through glycolysis or as a building block of salt-response carbohydrates or glycoproteins. For instance, ribose and inositol, which derive from glucose-6-phosphate (which also decreased significantly), were strongly increased. Similarly, glycine, serine and ethanolamine, which derive from 3-phosphoglyceric acid, and tyrosine and phenylalanine, which derive from phosphoenolpyruvate, all significantly increased (Fig. 2.6). Ethanolamine is a precursor for the synthesis of glycine betaine, a well-known osmolyte known to increase under salinity stress in plants (Suzuki et al., 2003). Tyrosine and phenylalanine are phenolic amino acids and are precursors of alkaloids and other secondary metabolites that have been shown to accumulate in plants under salinity stress.

2.4.5 Salt metabolism in leaves that have lost the ability for external salt sequestration in EBC

Our analysis (Table S2.1) revealed that the metabolite compositions of intact leaves and leaves with EBC removed were very similar, indicating that removal of EBC has no effect on the metabolite profiles of leaves when grown in control conditions. However, when plants were grown in salt conditions, a number of metabolites were significantly altered when intact leaves were compared with those with EBC removed (Table S2.2). Supervised and unsupervised clustering analysis (Fig. 2.7A,B) clearly shows separations between the two treatments, which reflects the differences in metabolite levels. GC–MS analysis detected 16 metabolites of which interestingly 15 were significantly decreased and only one was increased in the salt-treated leaves with EBC removed (Table S2.2). Here, we focus on the effect of brushing on GABA, inositol and sucrose biology, the metabolites with a known ability to regulate ionic relations in plants.

GABA is a non-protein amino acid known to modulate anion fluxes across the plasma membrane (Ramesh et al., 2015). In the current work, we show that brushing EBC reduces leaf GABA content by ~3-fold, from 1.5 to 0.5 mM, in quinoa. Given that EBCs represent about a quarter of the total leaf volume (see the preceding texts), the estimated concentration of GABA in EBC should be therefore at least 10-fold higher than in brushed leaf blade, that is about 5– 6 mM. This is clearly within the physiological range for reported effects of GABA on ion channels activity in plants (Gilliham and Tyerman, 2016; Ramesh et al., 2015; Shabala et al., 2014) and can therefore modulate salt loading into EBC, as shown in Fig. 2.9. Indeed, application of 5 mM GABA significantly reduced the magnitude of net Cl^- and Na^+ efflux from the stalk cell (Fig. 2.9), suggesting that increase accumulation of GABA in EBC may feedback on the rate of salt loading in salt bladders. Future studies should reveal the molecular nature and intracellular targets of such potential GABA targets in stalk and EBC.

The cyclic polyol myo-inositol is used in all organisms in many different metabolic pathways. Additionally, inositol plays an important role in plant osmotic adjustment (Adams et al., 2005). Importantly, both animal and plant studies have suggested that inositol transport may be tightly coupled with transport of Na^+. Myo-inositol concentrations increased in salt-stressed plants (Zhai et al., 2016), and expression of IMT (myo-inositol phosphate synthase) is enhanced in response to

salt stress. (Nelson et al., 1999) hypothesized that the loading of Na^+ into the xylem is coupled to myo-inositol transport and that myo-inositol acts as a facilitator of the Na^+ uptake and long-distance transport in halophytes. It remains to be answered whether such a mechanism operates in EBC.

The last aspect that warrants the discussion is a significant (3-fold) increase in leaf sucrose levels upon removal of EBC (from 0.27 to 0.86 mM). We believe that this phenomenon may be explained by an increased demand for non-enzymatic ROS scavenging in bladder-less leaves, a notion strongly supported by our observations that leaf mesophyll cells treated with exogenously supplied sucrose have a better ability to tolerate oxidative stress and retain K^+ in the cytosol (Fig. 2.8A,B). Salinity stress is known to result in a significant accumulation of various forms of ROS (Bose et al., 2014; Mittler et al., 2011), with hydrogen peroxide, superoxide radicals and hydroxyl radicals being the dominant ones. Of these, only the first two can be handled (kept under control) by means of enzymatic antioxidants. At the same time, hydroxyl radicals represent the most aggressive forms of ROS (Demidchik, 2014), causing damage to key cellular structures and significantly disturbing intracellular ion homeostasis (Demidchik et al., 2010), compromising leaf photosynthetic performance (Shabala et al., 2016). Sugars have been proposed to play a direct role in non-enzymatic antioxidant scavenging (Foyer and Shigeoka, 2011; Peshev et al., 2013; Stoyanova et al., 2010; Uemura and Steponkus, 2003; Van den Ende and Valluru, 2008) as fully supported by our electro-physiological data (Fig. 2.8). When sugars are compared at the same molar concentration, their greatest antioxidant capability is strongly correlated with their total number of hydroxyl groups, explaining why sucrose (with eight OH groups) is better compared with other sugars such as glucose and fructose (with five OH groups) (Smirnoff and Cumbes, 1989). Therefore, sucrose is well suited to protect the leaf mesophyll when hydroxyl radical production is expected to increase due to the failure of plants to load excessive salt into EBC (Fig. 2.9).

In conclusion, this work provides the explicit evidence for the important role of EBC as a component of salinity tolerance mechanisms in halophytes species. This role can be attributed to several mechanisms including EBC role as external NaCl storage space, improved K^+ retention in leaf mesophyll and as a storage space for several metabolites known to modulate plant ionic relations.

2.5 References

Adams, M.A., Richter, A., Hill, A.K., Colmer, T.D., 2005. Salt tolerance in *Eucalyptus* spp.: identity and response of putative osmolytes. Plant Cell Environ 28, 772-787.

Adams, P., Nelson, D.E., Yamada, S., Chmara, W., Jensen, R.G., Bohnert, H.J., Griffiths, H., 1998. Growth and development of *Mesembryanthemum crystallinum* (Aizoaceae). New Phytol 138, 171-190.

Adams, P., Thomas, J.C., Vernon, D.M., Bohnert, H.J., Jensen, R.G., 1992. Distinct cellular and organismic responses to salt stress. Plant Cell Physiol 33, 1215-1223.

Adolf, V.I., Jacobsen, S.-E., Shabala, S., 2013. Salt tolerance mechanisms in quinoa (*Chenopodium quinoa*). Environ Exp Bot 92, 43-54.

Agarie, S., Shimoda, T., Shimizu, Y., Baumann, K., Sunagawa, H., Kondo, A., Ueno, O., Nakahara, T., Nose, A., Cushman, J.C., 2007. Salt tolerance, salt accumulation, and ionic homeostasis in an epidermal bladder-cell-less mutant of the common ice plant *Mesembryanthemum crystallinum*. J Exp Bot 58, 1957-1967.

Anschütz, U., Becker, D., Shabala, S., 2014. Going beyond nutrition: regulation of potassium homoeostasis as a common denominator of plant adaptive responses to environment. J Plant Physiol 171, 670-687.

Barkla, B.J., Pantoja, O., 1996. Physiology of ion transport across the tonoplast of higher plants. Annu. Rev. Plant Biol 47, 159-184.

Barkla, B.J., Vera-Estrella, R., 2015. Single cell-type comparative metabolomics of epidermal bladder cells from the halophyte *Mesembryanthemum crystallinum.* Front Plant Sci 6, 10.

Barkla, B.J., Vera-Estrella, R., Camacho-Emiterio, J., Pantoja, O., 2002. Na^+/H^+ exchange in the halophyte *Mesembryanthemum crystallinum* is associated with cellular sites of Na^+ storage. Funct Plant Biol 29, 1017-1024.

Barkla, B.J., Vera-Estrella, R., Pantoja, O., 2012. Protein profiling of epidermal bladder cells from the halophyte *Mesembryanthemum crystallinum*. Proteomics 12, 2862-2865.

Bohnert, H.J., Nelson, D.E., Jensen, R.G., 1995. Adaptations to environmental stresses. Plant Cell 7, 1099-1111.

Bonales-Alatorre, E., Pottosin, I., Shabala, L., Chen, Z.-H., Zeng, F., Jacobsen, S.-E., Shabala, S., 2013. Differential activity of plasma and vacuolar membrane transporters contributes to genotypic differences in salinity tolerance in a halophyte species, *Chenopodium quinoa*. Int J Mol Sci 14, 9267-9285.

Bose, J., Shabala, L., Pottosin, I., Zeng, F., Velarde-Buendia, A.-M., Massart, A., Poschenrieder, C., Hariadi, Y., Shabala, S., 2014. Kinetics of xylem loading, membrane potential maintenance, and sensitivity of K^+-permeable channels to reactive oxygen species: physiological traits that differentiate salinity tolerance between pea and barley. Plant Cell Environ 37, 589-600.

Boughton, B.A., Callahan, D.L., Silva, C., Bowne, J., Nahid, A., Rupasinghe, T., Tull, D.L., McConville, M.J., Bacic, A., Roessner, U., 2011. Comprehensive profiling and quantitation of amine group containing metabolites. Anal Chem 83, 7523-7530.

Bressan, R.A., 2001. Learning from the Arabidopsis Experience. The next gene search paradigm. Plant Physiol 127, 1354-1360.

Chen, Z., Cuin, T.A., Zhou, M., Twomey, A., Naidu, B.P., Shabala, S., 2007. Compatible solute accumulation and stress-mitigating effects in barley genotypes contrasting in their salt tolerance. J Exp Bot 58, 4245-4255.

Chong, E.Y., Huang, Y., Wu, H., Ghasemzadeh, N., Uppal, K., Quyyumi, A.A., Jones, D.P., Yu, T., 2015. Local false discovery rate estimation using feature reliability in LC/MS metabolomics data. Sci Rep 5, 11.

Coutand, C., 2010. Mechanosensing and thigmomorphogenesis, a physiological and biomechanical point of view. Plant Sci 179, 168-182.

Cramer, G.R., Ergül, A., Grimplet, J., Tillett, R.L., Tattersall, E.A.R., Bohlman, M.C., Vincent, D., Sonderegger, J., Evans, J., Osborne, C., Quilici, D., Schlauch, K.A., Schooley, D.A., Cushman, J.C., 2006. Water and salinity stress in grapevines: early and late changes in transcript and metabolite profiles. Funct. Integr. Genomics 7, 111-134.

Cuin, T.A., Tian, Y., Betts, S.A., Chalmandrier, R., Shabala, S., 2009. Ionic relations and osmotic adjustment in durum and bread wheat under saline conditions. Funct Plant Biol 36, 1110-1119.

Demidchik, V., 2003. Free oxygen radicals regulate plasma membrane Ca^{2+}- and K^+-permeable channels in plant root cells. J Cell Sci 116, 81-88.

Demidchik, V., 2014. Mechanisms and physiological roles of K^+ efflux from root cells. J Plant Physiol 171, 696-707.

Demidchik, V., Cuin, T.A., Svistunenko, D., Smith, S.J., Miller, A.J., Shabala, S., Sokolik, A., Yurin, V., 2010. *Arabidopsis* root K^+-efflux conductance activated by hydroxyl radicals: single-channel properties, genetic basis and involvement in stress-induced cell death. J Cell Sci 123, 1468-1479.

Demidchik, V., Maathuis, F.J.M., 2007. Physiological roles of nonselective cation channels in plants: from salt stress to signalling and development. New Phytol 175, 387-404.

Dias, D.A., Hill, C.B., Jayasinghe, N.S., Atieno, J., Sutton, T., Roessner, U., 2015. Quantitative profiling of polar primary metabolites of two chickpea cultivars with contrasting responses to salinity. J Chromatogr B 1000, 1-13.

Flowers, T.J., Colmer, T.D., 2008. Salinity tolerance in halophytes. New Phytol 179, 945-963.

Flowers, T.J., Colmer, T.D., 2015. Plant salt tolerance: adaptations in halophytes. Ann Bot 115, 327-331.

Flowers, T.J., Munns, R., Colmer, T.D., 2015. Sodium chloride toxicity and the cellular basis of salt tolerance in halophytes. Ann Bot 115, 419-431.

Foyer, C.H., Shigeoka, S., 2011. Understanding oxidative stress and antioxidant functions to enhance photosynthesis. Plant Physiol 155, 93-100.

Gilliham, M., Tyerman, S.D., 2016. Linking metabolism to membrane signaling: the gaba–malate connection. Trends Plant Sci 21, 295-301.

Glenn, E.P., Brown, J.J., Blumwald, E., 2010. Salt tolerance and crop potential of halophytes. Crit Rev Plant Sci 18, 227-255.

Gong, Q., Li, P., Ma, S., Indu Rupassara, S., Bohnert, H.J., 2005. Salinity stress adaptation competence in the extremophile *Thellungiella halophila* in comparison with its relative *Arabidopsis thaliana*. Plant J 44, 826-839.

Hariadi, Y., Marandon, K., Tian, Y., Jacobsen, S.E., Shabala, S., 2010. Ionic and osmotic relations in quinoa (*Chenopodium quinoa*) plants grown at various salinity levels. J Exp Bot 62, 185-193.

Hill, C.B., Dias, D.A., Roessner, U., 2015. Current and emerging applications of metabolomics in the field of agricultural biotechnology. Adv Food Biotechnol 13, 26.

Ibdah, M., Krins, A., Seidlitz, H.K., Heller, W., Strack, D., Vogt, T., 2002. Spectral dependence of flavonol and betacyanin accumulation in *Mesembryanthemum crystallinum* under enhanced ultraviolet radiation. Plant Cell Environ 25, 1145-1154.

Jacobsen, S.-E., 2003. The worldwide potential for quinoa (*Chenopodium quinoa*). Food Rev Int 19, 167-177.

Jou, Y., Wang, Y.-L., Yen, H.E., 2007. Vacuolar acidity, protein profile, and crystal composition of epidermal bladder cells of the halophyte *Mesembryanthemum crystallinum*. Funct Plant Biol 34, 353-359.

Junker, B., Klukas, C., Schreiber, F., 2006. VANTED: a system for advanced data analysis and visualization in the context of biological networks. BMC Bioinformatics 7, 13.

Kamano, S., Kume, S., Iida, K., Lei, K.-J., Nakano, M., Nakayama, Y., Iida, H., 2015. Transmembrane topologies of ca^{2+}-permeable mechanosensitive channels MCA1 and MCA2 in *Arabidopsis thaliana*. J Biol Chem 290, 30901-30909.

Kumari, A., Das, P., Parida, A.K., Agarwal, P.K., 2015. Proteomics, metabolomics, and ionomics perspectives of salinity tolerance in halophytes. Front Plant Sci 6, 20.

Mittler, R., Vanderauwera, S., Suzuki, N., Miller, G., Tognetti, V.B., Vandepoele, K., Gollery, M., Shulaev, V., Van Breusegem, F., 2011. ROS signaling: the new wave? Trends Plant Sci 16, 300-309.

Monshausen, G.B., Haswell, E.S., 2013. A force of nature: molecular mechanisms of mechanoperception in plants. J Exp Bot 64, 4663-4680.

Moulia, B., Coutand, C., Julien, J.-L., 2015. Mechanosensitive control of plant growth: bearing the load, sensing, transducing, and responding. Front Plant Sci 6, 20.

Munns, R., Gilliham, M., 2015. Salinity tolerance of crops - what is the cost? New Phytol 208, 668-673.

Nelson, D.E., Koukoumanos, M., Bohnert, H.J., 1999. Myo-inositol-dependent sodium uptake in ice plant. Plant Physiol 119, 165-172.

Oh, D.-H., Barkla, B.J., Vera-Estrella, R., Pantoja, O., Lee, S.-Y., Bohnert, H.J., Dassanayake, M., 2015. Cell type-specific responses to salinity - the epidermal

bladder cell transcriptome of *Mesembryanthemum crystallinum*. New Phytol 207, 627-644.

Ozgur, R., Uzilday, B., Sekmen, A.H., Turkan, I., 2013. Reactive oxygen species regulation and antioxidant defence in halophytes. Funct Plant Biol 40, 832-847.

Panta, S., Flowers, T., Lane, P., Doyle, R., Haros, G., Shabala, S., 2014. Halophyte agriculture: success stories. Environ Exp Bot 107, 71-83.

Peshev, D., Vergauwen, R., Moglia, A., Hideg, É., Van den Ende, W., 2013. Towards understanding vacuolar antioxidant mechanisms: a role for fructans? J Exp Bot 64, 1025-1038.

Ramesh, S.A., Tyerman, S.D., Xu, B., Bose, J., Kaur, S., Conn, V., Domingos, P., Ullah, S., Wege, S., Shabala, S., Feijó, J.A., Ryan, P.R., Gilliham, M., 2015. GABA signalling modulates plant growth by directly regulating the activity of plant-specific anion transporters. Nat Commun 6, 9.

Ruan, C.-J., da Silva, J.A.T., Mopper, S., Qin, P., Lutts, S., 2010. Halophyte improvement for a salinized world. Crit Rev Plant Sci 29, 329-359.

Ruffino, A.M.C., Rosa, M., Hilal, M., González, J.A., Prado, F.E., 2009. The role of cotyledon metabolism in the establishment of quinoa (*Chenopodium quinoa*) seedlings growing under salinity. Plant Soil 326, 213-224.

Rygol, J., Zimmermann, U., Balling, A., 1989. Water relations of individual leaf cells of *Mesembryanthemum crystallinum* plants grown at low and high salinity. J Membrane Biol 107, 203-212.

Sanchez, D.H., Siahpoosh, M.R., Roessner, U., Udvardi, M., Kopka, J., 2008. Plant metabolomics reveals conserved and divergent metabolic responses to salinity. Physiol Plant 132, 209-219.

Shabala, L., Ross, T., McMeekin, T., Shabala, S., 2006. Non-invasive microelectrode ion flux measurements to study adaptive responses of microorganisms to the environment. Fems Microbiol Rev 30, 472-486.

Shabala, S., 2013. Learning from halophytes: physiological basis and strategies to improve abiotic stress tolerance in crops. Ann Bot 112, 1209-1221.

Shabala, S., Bose, J., Fuglsang, A.T., Pottosin, I., 2016. On a quest for stress tolerance genes: membrane transporters in sensing and adapting to hostile soils. J Exp Bot 67, 1015-1031.

Shabala, S., Bose, J., Hedrich, R., 2014. Salt bladders: do they matter? Trends Plant Sci 19, 687-691.

Shabala, S., Hariadi, Y., Jacobsen, S.-E., 2013. Genotypic difference in salinity tolerance in quinoa is determined by differential control of xylem Na^+ loading and stomatal density. J Plant Physiol 170, 906-914.

Shabala, S., Mackay, A., 2011. Ion Transport in Halophytes, in: Turkan, I. (Ed.), Plant Responses to Drought and Salinity Stress - Developments in a Post-Genomic Era. Academic Press, pp 151-199.

Shabala, S., Pottosin, I., 2014. Regulation of potassium transport in plants under hostile conditions: implications for abiotic and biotic stress tolerance. Physiol Plant 151, 257-279.

Smirnoff, N., Cumbes, Q.J., 1989. Hydroxyl radical scavenging activity of compatible solutes. Phytochemistry 28, 1057-1060.

Steudle, E., L[illegible]ttge, U., Zimmermann, U., 1975. Water relations of the epidermal bladder cells of the halophytic species *Mesembryanthemum crystallinum*: direct measurements of hydrostatic pressure and hydraulic conductivity. Planta 126, 229-246.

Stoyanova, S., Geuns, J., Hideg, É., Van Den Ende, W., 2010. The food additives inulin and stevioside counteract oxidative stress. Int J Food Sci Nutr 62, 207-214.

Suzuki, M., Yasumoto, E., Baba, S., Ashihara, H., 2003. Effect of salt stress on the metabolism of ethanolamine and choline in leaves of the betaine-producing mangrove species *Avicennia marina*. Phytochemistry 64, 941-948.

Szabados, L., Savouré, A., 2010. Proline: a multifunctional amino acid. Trends Plant Sci 15, 89-97.

Tsutsumi, K., Yamada, N., Cha-um, S., Tanaka, Y., Takabe, T., 2015. Differential accumulation of glycinebetaine and choline monooxygenase in bladder hairs and lamina leaves of *Atriplex gmelini* under high salinity. J Plant Physiol 176, 101-107.

Uemura, M., Steponkus, P.L., 2003. Modification of the intracellular sugar content alters the incidence of freeze-induced membrane lesions of protoplasts isolated from *Arabidopsis thaliana* leaves. Plant Cell Environ 26, 1083-1096.

Van den Ende, W., Valluru, R., 2008. Sucrose, sucrosyl oligosaccharides, and oxidative stress: scavenging and salvaging? J Exp Bot 60, 9-18.

Ventura, Y., Eshel, A., Pasternak, D., Sagi, M., 2015. The development of halophyte-based agriculture: past and present. Ann Bot 115, 529-540.

Widodo, Patterson, J.H., Newbigin, E., Tester, M., Bacic, A., Roessner, U., 2009. Metabolic responses to salt stress of barley (*Hordeum vulgare*) cultivars, Sahara and Clipper, which differ in salinity tolerance. J Exp Bot 60, 4089-4103.

Winter, K., 1973. Zum Problem der Ausbildung des Crassulaceens urestoffwechsels bei *Mesembryanthemum crystallinum* unter NaCl-Einflu. Planta 109, 135-145.

Wu, H., Shabala, L., Liu, X., Azzarello, E., Zhou, M., Pandolfi, C., Chen, Z.-H., Bose, J., Mancuso, S., Shabala, S., 2015. Linking salinity stress tolerance with tissue-specific Na^+ sequestration in wheat roots. Front Plant Sci 6, 13.

Yuan, Z., Druzhinina, I.S., Labbé, J., Redman, R., Qin, Y., Rodriguez, R., Zhang, C., Tuskan, G.A., Lin, F., 2016. Specialized microbiome of a halophyte and its role in helping non-host plants to withstand salinity. Sci Rep 6, 32467.

Zhai, H., Wang, F., Si, Z., Huo, J., Xing, L., An, Y., He, S., Liu, Q., 2016. Amyo-inositol-1-phosphate synthase gene, IbMIPS1, enhances salt and drought tolerance and stem nematode resistance in transgenic sweet potato. Plant Biotechnol J 14, 592-602.

Zuther, E., Koehl, K., Kopka, J., 2007. Comparative Metabolome Analysis of the Salt Response in Breeding Cultivars of Rice, in: Jenks, M.A., Hasegawa, P.M., Jain, S.M. (Eds.), Advances in Molecular Breeding Toward Drought and Salt Tolerant Crops. Springer Netherlands, Dordrecht, pp 285-315.

Chapter 3: Transcriptomics analysis of salt responsive genes related to epidermal bladder cells in quinoa

Abstract

Soil salinity is one of the most severe environmental stress that threatens crop production throughout the world. Contrary to traditional crop plants, halophytes have developed multiple adaptation mechanisms to cope with salt stress and hence, are perfect model plants to understand salinity tolerance traits and strategies and identify key genes related to salt tolerance. The ability of some halophytic plants such as *Chenopodium quinoa* to sequester large quantities of salt into external structures such as epidermal bladder cell (EBC), is one of hallmarks of salt tolerance in this plant. In the current study, plants were grown under non-saline condition for 4 weeks and one day prior the commencement of salt stress, EBCs were gently removed from all leaves and petioles by using a soft cosmetic brush. Plants were grown for 5 more weeks under 400 mM NaCl and transcriptome analysis in brushed and non-brushed leaves were compared. Comparing differently expressed genes (DEGs) of brushed and non-brushed leaves grown under 400 mM NaCl using a p-value < 0.05 and fold change > 2 as the significance cut-offs, indicated that 2014 genes were differently expressed, with 1398 genes being up-regulated and 616 genes down-regulated in bladder-bearing leaves. Significant alterations of genes related to response to stress, DNA replication, intracellular signalling pathway and ion and transmembrane transporters were determined. Altogether, the transcriptome analysis and reported differences between bladder-bearing and bladderless leaves, suggest that EBCs do not function as a passive external store place for salt as it was perceived before, but have active metabolic role(s) in quinoa plant.

3.1 Introduction

Salinity stress can significantly decrease crop production by causing massive metabolic disturbances due to osmotic stress and ionic toxicity (Zhang and Shi, 2013). Contrary to traditional crop plants, halophytes have developed multiple adaptation mechanisms to cope with salt stress (Flowers and Colmer, 2015) and hence, represent perfect models to understand salinity tolerance traits and strategies

that may be instrumental to identifying key genes related to salt tolerance (Shabala, 2013). Some halophytes including quinoa possess spherically-shaped external structures on their leaf surface called epidermal bladder cells (EBCs). These EBC are used to sequester toxic ions such as Na^+ and Cl^- and, in mechanistic terms, may be considered as 'inverted vacuoles' (Shabala et al., 2014). It has already been shown that EBCs operate as an external storage for Na^+ and removal of EBCs indicated an increase of salt load into leaf and as a result plant performance was affected under salinity stress (Chapter 2). The same study also showed that EBCs are preferentially accumulated certain metabolites that are known to have a role in modulating cellular ionic relations. It is estimated that about 50% of halophytes possess EBCs (Shabala et al., 2014) and thus these plant species could be potential plants to ameliorate saline soil or they could be considered as a source for crop improvement for salinity tolerance.

Characterisation of key salinity tolerance components in plants is essential for developing more salt tolerant genotypes. In this regards, next generation sequencing technologies such as RNA-sequencing has been broadly applied to study the molecular mechanism of adaptive responses to salt stress and to find salt-related candidate genes by analysing significantly different transcript abundance (Wang et al., 2009). Transcriptome analysis has great sensitivity and accuracy and could be used as one of the most applicable method to investigate the whole transcriptome (Jain, 2012). This technique has the ability to detect novel genes, identify low abundance genes and detect significantly expressed transcripts with higher fold-change (Jain, 2012; Wang et al., 2009).

Studies on *Mesembryanthemum crystallinum*, another halophytic species bearing EBCs, revealed that these structures have multiple functions such as accumulation of organic osmolytes, physical protection of leaves against UV, protection against water loss through providing a secondary epidermal layer, as well as having a role in energy generation (Jou et al., 2007; Oh et al., 2015). These findings also revealed an EBC-specific salt adaptive response under saline condition. Also, a metabolomic study comparing metabolic profile of *M. crystallinum* plants under saline condition with non-saline condition-grown plants indicated a significant change in metabolomic profile, with 352 metabolites being differently expressed in EBCs under salinity stress (Barkla and Vera-Estrella, 2015). These results indicate that EBCs do not solely function as a passive external store

for toxic ions as it was perceived before but instead may play important roles in the plant metabolism in halophytes. This conclusion is further corroborated by (Bohm et al., 2018) who speculated that the energy required for transport processes mediated ion sequestration in EBC may be provided by ATP from cyclic electron transport and mitochondria in these cells.

In this chapter, we assumed that EBCs operate as external salt store place and thus their removal should affect gene expression that would alter plant performance under saline conditions. As no quinoa mutants are currently available, in this investigation we used an alternate approach by removing the EBCs by the gentle brushing, and then compared the salt responsiveness of transcriptomes from intact leaves with those where EBCs were removed.

3.2 Materials and methods

3.2.1 Plant growth and salinity stress conditions

Quinoa (*Chenopodium quinoa*) seeds were grown in 20 cm diameter pots filled with standard potting mix, under controlled glasshouse conditions (mean day and night temperatures were 26 °C and 20 °C, respectively; humidity 65%; day length 16 hours) at the University of Tasmania in Hobart, Australia, from March to May 2017. Plants were grown for 4 weeks under non-saline conditions and one day prior to the commencement of salinity stress, EBCs of all leaves were gently removed from both sides of the leaves and stem by using a soft cosmetic brush (Chapter 2). Salinity stress commenced with 100 mM NaCl and reached to a final concentration of 400 mM NaCl in 4 days. EBCs were removed from the new emerged leaves on a basis of 3 to 4 times per week until the experiment was stopped after 4 weeks being under salt stress.

3.2.2 RNA-seq and data analysis

Total RNA was isolated from three biological replications of leaves using RNeasy Plant Mini Kit (Qiagen) following the manufacturer's instructions. RNA concentration and integrity were determined by Agilent Bioanalyzer 2100 system (Agilent Technologies Co. Ltd.) and samples with RIN value higher than 7 were used for sequencing. The NEBNext Ultra Directional RNA Library Prep Kit for Illumina (New England Biolabs) was used for mRNA-seq library following the manufacturer's protocol. In brief, 5 μg of total RNA was used to enriched mRNA

using polyT magnetic beads which was fragmented by divalent ions and then using random primers was subjected to first strand cDNA synthesis. The second strand cDNA was synthesised through replacing dT with U in the reaction. Then the end was repaired and dA-tailing and adaptor ligation were carried out. Using the USER enzyme, the second strand cDNA and part of the adaptor was removed and adaptor-ligated first strand cDNA was prepared for PCR amplification. As a quality control of libraries before conducting the sequencing process, the quality of libraries was tested using a Fragment Analyzer (Advanced Analytical Technologies, Inc) and the quantification was performed on a using Qubit (Thermo Fisher Scientific) and qPCR. The sequencing was performed on a HiSeq2500 using the SBS v4 reagent at the Core Facility for Genomics of the Shanghai Centre for Plant Stress Biology.

Raw reads were filtered to remove low quality reads and the quality control and adaptor trimming of raw sequencing reads was conducted using Trim Galore (http://www.bioinformatics.babraham.ac.uk/projects/trim_galore/). Cleaned reads were mapped to the quinoa reference genome (Jarvis et al., 2017) using the RNA-seq aligner STAR (version 2.5.4b) (Dobin et al., 2013). Differential expression analysis was performed using DESeq2 (version 1.22.2) (Love et al., 2014) in the R platform (version 3.5.1) (Team, 2018). Gene ontology (GO) term annotation was performed using AHRD (https://github.com/groupschoof/AHRD) and GO enrichment analysis was performed using agriGO (Tian et al., 2017).

3.2.3 Quantitative Real Time PCR (qRT-PCR) validation

About 2 μg of total extracted RNA (as described above) was used to synthesis cDNA using cDNA Synthesis SuperMix kit (TransGen, Beijing, China) according to the manufacturer's instruction. The RT-qPCR experiment was conducted for three biological replicates, with two technical repeats per experiment using an ABI StepOnePlus Real-Time PCR System with the TransStart Tip Green qPCR SuperMix (TransGen, Beijing, China) according to the manufacturer's instruction. The melting curve analysis was performed at the end of the cycles to ensure that the amplification of the target fragments was properly conducted. To calculate the relative gene expression, the relatively calculated cycle threshold values was produced using the $2^{-\Delta\Delta Ct}$ procedure with EF1-*a* as the internal reference gene.

3.3 Results

3.3.1 Sequencing statistics

To investigate the mechanisms underlying salinity tolerance of EBCs at the global transcriptional level, the transcriptome of quinoa leaves with and without EBCs grown under non-saline and 400 mM NaCl were analysed by a RNA-Sequencing study.

3.3.2 Identification of DEGs in bladderless and bladder-bearing leaves grown under saline condition

Comparing DEGs of bladder-bearing and bladderless leaves grown under 400 mM NaCl condition using a p-value < 0.05 and fold change > 2 as the significance cut-offs, revealed 2014 differently expressed genes. Of these, 1398 genes were down-regulated, and 616 genes were up-regulated in bladderless leaves (Fig. 3.1A; Suppl. Table 3.1). Comparing DEGs under non-saline condition also revealed that 701 genes were differently expressed; among them, 486 genes were down-regulated and 215 genes were up-regulated in bladderless leaves compared to bladder-bearing leaves (Fig. 3.1B; Suppl. Table 3.1).

Comparing similarity between DEGs of treatments showed that there were 103 down-regulated and 84 up-regulated genes that similarly expressed between bladderless and bladder-bearing leaves for saline and control grown plants (Fig. 3.1C).

3.3.3 GO terms enriched among DEGs

A Gene Ontology (GO) term enrichment analysis ($p \leq 0.05$) was conducted to provide insights into the function of DEGs. The DEGs of salt and control grown plants were annotated through GO classification analysis and grouped into biological process, cellular component, and molecular function categories (Suppl. Table 3.2; Suppl. Fig. 3.1). GO analysis of leaves with and without EBCs grown under saline conditions indicated the most enriched terms for groups such as phosphorylation, post-translational protein modification, DNA replication response to stress, intercellular signalling pathway, xyloglucan metabolic process, regulation of endopeptidase activity, cell wall polysaccharide metabolic process and transport. These groups acted as indicators of significant biological processes underlying the specific salinity-stress responses of EBCs. In the cellular component category GO,

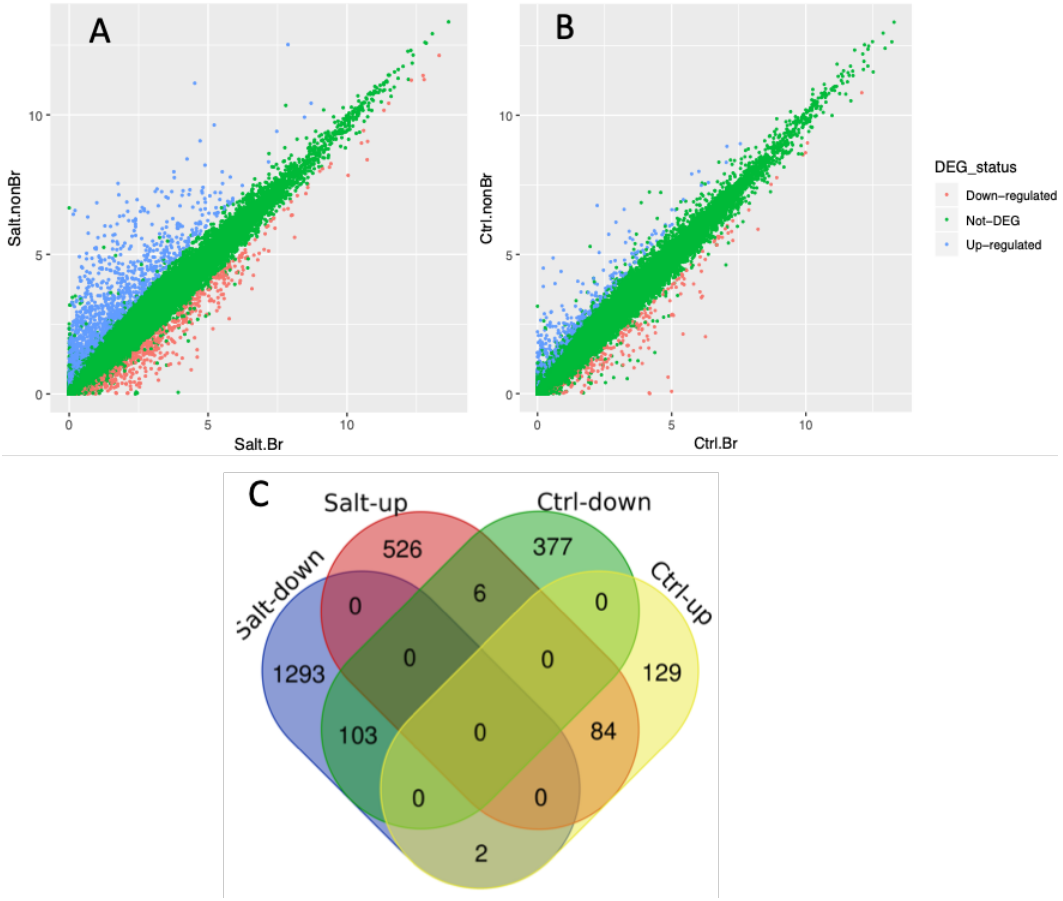

Fig. 3.1 Identification of differently expressed genes (DEGs) in the quinoa leaves with or without EBCs. Scatter plot showing mean genes for leaves with removed EBCs (x-axis) and intact leaves (y-axis) grown under (a) 400 mM NaCl and (b) non-saline conditions. DEGs were determined based on a false discovery rate (FDR) < 0.01 (Benjamini–Hochberg multiple testing adjustment). Blue and red spots signify DEGs up- and down-regulated by EBC removal treatment, respectively. The complete DEGs result is given in Suppl. Table S3.1. (c) Venn diagram of genes representing overlaps among DEGs of leaves with or without EBCs grown under saline and non-saline conditions.

the most dominant terms were nucleosome, protein-DNA complex, chromatin, chromosomal part, integral to membrane and apoplast (Fig. 3.2 and 3.3; Suppl. Table 3.2; Suppl. Fig. 3.1). In the molecular function category, the most enriched terms for over-expressed DEGs were protein kinase activity, phosphotransferase activity, transferase activity, protein serine/threonine kinase activity and transporter activity (Fig. 3.2 and 3.3; Suppl. Table 3.2; Suppl. Fig. 3.1). These transcriptional changes of genes categorized in different GO terms with regard to EBCs suggest that extensive metabolic activities occur in the EBCs under salinity stress.

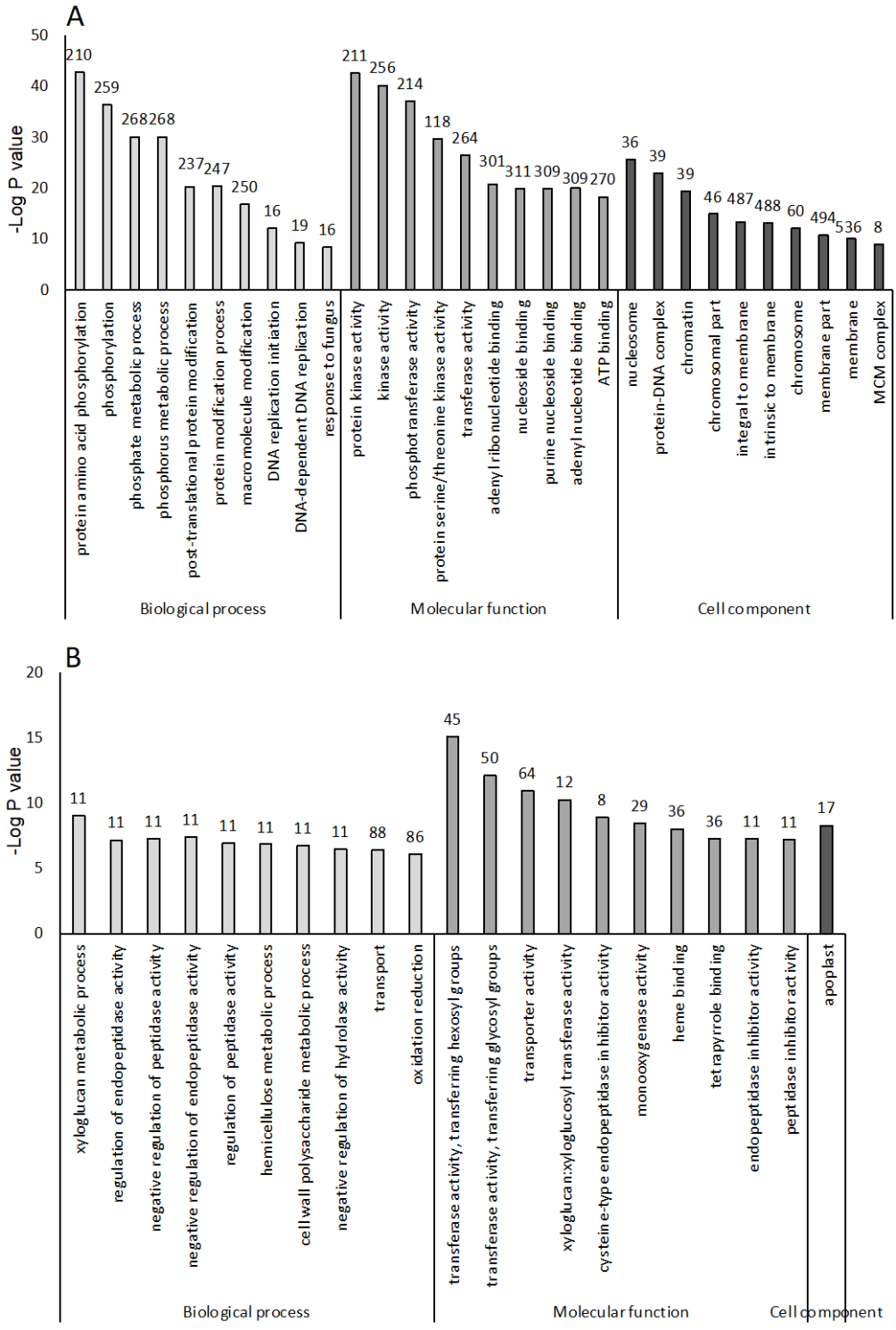

Fig. 3.2 Histogram of gene ontology (GO) classification of DEGs. (a) up-regulated and (b) down-regulated genes of leaves with or without EBCs grown under saline conditions were assigned to biological process, molecular function and cellular component. The value above bar shows number of GO term genes. The complete list of GO is given in Suppl. Table S3.2.

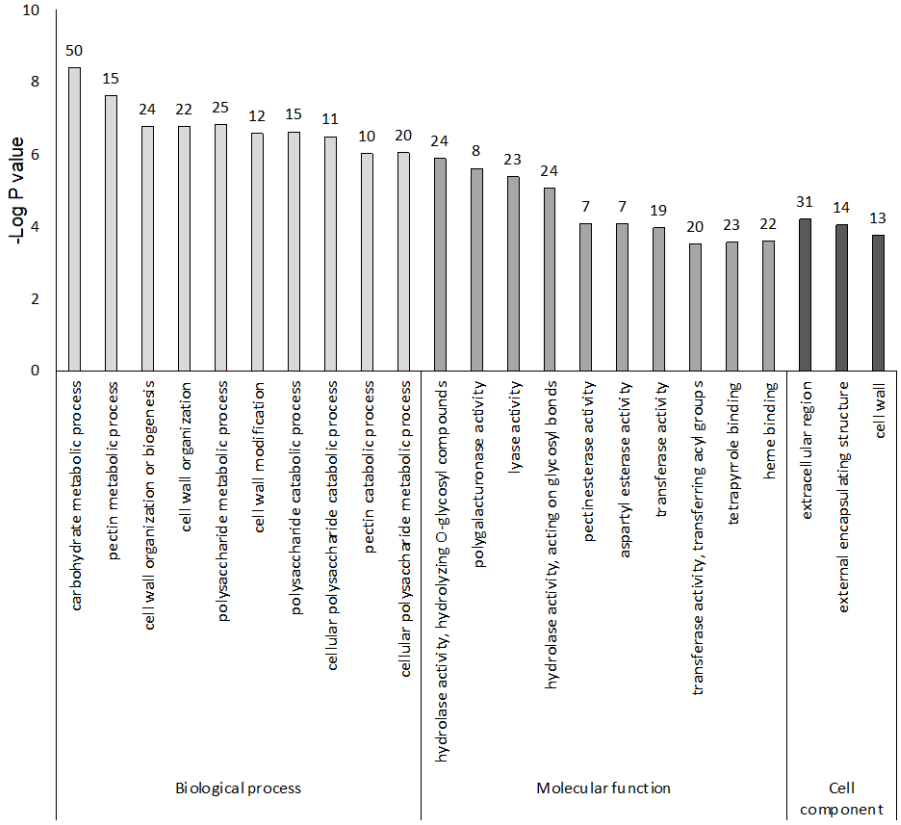

Fig. 3.3 Histogram of gene ontology (GO) classification of DEGs. The bar chart shows up-regulated genes of leaves with or without EBCs grown under non-saline conditions were assigned to biological process, molecular function and cellular component. The value above bar shows number of GO term genes. In down-regulated genes, there was not significant GO for molecular function and cellular component groups except "response to stimuli" that was significant in biological process group. The complete list of GO is given in Suppl. Table S3.2.

3.3.4 Salt response of the EBCs transcriptome

Based on GO enrichment analysis and visualisation of enriched GO terms using agroGO (Suppl. Table 3.2; Suppl. Fig. 3.1) of bladderless and bladder-bearing leaves of quinoa, we focused on gene families and pathways that highlighted different aspects of the collective salt response of EBCs transcriptome. These included genes involved in response to stress, DNA replication, intracellular signalling pathway and ion and transmembrane transporters (Suppl. Table 3.3).

3.3.5 Response to stress

Imposing 400 mM salt stress on bladderless quinoa plants resulted in a down-regulation of many gene responsible for salinity stress, with 115 genes up-regulated in bladder-bearing leaves grown under salinity stress (Suppl. Table 3.3). Ca^{2+}-binding proteins were among upregulated genes that were overexpressed in bladder-bearing plants under saline conditions. In this gene category, two homologues of calcium-dependent lipid-binding (CaLB domain) family protein were upregulated by 18.1- and 2.24-folds and three homologues of calmodulin-binding proteins were overexpressed between 2.4- and 4.7-folds change. The other gene in this category was the calcium-dependent protein kinase 29 that was upregulated by 6.9-fold in bladder-bearing leaves under saline condition (Suppl. Table 3.3). Five copies of ankyrin repeat family proteins (ANK) gene were up-regulated between 2.7- to 7.5-fold in intact leaves. Among up-regulated genes in intact leaves there were also genes related to disease resistance which appears to be present in EBCs which was not of surprise as one of suggested roles for EBCs is a protecting of leaves against diseases. Consistent with this, genes such as NB-ARC domain-containing disease resistance protein and disease resistance protein (CC-NBS-LRR class) family were upregulated (Suppl. Table 3.3). There were also many homologues of peroxidase superfamily protein and chaperone protein htpG family protein that were overexpressed in bladder-bearing leaves under saline condition (Suppl. Table 3.3).

3.3.6 DNA replication

EBCs are present on the both abaxial and adaxial leaf surfaces, as well as on plant stem. Our results indicated that numerous genes related to endoreduplication were upregulated in intact leaves (Suppl. Table 3.3). Eight homologues of minichromosome maintenance (MCM2/3/5) family protein which are DNA helicase and essential for DNA replication were upregulated between 2.3- to 3.4-fold in intact leaves under 400 mM NaCl. In accord with this, minichromosome maintenance 9 which is required for DNA replication initiation was also overexpressed by 5.5-fold (Suppl. Table 3.3). In the GO term “DNA replication”, other genes such as cell division cycle 45, DNA primase POLA3, DNA primase 2C large subunit family and DNA-directed DNA polymerase were among upregulated

genes in bladder-bearing leaves (Suppl. Table 3.3). This suggests that endopolyploidy occurs within EBCs under saline conditions.

3.3.7 Intracellular signalling pathway

Genes of sensing and signalling pathways related to salinity stress were upregulated in intact plants. Four homologues of glutamate receptor 2.7 gene alongside glutamate receptor 2.9 gene were among upregulated genes that overexpressed between 2.5- to 9.6-fold in bladder-bearing leaves (Suppl. Table 3.3). Six homologues of protein kinase superfamily protein as perceiving salt signals probably present in EBCs were upregulated in leaves with EBCs suggesting the presence of salt sensing mechanism in bladders (Suppl. Table 3.3). Four homologues of S-locus lectin protein kinase family protein, two homologues of UDP-galactose transporter 3 and G-type lectin S-receptor-like Serine/Threonine-kinase also were among upregulated genes in intact leaves under saline conditions (Suppl. Table 3.3).

3.3.8 Ion and transmembrane transporters

Under saline conditions ion transporters are involved in transportation and compartmentalisation of Na^+ and it appears that removal of EBCs resulted in over-expression of many ion and transmembrane transporters. The results of this investigation revealed 53 genes upregulated in bladderless leaves that were related to transmembrane transport and ion transport (Suppl. Table 3.3). Three genes encoding outward rectifying potassium channels were upregulated in bladderless leaves indicating K^+ leakage resulted from high Na^+ concentration in the absence of EBCs. On the contrary to intact leaves that contain EBCs and indicated levels of DNA replication, it appears that removal of EBCs stimulated DNA degradation activity where the expression levels of nuclease transporters which are associated with degradation of DNA were up-regulated by 2.5- to 11.3-fold in bladderless leaves (Suppl. Table 3.3).

Many genes related to cation exchangers such as cation exchanger 1, cation/H^+ exchanger 18, high-affinity K^+ transporter 1, organic cation/carnitine transporter 3 and sodium/calcium exchanger family protein/calcium-binding EF hand family protein were upregulated between 2.1- to 4.3-fold in bladderless leaves (Suppl. Table 3.3). In terms of anion transporters, two homologues of ammonium

transporter and four homologues of sulfate transporter were overexpressed in bladderless leaves (Suppl. Table 3.3). Five homologues of MATE (Multidrug and Toxic Compound Extrusion or Multi-Antimicrobial Extrusion) were also upregulated in leaves without EBCs under saline conditions (Suppl. Table 3.3).

As shown in early chapters, removal of EBCs from leaf surfaces had significantly disrupted ion homeostasis in bladderless leaves which resulted in upregulation of ion transporters which may act as a compensation mechanism in these plants. However, it comes with significant energy cost where the genes related to energising cells were increased. The transcript levels of genes regulating the energization across plasma membrane or tonoplast such as H^+-ATPase 4 (two homologues), ADP/ATP carrier 3, calcium ATPase 2, dicarboxylate carrier 2, ATPase E1-E2 type family protein/haloacid dehalogenase-like hydrolase family protein (two homologues) and tonoplast dicarboxylate transporter were upregulated in bladderless leaves (Suppl. Table 3.3).

3.3.9 Validation of the DEGs

Further verification of reliability of the transcriptome analysis results was conducted using randomly selected DEGs of this investigation for qRT-PCR analysis. Upregulation and downregulation of all the randomly selected genes were consistent with the corresponding gene expression levels determined by RNA-Seq (Fig. 3.4). This indicates the results obtained from RNA-Seq experiment were reliable.

3.4 Discussion

3.4.1 Removal of EBCs resulted in down-regulation of stress-responsive genes in bladderless leaves

Salt tolerance is a complex and multigenic trait and hence numerous genetic circuits are responsible for achieving salinity tolerance. In respect to this fact, identification of genes and gene products that play an important role in the plant adaptation to salt stress for overcoming this unfavourable condition in vital (Munns and Tester, 2008). In the current study GO enrichment analysis revealed that GO term

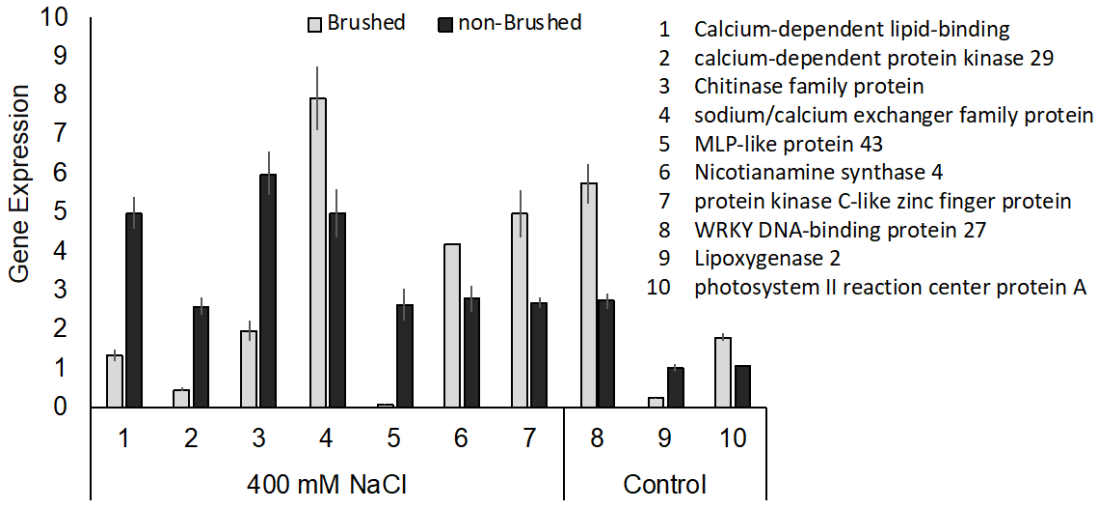

Fig 3.4 Bar plot indicating the expression analysis of randomly selected RNA-sequencing genes by RT-qPCR from leaves with or without bladders grown under saline and non-saline conditions. Gene expression was normalized against the housekeeping gene, EF1-*a*. Values are the average of three independent replications. > 1 is upregulation and < 1 is downregulation.

"response to stress" containing a large group of genes consisting of 115 genes (including copy numbers) was up-regulated in bladder-bearing leaves (Suppl. Tables 3.2 and 3.3).

In response to salinity stress, plants have evolved numerous survival mechanisms. Amongst them, Ca^{2+} has a fundamental role as the second messenger operating in different signalling transduction pathways (Tuteja and Mahajan, 2007). This role has been carried out through regulating the activity of different phosphatases and protein kinases families (e.g. control the activation of different ion transporters) (Batistic and Kudla, 2012). Under saline conditions, Na^{+} enters the cell and sensed by glucuronosyltransferase for glycosyl inositol phosphorylceramide (GIPC) sphingolipids in the plasma membrane. This excessive salt triggers an increase in the cytosolic Ca^{2+} concentration, which activate Ca^{2+}-binding proteins (Jiang et al., 2019). Three major group of Ca^{2+}-binding proteins including (i) Ca^{2+} dependent protein kinases (CDPK), (ii) calmodulins (CaM) and CaM-like proteins (CaML), (iii) calcineurin B-like proteins (CBL) have been determined in plants (Luan, 2009; McCormack et al., 2005). Here, genes related to

two of these classes were up-regulated in bladder-bearing leaves in this study (Suppl. Table 3.3). These Ca^{2+}-binding proteins regulate a broad spectrum of target proteins including proteins related to transporters for different ions (Zeng et al., 2015). Thus, many of the target proteins directly or indirectly play a role in regulating plant responses to unfavourable conditions such as salt stress. For instance, it has been shown that the overexpression of CaM gene induced by salinity stress from soybean in Arabidopsis results in an increased level of salinity tolerance by the up-regulation of DNA-binding activity of a MYB transcription factor MYB2 (Abe et al., 2003; Yoo et al., 2005). In light with this result, up- regulation of the Ca^{2+}-ATPases under salinity stress has been reported in various crop plants such as tobacco and soybean (Chung et al., 2000; Perez-Prat et al., 1992). This has been proposed to reduce Ca^{2+} concentration in the cytosol thus helping to maintain the homeostasis of Ca^{2+} (Singh et al., 2014).

Five homologues of genes encoding ankyrin repeat family proteins (ANK) were up-regulated in intact leaves (Suppl. Table 3.3). In plants, proteins containing ankyrin repeats have been indicated to be involved in diverse physiological processes (Huang et al., 2009) and different cellular functions, such as including cell cycle regulation, signal transduction and ion transport (Sedgwick and Smerdon, 1999). Also, they have important roles in responses to abiotic stresses in plants (Sharma and Pandey, 2015). For example, a novel gene with an ankyrin-repeat motif called itn1, was characterised in Arabidopsis (Sakamoto et al., 2008). It was suggested that this gene is involved in the ABA-dependent salt stress pathway and influences the ABA-mediated production of ROS (Sakamoto et al., 2008). Also, it has been reported that CaKR1 gene from ANK protein family may play a role in both biotic and abiotic stresses (Seong et al., 2007).

Another gene which highly up-regulated by 16.15-fold in bladder-bearing plants was MLP-like protein 43. MLP proteins belong to the Bet v 1 family, which trigger downstream signal transduction through binding ligands, such as cytokinins and secondary metabolites (Radauer et al., 2008). In a current investigation using physiological and biochemical analyses, it has been shown that MLP43 is a positive regulator in ABA and drought stress (Wang et al., 2016). This function by regulating expression ABA-responsive gene, ROS contents and of water loss efficiency. Hence, upregulation of this gene could confer salinity tolerance in bladder-bearing quinoa plants.

3.4.2 Salinity stress induced endopolyploidy in leaves containing EBCs

There is a growing bulk of evidence suggesting that the severity of stress tolerance in plants is causally linked with endopolyploidy (Barkla et al., 2018; Schoenfelder and Fox, 2015). For example, in cucumber UV-B irradiation stress resulted in a doubling of the ploidy level of epidermal cells and increased the cell size (Yamasaki et al., 2010). These cells with endopolyploidy also had higher peroxidase activity and the concentration phenolic compounds was changed.

In the current investigation, comparing significantly DEGs in response to salt stress between bladder-bearing and bladderless leaves revealed upregulation of many of the genes related to DNA replication in bladder-bearing leaves (Suppl. Table 3.3). Genes such as minichromosome maintenance (8 copies of MCM2/3/5) and minichromosome maintenance 9, were upregulated (Suppl. Table 3.3). It has been shown that MCM proteins are required for processive DNA replication and triggering DNA damage repair mechanisms (Hu et al., 2016). Additionally, the magnitude of response to salinity stress in bladder-bearing leaves by DNA primase POLA3 (2 copies), DNA-directed DNA polymerase, cell division cycle 45 (2 copies), DNA primase 2C large subunit is much higher than in bladderless leaves (Suppl. Table 3.3). These genes are crucial for polyploidisation (Guo and Han, 2014) and contribute the replicative helicase, elongation, and single-strand DNA-binding complexes that are essential for DNA replication (Takahashi et al., 2010).

Various cell types in plant species undergo one or two rounds of DNA duplication; however, it has been revealed that specialized cell types and cells that have high active metabolism generally indicating higher level of polyploidy (Cookson et al., 2006; Leitch and Dodsworth, 2017). In *M. crystallinum*, in addition to endopolyploidy which is controlled during plant development, salinity stress (200 mM NaCl) also induced polyploidy with 2 – 8 additional rounds of endoreduplication measured in nuclei of plant leaf (Barkla et al., 2018). In this study, salinity stress resulted in dramatically increased ploidy level in the EBCs of the flower bud where nuclei of EBCs were greater than 100 μm in diameter with estimated ploidy level of at least 32,768C.

Altogether, the result of our study suggests that increased endopolyploidy of bladder-bearing leaves of quinoa helps to mitigate salt stress damage, and this increases in ploidy and subsequent increase in EBC volume may contribute to salt

tolerance through increasing the external storage capacity for Na^+ compartmentalisation (Barkla et al., 2018).

3.4.3 Genes related to signalling pathway were up-regulated in bladder-bearing leaves

In addition to salt-responsive and transcriptional regulators genes that are involved in salinity stress, there are also sensing and signalling genes that mediate adaptation to salinity (Zhu, 2002). A generic signal transduction pathway starts with locally perceived special receptors on the cell membrane and is then followed by a series of intracellular reactions, including the secondary messengers; this phenomenon induces the expression of different stress-responsive genes, that finally resulting in protective responses in the whole plant (Xiong et al., 2002). Our results revealed that protein kinase superfamily protein, glutamate receptor and S-locus lectin protein kinase family protein have critical roles in perceiving salt signals in EBCs. Five homologues of Glutamate Receptor Ion Channel (GLRs) which were upregulated from 2.5 to 9.6 folds in bladder-bearing leaves (Suppl. Table 3.3) may play a role through signalling pathway and function as salt-responsive genes in EBCs. It is suggested that GLRs in plants can cause a rapid increase in cytosolic Ca^{2+} which is attributed to activation of plasma membrane Ca^{2+}-permeable channels (Dennison and Spalding, 2000). For example, in Arabidopsis it has been shown that increase of Ca^{2+} concentration in the cytosol and depolarisation of membrane induced by glutamate in Arabidopsis root cells are dependent on the presence of AtGLR3.3 (Qi et al., 2006; Stephens et al., 2008).

Protein kinases are among the most common cellular regulatory components of signal transduction that play important roles in plants response to environmental stresses (Xiong et al., 2002; Zhu, 2002). Hence, five up-regulated homologs of protein kinases in bladder-bearing leaves discovered in this investigation may play a role in adaptive responses to salinity in quinoa. In respect to this fact, fine mapping of an Arabidopsis population revealed that a protein kinase AtCIPK16, related to SOS2, was significantly overexpressed under saline conditions (Roy et al., 2013). The higher exclusion of Na^+ in Arabidopsis roots was linked with significantly higher up-regulation level of AtCIPK16 (Roy et al., 2013).

In this study, G-type lectin S-receptor-like Serine/Threonine-kinase gene also up-regulated by 4.78 folds which has been shown that is a positive regulator

of plant tolerance to salt stress. (Sun et al., 2013) provided evidence that GsSRK (a G-type lectin S-receptor-like serine/threonine protein kinase) could be a novel putative protein kinase in soybean that has a primary role in plant responses to salinity stress. Also, overexpression of this gene in Arabidopsis resulted in an increased level of salinity tolerance at various growth stages, as well as higher seed yield in Arabidopsis under saline conditions (Sun et al., 2013).

3.4.4 Disruption of EBCs increased transmembrane and ion transporters in bladderless plants to compensate for excessive salt load

Exposure of bladderless quinoa plants to salinity resulted in activation of many transporters, to deal with high amount of Na^+ in mesophyll in the absence of EBCs as an external salt store place. EBCs play a major role in Na^+ and toxic ions sequestration into their large vacuole which results in lower Na^+ content in metabolically active mesophyll cells. Our previous study indicated that brushing EBCs from leaf surface resulted in significantly higher Na^+ concentration in bladderless leaves (Chapter 2). The result of this transcriptome analysis revealed that this disruption in external Na^+ sequestration ability has significantly changed transmembrane and transporters profile in the leaf lamina (Suppl. Tables 3.2 and 3.3). To deal with higher Na^+ concentration in bladderless leaves, the genes coding for MATE efflux family protein, cation exchanger 1, organic cation/carnitine transporter, cation/H^+ exchanger 18 (a member of Putative Na^+/H^+ antiporter family), H^+-ATPase were amongst the up-regulated DEGs.

MATE transporters have prominent direct or indirect roles in cell detoxification and to this reason they are alternatively called DETOXIFICATION (DTX) proteins (Li et al., 2002). They also play role in transporting metabolites out of the cytosol using electrochemical gradient across the membrane, thus mediating the efflux or subcellular metabolites sequestration in the cell (Santos et al., 2017). The overexpression of five homologues encoding this protein family in the bladderless leaves may indicate the need for a higher detoxification in these leaves due to higher concentration of toxic ions such as Na^+ in the absence of EBCs.

Adaptation of plants to saline conditions requires ion homeostasis at the cellular level. This adaptation relies heavily on the vacuolar Na^+ and Cl^- sequestration, to reduce the ion concentration below the toxic levels in the cytosol. Overexpression of genes encoding Na^+ sequestration into the vacuole in leaves

without EBCs indicates that in the absence of EBCs and under high concentration of Na^+, transportation of Na^+ into the vacuole appears to be a compensation strategy. Up-regulation of cation/H^+ exchanger and vacuolar membrane localised organic cation/carnitine transporter (Kufner and Koch, 2008) in bladderless leaves in this study suggesting the compensation mechanism to maintain low cytoplasmic Na^+ concentration to minimize the toxicity impacts of salt. These membrane-bound transporters to pump toxic ions into vacuole play a key role for the salt tolerance.

Given the fact that K^+ content in plant cells equilibrates the toxic effects of Na^+, ion homeostasis in plants exposed to salt stress requires the maintaing of stable K^+ content (Demidchik et al., 2014). Up-regulation of genes related to outward rectifying K^+ channels in leaves without EBCs also indicates that electrolyte leakage resulted from salinity stress was higher in these leaves (Suppl. Table 3.3). Electrolyte leakage which can be triggered by salt stress (Shabala et al., 2006) and is mainly caused by the efflux of K^+. Under this circumstance, the activity of K^+ in the cytosol can decrease from 70–200 mM to 10–30 mM (Shabala et al., 2006). This salt-induced K^+ leakage is usually accompanied by higher levels of ROS which in turn results in programmed cell death (Demidchik et al., 2014). In light with this result, 4 homologues of genes encoding plant nuclease were up-regulated by 2.5- to 11.3-fold in bladderless leaves suggesting that DNA degradation activity was higher in leaves without EBCs (Suppl. Table 3.3). The higher DNA degradation may be a result of programmed cell death (Sakamoto and Takami, 2014) likely resulted from higher salt concentration of leaves without EBCs. Numerous genes encoding nucleases in plants have been reported as induced during cell-death events resulted from stressful conditions including salinity stress (Lombardi et al., 2007; Muramoto et al., 1999). This result implies significant role of higher salt load in programmed cell death in bladderless leaves.

Among up-regulated genes in bladderless leaves there were also H^+-ATPase genes that are central to membrane potential maintenance and membrane energization, required for transmembrane ion transport (Suppl. Table 3.3). It appears that removing EBCs which resulted in an increase of transporters required a great amount of energy to tackle the high load of salt within the cell. This considerable amount of carbon costs to the cell is required for ion transportation and flux across either tonoplast or plasma membrane and resultant feedbacks for maintenance of negative membrane potential. Furthermore, higher influx rate of

ions such as Na^+ and Cl^- in bladderless leaves will influence most other transport due to changes in membrane potential. Thus, it appears that the total energy invested into salinity tolerance in bladderless leaves is much more than that in bladder-bearing leaves.

In conclusion, the transcriptome analysis of bladder-bearing and bladderless leaves suggests that EBCs do not function as a passive external store place for salt as but have active metabolic role(s) in quinoa plant.

3.5 References

Abe, H., Urao, T., Ito, T., Seki, M., Shinozaki, K., Yamaguchi-Shinozaki, K., 2003. Arabidopsis AtMYC2 (bHLH) and AtMYB2 (MYB) function as transcriptional activators in abscisic acid signaling. Plant Cell 15, 63-78.

Barkla, B.J., Rhodes, T., Tran, K.T., Wijesinghege, C., Larkin, J.C., Dassanayake, M., 2018. Making epidermal bladder cells bigger: developmental- and salinity-induced endopolyploidy in a model halophyte. Plant Physiol 177, 615-632.

Barkla, B.J., Vera-Estrella, R., 2015. Single cell-type comparative metabolomics of epidermal bladder cells from the halophyte *Mesembryanthemum crystallinum*. Front Plant Sci 6, 435.

Batistic, O., Kudla, J., 2012. Analysis of calcium signaling pathways in plants. Biochim Biophys Acta 1820, 1283-1293.

Bohm, J., Messerer, M., Muller, H.M., Scholz-Starke, J., Gradogna, A., Scherzer, S., Maierhofer, T., Bazihizina, N., Zhang, H., Stigloher, C., Ache, P., Al-Rasheid, K.A.S., Mayer, K.F.X., Shabala, S., Carpaneto, A., Haberer, G., Zhu, J.K., Hedrich, R., 2018. Understanding the molecular basis of salt sequestration in epidermal bladder cells of *Chenopodium quinoa*. Curr Biol 28, 3075-3085 e3077.

Chung, W.S., Lee, S.H., Kim, J.C., Heo, W.D., Kim, M.C., Park, C.Y., Park, H.C., Lim, C.O., Kim, W.B., Harper, J.F., Cho, M.J., 2000. Identification of a calmodulin-regulated soybean Ca^{2+}-ATPase (SCA1) that is located in the plasma membrane. Plant Cell 12, 1393-1407.

Cookson, S.J., Radziejwoski, A., Granier, C., 2006. Cell and leaf size plasticity in Arabidopsis: what is the role of endoreduplication? Plant Cell Environ 29, 1273-1283.

Demidchik, V., Straltsova, D., Medvedev, S.S., Pozhvanov, G.A., Sokolik, A., Yurin, V., 2014. Stress-induced electrolyte leakage: the role of K^+-permeable channels and involvement in programmed cell death and metabolic adjustment. J Exp Bot 65, 1259-1270.

Dennison, K.L., Spalding, E.P., 2000. Glutamate-gated calcium fluxes in Arabidopsis. Plant Physiol 124, 1511-1514.

Dobin, A., Davis, C.A., Schlesinger, F., Drenkow, J., Zaleski, C., Jha, S., Batut, P., Chaisson, M., Gingeras, T.R., 2013. STAR: ultrafast universal RNA-seq aligner. Bioinformatics 29, 15-21.

Flowers, T.J., Colmer, T.D., 2015. Plant salt tolerance: adaptations in halophytes. Ann Bot 115, 327-331.

Guo, X., Han, F., 2014. Asymmetric epigenetic modification and elimination of rDNA sequences by polyploidization in wheat. Plant Cell 26, 4311-4327.

Hu, Z.B., Cools, T., De Veylder, L., 2016. Mechanisms used by plants to cope with dna damage. Annu Rev Plant Biol 67, 439-462.

Huang, J., Zhao, X., Yu, H., Ouyang, Y., Wang, L., Zhang, Q., 2009. The ankyrin repeat gene family in rice: genome-wide identification, classification and expression profiling. Plant Mol Biol 71, 207-226.

Jain, M., 2012. Next-generation sequencing technologies for gene expression profiling in plants. Brief Funct Genomics 11, 63-70.

Jarvis, D.E., Ho, Y.S., Lightfoot, D.J., Schmöckel, S.M., Li, B., Borm, T.J., Ohyanagi, H., Mineta, K., Michell, C.T., Saber, N., 2017. The genome of *Chenopodium quinoa*. Nature 542, 307.

Jiang, Z., Zhou, X., Tao, M., Yuan, F., Liu, L., Wu, F., Wu, X., Xiang, Y., Niu, Y., Liu, F., 2019. Plant cell-surface GIPC sphingolipids sense salt to trigger Ca^{2+} influx. Nature 572, 341-346.

Jou, Y., Wang, Y.L., Yen, H.C.E., 2007. Vacuolar acidity, protein profile, and crystal composition of epidermal bladder cells of the halophyte *Mesembryanthemum crystallinum*. Funct Plant Biol 34, 353-359.

Kufner, I., Koch, W., 2008. Stress regulated members of the plant organic cation transporter family are localized to the vacuolar membrane. BMC Res Notes 1, 43.

Leitch, I., Dodsworth, S., 2017. Endopolyploidy in plants. eLS.

Li, L., He, Z., Pandey, G.K., Tsuchiya, T., Luan, S., 2002. Functional cloning and characterization of a plant efflux carrier for multidrug and heavy metal detoxification. J Biol Chem 277, 5360-5368.

Lombardi, L., Ceccarelli, N., Picciarelli, P., Lorenzi, R., 2007. DNA degradation during programmed cell death in *Phaseolus coccineus* suspensor. Plant Physiol Biochem 45, 221-227.

Love, M.I., Huber, W., Anders, S., 2014. Moderated estimation of fold change and dispersion for RNA-seq data with DESeq2. Genome Biol 15, 550.

Luan, S., 2009. The CBL-CIPK network in plant calcium signaling. Trends Plant Sci 14, 37-42.

McCormack, E., Tsai, Y.C., Braam, J., 2005. Handling calcium signaling: Arabidopsis CaMs and CMLs. Trends Plant Sci 10, 383-389.

Munns, R., Tester, M., 2008. Mechanisms of salinity tolerance. Annu Rev Plant Biol 59, 651-681.

Muramoto, Y., Watanabe, A., Nakamura, T., Takabe, T., 1999. Enhanced expression of a nuclease gene in leaves of barley plants under salt stress. Gene 234, 315-321.

Oh, D.H., Barkla, B.J., Vera-Estrella, R., Pantoja, O., Lee, S.Y., Bohnert, H.J., Dassanayake, M., 2015. Cell type-specific responses to salinity - the epidermal bladder cell transcriptome of *Mesembryanthemum crystallinum*. New Phytol 207, 627-644.

Perez-Prat, E., Narasimhan, M.L., Binzel, M.L., Botella, M.A., Chen, Z., Valpuesta, V., Bressan, R.A., Hasegawa, P.M., 1992. Induction of a putative Ca-ATPase mRNA in NaCl-adapted cells. Plant Physiol 100, 1471-1478.

Qi, Z., Stephens, N.R., Spalding, E.P., 2006. Calcium entry mediated by GLR3.3, an Arabidopsis glutamate receptor with a broad agonist profile. Plant Physiol 142, 963-971.

Radauer, C., Lackner, P., Breiteneder, H., 2008. The Bet v1 fold: an ancient, versatile scaffold for binding of large, hydrophobic ligands. BMC Evol Biol 8, 286.

Roy, S.J., Huang, W., Wang, X.J., Evrard, A., Schmockel, S.M., Zafar, Z.U., Tester, M., 2013. A novel protein kinase involved in Na^+ exclusion revealed from positional cloning. Plant Cell Environ 36, 553-568.

Sakamoto, H., Matsuda, O., Iba, K., 2008. ITN1, a novel gene encoding an ankyrin-repeat protein that affects the ABA-mediated production of reactive oxygen species and is involved in salt-stress tolerance in *Arabidopsis thaliana*. Plant J 56, 411-422.

Sakamoto, W., Takami, T., 2014. Nucleases in higher plants and their possible involvement in DNA degradation during leaf senescence. J Exp Bot 65, 3835-3843.

Santos, A.L.D., Chaves-Silva, S., Yang, L., Maia, L.G.S., Chalfun-Junior, A., Sinharoy, S., Zhao, J., Benedito, V.A., 2017. Global analysis of the MATE gene family of metabolite transporters in tomato. BMC Plant Biol 17, 185.

Schoenfelder, K.P., Fox, D.T., 2015. The expanding implications of polyploidy. J Cell Biol 209, 485-491.

Sedgwick, S.G., Smerdon, S.J., 1999. The ankyrin repeat: a diversity of interactions on a common structural framework. Trends Biochem Sci 24, 311-316.

Seong, E.S., Choi, D., Cho, H.S., Lim, C.K., Cho, H.J., Wang, M.H., 2007. Characterization of a stress-responsive ankyrin repeat-containing zinc finger protein of *Capsicum annuum* (CaKR1). J Biochem Mol Biol 40, 952-958.

Shabala, S., 2013. Learning from halophytes: physiological basis and strategies to improve abiotic stress tolerance in crops. Ann Bot 112, 1209-1221.

Shabala, S., Bose, J., Hedrich, R., 2014. Salt bladders: do they matter? Trends Plant Sci 19, 687-691.

Shabala, S., Demidchik, V., Shabala, L., Cuin, T.A., Smith, S.J., Miller, A.J., Davies, J.M., Newman, I.A., 2006. Extracellular Ca^{2+} ameliorates NaCl-induced K^+ loss from Arabidopsis root and leaf cells by controlling plasma membrane K^+ -permeable channels. Plant Physiol 141, 1653-1665.

Sharma, M., Pandey, G.K., 2015. Expansion and function of repeat domain proteins during stress and development in plants. Front Plant Sci 6, 1218.

Singh, A., Kanwar, P., Yadav, A.K., Mishra, M., Jha, S.K., Baranwal, V., Pandey, A., Kapoor, S., Tyagi, A.K., Pandey, G.K., 2014. Genome-wide expressional and functional analysis of calcium transport elements during abiotic stress and development in rice. FEBS J 281, 894-915.

Stephens, N.R., Qi, Z., Spalding, E.P., 2008. Glutamate receptor subtypes evidenced by differences in desensitization and dependence on the GLR3.3 and GLR3.4 genes. Plant Physiol 146, 529-538.

Sun, X.L., Yu, Q.Y., Tang, L.L., Ji, W., Bai, X., Cai, H., Liu, X.F., Ding, X.D., Zhu, Y.M., 2013. GsSRK, a G-type lectin S-receptor-like serine/threonine protein kinase, is a positive regulator of plant tolerance to salt stress. J Plant Physiol 170, 505-515.

Takahashi, N., Quimbaya, M., Schubert, V., Lammens, T., Vandepoele, K., Schubert, I., Matsui, M., Inze, D., Berx, G., De Veylder, L., 2010. The MCM-binding protein ETG1 aids sister chromatid cohesion required for postreplicative homologous recombination repair. PLoS Genet 6, e1000817.

Team, R.C., 2018. R: A language and environment for statistical computing; 2015.

Tian, T., Liu, Y., Yan, H., You, Q., Yi, X., Du, Z., Xu, W., Su, Z., 2017. agriGO v2.0: a GO analysis toolkit for the agricultural community, 2017 update. Nucleic Acids Res 45, W122-W129.

Tuteja, N., Mahajan, S., 2007. Calcium signaling network in plants: an overview. Plant Signal Behav 2, 79-85.

Wang, Y., Yang, L., Chen, X., Ye, T., Zhong, B., Liu, R., Wu, Y., Chan, Z., 2016. Major latex protein-like protein 43 (MLP43) functions as a positive regulator during abscisic acid responses and confers drought tolerance in *Arabidopsis thaliana*. J Exp Bot 67, 421-434.

Wang, Z., Gerstein, M., Snyder, M., 2009. RNA-Seq: a revolutionary tool for transcriptomics. Nat Rev Genet 10, 57-63.

Xiong, L., Schumaker, K.S., Zhu, J.K., 2002. Cell signaling during cold, drought, and salt stress. Plant Cell 14 Suppl, S165-183.

Yamasaki, S., Shimada, E., Kuwano, T., Kawano, T., Noguchi, N., 2010. Continuous UV-B irradiation induces endoreduplication and peroxidase activity in epidermal cells surrounding trichomes on cucumber cotyledons. J Radiat Res 51, 187-196.

Yoo, J.H., Park, C.Y., Kim, J.C., Heo, W.D., Cheong, M.S., Park, H.C., Kim, M.C., Moon, B.C., Choi, M.S., Kang, Y.H., Lee, J.H., Kim, H.S., Lee, S.M., Yoon, H.W., Lim, C.O., Yun, D.J., Lee, S.Y., Chung, W.S., Cho, M.J., 2005. Direct interaction of a divergent CaM isoform and the transcription factor, MYB2, enhances salt tolerance in arabidopsis. J Biol Chem 280, 3697-3706.

Zeng, H., Xu, L., Singh, A., Wang, H., Du, L., Poovaiah, B.W., 2015. Involvement of calmodulin and calmodulin-like proteins in plant responses to abiotic stresses. Front Plant Sci 6, 600.

Zhang, J.L., Shi, H., 2013. Physiological and molecular mechanisms of plant salt tolerance. Photosynth Res 115, 1-22.

Zhu, J.K., 2002. Salt and drought stress signal transduction in plants. Annu Rev Plant Biol 53, 247-273.

Chapter 4: A large-scale screening of quinoa accessions reveals important role of epidermal bladder cells and stomatal patterning in salinity tolerance[2]

Abstract

The presence of epidermal bladder cells (EBCs) in halophytes allows considerable amount of Na^+ being accumulated in these external structures, away from the metabolically active mesophile cells. Also, stomatal patterning may represent a primary mechanism by which plants can optimise its water-use efficiency under saline condition. This investigation was aimed to explore the varietal differences in a salinity tolerance of quinoa (*Chenopodium quinoa*) by evaluating a broad range of accessions and linking the overall salinity tolerance with changes in stomatal characteristics and EBC parameters. One hundred and fourteen accessions were grown under temperature-controlled glasshouse under non-saline and 400 mM NaCl conditions, and different physiological and anatomical characteristics were measured. Accessions were classified into three classes (sensitive, intermediate and tolerant) based on a relative dry weight defined as salinity tolerance index (STI). Results showed a large variability in STI indicating a strong genetic variation in salinity tolerance in quinoa. Bladders density was increased in a majority of accessions under saline condition while the bladder's diameter remained unchanged; this resulted in a large variability in a bladder's volume as a dependant variable. Stomata density remained unchanged between saline and non-saline conditions while the stomata length declined between 3% to 43% amongst accessions. Leaf Na^+ concentration varied from 669 µmol/gDW to 3155 µmol/gDW under saline condition and, with an exception of a few accessions, leaf K^+ concentration increased under saline conditions. Correlation analysis indicated a significant positive association between EBC diameter and STI on one hand and

[2] This chapter has been published as: **Kiani-Pouya A,** Rasouli F, Bazihizina N, Zhang H, Hedrich R, Shabala S (2019) A large-scale screening of quinoa accessions reveals important role of epidermal bladder cells and stomatal patterning in salinity tolerance. Environ Exp Bot 168, 103885

EBC volume and STI on the other hand, in a salt-tolerant group. These observations are consistent with the role of EBCs in sequestration of toxic Na^+ in the external structures, away from the cytosol. A negative association was found between EBC density and diameter in salt-sensitive plants. A negative association between STI and stomata length was also found in a salt-tolerant group, suggesting that these plants were able to efficiently regulate stomatal patterning to balance water loss and CO_2 assimilation under saline conditions. Both salt-sensitive and salt-tolerant groups had the same Na^+ concentration in the shoot under saline conditions; however, a negative association between leaf Na^+ concentration and STI in salt-sensitive plants indicated a more efficient Na^+ sequestration process into the EBCs in salt-tolerant plants.

4.1 Introduction

While halophytes and glycophytes have similar salinity tolerance mechanisms at a basic level, halophytes have far superior salinity tolerance ability through developing numerous strategies to adapt to high saline conditions (Shabala and Mackay, 2011). These mechanisms include a range of anatomical and physiological traits (Munns and Tester, 2008; Shabala and Mackay, 2011).

One of the specialised features that distinguishes halophytes from glycophytes is the presence of the epidermal bladder cells (EBCs). EBCs have been found in about 50% of all halophyte species (Flowers and Colmer, 2008) and are located on the leaf surfaces, panicles and stem (Shabala, 2013). Given that EBCs are larger than epidermal cells, they are able to take up a considerable amount of Na^+ away from the photosynthetically active mesophyll cells (Shabala et al., 2014), making it an efficient strategy to confer salinity stress tolerance in halophytes (Ben Hassine et al., 2009). It was long suggested that EBC are essential in maintaining low concentration of Na^+ in leaves and particularly young leaves. Because of small and underdeveloped vacuoles in the mesophyll cells in younger leaves, they do not possess effective internal sequestration mechanisms and rely mainly on EBCs for salt sequestration (Bonales-Alatorre et al., 2013). In our previous work we have shown that a mechanical removal of EBC by gentle brushing results in a salt-sensitive phenotype in quinoa, thus providing the first direct evidence for the role of EBC in salinity tolerance (Kiani-Pouya et al., 2017). However, giving the pioneering nature of that study, many questions remain

unanswered. Is EBC density genetically predetermined or can it be adjusted for saline conditions? Will salinity impact EBC cell size (and, hence, volume)? No answers to these questions are available in the literature.

Many unanswered questions are also related to the stomata patterning as a component of the salt tolerance mechanism. Stomata control the gas exchange between plant and its surrounding environment and serve as a primary gateway for transpirational water loss and CO_2 influx in plant (Lawson and Blatt, 2014). As a result of this process, biomass accumulation in plants is directly proportionate to the amount of assimilated CO_2 and eventually is dependent on the regulation of stomatal aperture (Shabala, 2013). Under saline conditions, both osmotic stress and toxic Na^+ level in the cytosol negatively affect stomatal parameters (Tavakkoli et al., 2012). Why are halophytes capable to optimise their stomata performance? Are there any special strategies in stomata operation that halophytes utilise under salinity stress? How does salinity stress regulate epidermal the fate of epidermal cells leading to either an increase or decrease in the stomata numbers?

Significant advances have been made in understanding mechanisms that control stomatal function and also the signalling pathways that regulate guard cells operation in glycophytes (Casson and Hetherington, 2010). Also advanced is our understanding of the basal genetic pathways that regulate stomatal development, specifically in Arabidopsis (Assmann and Jegla, 2016; Bergmann and Sack, 2007; Wang et al., 2007). In contrast, much less is known about stomata operation in halophytes (Hedrich and Shabala, 2018), and a question on how environmental variables and particularly salinity stress modulates the basal stomatal development pathway requires more investigations. In light of this, understanding the genes regulatory network that control stomatal patterning and thus gas exchange under saline condition could be critical to reduce water loss in salinity-grown plants. Additionally, optimised gas exchange would maintain a high photosynthetic rate for better plant performance under saline conditions (Deinlein et al., 2014; Kim et al., 2010).

The ABA hormone is involved in controlling the closing and opening of stomata in response to alteration in plant water balance (Chen and Gallie, 2004). Can stomatal development be also affected by stress-induced ABA increase? An association between stomatal density and ABA levels was shown in tomato (Okuma et al., 2011) and Arabidopsis (Watkins et al., 2017), where the mutants of

these two plants which were defective in ABA biosynthesis produced higher stomatal numbers, supporting the above hypothesis.

Reduction in the stomatal conductance may occur via either physiological (e.g. changes in a stomatal aperture) or morphological (e.g. decrease in a stomatal density) pathways. It has been argued that alteration in the stomatal density may represent a primary mechanism by which plant can optimize water-use efficiency under salinity stress (Shabala et al., 2013). A comparison between halophyte *Thellungiella halophila* and its glycophyte counterpart Arabidopsis showed that salinity stress increased stomata density in Thellungiella leaves by about twofold (Inan et al., 2004). These results came in a contrast with the suggestion that reduced stomata density may reduce the residual (cuticular) transpiration through the closed stomata (Hasanuzzaman et al., 2018; Shabala, 2013) and, thus, be advantageous to plants. Thus, the question is: can these results from Thellungiella be extrapolated to all halophytes?

The aim of the current study was to evaluate effects of salinity on EBC and stomata patterning and development in quinoa plants and correlate the extent of variability in these traits with the genetic variation in a salinity stress tolerance amongst the large number of quinoa accessions.

4.2 Materials and methods

4.2.1 Plant materials and growth conditions

One hundred and fourteen quinoa accessions were grown from seeds in 15 cm diameter pots filled with standard potting mix under temperature-controlled glasshouse conditions. The standard potting mix was consisted of 90% composted pine bark; 5% coco peat; 5% coarse sand; gypsum at 1 kg/m^3; dolomite at 6 kg/m^3; ferrous sulphate at 1.5 kg/m^3; Osmoform Pre-mix at 1.25 kg/m^3 and controlled-release fertiliser, Scotts Pro at 3 kg/m^3. Day/night temperatures were 20 °C and 15.5 °C; mean humidity 74% and day length 16 h (incandescent lights were set at 6.00 to 9.00 and 16.00 to 22.00 hrs to give the day length hours). The experiment was carried out at the University of Tasmania in Hobart, Australia, between June and August 2017. Ten seeds were sown in each pot and germinating seedlings were then thinned to leave 3 uniform plants per pot a few days before salinity treatment commenced. Seedlings were watered for 14 days with tap water. Salt stress was commenced at 15th day after sowing and 50 mM NaCl was added to the irrigation

water twice daily over 4 days to a final concentration of 400 mM. Plants then were maintained under salt stress for six weeks. At harvesting date, one of the youngest fully expanded leaves from the top was taken for scanning electron microscope images.

4.2.2 Sampling and measurements

For fresh weight (FW) measurements, plants were cut at the base and whole plant immediately weighed. Plants were then dried at 60 °C for 96 hrs to obtain the dry weight (DW).

To quantify the stomata and EBC density of leaves, fresh samples were carefully harvested without causing any damage to the surfaces of one of the youngest fully expanded leaves from 5 individual plants of saline- and non-saline-grown quinoa plants. Leaf sections of 5 x 5 mm were mounted and two images from different leaf zones were taken from the abaxial side of the leaves using scanning electron microscopy (FEI MLA650 ESEM, ThermoFisher Scientific, Oregon, United States) at the environmental mode. A Peltier cooling element maintained the specimen temperature close to 5 °C. Stomatal and EBC density (number of cells per unit of leaf area) was counted from stored SEM images. For those accessions with very high density of bladders, EBCs were removed before images were taken to enable unobstructed view. To determine the EBCs volume we presumed that the EBC is spherical and the volume was calculated based on EBC density per leaf area and EBC diameter. Stomata length and epidermal cell area were measured using the ImageJ analysis software. Stomata and bladder indexes were determined as the ratio of the number of stomata/bladders in a given area divided by the total number of stomata/bladders and epidermal cells in that area. Presented data are the mean ± SE of measurements of 10 different fields of view of the abaxial side of leaves from five individual plants.

Leaf Na^+ and K^+ determinations were conducted from digested leaf samples. One of the youngest fully expanded leaf of plants was harvested and about 0.1 g aliquot of ground dry weight of leaves was used for determination of Na^+ and K^+. Dried leaf samples were mixed with 7 ml of 70% HNO_3 and digested in a Teflon digestion vessel using a microwave digester (MDS-2000 microwave digestion system, CEM Corporation). After digestion the solution was transferred to a 15 ml centrifuge tube and topped up with distilled water to a final volume of 15 ml. Then

an appropriately diluted solution was used to measure Na^+ and K^+ content using the flame photometer.

4.2.3 Grouping of accessions for salt tolerance

In order to allow comparisons among accessions, the measurements of plants DW at 400 mM NaCl were divided by their means under non-saline condition to convert to relative values. The relative DW was then considered as a salinity tolerance index (STI) and values were used to group the accessions. All the quinoa accessions were arbitrarily classified into three classes for salinity tolerance index (sensitive, intermediate and tolerant). The class intervals of tolerance classes were defined as the difference between the lowest and the highest relative values of DW divided by three.

4.2.4 Data analysis

The statistical analysis was carried out by IBM SPSS Statistics 24 software (IBM corp. Armonk, NY, USA). All presented data are mean values of five to ten replicates and accompanied by the standard errors. Significance between different treatments was determined by one-way ANOVA analysis based on Least Significant Distance test. The correlation analyses were applied to determine association between different characteristics under saline condition. To do this, all the studied characteristics measured under saline condition were correlated with STI for each of salt-tolerant, intermediate and sensitive groups.

4.3 Results

4.3.1 Salt stress affects physiological characteristics in quinoa

Imposing 400 mM NaCl on quinoa plants significantly impacted all the studied physiological traits, revealing a large variation among accessions for all characteristics. The mean individual results of physiological characteristics are shown in the Suppl. Table S4.1-2. Salinity stress caused a significant reduction in fresh weight (FW) and dry weight (DW) of all accessions. The FW ranged from 1.36 to 8.25 g $plant^{-1}$ under non-saline condition, and was significantly reduced under saline condition, where the FW varied from 0.62 to 2.92 g $plant^{-1}$ (Suppl. Table S4.1). In relative terms, FW of salt-grown plants were declined between 4% and 87% (Suppl. Table S4.1). Similar to FW, all the accessions had the highest DW under non-saline condition, ranging from 0.14 to 0.75 g $plant^{-1}$ (Suppl. Table S4.1).

DW significantly decreased under saline condition and ranged from 0.06 to 0.31 g plant^{-1}, showing relative variation between 7% and 84% (Fig. 4.1A-C and Suppl. Table S4.1). Collectively, these results indicate a strong genetic variation for salinity tolerance among quinoa accessions.

With an exception of a few accessions, salinity stress significantly increased bladder density in all the quinoa plants and at a maximum amount it increased by more than 3.5-fold (Suppl. Table S4.1). The regression analysis revealed no association between salinity tolerance index (STI) and bladder density for salt-tolerant, intermediate and sensitive groups (Suppl. Fig. S4.1A-C). Bladder diameter remained unchanged in the majority of accessions under saline condition; however, it slightly increased or decreased in a few accessions (Suppl. Table S4.1). In a salt-tolerant group, there was a significant association between STI and a bladder diameter under saline condition while there was not such a relation for intermediate and sensitive groups (Fig. 4.2). EBC volume, as a dependant variable of bladder density and diameter, had a great variation among accessions and ranged from 41% to 339% in relative terms (Suppl. Table S4.1). Ina salt-tolerant group, there was a significant positive correlation between STI and bladder volume under saline condition, while in intermediate and sensitive groups there was no association between these parameters (Fig. 4.2). Accessions also showed a great variation for the bladder index, which ranged from 64% to 291% in relative terms (Suppl. Table S4.1). There was no significant association between STI and the bladder index for all three groups (Suppl. Fig. S4.1D-F).

Salinity stress also significantly affected stomata characteristics. On average for all accessions, stomata density remained unchanged between saline and non-saline conditions. However, a large genetic variability was found for the stomata density amongst accessions, ranging from 67% to 159% in relative terms (Suppl. Table S4.2; Suppl. Fig. S4.2A, B), with some genotypes increasing and some decreasing stomata density. The regression analysis showed a significant positive correlation between STI and stomata density in a salt-tolerant group (Fig. 4.3).

However, the relative length of stomata declined by 3% to 43% in salt-grown plants (Suppl. Table S4.2; Suppl. Fig. 4.3A). This implies that quinoa plants manage to reduce stomatal gas exchange under saline condition by minimising the size of the pore.

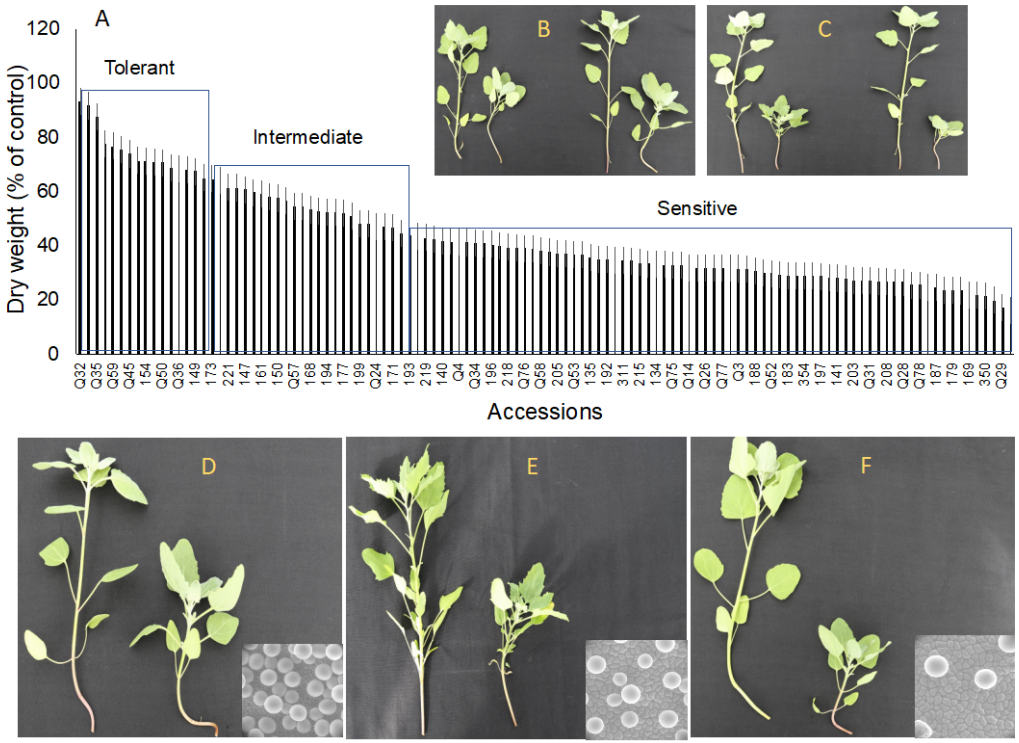

Fig. 4.1 Genetic variability of salinity tolerance in quinoa. A - salinity tolerance index defined as a relative dry weight of studied accession (% of control). Based on this result, all accessions were classified into three major groups including tolerant, intermediate and sensitive groups according to their performance under 400 mM NaCl. B, C - representative images of salt-tolerant and salt-sensitive accessions, respectively; D to F – images of representative plants from salt-tolerant(D), intermediate (E), and salt-sensitive (F) groups grown under non-saline and 400 mM NaCl conditions. The insets are scanning electron microscope images of leaf surface showing bladder density in plant of each group.

Salt-tolerant plants had a negative correlation between STI and stomatal length under saline condition while no association between these parameters was found in intermediate and sensitive groups (Fig. 4.3D-F). Relative changes in stomatal index ranged from 53% to 118% among accessions (Suppl. Table S4.2; Suppl. Fig. 4.3B) and there was no significant association between STI and stomata index in any group (Suppl. Fig. 4.4A-C).

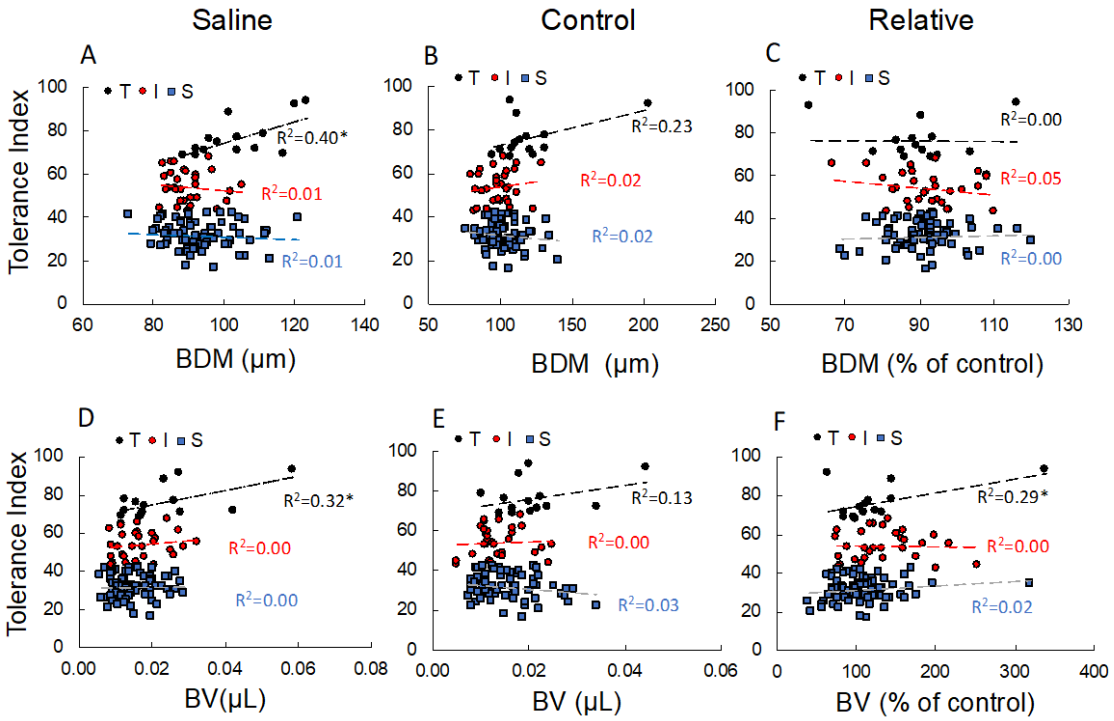

Fig. 4.2 Regression analysis (1) between salinity tolerance index (STI; defined as a relative dry weight) and bladder diameter, and (2) between STI and bladder volume. A, D – saline conditions; B, E – control conditions; C, F – relative change (% control). BDM, bladder cell diameter; BV, bladder cell volume. T, I and S letters in the figures stay for salt-tolerant, intermediate and sensitive groups. Each point represents one accession (a mean of 10 replications).

In respect to epidermal cell area (ECA), quinoa accessions responded differently to salt stress where ECA either declined or increased under saline condition so the relative change varied between 40% and 123% among accessions (Suppl. Table S4.2; Suppl. Fig. S4.2C, D).

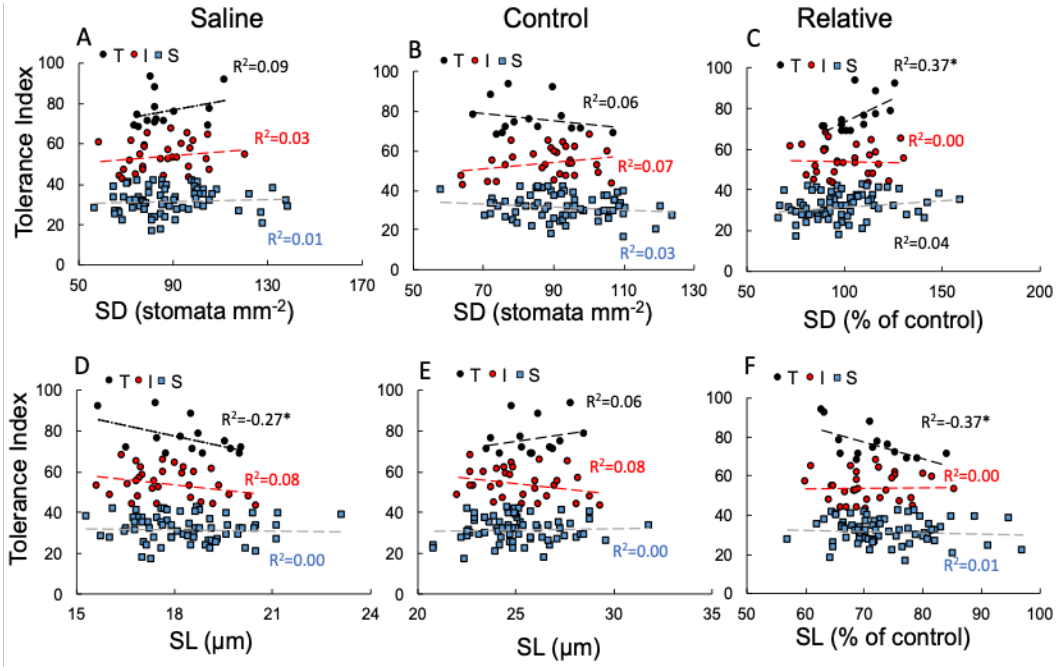

Fig. 4.3 Regression analysis (1) between STI and stomatal density, and (2) between STI and stomatal length. A, D – saline conditions; B, E – control conditions; C, F – relative change (% control). SD, stomatal density; SL, stomatal length. T, I and S letters in the figures stay for salt-tolerant, intermediate and sensitive groups. Each point represents one accession (a mean of 10 replications).

Salinity stress caused a significant increase in leaf Na^+ concentration, with Na^+ content varying between 669 µmol/gDW and 3155 µmol/gDW amongst accessions under saline condition (Suppl. Table S4.2). This result indicates significant genetic variation in quinoa's ability for Na^+ uptake (Suppl. Table S4.2; Suppl. Fig. 4.3C). With an exception of a few accessions, plants grown under saline condition showed higher K^+ content in their leaves compared with non-saline condition (Suppl. Table S4.2; Suppl. Fig. 4.3D). The K^+ concentration ranged from 89% to 258% in accessions grown under 400 mM salinity stress indicating that K^+ uptake was stimulated under saline condition.

4.3.2 Correlation analysis

All the accessions were assigned to three distinct classes based on the relative DW that defined as salinity tolerance indexes (STI). The major bulk of genotypes (70 accessions) was classified as salt-sensitive, while 30 and 14 accessions were categorised as intermediate and salt-tolerant, respectively. The STI of these three

groups were considered as dependent variables and correlated with measured physiological characteristics under 400 mM NaCl (Tables 4.1-4.3).

In the salt-tolerant group, there was a significant correlation between the EBC dimeter and STI (R^2= 0.63; P < 0.05) and also between STI and the bladder volume, indicating that the larger EBCs played a positive role in salinity tolerance (Table 4.1). In salt-sensitive plants on the other hand, there was a negative correlation between STI and leaf Na^+ concentration (R^2= -0.29; P < 0.05) (Table 4.3). This may imply a compromised Na^+ sequestration ability (to move away Na^+ from the photosynthetic active leaves) and, thus, a negative impact on a biomass production. In this regard, in a salt-sensitive group there was a strong negative correlation between bladder density and diameter (R^2 = -0.40; P < 0.01). Taking into account the positive relation between bladder density and bladder index (R^2 = 0.68; P < 0.01) it could be suggested that in salt-sensitive plants higher bladder density resulted in smaller bladders (Table 4.3). Also, there was no significant association between STI and a bladder volume or density in a salt-sensitive group. Instead, results revealed that increasing bladder density had a negative correlation with the bladder diameter and stomatal index (Table 4.3).

While there was a very significant positive correlation (R^2 = 0.73; P < 0.01) between EBC index and a stomata index in a salt-tolerant group (Table 4.1), these two parameters were negatively correlated (R^2 = -0.32; P < 0.01) in a salt-sensitive group (Table 4.3). The simultaneous increase in the bladder and stomata cells density in a salt-tolerant group was achieved through reducing the epidermal cell size (Suppl. Fig. S4.2).

A significant negative correlation between ECA and the bladder density was reported for the intermediate (R^2= -0.58; P < 0.01) and sensitive (R^2= -0.59; P < 0.01) clusters while no such correlation was found in the salt-tolerant group (Tables 4.1-4.3).

A negative correlation between bladder index and stomatal parameters (stomatal density (R^2 = -0.38; P < 0.01), stomatal length (R^2 = -0.28; P < 0.05) and stomatal index (R^2 = -0.32; P < 0.01)) were also found in salt-sensitive plants. This data suggests that the increasing bladder density affected stomatal characteristics which in turn finally affected plant performance under saline conditions (Table 4.3).

Table 4.1 Correlation between physiological characteristics and salinity tolerance index (relative dry weights) in a salt-tolerant cluster under saline condition

	STI	FW	BD	BDM	BV	BI	SD	SL	SI	ECA	Na^+	K^+
STI	1											
FW	0.79**	1										
BD	0.17	0.46	1									
BDM	0.63*	0.5	0.1	1								
BV	0.57*	0.70**	0.80**	0.65*	1							
BI	-0.25	0.11	0.41	0.55*	-0.03	1						
SD	0.3	-0.08	-0.31	0.54*	0.06	-0.40	1					
SL	-0.55*	-0.21	0.15	-0.05	-0.02	0.26	-0.26	1				
SI	-0.34	0.001	0.23	-0.42	-0.06	0.73**	-0.04	0.18	1			
ECA	-0.29	0.07	-0.005	-0.41	-0.19	0.37	0.71**	0.05	0.26	1		
Na^+	0.10	0.06	0.05	0.02	0.12	0.06	0.01	-0.17	0.21	0.32	1	
K^+	0.40	0.34	0.2	0.29	0.3	0.08	0.42	-0.28	0.02	-0.34	0.09	1

Abbreviations:

STI: relative dry weight (% of control); FW: relative fresh weight (% of control); BD: bladder density (cell mm^{-2}); BDM: bladder diameter (μm); BV: bladder volume (μl); BI: bladder index; SD: stomatal density (cell mm^{-2}); SL: stomatal length (μm); ECA: epidermal cell area (μm^2); Na^+: leaf Na^+ concentration (μmol/gDW); K^+: leaf K^+ concentration (μmol/gDW).

Table 4.2 Correlation between physiological characteristics and salinity tolerance index in plants from the intermediate cluster under saline condition

	STI	FW	BD	BDM	BV	BI	SD	SL	SI	ECA	Na^+	K^+
STI	1											
FW	0.64**	1										
BD	0.11	0.32	1									
BDM	-0.11	-0.18	0.15	1								
BV	0.15	0.19	0.82**	0.61**	1							
BI	0.23	0.39*	0.64**	0.28	0.64**	1						
SD	0.18	0.15	0.48**	-0.12	0.39	-0.132	1					
SL	-0.29	-0.28	-0.60**	-0.11	-0.59**	-0.125	-0.67**	1				
SI	0.001	0.42*	-0.06	0.02	-0.08	0.14	-0.008	0.04	1			
ECA	-0.17	-0.12	-0.59**	0.18	-0.42*	0.07	-0.84**	0.76**	0.31	1		
Na^+	-0.05	0.2	-0.1	0.04	-0.004	-0.018	-0.24	0.06	0.20	0.13	1	
K^+	0.02	0.09	0.09	-0.27	-0.171	0.21	-0.07	0.05	-0.02	0.06	-0.37*	1

Abbreviations:

STI: relative dry weight (% of control); FW: relative fresh weight (% of control); BD: bladder density (cell mm^{-2}); BDM: bladder diameter (μm); BV: bladder volume (μl); BI: bladder index; SD: stomatal density (cell mm^{-2}); SL: stomatal length (μm); ECA: epidermal cell area (μm^2); Na^+: leaf Na^+ concentration (μmol/gDW); K^+: leaf K^+ concentration (μmol/gDW).

Table 4.3 Correlation between physiological characteristics and salinity tolerance index in plants from salt-sensitive cluster under saline condition

	STI	FW	BD	BDM	BV	BI	SD	SL	SI	ECA	Na^+	K^+
STI	1											
FW	0.80**	1										
BD	0.09	0.25*	1									
BDM	-0.09	-0.08	-0.40**	1								
BV	0.07	0.22	0.68**	0.31**	1							
BI	-0.04	0.21	0.68**	-0.41**	0.46**	1						
SD	0.07	0.04	0.08	0.14	0.09	-0.38**	1					
SL	-0.04	-0.11	-0.45**	0.35**	-0.24*	-0.28*	-0.30*	1				
SI	-0.15	-0.08	-0.34**	0.38**	-0.14	-0.32**	0.48**	0.24*	1			
ECA	-0.18	-0.13	-0.59**	0.17	-0.40**	-0.01	-0.64**	0.59**	0.17	1		
Na^+	-0.29*	-0.01	0.11	-0.14	0.13	0.40**	-0.41**	-0.11	-0.19	0.27*	1	
K^+	-0.14	-0.13	0.08	-0.13	-0.05	0.06	0.05	-0.18	-0.10	-0.14	-0.14	1

Abbreviations:

STI: relative dry weight (% of control); FW: relative fresh weight (% of control); BD: bladder density (cell mm^{-2}); BDM: bladder diameter (μm); BV: bladder volume (μl); BI: bladder index; SD: stomatal density (cell mm^{-2}); SL: stomatal length (μm); ECA: epidermal cell area (μm^2); Na^+: leaf Na^+ concentration (μmol/gDW); K^+: leaf K^+ concentration (μmol/gDW).

4.4 Discussion

4.4.1 EBCs played an important role in salinity tolerance in quinoa

In a salt-tolerant group, the significant positive correlations between bladder diameter and STI in one hand and bladder volume and STI on the other hand (Table 4.1) indicate that higher external Na^+ sequestration capacity conferred by the larger bladder volume played a positive role in salinity tolerance in quinoa. The mechanistic basis for this is an increased capacity for compartmentalisation of significant amounts of toxic Na^+ in EBCs, as shown before in *Mesembryanthemum crystallinum* (Barkla et al., 2018) and quinoa, where bladderless plant possessed a salt-sensitive phenotype (Kiani-Pouya et al., 2017).

To better understand the contribution of EBCs towards salinity tolerance in quinoa, we have further selected 5 accessions with the highest and lowest bladder volume grown under 400 mM NaCl for detailed analysis (Fig. 4.4A-F). Plants with higher EBC volume had a significantly higher DW, bladder density, and bladder diameter than a group with low bladder volume (Fig. 4.4B-D). Also, plants with high EBC volume had about 5.5 times more EBC sequestration capacity compared to plants with low EBC volume (Table 4.4) indicating that tolerant plants had higher external Na^+ storage on their leaves where EBC act as a major sink for the toxic ions such as Na^+ and Cl^-. Using measured volumes of EBC (Table 4.4) and assuming that the thickness of leaf lamina is about 120 µm, the corresponding volume of the leaf lamina was about 0.12 µl. Thus, in accessions with a high bladder volume, about 40% of the total aerial volume was represented by EBCs while this value for plants with low EBC volume was about 10%. This 4-fold difference resulted in EBCs making a significant contribution towards the total aerial volume in salt-tolerant plants (Table 4.4) and therefore, provided them with a storage capacity for toxic Na^+ and Cl^-. In line with this, we have already calculated that Na^+ and Cl^- concentrations of quinoa EBC could be estimated around 850 mM and 1 M, respectively (Kiani-Pouya et al., 2017). Given that plants with high EBC volume had the same Na^+ concentration in their leaves as plants with a low EBC volume (Fig. 4.4F) and the fact that plant with high EBC volume had higher salt tolerance, it could be speculated that the majority of toxic Na^+ may be transported into the EBCs thus conferring the salinity tolerance of this group.

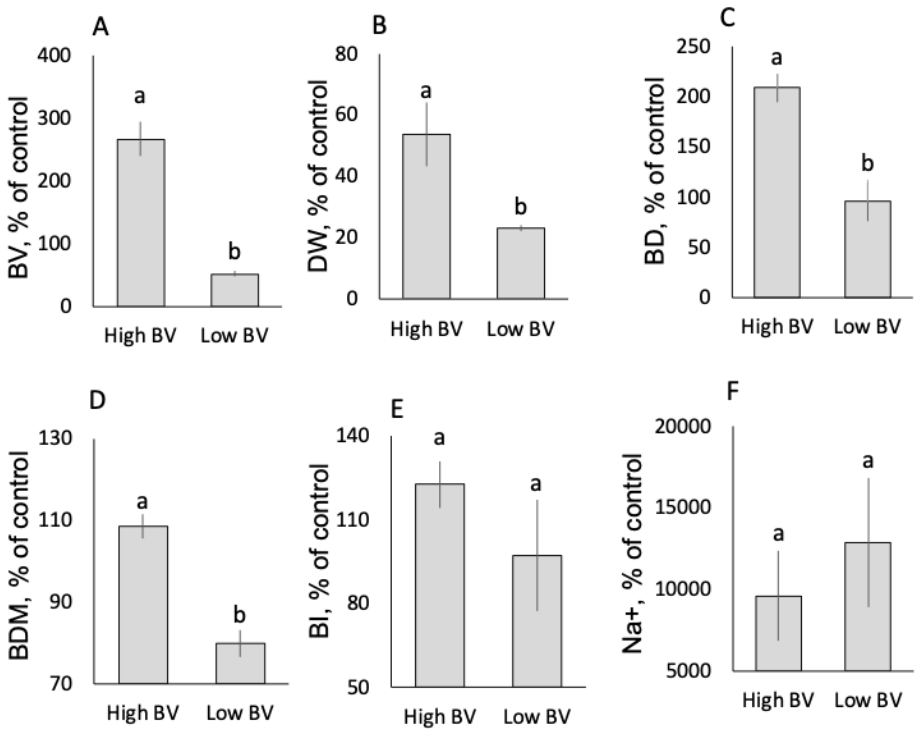

Fig. 4.4 Physiological characteristics of five quinoa accessions grouped based on the highest and lowest bladder volume. Bars show the average pooled data of five quinoa accessions. A - bladder volume, BV; B - dry weight, DW; C - bladder density, BD; D - bladder diameter, BDM; E - bladder index, BI; F - Na^+ concentration. The chosen accessions with higher BV were Q32, 195, 193, Q57, 127 and those with lower BV were Q5, 144, Q65, Q79, and 157. Mean ± SE (n = 5; 25 replications in total). Data labelled with different lower-case letters are significantly different at $P < 0.05$.

The bladder diameter had a major contribution towards salinity tolerance in quinoa; hence, increasing the size and quantity of EBCs may be beneficial to improving salinity tolerance through compartmentalization of Na^+ into EBCs. There is not much information on the mechanisms controlling EBC size in quinoa. Studies on Arabidopsis (Churchman et al., 2006) and *M. crystallinum* (Barkla et al., 2018) showed that, to a large extent, the trichome size is determined by the number of endoreduplications. It has also been revealed in *M. crystallinum* that salinity stress induced endopolyploidy in EBCs and leaves of this plant, with one or two additional rounds of endoreduplication occurring in salt-grown plants (Barkla et al., 2018). This increase in a cell size may contribute to salinity tolerance through increasing the external store volume for Na^+ sequestration. Endopolyploidy involves the tight control of molecular mechanisms that initiate and then maintain

endoreplication in the cell, allowing endocycling cells to replicate their DNA during the synthesis (S) phase but arresting progress to the mitosis phase, cycling instead between the S and gap (G) phases (Barkla et al., 2018). Cyclin-dependent kinases (CDKs), a conserved class of serine/threonine kinases, along with their regulatory subunit cyclins (CYCs) drive unidirectional and irreversible progression from one cell cycle phase to the next by phosphorylating target proteins (Kumar and Larkin, 2017). If similar mechanisms are involved in quinoa, they could be exploited to modify the bladder size through manipulating one or a few genes associated with cyclin production, to further improve external Na^+ storage capacity by controlling EBC size.

Table 4.4 Bladder-related information of five quinoa accessions grouped based on the highest and lowest bladder volume when grown under 400 mM NaCl conditions. It was assumed that the thickness of leaf lamina was about 120 μm. Mean ± SE (n = 5). *Significant and P< 0.01.

	Bladder density (EBC mm^{-2})	Bladder diameter (μm)	Bladder volume on both sides (μL)	% of total aerial volume
High EBC volume	66±5.9 *	104±4.1 *	0.077±0.01 *	38.2±3.24 *
Low EBC volume	16.9±1.8	90.3±0.8	0.014±0.001	10.5±0.51

4.4.2 Salt-sensitive plants failed to coordinate bladder size and density

The superior performance of plants under saline condition depends on numerous anatomical and physiological mechanisms (Ozgur et al., 2013; Shabala and Mackay, 2011). The cell elongation declines under saline conditions, first because of osmotic stress and then due to Na^+ build up (Munns and Tester, 2008; Zhu, 2002). Salt-sensitive plants showed a negative correlation between the bladder density and bladder diameter (Table 4.3). Given that EBCs play an important role in salinity tolerance in quinoa, the failure of this group to produce larger bladder cells resulted in a salt-sensitive phenotype. As it has been discussed in the previous section, this may be potentially explained by the number of endoreduplications occurring in salt-sensitive and tolerant groups.

Not much is known about the molecular mechanisms of EBCs patterning and formation in quinoa but based on the existing knowledge in Arabidopsis, the trichome formation is the result of an interaction between neighbouring epidermal cells (Glover, 2000; Larkin et al., 1996). This process is regulated by a number of

positive and negative regulators such as GLABRA1 and R2R3 MYB transcription factors (Pesch and Hulskamp, 2009) and is also under hormonal control.

On the contrary to the salt-sensitive group, salt-tolerant plants were able to concurrently keep constant density of both stomata and bladder cells under saline condition, mainly through reducing ECA (Table 4.1). The relation between decreasing ECA and salinity tolerance was further confirmed by analysis of 5 accessions with the highest and lowest ECA (Fig. 4.5A-H). As the relative ECA of group with highest area was increased to 119%, the ECA of group with the lowest was markedly reduced to 49.2% (Fig. 4.5A). Plants with a larger cell area significantly had less DW and bladder volume, bladder and stomata densities (Fig. 4.5B,C,E,F). This finding indicates that ECA had an association with all the important salt-responsive characteristics and thus could be considered as an important salt-responsive characteristic in quinoa. For instance, lower ECA resulted in higher bladder and stomata densities which correlated positively with biomass production. Furthermore, the group with bigger ECA also had bigger stomata length and higher leaf Na^+ concentration; as both play a negative role in salinity tolerance, they likely contributed to the salt-sensitive phenotype (Fig. 4.5G-H; Suppl. Fig. S4.5).

An increase in the stomata density was associated with a decrease in ECA (Fig. 4.5F). This strategy was rather different from those reported for other halophytes. For instance, it has been reported that stomatal density reduced under hypersaline condition in *Atriplex halimus* (Boughalleb et al., 2009), *Kochia prostrata* (Karimi et al., 2005) and *Suaeda maritima* (Flowers and Colmer, 2008). The reasons for this discrepancy should be a subject of a separate investigation.

4.4.3 Salt-tolerant plants effectively coordinate stomata length and density

Stomatal transpiration accounts for about 95% of the total water loss (Hedrich and Shabala, 2018) playing a significant role in water use efficiency in plants. Transpirational water loss through stomata are controlled by stomata parameters such as density, structure and aperture (Hetherington and Woodward, 2003) and the results of this investigation revealed that quinoa plants regulate this process through stomata length but not by stomata density. Indeed, while stomata density was not altered under either saline and non-saline conditions, stomata length (as a proxy for stomata aperture) declined on average by 30% in all accessions.

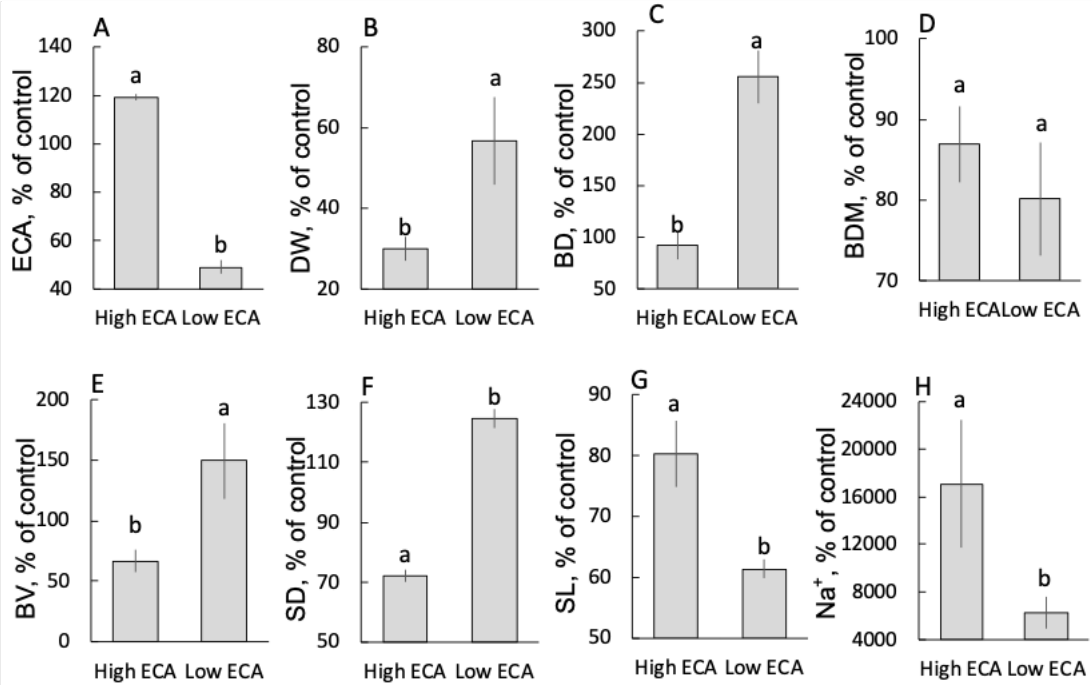

Fig. 4.5 Physiological characteristics of five quinoa accessions grouped based on the highest and lowest epidermal cell area. Bars show the average pooled data of five quinoa accessions. A - epidermal cell area, ECA; B - dry weight; C - bladder density, BD; D - bladder diameter, BDM; E - bladder volume, BV; F - stomata density, SD; G - Stomata length, SL; H - Na^+ concentration. The chosen accessions with higher ECA were 155, 146, 188, 157, Q65 and those with lower ECA were 193, Q68, 217, 208, and 173. Mean ± SE (n = 5; 25 replications in total). Data labelled with different lower-case letters are significantly different at $P < 0.05$.

Salt-tolerant plants, however, employed a different strategy. The negative correlation between STI and stomata length in the salt-tolerant group means that tolerant plants reduced guard cell aperture as a strategy to manage their water loss (Table 4.1). However, this mechanism has a cost for plants, as reduction in the stomatal conductance results in a reduction of photosynthetic rate and thereby decreasing plant biomass production that eventually leads to yield loss (Centritto et al., 2003). A further analysis revealed that salt-tolerant quinoa plants were able to increase stomata density as a compensation mechanism for reduced stomata length (Fig. 4.6D). As a result of this strategy, the gas exchange was efficiently controlled

in a way that it balanced leaf water loss and CO_2 assimilation under saline condition enabling plants to better deal with salt stress. Analysis of 5 accessions with the highest and lowest stomatal length revealed that the group with the smaller stomata length had significantly higher DW, bladder and stomatal densities (Fig. 4.6B-D) indicating that smaller guard cell aperture is compensated by the higher stomata density. Reducing ECA was a primary reason of the increased of other cell types densities e.g. bladder or stomata. In this regard, while ECA increased by 8% in plants with high stomatal length, the cell area decreased by 46% in group with smaller stomata length (Fig. 4.5E).

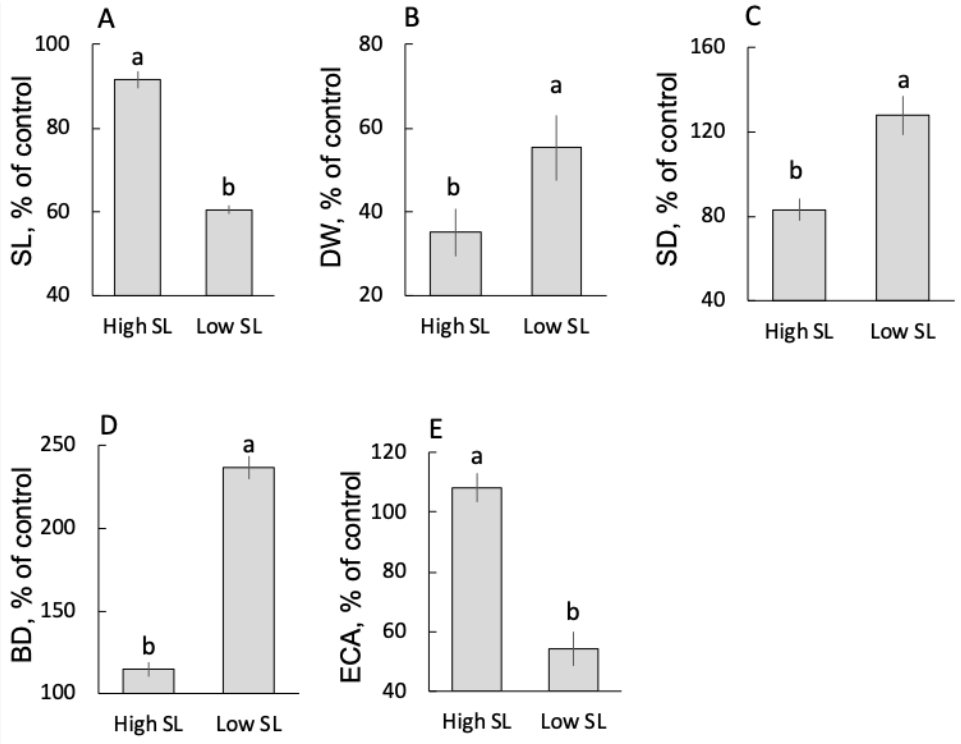

Fig. 4.6 Physiological characteristics of five quinoa accessions grouped based on the highest and lowest stomata length. Bars show the average pooled data of five quinoa accessions. A - Stomata length, SL; B - dry weight, DW; C - stomata density, SD; D - bladder density, BD; E - epidermal cell area, ECA. The chosen accessions with higher SL were Q65, Q58, Q54, 146, 178 and those with lower SL were Q32, 136, 173, 217, and 208. Mean ± SE (n = 5; 25 replications in total). Data labelled with different lower-case letters are significantly different at $P < 0.05$.

The stomatal lineage is dynamic and flexible, altering stomatal production in response to environmental change, with numerous transcriptional regulators,

cell-to-cell signaling and polarity proteins involved (Adrian et al., 2015; Lee and Bergmann, 2019). Like our knowledge of EBCs development, all available information comes from studies on Arabidopsis. Comparing transcriptional profiles of the above key genes between contrasting quinoa accessions may be an important step for targeting stomatal density as a salinity tolerance strategy in plant breeding programs.

4.4.4 Na^+ adversely affected salt-sensitive plants

It has been argued that prevention of Na^+ delivery to the leaves, and particularly young leaves, is a fundamental characteristic of Na^+ sequestration at the whole-plant level in different plant species (Munns, 2002). However, in addition to this general characteristic, halophytes are able to effectively compartmentalise Na^+ into vacuoles to prevent the toxic effects of Na^+ (Flowers and Colmer, 2008). Both salt-sensitive and salt-tolerant groups had the same leaf Na^+ concentration (on average 1649 µmol/gDW and 1700 µmol/gDW in salt-sensitive and tolerant group, respectively) suggesting that the ability of salt-tolerant and sensitive plants in preventing Na^+ entry to the shoot was the same. Also, there was a negative relation between leaf Na^+ concentration and STI in salt-sensitive plants (Table 4.3), which suggests that this group could not cope with high concentration of Na^+ that resulted in a lower biomass production (Table 4.3). Given that Na^+ sequestration into EBCs is one of the most important mechanisms for salinity tolerance in quinoa, this result further confirms the role of EBCs as salt dumpers for the sequestration of toxic ions away from the cytosol.

The findings of the current study revealed that in salt-tolerant quinoa genotypes a combination of higher bladder density and larger EBCs resulted in a higher EBC volume, increasing plant's external capacity for storage of toxic Na^+ and Cl^-. This result shows the important role of EBC in salinity tolerance in quinoa. Furthermore, although salt-tolerant plants had a negative association between STI and stomata length, they were also able to increase stomata density as a compensation strategy for the reduced stomata size. This mechanism indicates the superior ability of salt tolerant plants in regulating stomatal patterning to efficiently balance water loss and CO_2 assimilation under saline conditions.

4.5 References

Adrian, J., Chang, J., Ballenger, C.E., Bargmann, B.O.R., Alassimone, J., Davies, K.A., Lau, O.S., Matos, J.L., Hachez, C., Lanctot, A., Vaten, A., Birnbaum, K.D., Bergmann, D.C., 2015. Transcriptome dynamics of the stomatal lineage: birth, amplification, and termination of a self-renewing population. Develop Cell 33, 107-118.

Assmann, S.M., Jegla, T., 2016. Guard cell sensory systems: recent insights on stomatal responses to light, abscisic acid, and CO_2. Curr Opin Plant Biol 33, 157-167.

Barkla, B.J., Rhodes, T., Tran, K.T., Wijesinghege, C., Larkin, J.C., Dassanayake, M., 2018. Making epidermal bladder cells bigger: developmental- and salinity-induced endopolyploidy in a model halophyte. Plant Physiol 177, 615-632.

Ben Hassine, A., Ghanem, M.E., Bouzid, S., Lutts, S., 2009. Abscisic acid has contrasting effects on salt excretion and polyamine concentrations of an inland and a coastal population of the Mediterranean xero-halophyte species *Atriplex halimus*. Ann Bot 104, 925-936.

Bergmann, D.C., Sack, F.D., 2007. Stomatal development. Annu Rev Plant Biol 58, 163-181.

Bonales-Alatorre, E., Pottosin, I., Shabala, L., Chen, Z.H., Zeng, F., Jacobsen, S.E., Shabala, S., 2013. Differential activity of plasma and vacuolar membrane transporters contributes to genotypic differences in salinity tolerance in a halophyte species, *Chenopodium quinoa*. Int J Mol Sci 14, 9267-9285.

Boughalleb, F., Denden, M., Tiba, B.B., 2009. Anatomical changes induced by increasing NaCl salinity in three fodder shrubs, *Nitraria retusa, Atriplex halimus and Medicago arborea*. Acta Physiol Plant 31, 947-960.

Casson, S.A., Hetherington, A.M., 2010. Environmental regulation of stomatal development. Curr Opin Plant Biol 13, 90-95.

Centritto, M., Loreto, F., Chartzoulakis, K., 2003. The use of low [CO_2] to estimate diffusional and non-diffusional limitations of photosynthetic capacity of salt-stressed olive saplings. Plant Cell Environ 26, 585-594.

Chen, Z., Gallie, D.R., 2004. The ascorbic acid redox state controls guard cell signaling and stomatal movement. Plant Cell 16, 1143-1162.

Churchman, M.L., Brown, M.L., Kato, N., Kirik, V., Hulskamp, M., Inze, D., De Veylder, L., Walker, J.D., Zheng, Z., Oppenheimer, D.G., Gwin, T.,

Churchman, J., Larkin, J.C., 2006. SIAMESE, a plant-specific cell cycle regulator, controls endoreplication onset in *Arabidopsis thaliana*. Plant Cell 18, 3145-3157.

Deinlein, U., Stephan, A.B., Horie, T., Luo, W., Xu, G., Schroeder, J.I., 2014. Plant salt-tolerance mechanisms. Trends Plant Sci 19, 371-379.

Flowers, T.J., Colmer, T.D., 2008. Salinity tolerance in halophytes. New Phytol 179, 945-963.

Glover, B.J., 2000. Differentiation in plant epidermal cells. J Exp Bot 51, 497-505.

Hasanuzzaman, M., Shabala, L., Zhou, M., Brodribb, T.J., Corkrey, R., Shabala, S., 2018. Factors determining stomatal and non-stomatal (residual) transpiration and their contribution towards salinity tolerance in contrasting barley genotypes. Environ Exp Bot 153, 10-20.

Hedrich, R., Shabala, S., 2018. Stomata in a saline world. Curr Opin Plant Biol 46, 87-95.

Hetherington, A.M., Woodward, F.I., 2003. The role of stomata in sensing and driving environmental change. Nature 424, 901-908.

Inan, G., Zhang, Q., Li, P., Wang, Z., Cao, Z., Zhang, H., Zhang, C., Quist, T.M., Goodwin, S.M., Zhu, J., Shi, H., Damsz, B., Charbaji, T., Gong, Q., Ma, S., Fredricksen, M., Galbraith, D.W., Jenks, M.A., Rhodes, D., Hasegawa, P.M., Bohnert, H.J., Joly, R.J., Bressan, R.A., Zhu, J.K., 2004. Salt cress. A halophyte and cryophyte Arabidopsis relative model system and its applicability to molecular genetic analyses of growth and development of extremophiles. Plant Physiol 135, 1718-1737.

Karimi, G., Ghorbanli, M., Heidari, H., Khavari Nejad, R.A., Assareh, M.H., 2005. The effects of NaCl on growth, water relations, osmolytes and ion content in *Kochia prostrata*. Biol Plantarum 49, 301-304.

Kiani-Pouya, A., Roessner, U., Jayasinghe, N.S., Lutz, A., Rupasinghe, T., Bazihizina, N., Bohm, J., Alharbi, S., Hedrich, R., Shabala, S., 2017. Epidermal bladder cells confer salinity stress tolerance in the halophyte quinoa and *Atriplex* species. Plant Cell Environ 40, 1900-1915.

Kim, T.H., Bohmer, M., Hu, H., Nishimura, N., Schroeder, J.I., 2010. Guard cell signal transduction network: advances in understanding abscisic acid, CO_2, and Ca^{2+} signaling. Annu Rev Plant Biol 61, 561-591.

Kumar, N., Larkin, J.C., 2017. Why do plants need so many cyclin-dependent kinase inhibitors? Plant Signal Behavior 12, 2.

Larkin, J.C., Young, N., Prigge, M., Marks, M.D., 1996. The control of trichome spacing and number in Arabidopsis. Development 122, 997-1005.

Lawson, T., Blatt, M.R., 2014. Stomatal size, speed, and responsiveness impact on photosynthesis and water use efficiency. Plant Physiol 164, 1556-1570.

Lee, L.R., Bergmann, D.C., 2019. The plant stomatal lineage at a glance. J Cell Sci 132,

Munns, R., 2002. Comparative physiology of salt and water stress. Plant Cell Environ 25, 239-250.

Munns, R., Tester, M., 2008. Mechanisms of salinity tolerance. Annu Rev Plant Biol 59, 651-681.

Okuma, E., Jahan, M.S., Munemasa, S., Hossain, M.A., Muroyama, D., Islam, M.M., Ogawa, K., Watanabe-Sugimoto, M., Nakamura, Y., Shimoishi, Y., Mori, I.C., Murata, Y., 2011. Negative regulation of abscisic acid-induced stomatal closure by glutathione in Arabidopsis. J Plant Physiol 168, 2048-2055.

Ozgur, R., Uzilday, B., Sekmen, A.H., Turkan, I., 2013. Reactive oxygen species regulation and antioxidant defence in halophytes. Funct Plant Biol 40, 832-847.

Pesch, M., Hulskamp, M., 2009. One, two, three...models for trichome patterning in Arabidopsis? Curr Opin Plant Biol 12, 587-592.

Shabala, S., 2013. Learning from halophytes: physiological basis and strategies to improve abiotic stress tolerance in crops. Ann Bot 112, 1209-1221.

Shabala, S., Bose, J., Hedrich, R., 2014. Salt bladders: do they matter? Trends Plant Sci 19, 687-691.

Shabala, S., Hariadi, Y., Jacobsen, S.E., 2013. Genotypic difference in salinity tolerance in quinoa is determined by differential control of xylem Na^+ loading and stomatal density. J Plant Physiol 170, 906-914.

Shabala, S., Mackay, A., 2011. Ion transport in halophytes,. Adv Bot Res 57, 151-199.

Tavakkoli, E., Fatehi, F., Rengasamy, P., McDonald, G.K., 2012. A comparison of hydroponic and soil-based screening methods to identify salt tolerance in the field in barley. J Exp Bot 63, 3853-3867.

Wang, H., Ngwenyama, N., Liu, Y., Walker, J.C., Zhang, S., 2007. Stomatal development and patterning are regulated by environmentally responsive mitogen-activated protein kinases in Arabidopsis. Plant Cell 19, 63-73.

Watkins, J.M., Chapman, J.M., Muday, G.K., 2017. Abscisic acid-induced reactive oxygen species are modulated by flavonols to control stomata aperture. Plant Physiol 175, 1807-1825.

Zhu, J.K., 2002. Salt and drought stress signal transduction in plants. Annu Rev Plant Biol 53, 247-273.

Chapter 5: Understanding the role of root-related traits in salinity tolerance of quinoa accessions with contrasting epidermal bladder cells patterning [3]

Abstract

Our previous studies indicated that sequestration of toxic Na^+ and Cl^- ions into epidermal bladder cells (EBCs) is an efficient mechanism conferring salinity tolerance in quinoa. However, some halophytes do not develop EBCs but still possess superior salinity tolerance. To elucidate the possible compensation mechanism(s) underlying superior salinity tolerance in the absence of the external salt storage capacity, we have selected four quinoa accessions with contrasting patterns of EBC development. Whole-plant physiological and electrophysiological characteristics were assessed after 2 days and 3 weeks of 400 mM NaCl stress. Both accessions with low EBC volume utilised Na^+ exclusion at the root level and were capable to maintain low Na^+ concentration in leaves, to compensate for the inability to sequester Na^+ load in EBC. These conclusions were further confirmed by electrophysiological experiments showing higher Na^+ efflux from roots of these varieties (measured by a non-invasive microelectrode MIFE technique) as compared to accessions with high EBC volume. Furthermore, accessions with low EBC volume had significantly higher K^+ concentration in their leaves upon long-term salinity exposures compared to plants with high EBC sequestration ability, suggesting that the ability to maintain high K^+ content in the leaf mesophyll was as another important compensation mechanism.

5.1 Introduction

Halophytes are considered as plants with a superior ability to use specialized mechanisms to survive under high-saline conditions (Shao et al., 2014). Many of them are able to compartmentalise toxic ions such as Na^+ and Cl^- in the specialized epidermal bladder cell (EBC). The latter trait enables halophytes to effectively take

[3] This chapter has been submitted to Planta journal: **Kiani-Pouya A,** Rasouli F, Lana Shabala, Ayesha T.Tahir, Meixue Zhou, Shabala S (2019) Understanding the role of root-related traits in salinity tolerance of quinoa accessions with contrasting epidermal bladder cells patterning.

away excessive salt from the metabolically active tissues and transfer it into EBCs operating as salt dumps, therefore contributing to overall salinity tolerance (Shabala et al., 2014). Our previous study showed that sequestration of toxic Na^+ ions into EBCs is an efficient mechanism contributing to salinity tolerance in quinoa, as compromising this ability by the mechanical removal of EBC resulted in a salt-sensitive phenotype (Kiani-Pouya et al., 2017). Also, our large-scale quinoa germplasm screening revealed a strong correlation between the bladder's storage capacity and salinity tolerance indicating that the larger bladders with higher densities had a positive role in salinity tolerance (Kiani-Pouya et al., 2019). The molecular identity of key transporters involved in accumulation of Na^+ and Cl^- in EBCs in quinoa has been recently revealed (Bohm et al., 2018) and characterized at the functional level.

However, at least 50% of all halophytes do not utilize glands or EBCs to optimize their tissue ion concentrations (Shabala, 2013). For instance, Suaeda is representative of a group of very tolerant halophyte plants that are able to accommodate salt in the shoots without the need for salt compartmentalisation into external bladders (Flowers and Colmer, 2008). Given that these plants still possess superior salinity tolerance capability suggests the existence of multiple mechanisms for salinity tolerance, allowing plants to compensate for the lack of EBC sequestration ability. These mechanisms are numerous (Barkla et al., 2012; Bressan et al., 2001; Ozgur et al., 2013; Shabala et al., 2014; Shabala and Mackay, 2011), and it remains to be answered which of them plays a major role to compensate quinoa plants for the absence of external salt storage in EBCs, to deal with the salt stress.

In most cases, the lack of EBC is compensated by the pronounced succulency in plant shoots, allowing large amounts of salt to be stored in enlarged vacuoles in specialised storage tissues (Flowers and Colmer, 2008; Zeng et al., 2018). In lay terms, these plants simply switched from external to internal salt storage. However, the succulency is typically found in halophytic dicots and often not observed in grass species (Flowers and Colmer, 2008); it is also not pronounced in quinoa. This suggests that other compensation mechanisms (such as root traits) may also confer salinity tolerance in halophytes. What are their roles in quinoa?

In this work, we hypothesised that EBC sequestration is not the only mechanism behind the salinity tolerance in quinoa, and plants with low EBC

volume (and, hence, compromised ability for the external Na^+ storage) should have compensation mechanism(s) to deal with excessive salt. Amongst possible candidates are efficient osmotic adjustment and osmoprotection, traits that maintain optimal ion homeostasis, and developmental and physiological control of stomatal operation (Flowers and Colmer, 2008; Munns and Tester, 2008; Shabala et al., 2014; Shabala and Mackay, 2011). Of specific interest are mechanisms regulating Na^+ and K^+ transport and homeostasis (Schroeder et al., 2013). Plants are able to reduce the amount of accumulated Na^+ by its efficient exclusion at the root level. This exclusion is mediated by the plasma membrane-localized salt overly sensitive 1 (SOS1) transporter (Qiu et al., 2002). Halophytes like quinoa also rely heavily on the use of inorganic ions to maintain cell turgor (Shabala, 2013). Potassium is the major cation present in the cytosol (with concentrations 100 mM and above) and thus is critical for this purpose. However, a massive K^+ leakage from the cytosol of root and leaf tissues occurs under salinity stress in all plants (Shabala et al., 2006) which leads to K^+ pool depletion and may trigger programmed cell death in plant tissues through activation of enzymes associated with protein catabolism (Demidchik et al., 2010). Under this circumstances, efficient K^+ retention ability has the main contribution to salinity tissue tolerance. Can the lack of EBC sequestration ability for Na^+ be then compensated by a better K^+ retention in plant tissue(s)?

In this study, four quinoa accessions were selected from our previous experiment that possessed different EBC patterning and contrasting salt tolerance. These accessions were used in a series of glasshouse and laboratory experiments to understand the mechanistic basis of compensatory mechanisms conferring salinity stress tolerance.

5.2 Materials and Methods

5.2.1 Plant material and growth conditions

Two relatively salt-sensitive quinoa accessions (195 and Q30) and two salt-tolerant accessions (Q68 and Q21) were used in this study (Fig. 5.1). Throughout the text, these are abbreviated as S (for sensitive) and T (tolerant) and referred as HBV and LBV for high- and low-EBC bladder volume, respectively. Plants were grown from seeds in 20 cm diameter pots filled with a mixture of 70% sand and 30% perlite under temperature-controlled glasshouse conditions at the University of Tasmania

in Hobart, Australia. Seeds were irrigated with a half-strength modified Hoagland's nutrient solution. The nutrient solution composition was as follows: KNO_3 (3 mM), Ca $(NO_3)_2$ $4H_2O$ (2.5 mM), KH_2PO_4 (0.17 mM), $MgSO_4.7H_2O$ (1.5 mM), Fe as sodium ferric diethylenetriamine pentaacetate (NaFeDTPA) (50 µM), H_3BO_3 (23 µM), $MnSO_4$ H_2O (5 µM), $ZnSO_4$ $7H_2O$ (0.4 µM), $CuSO_4$ $7H_2O$ (0.2 µM), and H_2MoO_4 (0.1 µM). After germination, the nutrient solutions were replaced with a full-strength modified Hoagland's solution. Day/night temperatures was 22 °C and 16 °C; the mean humidity 74% and a day length 16 h (incandescent lights were set at 6.00 to 9.00 and 16.00 to 22.00 hrs to give the day length hours). Fifteen seeds were sown in each pot. Germinated seedlings were then thinned to leave 4 uniform plants per pot a few days before salinity treatment commenced. Experiment was organised in a completely randomised design, with each treatment including four replications. Seedlings were watered for 14 days with a tap water and the salt stress was then commenced at 15th day after sowing, with NaCl salt added to the irrigation water. Plants were watered twice daily, and salinity concentration was increased by 50 mM increments over 4 days to reach a final concentration of 400 mM NaCl. Plants then were maintained under salt stress for 3 weeks. Different physiological and electrophysiological parameters were assessed after short (2 days) and long-term (3 weeks) of 400 mM NaCl stress.

5.2.2 Leaf sap Na^+ and K^+ concentration

To measure Na^+ and K^+ concentrations, one of the youngest fully expanded leaves was harvested at two days and three weeks after imposing 400 mM NaCl. The harvested leaves placed into Eppendorf tubes (Eppendorf South Pacific, NSW, Australia) and immediately frozen. For ion content and osmolality determinations, the leaves were thawed and the sap then was extracted through squeezing the leaves. To remove debris, the extracted sap was centrifuged at 7000 rpm for 5 min. About 25-50 µL of the collected leaf sap was diluted with an appropriate volume of distilled water to measure K^+ and Na^+ contents using a flame photometer (Corning 410C, Essex, UK). Five replicates were used for each treatment.

5.2.3 MIFE non-invasive ion flux measurements

Net Na^+ and K^+ fluxes were measured using non-invasive ion-selective vibrating microelectrodes (the MIFE technique; University of Tasmania, Hobart, Australia).

The principles of MIFE ion flux measurements and details of microelectrodes fabrication and calibration are fully described elsewhere (Shabala et al., 2006; Shabala et al., 1997). In brief, borosilicate glass capillaries (GC150-10; Clark Electrochemical instruments, Pangbourne, Berks, UK) were pulled out using a vertical puller, then dried overnight at 225 °C, and silanized with tributilchlorosilane (Cat. no. 90796; Fluka, Busch, Switzerland). Electrodes were then back-filled using backfilling solutions (200 mM/L KCl for K^+ and 500 mM/L NaCl for Na^+) and tips of respective electrodes were front-filled with commercially available ionophore cocktails (Na^+ catalogue No. 71176 and K^+, catalogue No. 71176; both from Sigma-Aldrich, Castle Hill, NSW, Australia) and finally calibrated with respective standards. The electrodes that had a slope above 50 mV per decade with a correlation above 0.999 were used for measurement.

5.2.4 MIFE experimental protocols for Na^+ and K^+ flux measurements

For K^+ flux measurement, seeds of quinoa accessions were surface sterilized with 10% commercial bleach for 10 min and then rinsed thoroughly with deionized water for 30 min. Seeds were sown on the filter paper in 90-mm Petri dish and grown for 3 days in an incubator at 24 °C. The germinated seedlings were then immobilized in a Petri dish and pre-conditioning in a Basic Salt Media solution (BSM: 0.1 mmol/L $CaCl_2$ and 0.5 mmol/L KCl) for 30 min. Steady-state K^+ fluxes were recorded for 5 min from the mature zone of the root (5 mm from the root tip). Then, treatment of 200 mM NaCl was administered and net fluxes of K^+ were measured for further 30 min.

To measure Na^+ efflux, plants were grown in a mixture of 70% sand and 30% perlite for two weeks with tap water and then continue growing under non-saline and 400 mM NaCl conditions for additional three weeks as described above. A so-called 'recovery protocol' (Cuin et al., 2011) was then used to measure the magnitude of Na^+/H^+ exchanger-mediated Na^+ efflux from the epidermal root tissue. An apical root segment was cut and thoroughly rinsed with 10 mM $CaCl_2$ solution, to remove apoplastic NaCl. The root segment was then transferred into a clean chamber containing Na^+-free BSM solution (with/without 0.1 mM amiloride). Na^+ flux measurements were conducted in the elongation zone, between 250-500 μm from the root cap.

5.2.5 RNA extraction and RT-qPCR experiments

Harvesting plant samples for real-time qPCR was carried out at 3 weeks after imposing 400 NaCl salt stress. About 100 mg of fresh roots were harvested and used immediately for extraction. The total RNA was extracted from roots by grinding in a liquid nitrogen using Isolate II RNA Mini Kit (Bioline, NSW, Australia) according to the manufacturer's instructions. The first-strand cDNA was synthetised using QuantiTect Reverse Transcription Kit (Qiagen). Relative transcript levels of CqSOS1, CqNHX, CqSKOR, CqGORK and CqEF-1a as a reference gene were determined using a real-time qPCR analysis by Qiagen Rotor-gene PCR system. RT-qPCR experiments were as follows: 95 °C for 2 min, 95 °C for 10 sec, 55 °C for 15 sec and 72 °C for 20 sec. Amplified gene products were detected using QuantiNova SYBR Green PCR Kit (Qiagen). Each data point consisted of three biological and two technical replicates and as shown as mean ± SE. Details on primers are presented in Suppl. Table S5.1. The reported data is presented as relatively values (e.g. transcript levels under saline conditions divided by the corresponding values under control conditions) with normalization of data to the average of the internal control of the housekeeping gene.

5.2.6 Statistical analysis

Data were analysed using IBM SPSS Statistics 24 software (IBM corp. Armonk, NY, USA). Unless stated otherwise, the presented data represent a mean of five replicates and is accompanied by the standard errors. A one-way analysis of variance and treatment mean separations were performed using Duncan's multiple range test at 5% level of significance.

5.3 Results

5.3.1 Biomass and EBCs characteristics of selected accessions

Four contrasting quinoa accessions were chosen for this study from a large-scale screening experiment (Fig. 5.1). Accessions Q68 and Q21 with 68.9% and 71.9% relative DW under saline conditions were classified as salt-tolerant plants (T), representing HBV and LBV accessions, respectively. Accessions Q195 and Q30 with a relative DW of 41.9% and 42.8% respectively, were deemed as salt-sensitive. They also had contrasting EBC volume (HBV and LBV, respectively; Fig. 5.1).

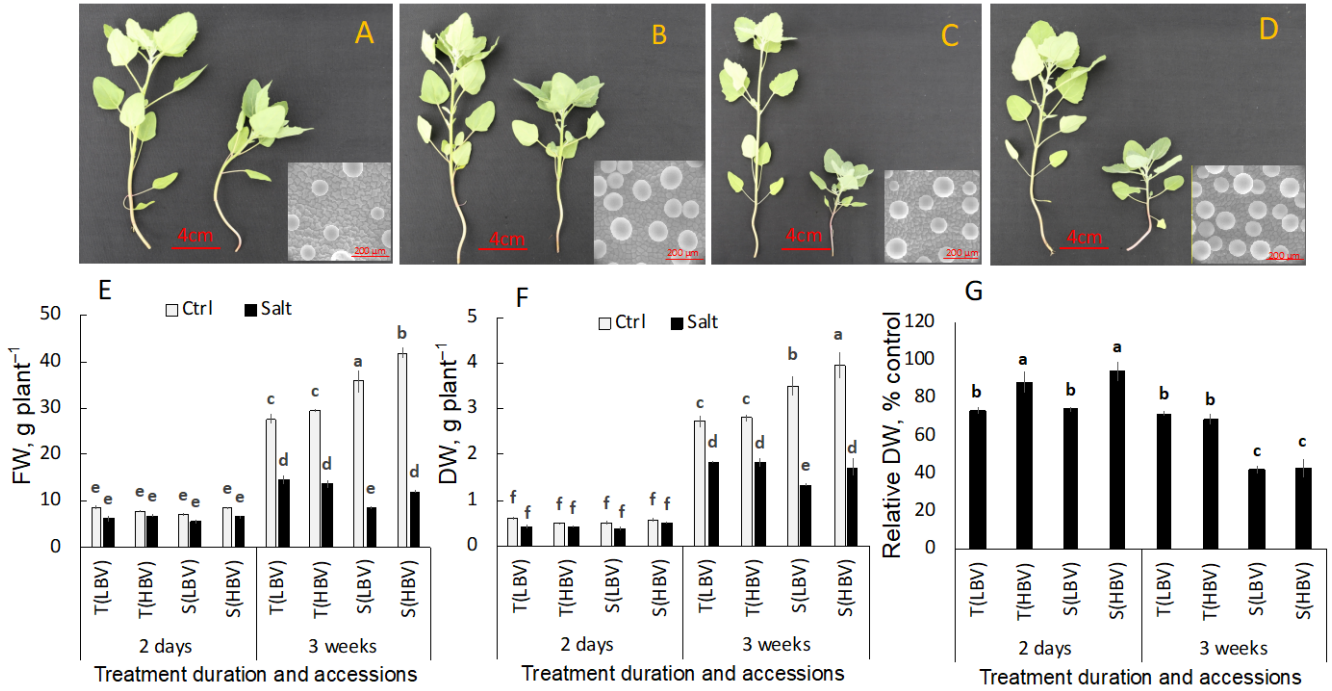

Fig. 5.1 Biomass and epidermal bladder cells (EBCs) patterning of selected accessions. Accessions used are: (A) accession Q21 - salt-tolerant with low EBC volume; abbreviated as T(LBV); (B) accession Q68 - salt-tolerant with high EBC volume, T(HBV); (C) accession Q30 - salt-sensitive with low EBC volume, S(LBV); (D) accession 195 - salt-sensitive with low EBC volume, S(HBV). The insets are scanning electron microscope images of leaf surface showing bladder density in each accession. E-G - fresh and dry weights of four quinoa accessions grown under control and saline (400 mM NaCl) conditions. Mean ± SE (n = 5). E - fresh weigh (g plant^{-1}); F - dry weight (g plant^{-1}); G - relative weight (% control). Data labelled with different lower-case letters are significantly different at $P < 0.05$. FW = fresh weight; DW = dry weight; Ctrl = control.

The specific information on the bladder density and EBC diameters of studied accessions grown in the presence of 400 mM NaCl is given in Table 5.1. As one can see, the difference in the EBC volume between HBV and LBV varieties was at least two-fold (Table 5.1). Assuming that the EBC density is equal at the both sides of the leaf and the thickness of the leaf lamina is about 120 μm, the corresponding volume of the leaf lamina would be about 0.12 μl. Thus, as shown in Table 5.1, in HBV accessions EBC comprised about one-third of the total aerial volume, representing a major potential sink for external Na^+ storage.

Table 5.1 Bladder-related information of 4 quinoa accession grown under 400 mM NaCl conditions. It was assumed that the thickness of leaf lamina was about 120 μm. Mean ± SE (n = 5).

	Accession	Bladder density (cell/mm^2)	Bladder diameter (μm)	Bladder volume (μl)	% of total aerial volume
Salt-tolerant	T(LBV)	17.5±1.3	111.5±5.5	0.025±0.001	17.5±1.23
	T(HBV)	29.8±2.2	120.3±2.7	0.055±0.002	31.5±2.45
Salt-sensitive	S(HBV)	82.4±8.6	84.6±2.3	0.056±0.002	31.8±2.3
	S(LBV)	58±3.5	80.2±3.3	0.031±0.001	20±1.91

5.3.2 Leaf and root sap ionic analysis

Two days after imposing 400 mM salt stress, Na^+ contents in leaves and roots of both salt-sensitive and tolerant plants significantly increased compared to control plants; the numbers were even higher after 3 weeks of salt stress (Fig. 5.2A, B). In leaves, the highest Na^+ content was recorded in accession S(HBV) and there was not significant difference among other accessions (Fig. 5.2A). Consistent with this result, S(LBV) had Na^+ concentration as low as salt-tolerant plants (Fig. 5.2A). In roots, Na^+ concentration in T(LBV) was the lowest after 2 days of salt exposure whereas T(HBV) had Na^+ concentration (Fig. 5.2B). However, after 3 weeks of salinity stress both salt-tolerant accessions had the same Na^+ concentration in their roots which were significantly lower compared with those in salt-sensitive plants (Fig. 5.2B).

There was not significant difference in the leaf K^+ content amongst accessions either before stress or after 2 days of salt exposure. After 3 weeks of salinity stress, leaf K^+ concentration was significantly increased in all accessions (Fig. 5.2C).

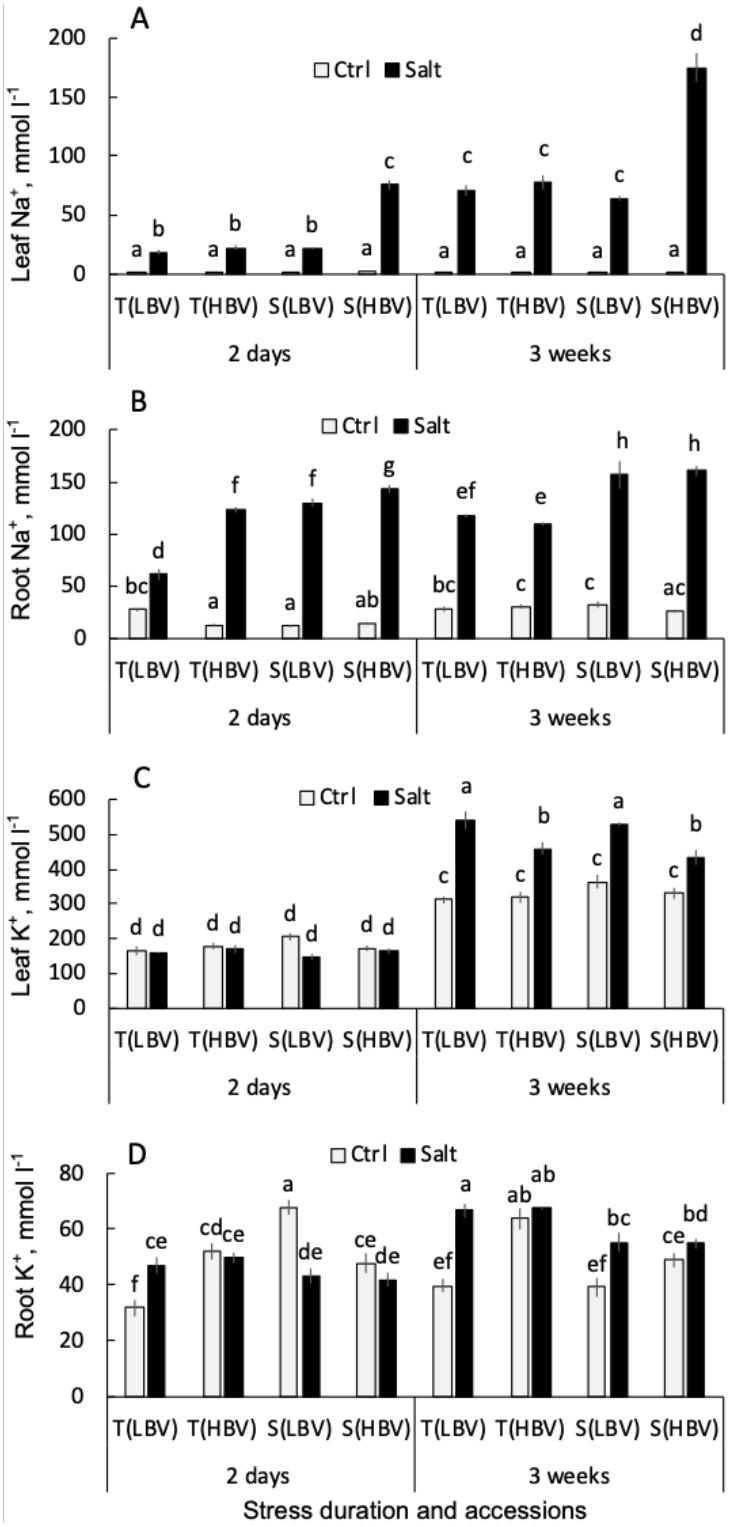

Fig. 5.2 Na^+ and K^+ concentrations (mmol/l) of leaf and root sap of four quinoa accessions grown under control and saline (400 mM NaCl) conditions. Mean ± SE (n = 5). A - leaf sap Na^+; B - root sap Na^+; C - leaf sap K^+; D - root sap K^+. Data labelled with different lower-case letters are significantly different at $P < 0.05$.

T(LBV) and S(LBV) had significantly higher K^+ concentration compared to their counterparts (Fig. 5.2C). K^+ concentration in roots of all accessions increased significantly upon long-term salinity exposure, with salt-tolerant accessions having higher K^+ concentration than salt-sensitive plants; however, there was not significant difference between plants with high and low EBC volume (Fig. 5.2D).

5.3.3 Na^+ flux from the root

Salt-treated and control roots of quinoa accessions grown for 2 days and 3 weeks under 400 mM NaCl were compared for their ability to exclude Na^+. When transferred to Na^+-free media, net Na^+ efflux was recorded from the root epidermis in all accessions. This efflux was strongest in the root elongation zone (where SOS1 Na^+/H^+ exchanger is predominantly located; Shi et al., 2002) and observed only in salt-grown plants (Fig. 5.3). Net Na^+ efflux was higher in plants exposed to longer salinity treatments (Fig. 5.3). At short-term salt stress, the highest net Na^+ efflux (-37.9 nmol/m^2 s^1) was measured from salt-tolerant accession T(LBV) and the lowest (-8.1 nmol/m^2 s^1) signal was from salt-sensitive accession S(HBV) (Fig. 5.3). Under long-term salinity stress, accession T(HBV) with -56.5 nmol/m^2 s^1 and S(HBV) with -12.9 nmol/m^2 s^1 had the highest and lowest Na^+ efflux, respectively (Fig. 5.3). Roots pre-treatment with 0.5 mM amiloride (a known inhibitor of Na^+/H^+ SOS1 exchanger; Wu et al. 2019) reduced root Na^+ extruding ability by ca 90% (Fig. 5.3).

5.3.4 NaCl-induced K^+ flux from root

Adding 200 mM NaCl to the bath solution resulted in a rapid and massive net K^+ efflux from mature root zone in all accessions (Fig. 5.4A). The peak K^+ efflux was highest in salt sensitive accessions compared with their salt-tolerant counterparts. The lowest response was measured form T(LBV) (Fig. 5.4). In both sensitive and tolerant groups, varieties with LBV had less net K^+ efflux compared with varieties with HBV (Fig. 5.4), indicative of a compensation mechanism. Both salt tolerant accessions showed a higher steady-state K^+ efflux compared to sensitive plants after exposing to salt stress where K^+ efflux for T(LBV) and T(HBV) were -37.5 and -33.2 nmol/m^2 s^1 respectively and these values for S(LBV) and S(HBV) were -63.3 and -66.2 nmol/m^2 s^1 (Fig. 5.4).

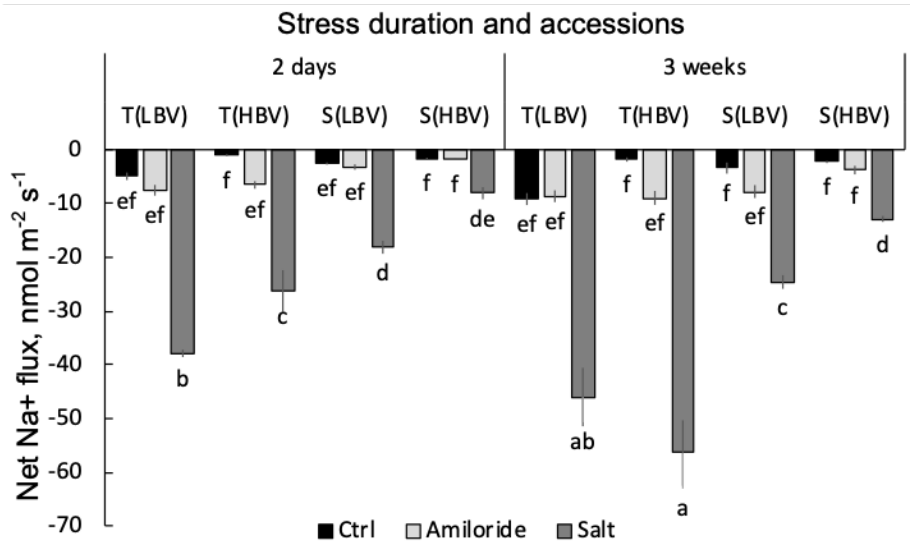

Fig. 5.3 Net Na^+ fluxes measured in 'recovery protocols' from the elongation zone (250-500 μm from root tip) of four quinoa accessions after pre-conditioning in Basic Salt Media solution (BSM: 0.1 mmol/L $CaCl_2$ and 0.5 mmol/L KCl) containing 100 μM amiloride for 20 min. Before measurement, plants were grown in a mixture of 70% sand and 30% perlite for two weeks with tap water and then continue growing under non-saline and 400 mM NaCl conditions for additional 3 weeks. Mean ±SE (n=6-8). Inserts in each panel denote the steady-state Na^+ efflux 5 min after the removal of the pre-conditioning solution. Data labelled with different lower-case letters are significantly different at $P < 0.05$. The flux convention is "efflux negative".

5.3.5 Transcript levels of salt transporters under saline conditions

The transcript levels of CqSOS1, CqNHX, CqGORK, and CqSKOR were measured in root tissues of all quinoa accessions grown for 3 weeks under 400mM salinity stress compared to their corresponding plants grown under non-saline conditions, and then normalized to the expression level of housekeeping gene CqEF-1a.

A comparative analysis of CqSOS1 indicated that this gene was significantly up-regulated under saline conditions in all accessions (Fig. 5.5). However, the expression level of salt-tolerant genotypes was higher compared with their sensitive counterparts. The highest increase in CqSOS1 expression level

(more than 5-fold) was observed in T(HBV) (Fig. 5.5). Similar to CqSOS1, the transcript level of

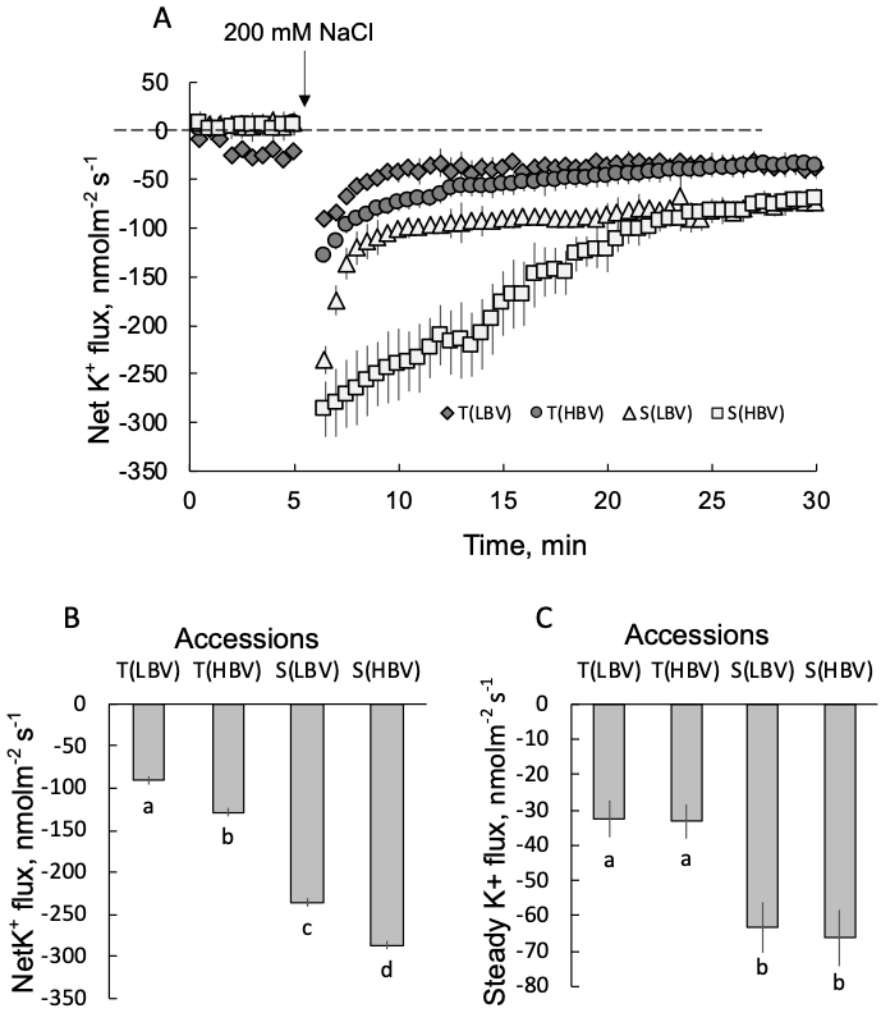

Fig. 5.4 A - kinetics of NaCl-induced K^+ efflux from roots of four quinoa accessions. Net K^+ fluxes were measured from the mature zone (5 mm from root tip) of 3 days old seedlings pre-conditioned in Basic Salt Media solution. B - peak K^+ efflux values from root samples exposed to 200 mM NaCl; C - steady-state K^+ efflux measured from root samples 40 min after exposure to salt stress. Mean ± SE (n=6-8). Data labelled with different lower-case letters are significantly different at $P < 0.05$.

CqNHX1 was higher in salt-tolerant plants compared to sensitive ones, with the strongest response in T(LBV) (Fig. 5.5). On the contrary to above mentioned trends, the transcript level of GORK and SKOR genes in salt-tolerant accessions either

remained unchanged or reduced while the activity of these genes increased in salt-sensitive accessions under saline conditions (Fig. 5.5).

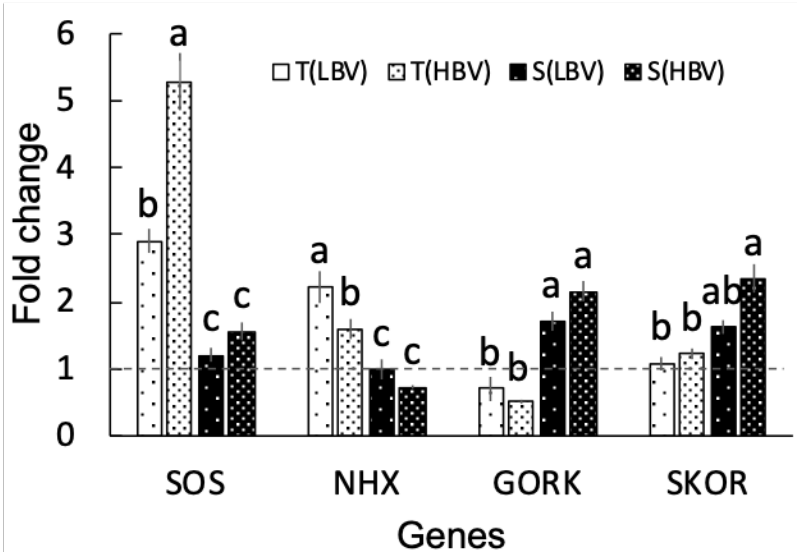

Fig. 5.5 The relative transcript level of CqSOS1, CqNHX, CqSKOR, CqGORK in roots of four quinoa accessions (from plants exposed to 400 mM NaCl for 3 weeks). Each data point is mean ± SE of three technical replicates each representing six biological samples.

5.4 Discussion

5.4.1 Na^+ exclusion ability from the root compensates for the lack of EBC

Na^+ exclusion from the shoot and its restriction from entry to the plant at the root level are among the most important salinity tolerance mechanisms in plant species. However, as the amount of Na^+ that can be retrieved from the shoot and moved be backed to the root is very small (Lei et al., 2014), Na^+ exclusion from roots has long been recognised as a key physiological characteristic contributing to salt tolerance (Munns and Tester, 2008). In the presence of EBCs, quinoa plants have the ability to sequester toxic Na^+ away from metabolically-active cellular compartments in the leaf. In the absence of a possibility for large external Na^+ storage in low EBC volume (LBV) accessions, Na^+ exclusion at the root level and maintaining low Na^+ concentration in leaves could be considered as primary compensation mechanism (Fig. 5.2A, B). Both T(LBV) and S(LBV) accessions had lower Na^+ content at the root level after 2 days of salt stress in comparison to their counterparts with high EBC volume (Fig. 5.2B). Also, both accessions had low leaf Na^+ concentration

after 3 weeks of salinity stress showing that they were able to limit Na^+ entry to the shoot in the absence of high external Na^+ storage (Fig. 5.2A).

T(LBV) and S(LBV) had efficient Na^+ extrusion at the root level resulted in higher ability for net Na^+ efflux ability from the root epidermis compared with plants with higher EBC volume, upon short-term salt exposures (Fig. 5.3). Thus, these accessions employed Na^+ exclusion from the root uptake as a compensation mechanism for the lack of a high EBC volume. This finding suggests that an active Na^+ efflux system is present to remove the Na^+ out of the root cells of plants with low EBC volume. The most suitable candidates for this role are Na^+/H^+ exchangers at the plasma membrane encoded by SOS1 gene. Earlier pharmacological and genetic experiments showed operation of such exchangers in roots of wheat (Cuin et al., 2011; Feki et al. 2014), Arabidopsis (Ullah et al., 2016) and barley (Wu et al., 2019). Gene expression results are consistent with the notion that the plasma membrane Na^+ efflux transporter CqSOS1 operates in the removal of Na^+ out of the root cells (Fig. 5.5), with higher CqSOS1 transcript levels found in salt-tolerant accessions. Consistent with previous findings (Ruiz-Carrasco et al., 2011), salinity exposure resulted in a 5-fold upregulation of CqSOS1 transcript levels in T(HBV). This is in agreement with the observed changes in root Na^+ concentration of studied plants in physiological experiments (Fig. 5.2B).

Vacuolar NHX1 exchangers play a critical role in the intracellular Na^+ sequestration in glycophytes (Xu et al., 2008; Zhang et al., 2001). Most of these studies, however, deal with vacoular Na^+ sequestration in the shoot. In the current study the significantly higher transcript level of CqNHX1 at the root level in T(LBV) compared to T(HBV) may indicate that this antiporter has an active role in compartmentalisation of Na^+ into the vacuole in *roots* thus conferring a compensation strategy when plants lack high EBC volume as an external Na^+ storage in the shoot (Fig. 5.5).

5.4.2 K^+ retention as a component of the compensation mechanism

K^+ plays a vital role in many cell functions. A strong correlation between salinity tolerance and root K^+ retention ability has been found in glycophytes such as wheat (Cuin et al., 2011), rice (Feng et al., 2019), maize (Cao et al., 2019) and barley (Chen et al., 2007). Quinoa as a halophytic plant has a high ability to retain K^+ under unfavorite conditions (Bonales-Alatorre et al., 2013). In a line with the role

of K^+ in salinity tolerance, T(LBV) and S(LBV) had significantly higher K^+ concentration in their leaves at long-term (3 weeks) salinity stress compared to plants with high EBC sequestration ability (Fig. 5.2B), suggesting that the ability to maintain high K^+ content under saline condition may play an important role as a component of the tissue-tolerance mechanism, to compensate for the lack of ability to sequester salt lead in EBCs. Given the fact that plants with low EBC sequestration may have higher Na^+ concentration in their cytosol, taking up high level of K^+ can improve salinity tolerance.

Potassium is known to activate over 50 enzymes (Marschner et al., 1995) including Rubisco and enzymes that playing a role in the chlorophyll biosynthesis. Thus, reduced K^+/Na^+ ratio in the cytosol as a result of accumulation of higher concentration of Na^+ in leaf may compromise plant's CO_2 assimilation capacity. Consistent with this notion, Wu et al., (2015) showed that K^+ retention ability in photosynthetically active mesophyll tissue was an important characteristic contributing to the overall salt tolerance in barley plants. Under this circumstance, the higher ability of quinoa to avoid reduction of K^+ content and to keep optimal K^+/Na^+ ratio in their cytosol, as observed in T(LBV) and S(LBV), may be considered as an important compensation strategy for the lack of EBC sequestration ability. NaCl-induced K^+ leakage of studied accessions showed that accessions with low EBC volume (T(LBV) and S(LBV)) had less K^+ loss when imposed to 200 mM NaCl (Fig. 5.4A-C) and also had significantly higher leaf K^+ content than their counterparts with HBV (T(HBV) and S(HBV)) (Fig. 5.2C). As the loss of K^+ from leaves may trigger programmed cell death (Shabala, 2009) and accelerate leaf senescence, such K^+ retention in the mesophyll may be a critical component of the tissue tolerance mechanism. For example, Arabidopsis *gork1-1* mutant plants which lacking functional outward- rectifying K^+ channels had tenfold lower of number of cells undergoing programmed cell death compared with wild type (Demidchik et al., 2010). The mechanism behind is that reactive oxygen species activated K^+ efflux through GORK channels in wild type plant that resulted in significantly higher K^+ loss from plant cells that stimulates programmed cell death (Demidchik et al., 2014).

Electrophysiological and genetic studies showed that depolarization-activated outward rectifying K^+ channels (GORK in Arabidopsis) are the major

route for the NaCl-induced K^+ efflux from cells (Bose et al., 2014; Gaymard et al., 1998). Here we found a higher transcript level of CqGORK in S(LBV) and S(HBV) explaining the greater extent of K^+ loss from these accessions. The physiological rationale behind this upregulation may be a need for K^+ efflux as a safety valve to cope with the initial depolarization of the plasma membrane under saline conditions (Alvarez-Pizarro et al., 2009) in these plants.

Altogether, to compensate for the lack of capacity for external salt storage in epidermal bladder cells, quinoa plants employ compensation mechanisms such as higher Na^+ extrusion from the root and better K^+ retention in mesophyll, to confer salinity stress tolerance.

5.5 References

Alvarez-Pizarro, J.C., Gomes-Filho, E., de Lacerda, C.F., Alencar, N.L.M., Prisco, J.T., 2009. Salt-induced changes on H^+-ATPase activity, sterol and phospholipid content and lipid peroxidation of root plasma membrane from dwarf-cashew (*Anacardium occidentale*) seedlings. Plant Growth Regul 59, 125-135.

Barkla, B.J., Vera-Estrella, R., Pantoja, O., 2012. Protein profiling of epidermal bladder cells from the halophyte *Mesembryanthemum crystallinum*. Proteomics 12, 2862-2865.

Bohm, J., Messerer, M., Muller, H.M., Scholz-Starke, J., Gradogna, A., Scherzer, S., Maierhofer, T., Bazihizina, N., Zhang, H., Stigloher, C., Ache, P., Al-Rasheid, K.A.S., Mayer, K.F.X., Shabala, S., Carpaneto, A., Haberer, G., Zhu, J.K., Hedrich, R., 2018. Understanding the molecular basis of salt sequestration in epidermal bladder cells of *Chenopodium quinoa*. Curr Biol 28, 3075-3085.

Bonales-Alatorre, E., Pottosin, I., Shabala, L., Chen, Z.H., Zeng, F., Jacobsen, S.E., Shabala, S., 2013. Differential activity of plasma and vacuolar membrane transporters contributes to genotypic differences in salinity tolerance in a halophyte species, *Chenopodium quinoa*. Int J Mol Sci 14, 9267-9285.

Bose, J., Shabala, L., Pottosin, I., Zeng, F., Velarde-Buendia, A.M., Massart, A., Poschenrieder, C., Hariadi, Y., Shabala, S., 2014. Kinetics of xylem loading, membrane potential maintenance, and sensitivity of K^+-permeable channels to

reactive oxygen species: physiological traits that differentiate salinity tolerance between pea and barley. Plant Cell Environ 37, 589-600.

Bressan, R.A., Zhang, C., Zhang, H., Hasegawa, P.M., Bohnert, H.J., Zhu, J.K., 2001. Learning from the Arabidopsis experience. The next gene search paradigm. Plant Physiol 127, 1354-1360.

Cao, Y., Liang, X., Yin, P., Zhang, M., Jiang, C., 2019. A domestication-associated reduction in K^+-preferring HKT transporter activity underlies maize shoot K^+ accumulation and salt tolerance. New Phytol 222, 301-317.

Chen, Z.H., Cuin, T.A., Zhou, M.X., Twomey, A., Naidu, B.P., Shabala, S., 2007. Compatible solute accumulation and stress-mitigating effects in barley genotypes contrasting in their salt tolerance. J Exp Bot 58, 4245–4255. .

Cuin, T.A., Bose, J., Stefano, G., Jha, D., Tester, M., Mancuso, S., Shabala, S., 2011. Assessing the role of root plasma membrane and tonoplast Na^+/H^+ exchangers in salinity tolerance in wheat: in planta quantification methods. Plant Cell Environ 34, 947-961.

Demidchik, V., Cuin, T.A., Svistunenko, D., Smith, S.J., Miller, A.J., Shabala, S., Sokolik, A., Yurin, V., 2010. Arabidopsis root K^+-efflux conductance activated by hydroxyl radicals: single-channel properties, genetic basis and involvement in stress-induced cell death. J Cell Sci 123, 1468-1479.

Demidchik, V., Straltsova, D., Medvedev, S.S., Pozhvanov, G.A., Sokolik, A., Yurin, V., 2014. Stress-induced electrolyte leakage: the role of K^+-permeable channels and involvement in programmed cell death and metabolic adjustment. J Exp Bot 65, 1259-1270.

Feng, H., Tang, Q., Cai, J., Xu, B., Xu, G., Yu, L., 2019. Rice OsHAK16 functions in potassium uptake and translocation in shoot, maintaining potassium homeostasis and salt tolerance. Planta 250, 549-561.

Flowers, T.J., Colmer, T.D., 2008. Salinity tolerance in halophytes. New Phytol 179, 945-963.

Gaymard, F., Pilot, G., Lacombe, B., Bouchez, D., Bruneau, D., Boucherez, J., Michaux-Ferriere, N., Thibaud, J.B., Sentenac, H., 1998. Identification and disruption of a plant shaker-like outward channel involved in K^+ release into the xylem sap. Cell 94, 647-655.

Kiani-Pouya, A., Rasouli, F., Bazihizina, N., Zhang, H., Hedrich, R., Shabala, S., 2019. A large-scale screening of quinoa accessions reveals an important role

of epidermal bladder cells and stomatal patterning in salinity tolerance. Environ Exp Bot, 103885.

Kiani-Pouya, A., Roessner, U., Jayasinghe, N.S., Lutz, A., Rupasinghe, T., Bazihizina, N., Bohm, J., Alharbi, S., Hedrich, R., Shabala, S., 2017. Epidermal bladder cells confer salinity stress tolerance in the halophyte quinoa and *Atriplex* species. Plant Cell Environ 40, 1900-1915.

Lei, B., Huang, Y., Sun, J., Xie, J., Niu, M., Liu, Z., Fan, M., Bie, Z., 2014. Scanning ion-selective electrode technique and X-ray microanalysis provide direct evidence of contrasting Na^+ transport ability from root to shoot in salt-sensitive cucumber and salt-tolerant pumpkin under NaCl stress. Physiol Plant 152, 738-748.

Marschner, H., George, E., Römheld, V., 1995. Preface to Second Edition, in: Marschner, H. (Ed.), Mineral Nutrition of Higher Plants. Academic Press, London, pp vii-viii.

Munns, R., Tester, M., 2008. Mechanisms of salinity tolerance. Annu Rev Plant Biol 59, 651-681.

Ozgur, R., Uzilday, B., Sekmen, A.H., Turkan, I., 2013. Reactive oxygen species regulation and antioxidant defence in halophytes. Funct Plant Biol 40, 832-847.

Qiu, Q.S., Guo, Y., Dietrich, M.A., Schumaker, K.S., Zhu, J.K., 2002. Regulation of SOS1, a plasma membrane Na^+/H^+ exchanger in *Arabidopsis thaliana*, by SOS2 and SOS3. Proc Natl Acad Sci 99, 8436-8441.

Ruiz-Carrasco, K., Antognoni, F., Coulibaly, A.K., Lizardi, S., Covarrubias, A., Martinez, E.A., Molina-Montenegro, M.A., Biondi, S., Zurita-Silva, A., 2011. Variation in salinity tolerance of four lowland genotypes of quinoa (*Chenopodium quinoa*) as assessed by growth, physiological traits, and sodium transporter gene expression. Plant Physiol Biochem 49, 1333-1341.

Schroeder, J.I., Delhaize, E., Frommer, W.B., Guerinot, M.L., Harrison, M.J., Herrera-Estrella, L., Horie, T., Kochian, L.V., Munns, R., Nishizawa, N.K., Tsay, Y.F., Sanders, D., 2013. Using membrane transporters to improve crops for sustainable food production. Nature 497, 60-66.

Shabala, S., 2009. Salinity and programmed cell death: unravelling mechanisms for ion specific signalling. J Exp Bot 60, 709-712.

Shabala, S., 2013. Learning from halophytes: physiological basis and strategies to improve abiotic stress tolerance in crops. Ann Bot 112, 1209-1221.

Shabala, S., Bose, J., Hedrich, R., 2014. Salt bladders: do they matter? Trends Plant Sci 19, 687-691.

Shabala, S., Demidchik, V., Shabala, L., Cuin, T.A., Smith, S.J., Miller, A.J., Davies, J.M., Newman, I.A., 2006. Extracellular Ca^{2+} ameliorates NaCl-induced K^+ loss from Arabidopsis root and leaf cells by controlling plasma membrane K^+-permeable channels. Plant Physiol 141, 1653-1665.

Shabala, S., Mackay, A., 2011. Ion Transport in Halophytes, in: Turkan, I. (Ed.), Plant Responses to Drought and Salinity Stress - Developments in a Post-Genomic Era. Academic Press, pp 151-199.

Shabala, S.N., Newman, I.A., Morris, J., 1997. Oscillations in H^+ and Ca^{2+} ion fluxes around the elongation region of corn roots and effects of external pH. Plant Physiol 113, 111-118.

Shao, Q., Han, N., Ding, T., Zhou, F., Wang, B., 2014. SsHKT1;1 is a potassium transporter of the C3 halophyte (*Suaeda salsa*) that is involved in salt tolerance. Funct Plant Biol 41, 790-802.

Ullah, A., Dutta, D., Fliegel, L., 2016. Expression and characterization of the SOS1 Arabidopsis salt tolerance protein. Mol Cell Biochem 415, 133-143.

Wu, H., Shabala, L., Zhou, M., Su, N., Wu, Q., Ul-Haq, T., Zhu, J., Mancuso, S., Azzarello, E., Shabala, S., 2019. Root vacuolar Na^+ sequestration but not exclusion from uptake correlates with barley salt tolerance. The Plant Journal.

Wu, H., Zhu, M., Shabala, L., Zhou, M., Shabala, S., 2015. K^+ retention in leaf mesophyll, an overlooked component of salinity tolerance mechanism: a case study for barley. J Integr Plant Biol 57, 171-185.

Xu, H., Jiang, X., Zhan, K., Cheng, X., Chen, X., Pardo, J.M., Cui, D., 2008. Functional characterization of a wheat plasma membrane Na^+/H^+ antiporter in yeast. Arch biochem and biophys 473, 8-15.

Zeng, F., Shabala, S., Maksimovic, J.D., Maksimovic, V., Bonales-Alatorre, E., Shabala, L., Yu, M., Zhang, G., Zivanovic, B.D., 2018. Revealing mechanisms of salinity tissue tolerance in succulent halophytes: a case study for *Carpobrotus rossi*. Plant Cell Environ 41, 2654-2667.

Zhang, H.X., Hodson, J.N., Williams, J.P., Blumwald, E., 2001. Engineering salt-tolerant *Brassica* plants: characterization of yield and seed oil quality in transgenic plants with increased vacuolar sodium accumulation. Proc Natl Acad Sci 98, 12832-12836.

Chapter 6: Stomatal traits as a determinant of superior salinity tolerance in wild barley [4]

Abstract

Wild barley *Hordeum spontaneum* (WB) is the progenitor of a cultivated barley *Hordeum vulgare* (CB). WB plants have evolved efficient mechanisms to survive in harsh environments. Understanding mechanisms by which WB cope with abiotic stresses may open prospects of transferring these promising traits to the high yielding CB genotypes. This study aimed to investigate the strategies that WB plants utilise in regard to the control of stomatal operation and ionic homeostasis to deal with salinity stress, one of the major threats to the global food security. Twenty-six genotypes of WB and CB were grown under glasshouse conditions and exposed to 300 mM NaCl salinity treatment for 5 weeks followed by their comprehensive physiological assessment. WB had higher relative biomass than CB when exposed to salinity stress. Under saline conditions, WB plants were able to keep constant stomatal density (SD) while SD significantly decreased in CB. The higher SD in WB also resulted in a higher stomatal conductance (g_s) under saline conditions, with g_s reduction being 51% and 72% in WB and CB, respectively. Furthermore, WB showed faster stomatal response to light, indicating their better ability to adapt to changing environmental conditions. Experiments with isolated epidermal strips indicated that CB genotypes have the higher stomatal aperture when incubated in 80 mM KCl solution, and its aperture declined when KCl was substituted by NaCl. On the contrary, WB genotype had the highest stomatal aperture being exposed to 80 mM NaCl suggesting that WB plants may use Na^+ instead of K^+ for stomata movements. Overall, o*ur* data suggest that CB employ a stress-escaping strategy by reducing stomata density via developmental mechanisms controlling stomatal lineage, to conserve water, when grown under salinity conditions. WB, on a contrary, is capable to utilize Na^+ for stomatal

[4] This chapter has been submitted to J Plant Physiol, **Kiani-Pouya A,** Rasouli F, Rabbi B, Falakboland Z, Yong M, Chen Z, Zhou M, Shabala S (2019) Stomatal traits as a determinant of superior salinity tolerance in wild barley.

operation. Understanding the molecular basis of this process may allow incorporating these traits in elite CB varieties to improve its salinity stress tolerance.

6.1 Introduction

Soil salinization is becoming a serious problem in agricultural systems and is a major factor which affects crop productivity in irrigated land (Zorb et al., 2019). Thus, salt tolerant crops are required to ensure global food security and meet a target of feeding predicted 9.6 Bln people by 2050 (Fita et al., 2015). In this context, understanding plant salinity tolerance mechanisms is vital to develop sustainable plant production strategies. Salinity stress inhibits plant growth and productivity by imposing several major constraints including reduced water availability (osmotic stress), specific ion (Na^+ or Cl^-) toxicity, and increased ROS production (oxidative stress) (Munns and Tester, 2008). Accordingly, plant adaptation to hypersaline conditions relies on a plethora of anatomical (leaf succulence; stomatal structure and patterning; root suberization; salt glands or bladders), physiological (rapid osmotic adjustment; intracellular ion sequestration; exclusion from uptake) and biochemical (e.g. higher antioxidant activity) mechanisms (Ahmed et al., 2013; Flowers et al., 1986; Shabala and Munns, 2012). Salinity stress tolerance is very complex and cannot be attributed to operation of one specific gene. Pyramiding several genes or physiological traits contributing to salt tolerance, in one ideotype, can be considered as the rationale strategy to improve crop performance under saline conditions (Hedrich and Shabala, 2018; Shabala and Cuin, 2008; Yeo and Flowers, 1985; Zhu, 2002).

Salinity stress tolerance was largely reduced during crop domestication as a result of selection for high yield and quality under optimal conditions (El-Esawi et al., 2018). In this regard, genetic improvement of crops by introgression of important agronomic genes from their wild relatives has been considered as one of the most economically viable solutions to enhance crop performance to increase tolerance to salinity stress (Ashraf et al., 2009). Although barley (*Hordeum vulgare*) as a cultivated crop has the highest salt-tolerance potential amongst cereal crops (Steppuhn et al., 2005), it has been argued that the narrow genetic diversity of this species has increased its sensitivity to salt stress (Zhu, 2002). On the other hand, WB has shown wider genetic diversity in salinity tolerance as compared with CB (Ahmed et al., 2013). WB species have a promising adaptive genetic variation for

biotic and environmental stresses and these genetic variations and adaptabilities suggest the potential of WB as a valuable germplasm source for improving barley salt tolerance. It was reported that more than 50% of wild *Hordeum* species occupy habitats ranging from mildly saline pastures to highly saline lands (Garthwaite et al., 2005). Salinity stress tolerance of wild barley has been previously reported (Han et al., 2018; Nevo and Chen, 2010; Wu et al., 2013), but there is still a lack of information to decipher the underlying mechanisms of salinity tolerance of WB species (Garthwaite et al., 2005).

Plant yield is ultimately determined by their ability to gain and assimilate carbon dioxide (CO_2) which is regulated by the fine-tune of the stomatal aperture (Chen et al., 2017; Zhao et al., 2019). Efficient stomatal operation involves balancing CO_2 intake for photosynthesis and commitment to transpiration that accounts for about 95% of total water loss by the plant (Hetherington and Woodward, 2003). Stomatal operation is strongly affected by salinity (Liu et al., 2017); such operation is more efficient in halophytes (naturally salt-loving plants) compared with their glycophytic counterparts (Hedrich and Shabala, 2018). Effect of salinity on stomatal characteristics is complex, with both stomatal conductance, and stomatal size and density being affected (Liu et al., 2014; Peng et al., 1998). For instance, a positive correlation between transpiration rate and stomatal density have been reported in barley (Miskin et al., 1972) and wheat (Wang and Clarke, 1993). Also, significant association has been found between stomatal traits (e.g. guard cell size and stomatal aperture width) and grain yield in salt-tolerant cultivars indicating that stomatal parameters may have contribution to salt tolerance in this crop (Liu et al., 2017). However, none of these studies employed wild relatives of cereal crops to explore the links between the stomatal traits and salinity tolerance.

The wild barley (*Hordeum spontaneum*) is a progenitor of CB, which has evolved efficient mechanisms to survive in harsh environments (Dai et al., 2018; Wang et al., 2018) and have a wide range of environmental adaptability to limited water availability, soil conditions, and extreme temperatures (Garthwaite et al., 2005). These mechanisms are numerous and include, but are not limited to, root system anatomy, thick and complex cuticular waxes, efficient exclusion of toxic ions, and regulation of stress-responsive genes and metabolites (Wang et al., 2018). However, little is known about differences in stomatal patterning and operation between WB and CB genotypes. Do WB and CB reduce their stomatal apertures to

save water under salinity stress? Or does WB as a salt-tolerant species has a superior ability to maintain a constant stomatal operation under saline conditions, regardless of the soil water potential imposed by high salt? Do WB and CB use identical stomatal patterning strategy to cope with salinity stress? Given the fact that plant biomass production is ultimately associated with the amount of water evaporated through the stomatal pores, different adaptive strategies for WB and CB under saline conditions are of high importance. Improving our understanding on this matter could be beneficial for plant breeding efforts through proposing appropriate traits to be designed and included in breeding programs for saline tolerance in crops.

Another important aspect in tackling salinity stress is for plants deal with Na^+ toxicity. Under saline conditions, Na^+ and K^+ are amongst the most abundant ions for plants and K^+ is highly accumulated in guard cells because its main role in stomata opening (Wang et al., 2013; Zhao et al., 2019). However, early experiments with epidermal peels of *Commelina communis* have shown that Na^+ was equally effective as K^+ in promoting stomatal opening although the stomatal responses to different treatments such as CO_2, darkness and ABA inhibition of opening were higher in KCl than in NaCl (Jarvis and Mansfield, 1980; MacRobbie, 1983). More recent study using halophyte *Mesembryanthemum crystallinum* plants showed that Na^+ concentration dramatically is increased in the guard cells during stomatal opening, indicating that guard cells can use Na^+ instead of K^+ to increase osmotic pressure (Chiang et al., 2016). Together, these findings suggest that Na^+ is potentially able to drive the stomatal opening in relatively low concentrations and stomatal closure under salinity stress. However, whether guard cells can use Na^+ instead of K^+ to increase osmotic pressure for stomatal opening needs to be carried out on a broader range of ecologically, evolutionarily and economically important plant species including halophytes and glycophytes. In respect to barley, it remains to be answered of whether wild and cultivated genotypes respond differently to Na^+ for stomatal opening under saline conditions, or they have the same mechanism.

This study aimed to investigate the difference in stomata operation and patterning between WB and CB under condition of soil salinity. It also aimed to identify how WB and CB plants respond to Na^+ toxicity and whether Na^+ has a role in stomatal movements under saline conditions. Understanding of these mechanisms in WB would be beneficial for introducing desirable physiological

traits that have the potential to be selected as a screening criterion for salinity tolerance, ultimately to be incorporated into CB through breeding programs.

6.2 Materials and methods

6.2.1 Plant material and growth conditions

Salinity tolerance was assessed in 26 genotypes of WB and CB species. Seeds were obtained from the barley genotype collection of Zhejiang University and Yangzhou University in China and the Australian Winter Cereal Collection and reproduced in the greenhouse facilities of Tasmanian Institute of Agriculture in Hobart, Australia. Plants were grown under glasshouse conditions from August - October in 2016. The mean daily temperatures were 22°C (day) and 15°C (night) and relative humidity was 65% - 75%. Plants were grown in 8 inches pots filled with the standard potting mixture that consisted of 90% composted pine bark; 5% coco peat; 5% coarse sand; gypsum at 1 kg/m^3; dolomite at 6 kg/m^3; ferrous sulphate at 1.5 kg/m^3; Osmoform Pre-mix at 1.25 kg/m^3 and controlled-release fertiliser, Scotts Pro at 3 kg/m^3 (Chen et al., 2007). Six seeds were planted in each pot; after emergence, four uniformed plants were then kept. Ten days after emergence, salt stress commenced, applying NaCl with a 50 mM daily increments until reaching a final concentration of 300 mM NaCl. Plants were watered three times per day and were kept under non-saline and saline conditions for more 5 weeks.

6.2.2 Biomass and SPAD measurements

The fresh and dry weights were measured from five replications at the harvest time. For dry weight, plants were oven-dried at 60 °C for 96 hours. The chlorophyll content was determined on the youngest fully-expanded leaf using chlorophyll meter readings (Minolta SPAD-502, Japan).

6.2.3 Stomatal aperture measurements in response to Na^+ and K^+

To measure stomatal conductance, the youngest fully-expanded leaf was selected, and stomatal conductance was measured using a leaf porometer (model SC-1, Decagon, Castle Hill NSW, Australia). All the measurements were conducted under glasshouse conditions, during the sunny days (PAR: 1000–1200 µmol m^{-2} s^{-1}).

To quantify the stomatal density on leaves using scanning electron microscopy (SEM), fresh leaf samples were harvested from 5 fully expanded leaves

of saline and control plants. Leaf sections of 5 mm × 5 mm were mounted and two images from different leaf zones were taken from the leaf surface using SEM (FEI MLA650 ESEM, ThermoFisher Scientific, Oregon, USA) operating in environmental mode. As our preliminary experiments have shown that stomata patterning and size were not significantly different between abaxial and adaxial leaf surfaces (Suppl. Fig. 6.1), only adaxial surface was studied. The number of stomata were counted from the SEM images, and stomatal density (number of stomata per surface area) and stomata index (number of stomata in a field of view divided by the total number of stomata and epidermal cells in that field of view) were then calculated. Stomatal aperture length was measured manually using the ImageJ software. Presented data are the mean ± SE of measurements 10 different fields of view of the adaxial side of leaves from 5 individual plants.

6.2.4 Leaf elemental content and osmolality

To measure osmolality and Na^+ and K^+ contents of the leaves, the youngest fully expanded leaf was harvested (five replicates for each cultivar for both salt-treated and control plants). To extract the leaf sap, samples were freeze-thaw followed by hand squeeze in the 2 mL Eppendorf tubes, and then were centrifuged at 4,000 rpm for 5 min; 20 mL of the collected supernatant was measured for its osmolality using a vapour pressure osmometer (Vapro, Wescor Inc., Logan, UT, USA). For determination of Na^+ and K^+, 50 µL of the leaf sap was mixed with appropriate content of distilled water and the mixture was assessed in a flame photometer (Corning 410C, Essex, UK) to quantify K^+ and Na^+ concentrations in the leaf sap.

6.2.5 Epidermal strips response to Na^+ and K^+

The effects of apoplastic ion composition on the ability of guard cells to respond to external stimuli were investigated by conducting epidermal strip assays. The fully expanded leaves were selected from plants grown in glasshouse under 12/12 h light/dark conditions for 4 weeks. Plants were kept in dark for 16 h and leaves were excised, and leaf epidermis were removed with razor blade and fine forceps. Then, the epidermal strips were mounted on a medical adhesive coated-coverslip with abaxial side facing down. Leaf peels were incubated in different solutions as follows: K^+ solution (7.5 mM iminodiacetic acid, 80 mM KCl and 10 mM MES, pH 6.1), Na^+ solution (7.5 mM iminodiacetic acid, 80 mM NaCl and 10 mM MES,

pH 6.1), K^+/Na^+ Solution (7.5 mM iminodiacetic acid, 40 Mm KCl + 40 mM NaCl and 10 mM MES, pH 6.1). All the solutions containing epidermal strips were kept in the dark for 2 hours. Pictures of epidermal peels were taken using a digital camera attached to a Leica DMi8 microscope (Leica Microsystems, Germany). The peels were then illuminated with a white light of 200 μmol m^{-2} s^{-1} intensity) for 3.5 h. The peels were photographed, and stomatal apertures was measured using ImageJ software.

6.2.6 Measurement of kinetics of stomatal response to light

Plants were kept in the dark for 16 hours and then exposed to bright (1500 μmol m^{-2} s^{-1}) white light, to compare the kinetics of stomata opening between one representative genotype from each group. Stomatal conductance was measured from the youngest fully expanded leaf using a LI-6400XT portable photosynthesis system (LiCor Inc., Lincoln, NE, USA) with the following settings: leaf chamber temperature, 20 °C; light, 1500 μmol m^{-2} s^{-1}; CO_2 reference, 400 ppm; flow rate, 500 μmol s^{-1}. The sampling rate was 3 samples/min. Measurements were recorded every until the stomatal conductance reached a steady state.

6.2.7 Data analysis

Data analysis was performed using IBM SPSS Statistics 24 software (IBM corp. Armonk, NY, USA). All presented data are mean values of five to ten replicates with standard errors. One-way ANOVA was performed on the studied traits to determine the significance of differences between treatments. The correlation analyses were applied to determine association between different traits under saline conditions.

6.3 Results

Twenty-six WB and CB genotypes were grown under 300 mM salt stress for 5 weeks under glasshouse conditions. Exposure to 300 mM NaCl significantly affected the fresh (FW) and dry (DW) weights of CB and WB genotypes (Table 6.1).

Table 6.1 Mean relative values (% control) of studied physiological and morphological characteristics for cultivated and wild barley groups. FW - fresh weight; DW - dry weight; SPAD – chlorophyll content; SD - stomatal density; SAL - stomatal aperture length; SI - stomatal index; gs - stomatal conductance; Osm - leaf sap osmolality; Na^+ - leaf sap Na^+ concentration; K^+ - leaf sap K^+ concentration. *Significant and P< 0.05.

	FW	DW	SPAD	SD	SAL	SI	gs	Osm	Na^+	K^+
Cultivated	22.5±1.2*	31.5±1.3*	128±1.9*	84±4.2	95.9±1.1	93.5±3.7	28.3±3.1	246±9	1669±118	112±7
Wild	35.1±1.9	45.3±2.4	135±2.1	102±4.3	93.4±1.2	97.6±2.4	41.2±5.4	239±10	1810±262	105±9
LSD (5%)	2.9	3.9.	6.5	10.2	2.3	5.2	10.6	22.8	490	16

In relative terms, FW and DW values ranged from 27.3% to 50.7% and 30.1% to 61.7% in WB plants, respectively (Fig. 6.1 & 6.2A, B and Suppl. Tables 6.1 & 6.2). In CB plants, FW and DW values ranged from 16.38% to 32.35% and from 26.04% to 50.37%, respectively, showing that salinity stress significantly affected CB more than WB (Fig. 6.2A, B and Suppl. Tables 6.1 and 6.2). SPAD values significantly increased under saline condition for both WB and CB groups (Fig. 6.2C), with WB plants having higher values than CB in relative terms (Table 6.1). While there was no significant difference for shoot sap osmolality between CB and WB under non-saline conditions, it increased under saline conditions in both groups, with CB having significantly higher osmolality than WB (Fig. 6.2D). Given that there was no significant difference for sap osmolality between CB and WB groups in relative terms, it appears that WB plants had more relied on inorganic components to increase sap osmolality (Table 6.1; Fig. 6.2D). Leaf sap Na^+ and K^+ concentrations had significantly changed in CB and WB under salt stress conditions, but no significant difference was found between both the CB and WB groups under either saline or non-saline conditions (Fig. 6.2E, F). Under saline conditions, leaf sap Na^+ concentration in CB values ranged from 152 mmol L^{-1} to 351 mmol L^{-1} whereas these values varied between 154 mmol L^{-1} and 752 mmol L^{-1} in WB (Suppl. Tables 6.1 and 6.2).

A significant decrease in stomatal conductance (g_s) under salt stress conditions was reported for all genotypes. The g_s of CB was higher than WB under non-saline conditions; however, no significant differences between two groups was reported for saline conditions (Fig. 6.3A). As a result, relative stress-induced reduction in stomatal conductance was much higher for CB compared with WB (72

± 5.4% and 51 ± 3.1%, respectively; Table 6.1). There was a significant difference between CB and WB for stomatal density under non-saline conditions, with CB showed higher stomatal density (47.3 ± 2.2 stomata/mm^2) than WB (39.4 ± 2.1 stomata/mm^2). No significant difference for this characteristic was found between CB and WB plants under saline conditions (Fig. 6.3B). This resulted in a 16% reduction in stomatal density under saline conditions in CB plants, while the relative stomatal density of WB plants remained unchanged (Table 6.1).

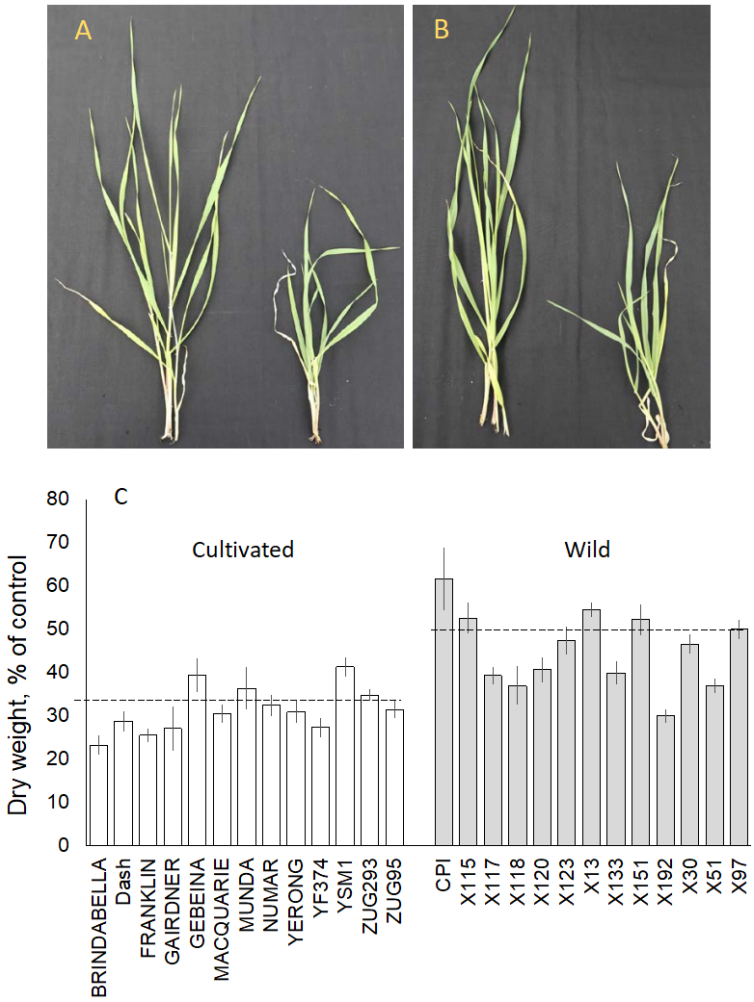

Fig. 6.1 Relative dry weight (% control) of 26 cultivated and wild barley genotypes. Plants were grown under control and 300 mM NaCl for 35 days. Above photos show Gairdner genotype (A) as a representative of cultivated barley group and CPI genotype (B) as a representative of wild barley group. Data are Mean ± S.E. (n=5).

In this regard, there was no significant difference in stomatal index for WB plants under saline and non-saline conditions while stomatal index significantly declined in CB plants in saline conditions than non-saline conditions (Fig. 6.3C). No

significant ($P < 0.05$) difference for stomatal aperture length between saline and non-saline conditions was reported for CB. In WB, however, it was significantly reduced under saline conditions compared to non-saline conditions (Fig. 6.3D) suggesting that reducing stomatal aperture length in WB was a salt-adaptive characteristic.

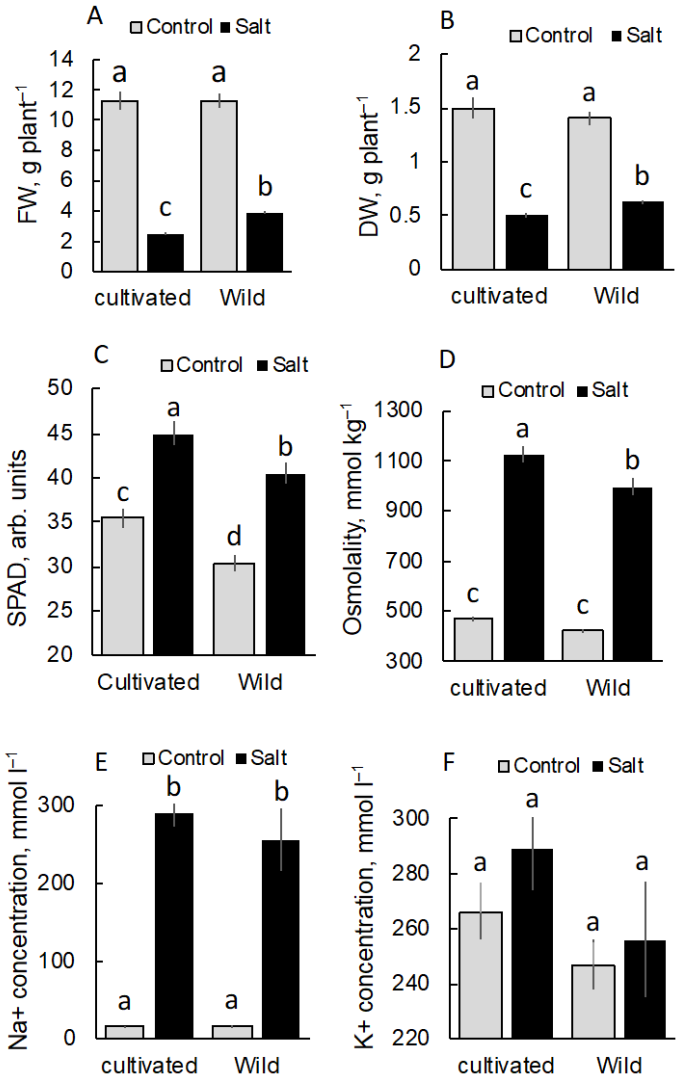

Fig. 6.2 Physiological characteristics of wild and cultivated barley genotypes grown under control and salt (300 mM NaCl for 35 days) conditions. (A) - fresh weight (g per plant), (B) - dry weight (g per plant), (C) - SPAD value, (D) - leaf sap osmolality (mmol kg^{-1}), (E) - leaf sap Na^+ concentration (mmol L^{-1}) (F) - leaf sap K^+ concentration (mmol L^{-1}). Data are Mean ± S.E. (n=13). Data labelled with different lower-case letters are significantly different at $P < 0.05$.

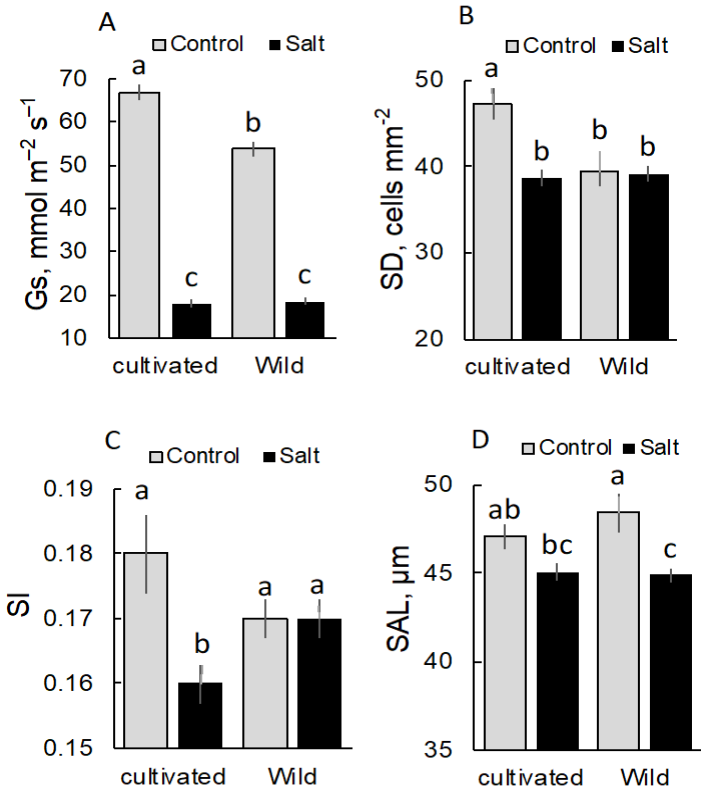

Fig. 6.3 Anatomical characteristics of wild and cultivated barley genotypes grown under control and salt (300 mM NaCl for 35 days) conditions. (A) - stomatal conductance (mmol m^{-2} s^{-1}), (B) - stomatal density (stomata mm^{-2}), (C) - stomatal index (number of stomata cells divided by number of epidermal cells in the field of view), (D) - stomatal aperture length (µm). Mean ± S.E (n=13). Data labelled with different lower-case letters are significantly different at $P < 0.05$.

6.3.1 Stomatal responses to light and Na^+ and K^+ treatments on epidermal strips

As the next step, we have compared kinetics of responses of stomata in CB and WB genotypes to light transition. The rationale behind these experiments was that faster stomata opening to external stimuli (light in this case) may give plants a competitive advantage and optimize the water use efficiency under saline conditions. Our data showed that WB had higher speed of stomatal response to light compared with CB (Fig. 6.4A). To reach a steady-state level of stomatal conductance, CB and WB needed 26.3 ± 1.7 and 19.7 ± 1.6 min, respectively (significant at $P < 0.05$).

The next question to answer was of whether barley plants can substitute K^+ with Na^+ for stomata operation. To do this, we have chosen one representative genotype (X133) from WB group and compared it with variety Gairdner from the

CB group (as a typical CB). As shown in Fig. 6.4, stomata of WB and CB behaved differently when K^+ was substituted by Na^+ in the bath solution. Gairdner, had the biggest stomatal aperture under 80 mM KCl treatment, and its stomatal aperture declined with increasing NaCl levels, indicating that this genotype relied mostly on K^+ for stomatal opening (Fig. 6.4B). On the contrary, X133, as a representative of WB plants, had the highest stomatal aperture under 80 mM NaCl treatment, showing that Na^+ had a positive role in stomata opening in this genotype (Fig. 6.4B). This result suggests that WB plants may utilize Na^+ instead of K^+ for stomatal movements under saline conditions.

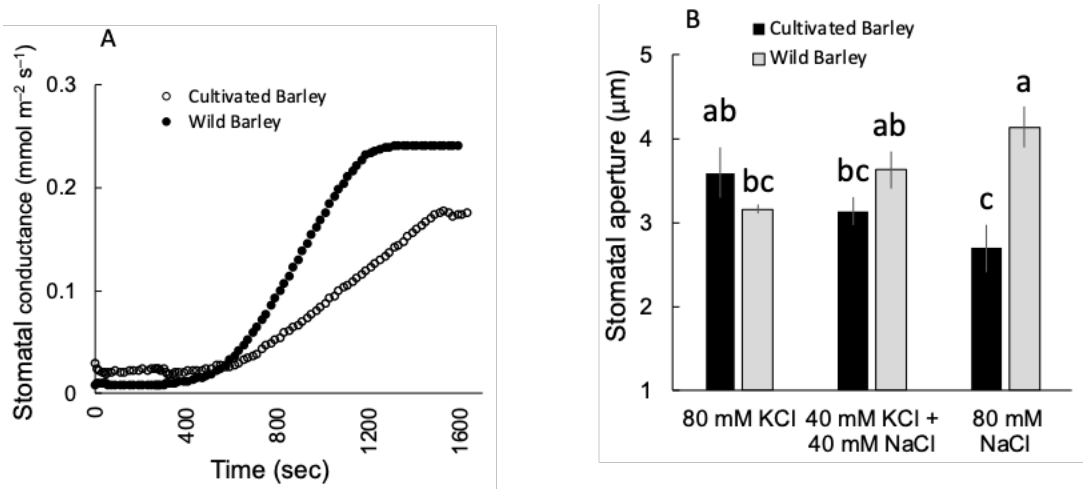

Fig. 6.4 Stomatal responses to light and measurement of stomata aperture in epidermal strip assays in solutions containing different amounts of Na^+ and K^+. Two representative genotypes were selected: one form from wild barley group (genotype X133), and one from cultivated group (genotype Gairdner). (A) – Kinetics of stomatal response during the transition from dark to light. Stomatal conductance was measured with a portable photosynthesis system (LiCor Inc., Lincoln, NE, USA) at 20 °C leaf temperature, 1500 µmol m^{-2} s^{-1} light, 400 ppm CO_2 reference, and 500 µmol s^{-1} flow rate. Measurements were recorded every 20 seconds until stomatal conductance approach steady state. (B) - Effect of different solutions in promotion of stomatal aperture in cultivated and wild barley genotypes. Plants were kept in the dark for 16 hours and leaf epidermis was removed from excised leaves. Leaf peels were incubated in NaCl, KCl and NaCl + KCl solutions and were kept in the dark for 2 hours. Data labelled with different lower-case letters are significantly different at $P < 0.05$.

6.3.2 Correlation analysis

The correlation analysis of WB group indicated a positive relation between DW and stomatal conductance (R^2= 0.55, $P < 0.05$) and DW and stomata density (R^2= 0.58, $P < 0.05$) under saline conditions showing that the higher stomatal density resulted in a higher stomatal conductance that eventually led to higher biomass production under salinity stress (Table 6.2). The CB group showed a negative correlation between stomata density and DW (R^2= -0.56, $P < 0.05$) under salt stress conditions (Table 6.3). In CB, the higher epidermal cell density resulted in less DW (R^2= -0.68, $P < 0.05$) whereas WB did not show such a negative relation (Table 6.2 and 3). In CB group, a negatively correlation between osmolality and DW was found under saline conditions (R^2= 0.69, $P < 0.01$) (Table 6.3).

Table 6.2 Correlation between studied physiological and anatomical characteristics of wild barley genotypes under saline conditions

	FW	DW	SPAD	Gs	SD	SAL	SI	Na^+	K^+	Osm
FW	1									
DW	0.80**	1								
SPAD	-0.21	-0.2	1							
Gs	0.40	0.55*	-0.19	1						
SD	0.51	0.58*	0.28	0.39	1					
SAL	0.10	-0.09	0.002	-0.32	-0.56*	1				
SI	0.13	0.17	0.06	-0.17	0.10	0.47	1			
Na^+	-0.08	-0.46	-0.38	-0.27	-0.29	0.21	-0.11	1		
K^+	0.40	0.71**	-0.17	0.26	0.55*	-0.45	0.18	-0.59*	1	
Osm	-0.23	-0.36	-0.53	-0.15	-0.25	0.07	0.09	0.67*	-0.18	1

Abbreviations: FW - fresh weight (g per plant); DW - dry weight (g per plant); SPAD – chlorophyll content (arb. units); SD - stomatal density (cells mm^{-2}); SAL - stomatal aperture length (μM); SI - stomatal index (number of stomata cells divided by number of epidermal cells); Gs - stomatal conductance (mmol m^{-2} s^{-1}); Osm - leaf sap osmolality (mmol kg^{-1}); Na^+ - leaf sap Na^+ concentration (mmol L^{-1}); K^+ - leaf sap K^+ concentration (mmol L^{-1}).

Table 6.3 Correlation between studied physiological and anatomical characteristics of cultivated barley genotypes under saline conditions

	FW	DW	SPAD	Gs	SD	SAL	SI	Na^+	K^+	Osm
FW	1									
DW	0.88**	1								
SPAD	-0.15	-0.44	1							
Gs	0.09	0.21	0.185	1						
SD	-0.48	-0.56*	0.55	-0.16	1					
SAL	0.12	0.22	-0.17	0.06	-0.59*	1				
SI	0.27	0.04	0.32	-0.49	0.47	-0.14	1			
Na^+	-0.26	-0.19	-0.11	0.34	-0.21	0.05	-0.51	1		
K^+	0.39	0.67*	0.09	-0.34	0.25	-0.07	0.05	0.05	1	
Osm	-0.68**	-0.69**	-0.02	-0.08	0.19	-0.31	-0.31	0.64*	0.2	1

Abbreviations: FW - fresh weight (g per plant); DW - dry weight (g per plant); SPAD – chlorophyll content (arb. units); SD - stomatal density (cells mm^{-2}); SAL - stomatal aperture length (µM); SI - stomatal index (number of stomata cells divided by number of epidermal cells); Gs - stomatal conductance (mmol m^{-2} s^{-1}); Osm - leaf sap osmolality (mmol kg^{-1}); Na^+ - leaf sap Na^+ concentration (mmol L^{-1}); K^+ - leaf sap K^+ concentration (mmol L^{-1}).

6.4 Discussion

6.4.1 Wild barley plants maintain constant stomatal density under saline conditions to maximise photosynthesis

In WB plants, a positive correlation was found between DW and stomatal density (R^2= 0.58; $P < 0.05$) while this correlation was negative in CB (R^2= -0.57; $P < 0.05$) (Tables 6.2 and 6.3) suggesting that WB and CB had used different mechanism to tackle salt stress. Comparing stomata density in WB and CB under saline and non-saline conditions revealed that CB had significantly higher stomatal density than WB under non-saline conditions, but this amount decreased by 16% in CB while slightly increased in WB under saline conditions (Fig. 6.3B; Table 6.1). Also, CB plants had significantly lower stomata index under saline conditions while WB had the ability to keep its stomata index constant under normal and saline conditions (Fig. 6.3C). Thus, these results suggest that CB employ a stress-escaping strategy by reducing stomata density via developmental mechanisms, to conserve water when grown under conditions of hyperosmotic stress. WB, on the contrary, is capable to use Na^+ as a cheap osmoticum (including also for stomatal operation)

and, hence, can afford to maintain stomatal density unchanged. This strategy allows WB plants to maintain the constant rate of CO_2 assimilation, while in CB reduced g_s resulting from reduced stomata density comes with yield penalties.

6.4.2 Wild barley plants have faster stomatal regulation and superior stomatal conductance under saline conditions

Photosynthesis depends on many resources such as water, light and the availability of CO_2. Under salt stress conditions stomata are closed, and CO_2 acquisition is reduced, becoming a limiting parameter in photosynthesis (Chaves et al., 2009). Also, leaf transpiration is regulated by stomatal parameters (e.g. stomatal density, structure and aperture) and accounts for about 95% of all water lost by the plant, indicating the significance role of stomata in water use in plants (Hetherington and Woodward, 2003). In this study, g_s of CB was higher than WB under non-saline conditions (Fig. 6.3A), showing their higher gas exchange capacity under normal conditions. Salinity stress decreased stomatal conductance capacity by 72% and 59% in CB and WB, respectively, indicating that CB have severely lost their gas exchange ability under saline conditions (Table 6.1). Furthermore, the significant association between stomatal conductance and salinity tolerance in WB plants (Table 6.2) also reveals that this group was benefited from higher gas exchange rate.

In addition to superior stomatal conductance, WB was also able to respond to light faster than CB (Fig. 6.4A). The speed of changes in gas exchange in response to light is different among species (Lawson et al., 2010). Faster stomatal regulation of WB also suggests that WB plants potentially had better adaptation between stomatal responses and light intensity that could result in higher water use efficiency (WUE) and efficient conversion of light energy for more biomass and yield (Lawson and Blatt, 2014; Moualeu-Ngangue et al., 2016). This was confirmed in this study by significantly higher DW and relatively higher g_s in WB plants under saline conditions (Fig. 6.1 and Fig. 6.2B; Table 6.1).

The closing and opening of stomata are driven by guard cell signalling mechanisms and a number of external environmental cues (Blatt, 2000) and there is a significant variation in stomatal sensitivity among different plant species (Lawson et al., 2012). Studies have shown that stomatal density and size play a significant role in stomatal opening and closing (Franks and Beerling, 2009; Lawson and Blatt, 2014). For instance, in *Phaseolus vulgaris*, which has smaller

and more stomata, responded faster than *Vicia faba*, which has larger and fewer stomata under well-watered condition (Lawson and Blatt, 2014). The mechanism used in CB was similar to this strategy under control, where CB plants had higher stomatal density and smaller stomatal aperture (Fig. 6.3B, D). However, it is a very different mechanism for CB and WB under salinity stress. WB plants had faster g_s and relatively higher stomatal index, which enable plants to open and close more rapidly while maintaining photosynthesis. Under these circumstances, CO_2 diffusion into the leaf for photosynthesis would be maximized that eventually leads to superior salinity tolerance ability of WB group than CB group.

In this study, faster stomatal regulation of WB may play an important role in plant WUE and consequently in biomass production, as the idea of manipulation of stomatal response to changing environmental conditions could provide a means to both improving WUE and increasing the photosynthetic rate of plants (Lawson and Blatt, 2014; Papanatsiou et al., 2019).

6.4.3 Wild barley plants use Na^+ for stomatal movements

WB plants are more tolerant to salinity stress, standing close to their halophytic relatives. The latter is known to use Na^+ to drive the guard cell osmotic motor by Na^+ (Hedrich and Shabala, 2018). The reliance of CB plants on K^+ ion for stomatal operation (Fig. 6.4B) suggests that Na^+ may cause a disruption in the normal control of guard cell turgor as it does in other non-halophyte plants (Robinson et al., 1997). However, this did not occur in WB plants, where stomatal operation was more efficient in the presence of 80 mM NaCl (Fig. 6.4B). This suggests that WB may use Na^+ instead of K^+ for stomata operation. This is consistent with previous findings on guard cells in some halophyte species (e.g. *Aster trifolium*; (Very et al., 1998) and a general view that, under conditions of reduced K^+ availability, Na^+ can replace K^+ in several physiological processes (Erel et al., 2014). We suggest that a facultative ability of WB to use either K^+ or Na^+ for stomatal movements give them a competitive advantage under saline conditions. It appears that WB genotypes showed a mechanism that has been reported in some halophytic plants. While inability of guard cells to exclude Na^+ in non-halophytes under saline condition may leads to subsequent loss of stomatal regulation of water relations that eventually contribute to damage, halophytes may have evolved various stomatal ionic properties as adaptive features to deal with Na^+ entry to the cytoplasm of the

guard cells (Robinson et al., 1997; Very et al., 1998). It has been proposed that guard cells in halophytes can overcome high concentration of Na^+ either through ability to substitute Na^+ for K^+ as the primary ion determining their alterations of turgor, or by Na^+ excluding, to enable K^+ to retain the main role (Robinson et al., 1997; Very et al., 1998). In halophytic *Suaeda maritima* L, Na^+ was the major cation in the guard cells under saline condition and the concentration of this ion were lower in guard cells when stomata closed (Flowers et al., 1986).

Given the fact that there was no significant difference between WB and CB in terms of leaf Na^+ concentration under saline condition it appears that they had different mechanism to deal with this ion at guard cell level. Accumulated Na^+ in the leaf apoplast of WB plants provide a driving force for Na^+ entry into guard cells, which could result in stomatal opening through increasing the osmotic pressure within guard cells. CB plants, on the other hand, utilised a stress avoidance mechanism to prevent stomatal opening by Na^+, providing a regulatory strategy for the control of water loss and Na^+ accumulation in the shoot through the decreased transpiration under salinity stress. This mechanism plays an important role when salt accumulation in the shoot begins to exceed the capacity for vacuole sequestration. Depsite early indication of the role of Na^+ for stomatal closure in a halophyte (Very et al., 1998), the molecular mechanisms allowing WB to use Na^+ in stomatal operation remain a subject for further studies.

6.4.4 Osmotic adjustment in cultivated barley comes with higher cost than wild barley

DW had negative association with the leaf sap osmolality in CB (Table 6.3), with CB plants having significantly higher value (1127 mmol kg^{-1}) compared with WB (998 mmol kg^{-1}) (Fig. 6.2D). Both inorganic ions and organic osmolytes determine cell osmolarity. As leaf ionorganic ion content was not significant different between WB and CB (Fig. 6.2E, F), the difference in osmolarity between CB and WB is then most likely attributed to the difference in the concentration of organic osmolytes.

For the successful adaptation, plants need to achieve right balance between excluding most of the salt to prevent it concentrating to toxic level in leaves and taking it up, for optimal osmotic adjustment. By relying on Na^+ and Cl^- for osmotic adjustment plants can avoid the high carbon cost of synthesis of organic solutes

used as the same purpose (Tyerman et al., 2019), assuming that plants are able to securely compartmentalized toxic salt load in vacuoles. In this regard, it is estimated that biosynthesis of one compatible solute molecule requires 30 to 109 ATP molecules whereas the uptake of two K^+ and two Cl^- ions requires one molecule of ATP (Oren et al., 1999). At the same time, increasing osmolarity of the vacuolar sap needs to be osmotically balanced by increasing amounts of compatible solutes in the cytosol (Chen et al., 2007). In our case, WB accumulated the same concentration of Na^+ as CB but had ~13% lower leaf sap osmolarity (Fig. 6.2D), WB genotypes were thus required to produce much fewer compatible solutes for the osmotic adjustment in the cytosol. As the synthesis of compatible solutes costs large amount of energy to the plant (Tyerman et al., 2019), the higher energy efficiency in WB genotypes might explain the observed less yield penalties in this group.

In conclusion, cultivated barley employs a stress-escaping strategy, reducing stomata density, in an attempt to preserve water under saline condition. On the contrary, superior salinity tolerance in a wild barley is related to its ability to maintain relatively constant stomata density but utilize Na^+ (in addition, or instead of, K^+) for stomatal movements. Understanding the molecular basis of this process may allow incorporating this stomatal trait in elite CB varieties in plant breeding programs.

6.5 References

Ahmed, I.M., Cao, F., Zhang, M., Chen, X., Zhang, G., Wu, F., 2013. Difference in yield and physiological features in response to drought and salinity combined stress during anthesis in Tibetan wild and cultivated barleys. PloS One 8, e77869.

Ashraf, M., Rahmatullah, Ahmad, R., Afzal, M., Tahir, M.A., Kanwal, S., Maqsood, M.A., 2009. Potassium and silicon improve yield and juice quality in sugarcane (*Saccharum officinarum*) under salt stress. J Agron Crop Sci 195, 284-291.

Blatt, M.R., 2000. Cellular signaling and volume control in stomatal movements in plants. Annu Rev Cell Dev Biol 16, 221-241.

Chaves, M.M., Flexas, J., Pinheiro, C., 2009. Photosynthesis under drought and salt stress: regulation mechanisms from whole plant to cell. Ann Bot 103, 551-560.

Chen, Z.H., Chen, G., Dai, F., Wang, Y., Hills, A., Ruan, Y.L., Zhang, G., Franks, P.J., Nevo, E., Blatt, M.R., 2017. Molecular evolution of grass stomata. Trends Plant Sci 22, 124-139.

Chen, Z.H., Cuin, T.A., Zhou, M.X., Twomey, A., Naidu, B.P., Shabala, S., 2007. Compatible solute accumulation and stress-mitigating effects in barley genotypes contrasting in their salt tolerance. J Exp Bot 58, 4245–4255.

Chiang, C.P., Yim, W.C., Sun, Y.H., Ohnishi, M., Mimura, T., Cushman, J.C., Yen, H.E., 2016. Identification of ice plant (*Mesembryanthemum crystallinum*) micrornas using RNA-seq and their putative roles in high salinity responses in seedlings. Front Plant Sci 7, 1143.

Dai, F., Wang, X., Zhang, X.Q., Chen, Z., Nevo, E., Jin, G., Wu, D., Li, C., Zhang, G., 2018. Assembly and analysis of a qingke reference genome demonstrate its close genetic relation to modern cultivated barley. Plant Biotechnol J 16, 760-770.

El-Esawi, M.A., Alaraidh, I.A., Alsahli, A.A., Ali, H.M., Alayafi, A.A., Witczak, J., Ahmad, M., 2018. genetic variation and alleviation of salinity stress in barley (*Hordeum vulgare*). Molecules 23.

Erel, R., Ben-Gal, A., Dag, A., Schwartz, A., Yermiyahu, U., 2014. Sodium replacement of potassium in physiological processes of olive trees (var. Barnea) as affected by drought. Tree physiol 34, 1102-1117.

Fita, A., Rodriguez-Burruezo, A., Boscaiu, M., Prohens, J., Vicente, O., 2015. Breeding and domesticating crops adapted to drought and salinity: a new paradigm for increasing food production. Front Plant Sci 6, 978.

Flowers, T.J., Hajibagheri, M.A., Clipson, N.J.W., 1986. Halophytes. Q Rev Biol 61, 313-337.

Franks, P.J., Beerling, D.J., 2009. Maximum leaf conductance driven by CO_2 effects on stomatal size and density over geologic time. Proc Natl Acad Sci 106, 10343-10347.

Garthwaite, A.J., von Bothmer, R., Colmer, T.D., 2005. Salt tolerance in wild *Hordeum* species is associated with restricted entry of Na^+ and Cl^- into the shoots. J Exp Bot 56, 2365–2378.

Han, Y., Yin, S., Huang, L., Wu, X., Zeng, J., Liu, X., Qiu, L., Munns, R., Chen, Z.H., Zhang, G., 2018. A sodium transporter HvHKT1;1 confers salt tolerance

in barley via regulating tissue and cell ion homeostasis. Plant Cell Physiol 59, 1976-1989.

Hedrich, R., Shabala, S., 2018. Stomata in a saline world. Curr Opin Plant Biol 46, 87-95.

Hetherington, A.M., Woodward, F.I., 2003. The role of stomata in sensing and driving environmental change. Nature 424, 901-908.

Jarvis, R.G., Mansfield, T.A., 1980. Reduced stomatal responses to light, carbon dioxide and abscisic acid in the presence of sodium ions. Plant Cell Environ 3, 279-283.

Lawson, T., Blatt, M.R., 2014. Stomatal size, speed, and responsiveness impact on photosynthesis and water use efficiency. Plant Physiol 164, 1556-1570.

Lawson, T., Kramer, D.M., Raines, C.A., 2012. Improving yield by exploiting mechanisms underlying natural variation of photosynthesis. Curr Opin Biotechnol 23, 215-220.

Lawson, T., von Caemmerer, S., Baroli, I., 2010. Photosynthesis and Stomatal Behaviour, in: Lüttge, U.E., Beyschlag, W., Büdel, B., Francis, D. (Eds.), Progress in Botany 72. Springer Berlin Heidelberg, Berlin, Heidelberg, pp 265-304.

Liu, X., Fan, Y., Mak, M., Babla, M., Holford, P., Wang, F., Chen, G., Scott, G., Wang, G., Shabala, S., Zhou, M., Chen, Z.H., 2017. QTLs for stomatal and photosynthetic traits related to salinity tolerance in barley. BMC Genomics 18, 9.

Liu, X., Mak, M., Babla, M., Wang, F., Chen, G., Veljanoski, F., Wang, G., Shabala, S., Zhou, M., Chen, Z.H., 2014. Linking stomatal traits and expression of slow anion channel genes HvSLAH1 and HvSLAC1 with grain yield for increasing salinity tolerance in barley. Front Plant Sci 5, 634.

MacRobbie, E.A.C., 1983. Effects of light/dark on cation fluxes in guard cells of *Commelina communis*. J Exp Bot 34, 1695-1710.

Miskin, K.E., Rasmusson, D.C., Moss, D.N., 1972. Inheritance and physiological effects of stomatal frequency in barley. Crop Sci 12, 780–783.

Moualeu-Ngangue, D.P., Chen, T.W., Stutzel, H., 2016. A modeling approach to quantify the effects of stomatal behavior and mesophyll conductance on leaf water use efficiency. Front Plant Sci 7, 875.

Munns, R., Tester, M., 2008. Mechanisms of salinity tolerance. Annu Rev Plant Biol 59, 651-681.

Nevo, E., Chen, G., 2010. Drought and salt tolerances in wild relatives for wheat and barley improvement. Plant Cell Environ 33, 670-685.

Oren, R., Sperry, J.S., Katul, G.G., Pataki, D.E., Ewers, B.E., Phillips, N., Schäfer, K.V.R., 1999. Survey and synthesis of intra- and interspecific variation in stomatal sensitivity to vapour pressure deficit. Plant Cell Environ 22, 1515-1526.

Papanatsiou, M., Petersen, J., Henderson, L., Wang, Y., Christie, J.M., Blatt, M.R., 2019. Optogenetic manipulation of stomatal kinetics improves carbon assimilation, water use, and growth. Science 363, 1456-1459.

Peng, S., Laza, R.C., Khush, G.S., Sanico, A.L., Visperas, R.M., Garcia, F.V., 1998. Transpiration efficiencies of Indica and improved tropical Japonica rice grown under irrigated conditions. Euphytica 103, 103–108.

Robinson, M.F., Very, A.A., Sanders, D., Mansfield, T.A., 1997. How can stomata contribute to salt tolerance? . Ann Bot 80, 387-393.

Shabala, S., Cuin, T.A., 2008. Potassium transport and plant salt tolerance. Physiol Plant 133, 651-669.

Shabala, S., Munns, R., 2012. Salinity stress: physiological constraints and adaptive mechanisms. Plant Stress Physiol 1, 59-93.

Steppuhn, H., van Genuchten, M.T., Grieve, C.M., 2005. Root-zone salinity: I. selecting a product-yield index and response function for crop tolerance. Crop Sci 45, 209-220.

Tyerman, S.D., Munns, R., Fricke, W., Arsova, B., Barkla, B.J., Bose, J., Bramley, H., Byrt, C., Chen, Z., Colmer, T.D., Cuin, T., Day, D.A., Foster, K.J., Gilliham, M., Henderson, S.W., Horie, T., Jenkins, C.L.D., Kaiser, B.N., Katsuhara, M., Plett, D., Miklavcic, S.J., Roy, S.J., Rubio, F., Shabala, S., Shelden, M., Soole, K., Taylor, N.L., Tester, M., Watt, M., Wege, S., Wegner, L.H., Wen, Z., 2019. Energy costs of salinity tolerance in crop plants. New Phytol 221, 25-29.

Very, A.-A., Robinson, M.F., Mansfield, T.A., Sanders, D., 1998. Guard cell cation channels are involved in Na^+-induced stomatal closure in a halophyte. Plant J 14, 509-521.

Wang, H., Clarke, J.M., 1993. Relationship of excised-leaf water-loss and stomatal frequency in wheat. Can J Plant Sci 73, 93-99.

Wang, L.M., Wei, S.W., Chen, J.B., Zhang, Y.D., Huang, D.F., 2013. Regulation of the inward rectifying K^+ channel MIRK and ion distribution in two melon cultivars (*Cucumis melo*) under NaCl salinity stress. Acta Physiol Plant 35, 2789-2800.

Wang, X., Chen, Z.H., Yang, C., Zhang, X., Jin, G., Chen, G., Wang, Y., Holford, P., Nevo, E., Zhang, G., Dai, F., 2018. Genomic adaptation to drought in wild barley is driven by edaphic natural selection at the Tabigha Evolution Slope. Proc Natl Acad Sci 115, 5223-5228.

Wu, D., Shen, Q., Cai, S., Chen, Z.H., Dai, F., Zhang, G., 2013. Ionomic responses and correlations between elements and metabolites under salt stress in wild and cultivated barley. Plant Cell Physiol 54, 1976-1988.

Yeo, A.R., Flowers, T.J., 1985. The absence of an effect of the Na^+/Ca^{2+} ratio on sodium chloride uptake by rice (*Oryza sativa*). New Phytol 99, 81-90.

Zhao, C., Wang, Y., Chan, K.X., Marchant, D.B., Franks, P.J., Randall, D., Tee, E.E., Chen, G., Ramesh, S., Phua, S.Y., Zhang, B., Hills, A., Dai, F., Xue, D., Gilliham, M., Tyerman, S., Nevo, E., Wu, F., Zhang, G., Wong, G.K., Leebens-Mack, J.H., Melkonian, M., Blatt, M.R., Soltis, P.S., Soltis, D.E., Pogson, B.J., Chen, Z.H., 2019. Evolution of chloroplast retrograde signaling facilitates green plant adaptation to land. Proc Natl Acad Sci 116, 5015-5020.

Zhu, J.K., 2002. Salt and drought stress signal transduction in plants. Annu Rev Plant Biol 53, 247-273.

Zorb, C., Geilfus, C.M., Dietz, K.J., 2019. Salinity and crop yield. Plant Biol 21 Suppl 1, 31-38.

Chapter 7: General Discussion

Environmental stresses such as salinity significantly hinders plant growth that finally result in reduction of the crop yield. To match global food production for increasing world population, agriculture needs to move into marginal lands that expose crop plants to unfavourable conditions. Therefore, understanding the mechanisms of salinity tolerance play important role to deal with this abiotic stress (Cheeseman, 2015). Yet, the majority of investigations on plant responses to salt stress have been carried out with Arabidopsis as a model plant, which has a significantly low tolerance to environmental stresses including as salinity. Although studies on Arabidopsis and some other model species have increased our knowledge of stress tolerance mechanisms based on individual gene functions in different pathways however, in almost all cases, genes with a stress-alleviating feature under controlled conditions have not resulted in stress-tolerance character under field conditions (Wu et al., 2012). This failure urges to develop model plants that can provide primary insights into strategies that confer high stress-tolerance levels in plant species that naturally are tolerant to stresses (Amtmann, 2009; Bressan et al., 2001). Hence, investigation on the halophytic plant which are naturally tolerant to salinity stress or study on salinity tolerant crop plants is necessary (Flowers et al., 2015).

Halophytic species can be considered as model plants to study the salt tolerance mechanism. Halophytes only consists of a small numbers of all flowering plants (Flowers et al., 2010) which have evolved independently in a diverse plant families indicating the convergent evolved adaptations to saline condition (Bromham, 2015). The capacity to generate high-throughput metabolomic and transcriptomic data from halophytic plants provides opportunities for understanding the salinity tolerance mechanisms and also provides the adaptation strategies could be learnt to improving the salinity tolerance of agriculturally important crop plants.

Despite high salinity tolerance of halophytes, the mechanisms of this superior ability have not been completely studied. This study has focused on stomata and epidermal bladder cells and their involvement in salinity tolerance in halophytic plant *Chenopodium quinoa*. Additionally, and as a case study, stomatal

traits as a salinity tolerance mechanism component was compared between halophytic crops and their wild relatives using cultivated and wild barley plants.

Plants need to efficiently balance gaseous exchange of leaf to maximize CO_2 uptake for photosynthesis and to minimize water loss through transpiration. Salinity stress severely influences water balance in plants and given the role of stomata that regulate all gaseous diffusion, it can be concluded that they are ultimate boundary line for regulating water relation in plants under saline condition.

Our results of a large-scale screening of quinoa revealed that stomata density remained unchanged between saline and non-saline conditions while stomata length declined between 3% to 43% among accessions. There was also a negative association between the relative dry weight and stomata length in a salt-tolerant group, suggesting that these plants were able to efficiently regulate stomatal patterning to efficiently balance water loss and CO_2 assimilation under saline condition. In the light of importance of stomatal traits as a determinant of salinity tolerance in quinoa, we have extrapolated this work to barley plants through comparing cultivated (*Hordeum vulgare*) and wild (*Hordeum spontaneum*) barley genotypes under saline and non-saline conditions. The results revealed similar finding as quinoa where wild barley plants were able to keep constant SD while this trait significantly decreased in cultivated barley. Also, our results indicated the higher SD in wild barley which led to higher stomatal conductance (g_s) under saline conditions, with g_s reduction being 51% and 72% in wild barley and cultivated barley, respectively. Hence, cultivated barley employ a stress-escaping strategy by reducing SD, in an attempt to conserve water when grown under salinity conditions.

Stomatal pores represent less than 3% of total leaf surface (Chaves et al., 2016) but are responsible for about 95% of total water loss in plants (Hedrich and Shabala, 2018) and hence, their alteration should have great impacts on WUE. In light to this fact, stomata also indicated a diverse range of anatomical and morphological differences such as variation in shapes, sizes, and numbers across plant species. This broad range of genetic variation in turn have the potential to influence stomatal movement and, consequently, plant photosynthesis rate and WUE (Bertolino et al., 2019). Although different stomatal properties such as patterning playing an important role on plant performance (Lawson and Vialet-Chabrand, 2019), however, there is scarce information about how targeted alteration of stomatal characteristics affect physiological responses in crop plants

(Chaves et al., 2016). It noteworthy to emphasise that there is almost no information in this regard for halophytes. Thus, targeted genetic modifications of stomatal density under unfavourable environmental conditions such as salinity stress could be an important approach for the engineering of higher WUE in crop plants. Although stomata are not the only limiting factor for water loss by plants but they have a main role in this process and hence needs appropriate considerations in this context.

Recent investigations have been shown that numerous components of the stomatal signalling network such as bHLH transcription factors (Liu et al., 2009; Raissig et al., 2016; Raissig et al., 2017) and peptide signals regulating stomatal density (Caine et al., 2019; Hughes et al., 2017). These findings have provided this opportunity for investigators to examine the implications of targeted alterations in stomatal density in agriculturally important crop plants such as barley. Studies on barley has been indicated that the upregulation of EPF1 can improve WUE without any reduction in grain yield, although in some cases photosynthetic rate slightly decreased under non-saline conditions (Caine et al., 2019; Hughes et al., 2017; Hunt et al., 2010).

From the breeding point of view, key features including morphological and physiological characteristics could be targeted to breed desire plants for saline conditions. In case of barley and quinoa, our investigation indicated that plants with higher stomatal density and conductance and lower Na^+ content in their leaves under saline conditions indicated better tolerance to salinity. The wide genetic variation in traits such as stomatal density and stomatal length reported in the current investigation under saline conditions make it possible to identify the contrasting genotypes for QTL mapping of these traits for development of salt-tolerant barley and quinoa genotypes.

A significant proportion of halophytes are able to sequester salt from their leaves into the external store cells. One of these external anatomical features that is called epidermal bladder cells (EBC) which has a unique structure directly sequester toxic ions out of the plant (Shabala et al., 2014). EBCs is one of mechanism used by a group of halophytes to deal with salinity stress (Barkla et al., 2002; Oh et al., 2015; Shabala et al., 2014) and hence understanding the function of EBCs may eventually play an important role in transferring this ability to crop plants.

It has long been suggested that EBCs to play an important role in plant performance under saline conditions. Some suggested roles include (i) sequestration sites for excessive salt load; (ii) storage of metabolites; (iii) a secondary epidermis for protection against UV radiation; (iv) external water reservoirs and (v) a reservoir for reactive oxygen species (ROS)- scavenging metabolites and organic osmo-protectants (Adams et al., 1998; Agarie et al., 2007; Barkla and Vera-Estrella, 2015; Ibdah et al., 2002; Jou et al., 2007; Oh et al., 2015; Rygol et al., 1989; Steudle et al., 1975).

In the current study we provide direct supporting evidence for the role of EBCs to assist halophytic plant, *Chenopodium quinoa*, to cope with salinity stress. The results indicated a significant role of EBCs in salinity adaptation of quinoa where it indicated a key role of EBC as a salt dumper to externally sequester salt load; improved K^+ retention in leaf mesophyll and as a storage space for several metabolites known to modulate plant ionic relations.

Our metabolomics study indicated a dramatically modified metabolic changes in bladder-bearing leaves compared bladderless leaves, with the biggest differences reported for gamma-aminobutyric acid (GABA), proline, sucrose and inositol, affecting ion transport across cellular membranes. In addition to this, the transcriptome investigation showed significant alterations of genes related to ion transport, DNA replication, and genes related to stress signalling in response to salinity stress were determined. This finding that the transcriptome of bladder-bearing leaves differed from those of bladderless leaves suggests that EBCs do not function as a passive external store place for salt as it was perceived before (Steudle et al., 1975) but play active metabolic role in quinoa plant.

Our large-scale screening of quinoa accessions also showed a large variability for fresh and dry weights indicating a strong genetic variation for salinity tolerance in quinoa. Bladder density increased in majority of accessions under saline condition while bladder diameter remained unchanged; this resulted in a large variability in a bladder volume as a dependant variable.

Although studying EBCs at the molecular and cellular levels are challenging however, new technologies have been applied to elucidate the mechanisms by which EBCs alleviate salinity stress (Bohm et al., 2018). Thus, applying lessons from salt gland physiology to improving the salt tolerance of agricultural crops through engineering trichomes of a non-halophyte plants into functional EBCs

might be feasible. In this context, a detailed understanding of molecular basis of salt sequestration in EBCs and available knowledge of trichome development (Bohm et al., 2018; Shabala et al., 2014), in combination with new gene assembly technologies that assist transferring whole pathways to plant genomes (Patron, 2014), suggest that attempting to alter crop plants trichomes to function as salt glands may be applicable (Shabala et al., 2014). For example and based on available information (Bohm et al., 2018) it might be possible to engineer expression of salt-responsive genes such as plasma membrane H^+-ATPase and tonoplast Na^+/H^+ antiporter (NHX1) in trichomes, along with other important genes for salt transportation from metabolically active cells into trichomes. In this regard, Solanaceae crops provide potential candidates for engineering multicellular salt glands into crops (Dassanayake and Larkin, 2017). For instance, given that substantial molecular resources for tomato or potato are already available, engineering trichomes of these crops could be advantageous. The reference genomes of main commercial cultivars of both tomato and potato are available as well as the genomes of more stress tolerant wild relatives in this family (Aversano et al., 2015; Consortium, 2011). In addition to this, in Solanaceae family there are some cultivars that can tolerate moderate levels of salinity stress (Shahbaz et al., 2012), and more importantly they have naturally developed secretory trichomes in terms of structural features are similar to recretohalophytes (Dassanayake and Larkin, 2017). However, the idea of modifying a glandular trichome to a salt sequestering trichome requires the information of linking stress signalling and also coordination of salt transport from roots to shoots and finally to be sequestered to the converted glandular trichomes at a metabolic energy cost applicable for a crop plant (Dassanayake and Larkin, 2017).

In conclusion, this investigation has demonstrated that stomatal characteristics such as stomatal density and length as well as tissue-tolerance mechanisms such as salt sequestration into EBCs represent critical traits enabling plants adaptation to saline environment. These traits should become a focus of future breeding programs aimed to improve salinity tolerance in traditional crops.

7.1 References

Adams, P., Nelson, D.E., Yamada, S., Chmara, W., Jensen, R.G., Bohnert, H.J., Griffiths, H., 1998. Growth and development of *Mesembryanthemum crystallinum* (Aizoaceae). New Phytol 138, 171-190.

Agarie, S., Shimoda, T., Shimizu, Y., Baumann, K., Sunagawa, H., Kondo, A., Ueno, O., Nakahara, T., Nose, A., Cushman, J.C., 2007. Salt tolerance, salt accumulation, and ionic homeostasis in an epidermal bladder-cell-less mutant of the common ice plant *Mesembryanthemum crystallinum*. J Exp Bot 58, 1957-1967.

Amtmann, A., 2009. Learning from evolution: *Thellungiella* generates new knowledge on essential and critical components of abiotic stress tolerance in plants. Mol Plant 2, 3-12.

Aversano, R., Contaldi, F., Ercolano, M.R., Grosso, V., Iorizzo, M., Tatino, F., Xumerle, L., Dal Molin, A., Avanzato, C., Ferrarini, A., 2015. The *Solanum commersonii* genome sequence provides insights into adaptation to stress conditions and genome evolution of wild potato relatives. Plant Cell 27, 954-968.

Barkla, B.J., Vera-Estrella, R., 2015. Single cell-type comparative metabolomics of epidermal bladder cells from the halophyte *Mesembryanthemum crystallinum*. Front Plant Sci 6, 10.

Barkla, B.J., Vera-Estrella, R., Camacho-Emiterio, J., Pantoja, O., 2002. Na^+/H^+ exchange in the halophyte *Mesembryanthemum crystallinum* is associated with cellular sites of Na^+ storage. Funct Plant Biol 29, 1017-1024.

Bertolino, L.T., Caine, R.S., Gray, J.E., 2019. Impact of stomatal density and morphology on water-use efficiency in a changing world. Front Plant Sci 10, 225.

Bohm, J., Messerer, M., Muller, H.M., Scholz-Starke, J., Gradogna, A., Scherzer, S., Maierhofer, T., Bazihizina, N., Zhang, H., Stigloher, C., Ache, P., Al-Rasheid, K.A.S., Mayer, K.F.X., Shabala, S., Carpaneto, A., Haberer, G., Zhu, J.K., Hedrich, R., 2018. Understanding the molecular basis of salt sequestration in epidermal bladder cells of *Chenopodium quinoa*. Curr Biol 28, 3075-3085 e3077.

Bressan, R.A., Zhang, C., Zhang, H., Hasegawa, P.M., Bohnert, H.J., Zhu, J.K., 2001. Learning from the Arabidopsis experience. The next gene search paradigm. Plant Physiol 127, 1354-1360.

Bromham, L., 2015. Macroevolutionary patterns of salt tolerance in angiosperms. Ann Bot 115, 333-341.

Caine, R.S., Yin, X., Sloan, J., Harrison, E.L., Mohammed, U., Fulton, T., Biswal, A.K., Dionora, J., Chater, C.C., Coe, R.A., 2019. Rice with reduced stomatal density conserves water and has improved drought tolerance under future climate conditions. New Phytol 221, 371-384.

Chaves, M., Costa, J., Zarrouk, O., Pinheiro, C., Lopes, C., Pereira, J., 2016. Controlling stomatal aperture in semi-arid regions—The dilemma of saving water or being cool? Plant Sci 251, 54-64.

Cheeseman, J.M., 2015. The evolution of halophytes, glycophytes and crops, and its implications for food security under saline conditions. New Phytol 206, 557-570.

Consortium, P.G.S., 2011. Genome sequence and analysis of the tuber crop potato. Nature 475, 189.

Dassanayake, M., Larkin, J.C., 2017. Making plants break a sweat: the structure, function, and evolution of plant salt glands. Front Plant Sci 8, 406.

Flowers, T.J., Galal, H.K., Bromham, L., 2010. Evolution of halophytes: multiple origins of salt tolerance in land plants. Funct Plant Biol 37, 604-612.

Flowers, T.J., Munns, R., Colmer, T.D., 2015. Sodium chloride toxicity and the cellular basis of salt tolerance in halophytes. Ann Bot 115, 419-431.

Hedrich, R., Shabala, S., 2018. Stomata in a saline world. Curr Opin Plant Biol 46, 87-95.

Hughes, J., Hepworth, C., Dutton, C., Dunn, J.A., Hunt, L., Stephens, J., Waugh, R., Cameron, D.D., Gray, J.E., 2017. Reducing stomatal density in barley improves drought tolerance without impacting on yield. Plant Physiol 174, 776-787.

Hunt, L., Bailey, K.J., Gray, J.E., 2010. The signalling peptide EPFL9 is a positive regulator of stomatal development. New Phytol 186, 609-614.

Ibdah, M., Krins, A., Seidlitz, H.K., Heller, W., Strack, D., Vogt, T., 2002. Spectral dependence of flavonol and betacyanin accumulation in *Mesembryanthemum*

crystallinum under enhanced ultraviolet radiation. Plant Cell Environ 25, 1145-1154.

Jou, Y., Wang, Y.-L., Yen, H.E., 2007. Vacuolar acidity, protein profile, and crystal composition of epidermal bladder cells of the halophyte *Mesembryanthemum crystallinum*. Funct Plant Biol 34, 353-359.

Lawson, T., Vialet-Chabrand, S., 2019. Speedy stomata, photosynthesis and plant water use efficiency. New Phytol 221, 93-98.

Liu, Y., Sheng, Z., Liu, H., Wen, D., He, Q., Wang, S., Shao, W., Jiang, R.J., An, S., Sun, Y., Bendena, W.G., Wang, J., Gilbert, L.I., Wilson, T.G., Song, Q., Li, S., 2009. Juvenile hormone counteracts the bHLH-PAS transcription factors MET and GCE to prevent caspase-dependent programmed cell death in Drosophila. Development 136, 2015-2025.

Oh, D.H., Barkla, B.J., Vera-Estrella, R., Pantoja, O., Lee, S.Y., Bohnert, H.J., Dassanayake, M., 2015. Cell type-specific responses to salinity - the epidermal bladder cell transcriptome of *Mesembryanthemum crystallinum*. New Phytol 207, 627-644.

Patron, N.J., 2014. DNA assembly for plant biology: techniques and tools. Curr Opin Plant Biol 19, 14-19.

Raissig, M.T., Abrash, E., Bettadapur, A., Vogel, J.P., Bergmann, D.C., 2016. Grasses use an alternatively wired bHLH transcription factor network to establish stomatal identity. Proc Natl Acad Sci 113, 8326-8331.

Raissig, M.T., Matos, J.L., Anleu Gil, M.X., Kornfeld, A., Bettadapur, A., Abrash, E., Allison, H.R., Badgley, G., Vogel, J.P., Berry, J.A., Bergmann, D.C., 2017. Mobile MUTE specifies subsidiary cells to build physiologically improved grass stomata. Science 355, 1215-1218.

Rygol, J., Zimmermann, U., Balling, A., 1989. Water relations of individual leaf cells of *Mesembryanthemum crystallinum* plants grown at low and high salinity. J Membr Biol 107, 203-212.

Shabala, S., Bose, J., Hedrich, R., 2014. Salt bladders: do they matter? Trends Plant Sci 19, 687-691.

Shahbaz, M., Ashraf, M., Al-Qurainy, F., Harris, P.J., 2012. Salt tolerance in selected vegetable crops. Crit Rev Plant Sci 31, 303-320.

Steudle, E., Luttge, U., Zimmermann, U., 1975. Water relations of the epidermal bladder cells of the halophytic species *Mesembryanthemum crystallinum*:

direct measurements of hydrostatic pressure and hydraulic conductivity. Planta 126, 229-246.

Wu, H.J., Zhang, Z., Wang, J.Y., Oh, D.H., Dassanayake, M., Liu, B., Huang, Q., Sun, H.X., Xia, R., Wu, Y., Wang, Y.N., Yang, Z., Liu, Y., Zhang, W., Zhang, H., Chu, J., Yan, C., Fang, S., Zhang, J., Wang, Y., Zhang, F., Wang, G., Lee, S.Y., Cheeseman, J.M., Yang, B., Li, B., Min, J., Yang, L., Wang, J., Chu, C., Chen, S.Y., Bohnert, H.J., Zhu, J.K., Wang, X.J., Xie, Q., 2012. Insights into salt tolerance from the genome of *Thellungiella salsuginea*. Proc Natl Acad Sci 109, 12219-12224.

Supplementary Figures

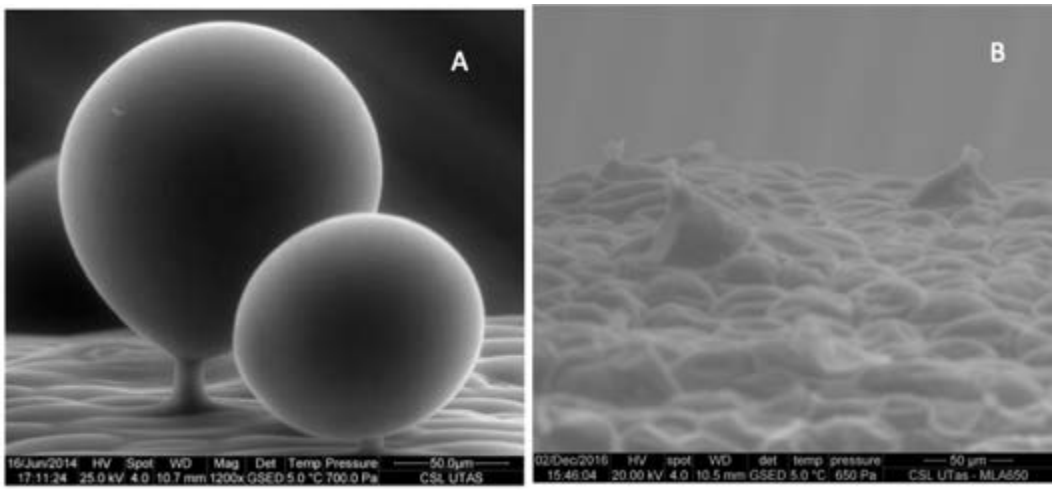

Suppl. Fig. S2.1 Anatomical structure of epidermal bladder cell (EBC)–stalk cell (SC) complex in *Chenopodium quinoa* leaves (a). Upon gentle brushing, EBC is detached from the SC, causing no damage to leaf lamella (b).

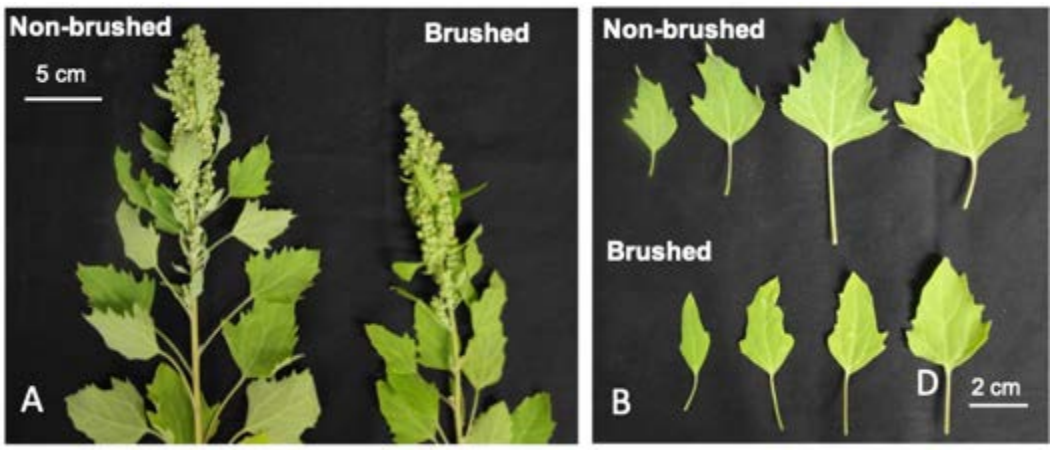

Suppl. Fig. S2.2 Severe leaf brushing results in altered plant phenotype. Quinoa plants were grown under control conditions, and EBCs were mechanically removed from each newly developed leaf by severe brushing causing thigmomorphogenetic responses. As a result, brushed plants were more stunted (a) and had smaller leaves (b).

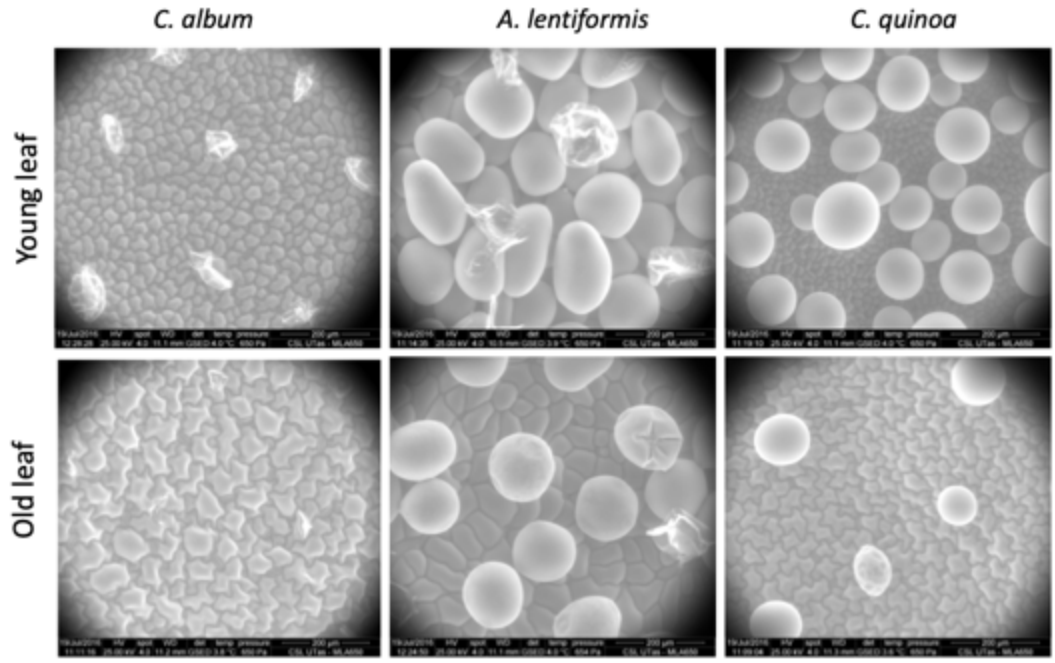

Suppl. Fig. S2.3 Differences in EBC density between young (top panels) and old (lower panels) leaves of three species used in this study. *Atriplex lentiformis* (another halophyte species) had EBC density even higher than *Chenopodium quinoa*, while in closely related *Chenopodium album*, only a few EBC could be observed in one field of view in young (but not old) leaves. Hence, adaptive strategy of *C. album* to saline stress is different from two other species and does not rely on salt sequestration in EBC.

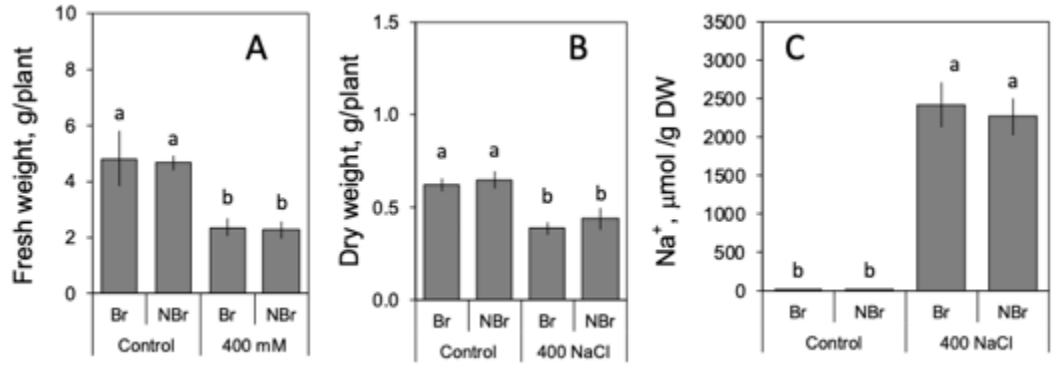

Suppl. Fig. S2.4 Effect of leaf brushing on physiological and agronomical characteristics of *Chenopodium album* plants. A – shoot fresh weigh; B - shoot dry weight; C – shoot Na^+ content. Mean ± SE (n = 5 to 7). Plants were treated with 400 mm NaCl for 5 weeks. Br – brushed; NBr – non-brushed. Different lowercase letters indicate significant difference at $P < 0.05$. As seen from the figure, contrary to *Chenopodium quinoa* plants, brushing the leaf surface of *C. album* did not result in a salt-sensitive phenotype and did not led to higher Na^+ accumulation in the leaf lamina.

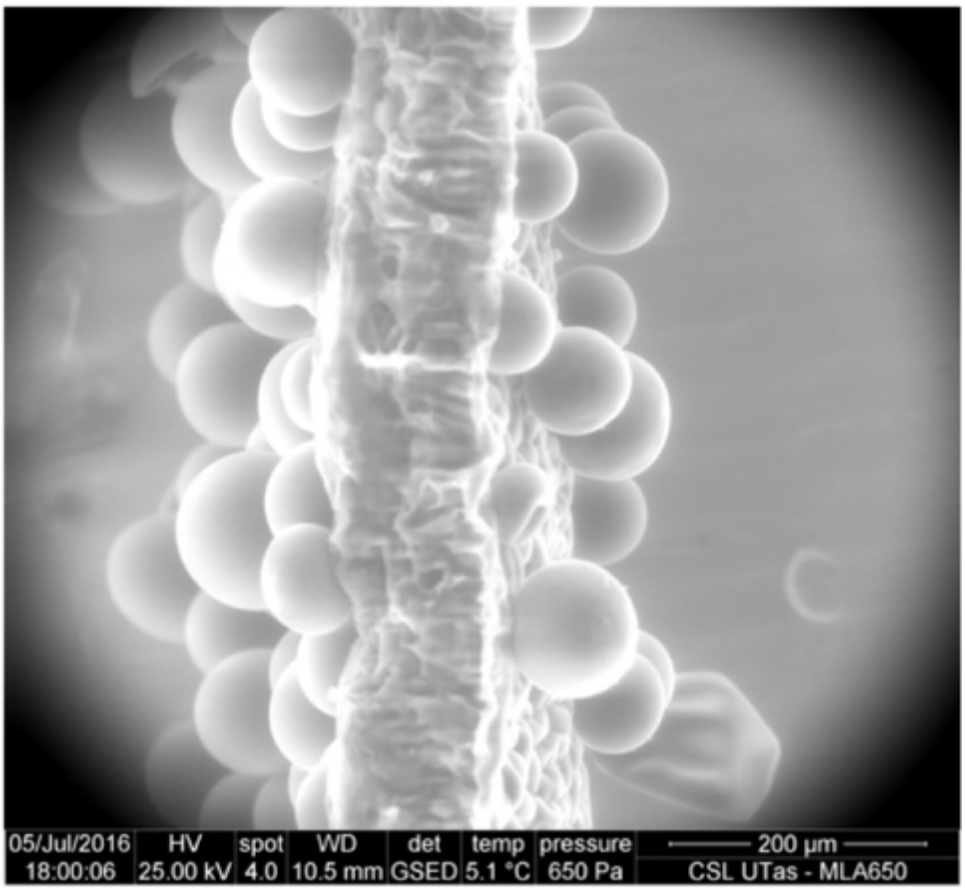

Suppl. Fig. S2.5 Cross section of salt-grown *Chenopodium quinoa* leaf showing the relative size of EBC compared with the thickness of the leaf lamina.

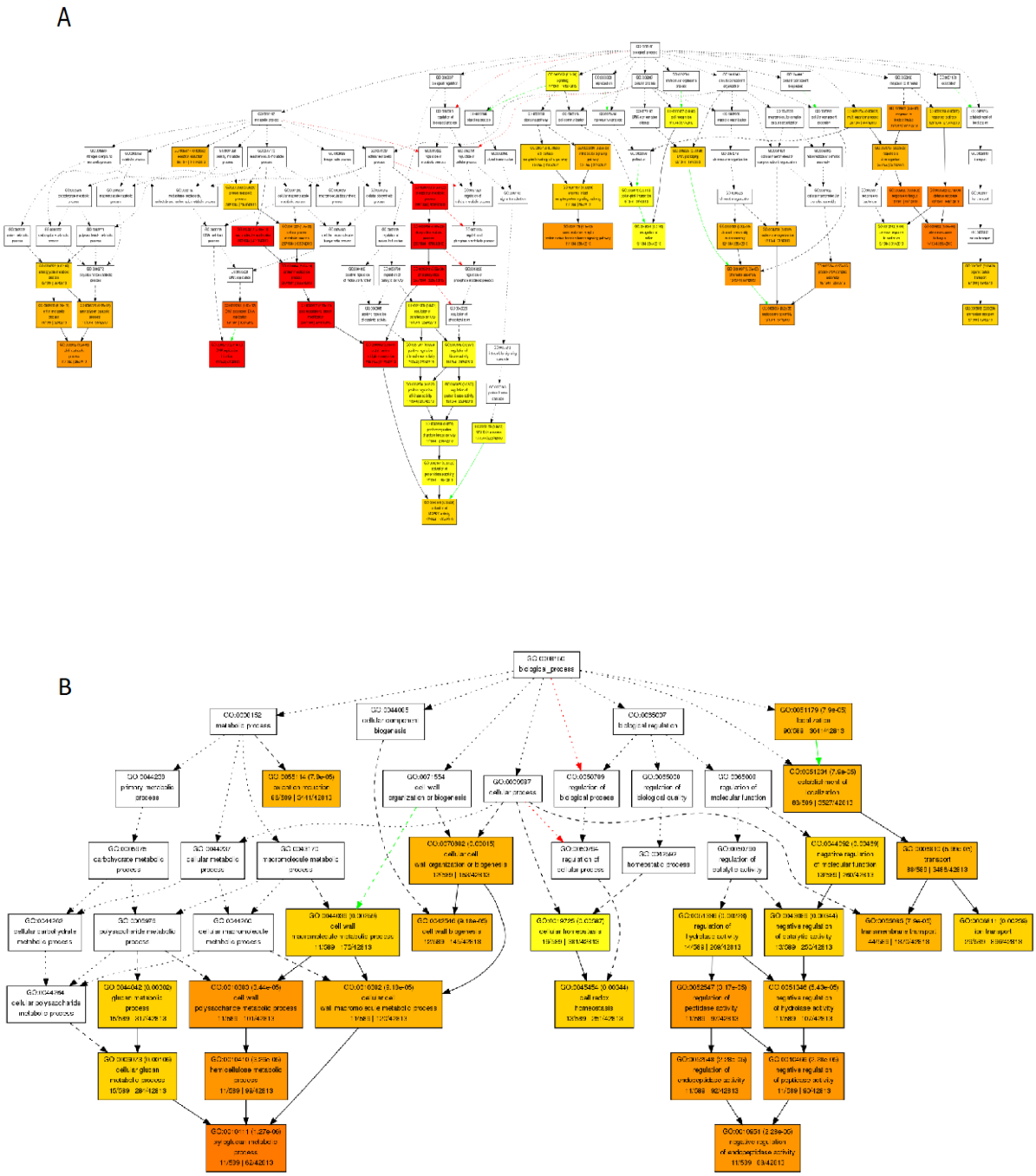

Suppl. Fig. 3.1 Differentially expressed genes (DEGs) in the quinoa leaves with and without EBCs grown under 400 mM NaCl according to agriGO term annotation analysis assigned to biological process (a) downregulated DEGs (b) upregulated DEGs

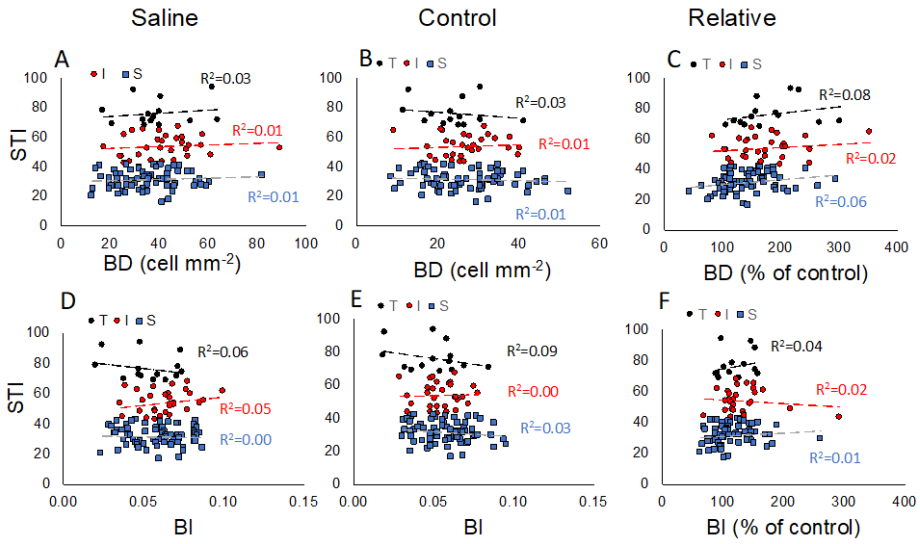

Suppl. Fig. S4.1 Regression analysis (1) between salinity tolerance index and bladder density, and (2) between STI and bladder index. A, D – saline conditions; B, E – control conditions; C, F – relative change (% control). BD, bladder density; BI, bladder index. T, I and S letters in the figures stay for salt-tolerant, intermediate and sensitive groups. Each point represents one accession which is a mean of 10 replications.

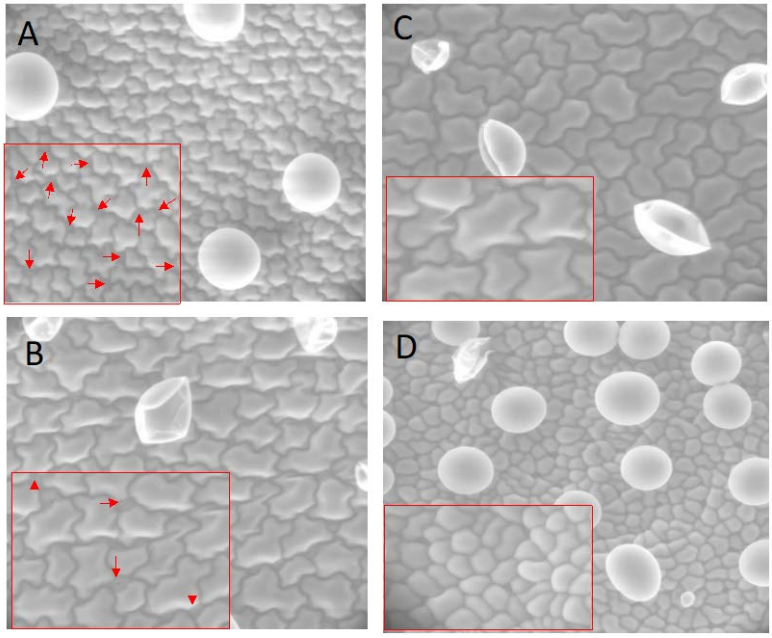

Suppl. Fig. S4.2 Scanning electron microscope images of leaf surface of a plant with A) high stomata density (accession 197); B) low stomata density (accession 141) under saline condition (The red arrows in the inset show stomata in an area of 0.063 mm^2 of the image); C) images of leaf surface of a plant with high epidermal cell area (accession Q28) and D) low epidermal cell area (accession 208) under saline condition (The inset show epidermal cells in an area of 0.026 mm^2 of the image).

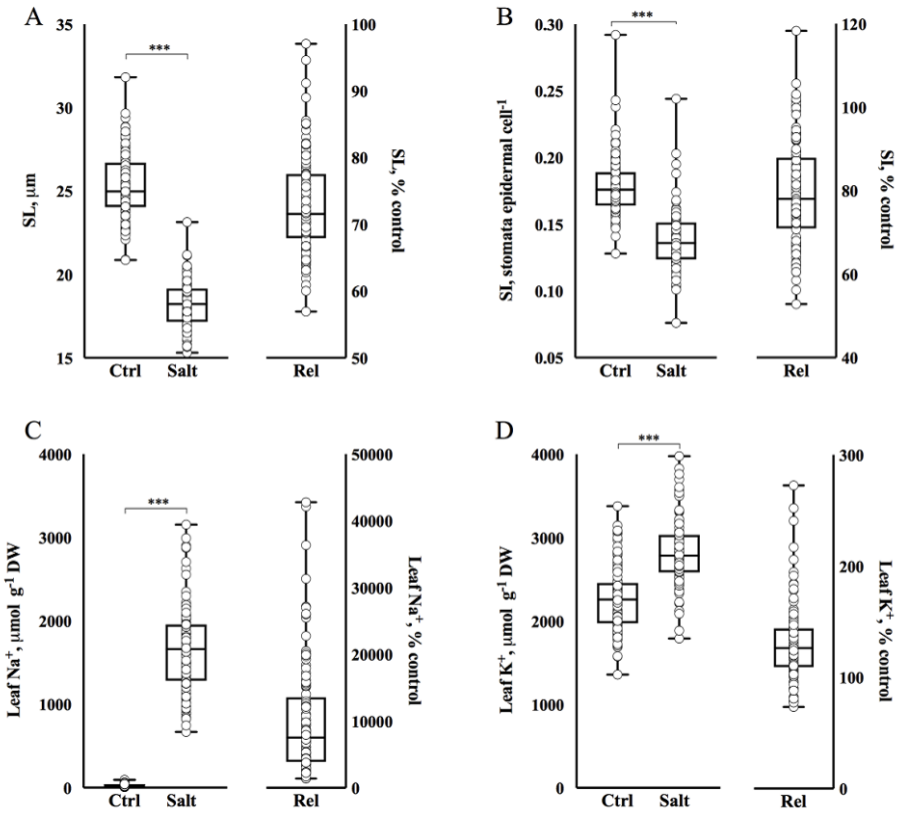

Suppl. Fig. S4.3 Genetic variation in stomatal characteristics and Na^+ and K^+ concentrations in leaves. A - stomatal length, SL; B - stomatal index, SI; C – leaf Na^+ ; D – leaf K^+ . Each dot in the box plot representing a mean value of a single accession under control (Ctrl), saline (Salt) and in relative term (Rel). The middle line in the box plot denotes the median. *** shows significant difference (P <0.001)

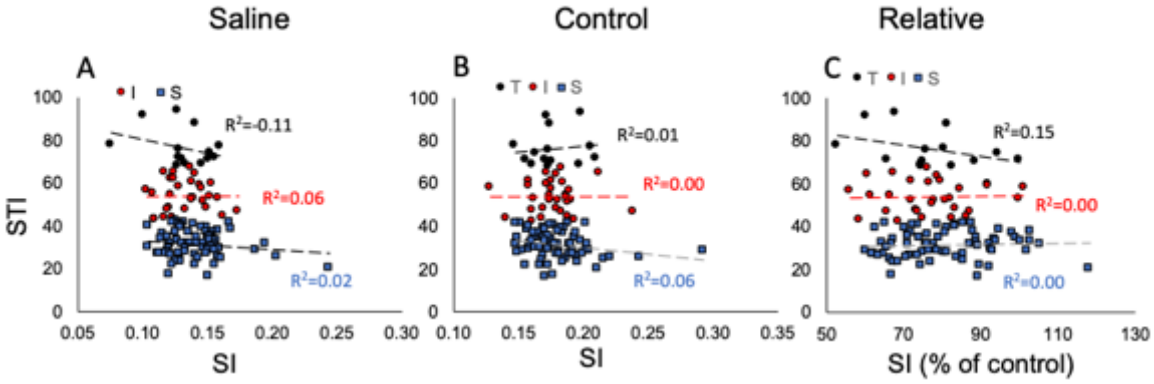

Suppl. Fig. S4.4 Regression analysis between salinity tolerance index and bladder index. A – saline conditions; B – control conditions; C – relative change (% control). SI, stomata index. T, I and S letters in the figures stay for salt-tolerant, intermediate and sensitive groups. Each point represents one accession which is a mean of 10 replications.

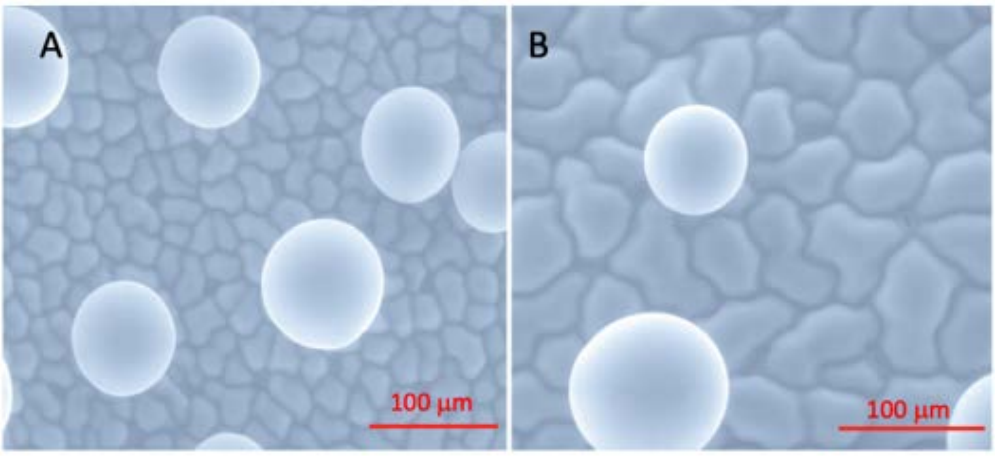

Suppl. Fig. S4.5 Scanning electron microscope images of leaf surface of a plant with A) low epidermal cell area and smaller stomatal length (accession 208) and B) high epidermal cell area and bigger stomatal length (accession Q28) under saline condition

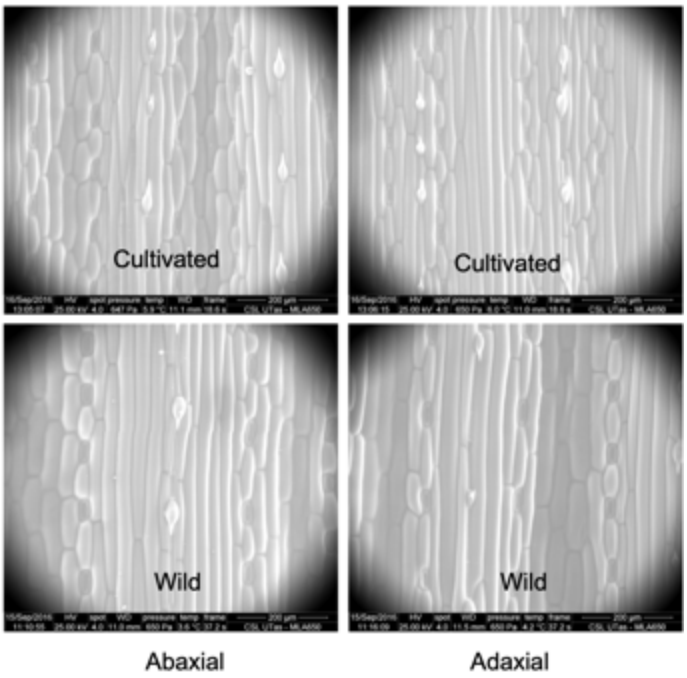

Suppl. Fig 6.1 Typical images of abaxial and adaxial surfaces of one representative cultivated (cv Gairdner) and one wild (X133) barley genotypes.

Supplementary Tables

Suppl. Table S2.1 Untargeted gas chromatography–mass spectrometry (GC–MS) metabolite profile comparisons of brushed versus non-brushed grown under control conditions. CNB = control non-brushed; CB = control brushed. Data are presented as x-fold with CNB set to 1 (n = 5). The blue cells indicate statistical significance determined with Student's t-test ($P > 0.05$)

	Control NBr		Control Br	
ORGANIC ACIDS	**x-fold**	**sem**	**x-fold**	**sem**
Oxalate	1.000	± 0.567	-1.404	± 0.366
Benzoate	1.000	± 0.141	-1.292	± 0.089
Nicotinic acid	1.000	± 0.185	-1.349	± 0.190
Succinate	1.000	± 0.152	-1.066	± 0.064
Fumarate	1.000	± 0.152	-1.162	± 0.216
Malate	1.000	± 0.142	1.306	± 0.278
Pyroglutamate	1.000	± 0.317	-1.063	± 0.135
Citrate	1.000	± 0.266	-1.307	± 0.160
Ascorbic acid/ Iso ascorbic	1.000	± 0.240	-1.178	± 0.222
4_hydroxy cinnamic acid	1.000	± 0.183	-1.260	± 0.244
Mucic/saccharic	1.000	± 0.142	1.218	± 0.137
SUGARS AND SUGAR ALCOHOLS	**x-fold**	**sem**	**x-fold**	**sem**
Threitol	1.000	± 0.184	-1.292	± 0.150
Erythronate	1.000	± 0.066	1.291	± 0.135
Threonate	1.000	± 0.193	1.202	± 0.086
Xylose	1.000	± 0.156	1.057	± 0.167
Arabinose	1.000	± 0.078	1.021	± 0.091
Ribose	1.000	± 0.072	-1.010	± 0.058
Rhamnose	1.000	± 0.097	1.061	± 0.076
Arabitol	1.000	± 0.140	-1.120	± 0.168
Ribonate	1.000	± 0.371	-1.758	± 0.211
Galactose	1.000	± 0.122	-1.095	± 0.155
Galactitol	1.000	± 0.138	-1.258	± 0.144
Galactonate	1.000	± 0.177	-1.303	± 0.031

Inositol	1.000	±	0.043	-1.016	±	0.065
Fructose-6-P	1.000	±	0.190	1.529	±	0.192
Glucose-6-P	1.000	±	0.197	1.773	±	0.196
Maltose	1.000	±	0.124	1.233	±	0.170
Trehalose	1.000	±	0.220	-1.343	±	0.125
Fructose	1.000	±	0.165	1.072	±	0.175
Glucose	1.000	±	0.313	-1.145	±	0.267
Inositol	1.000	±	0.036	-1.057	±	0.067
Sucrose	1.000	±	0.035	-1.135	±	0.075
OTHERS	**x-fold**		**sem**	**x-fold**		**sem**
Monomethylphosphate	1.000	±	0.259	1.017	±	0.240
Diethylene_glycol	1.000	±	0.313	-1.453	±	0.266
Glycerate	1.000	±	0.097	1.549	±	0.243
Threonate-1,4-lactone	1.000	±	0.178	-1.039	±	0.202
Cytosine	1.000	±	0.177	-1.267	±	0.100
Glycerol-3-P	1.000	±	0.139	1.161	±	0.122
Pantothenic acid	1.000	±	0.134	-1.172	±	0.108
Phosphate	1.000	±	0.199	1.729	±	0.174
AMINO ACIDS AND AMINES	**x-fold**		**sem**	**x-fold**		**sem**
Aspartate	1.000	±	0.154	1.239	±	0.161
Ethanolamine	1.000	±	0.212	1.014	±	0.186
GABA	1.000	±	0.378	1.239	±	0.272
Glutamate	1.000	±	0.226	1.200	±	0.216
Glycine	1.000	±	0.117	1.119	±	0.124
Isoleucine	1.000	±	0.295	-1.376	±	0.279
Phenylalanine	1.000	±	0.329	-1.137	±	0.267
Proline	1.000	±	0.261	-1.038	±	0.177
Serine	1.000	±	0.160	1.390	±	0.154
Threonine	1.000	±	0.322	-1.182	±	0.245
Tyrosine	1.000	±	0.433	1.186	±	0.341
Valine	1.000	±	0.239	-1.105	±	0.170
UNKNOWNS	**x-fold**		**sem**	**x-fold**		**sem**
UN_2_276_13.279	1.000	±	0.229	1.275	±	0.185
UN_3_205_13.816	1.000	±	0.382	1.107	±	0.297
UN_4_262_14.466	1.000	±	0.050	**-1.244**	**±**	**0.025**

UN_6_306_16.105	1.000 ± 0.095	-1.067 ± 0.039
UN_7_306_16.255	1.000 ± 0.092	-1.152 ± 0.034
UN_8_292_16.499?	1.000 ± 0.151	-1.299 ± 0.075
UN_9_204_18.259	1.000 ± 0.136	-1.084 ± 0.156
UN_10_217_18.860	1.000 ± 0.403	-1.346 ± 0.153
UN_11_292_19.232	1.000 ± 0.125	-1.003 ± 0.100
UN_12_275_20.337	1.000 ± 0.086	1.011 ± 0.069
UN_13_285_20.524	1.000 ± 0.367	-1.605 ± 0.364
UN_14_275_20.752	1.000 ± 0.161	-1.189 ± 0.077
UN_15_273_21.216	1.000 ± 0.095	-1.406 ± 0.209
UN_16_361_21.963	1.000 ± 0.433	-1.374 ± 0.240
UN_17_174_23.147	1.000 ± 0.181	-1.705 ± 0.142
UN_18_319_23.921	1.000 ± 0.074	-1.091 ± 0.115
UN_19_445_25.068	1.000 ± 0.166	-1.072 ± 0.143
UN_20_204_25.590	1.000 ± 0.214	1.049 ± 0.167
UN_21_290_26.044	1.000 ± 0.088	1.010 ± 0.124
UN_22_318_27.667	1.000 ± 0.174	1.488 ± 0.211
UN_23_321_28.613	1.000 ± 0.073	-1.101 ± 0.064
UN_24_191_29.266	1.000 ± 0.211	1.075 ± 0.089
UN_25_204_30.286	1.000 ± 0.056	-1.041 ± 0.059
UN_26_328_31.254	1.000 ± 0.122	-1.195 ± 0.129
UN_27_318_31.709	1.000 ± 0.159	1.025 ± 0.102
UN_31_297_33.138	1.000 ± 0.158	-1.083 ± 0.129
UN_32_327_33.739	1.000 ± 0.197	-1.514 ± 0.186
UN_33_647_35.483	1.000 ± 0.284	-1.308 ± 0.385
UN_154_7.967	1.000 ± 0.418	-1.584 ± 0.440
UN_14_275_20.752	1.000 ± 0.134	-1.124 ± 0.045
UN_18.033	1.000 ± 0.118	-1.061 ± 0.094

Suppl. Table S2.2 Untargeted GC-MS metabolite profile comparison of brushed versus non-brushed quinoa leaves grown under saline conditions. TNB = Treated Non-Brushed; TB = Treated Brushed. Data are presented as x-fold with TNB set to 1 (n=5). Blue cells indicate statistical significance determined with Students t-test (P > 0.05).

	Salt NBr		**Salt Br**	
ORGANIC ACIDS	**x-fold**	**sem**	**x-fold**	**sem**
Ascorbic acid/ Iso ascorbic	1.000	± 0.289	2.175	± 0.210
Benzoate	1.000	± 0.025	1.003	± 0.051
Citrate	1.000	± 0.200	**-2.586**	**± 0.247**
Fumarate	1.000	± 0.287	-3.558	± 0.413
Glycerate	1.000	± 0.160	-1.551	± 0.157
Glycolic acid	1.000	± 0.072	**-1.717**	**± 0.076**
Malate	1.000	± 0.219	-2.472	± 0.496
Mucic/saccharic	1.000	± 0.165	-1.156	± 0.234
Nicotinic acid	1.000	± 0.059	-1.604	± 0.256
Oxalate	1.000	± 0.224	**-6.247**	**± 0.484**
Pipercolic acid	1.000	± 0.278	-2.319	± 0.414
Salicylic acid	1.000	± 0.223	-2.100	± 0.489
Succinate	1.000	± 0.074	1.240	± 0.189
Threonate	1.000	± 0.176	**-3.678**	**± 0.334**
Threonate-1,4-lactone	1.000	± 0.045	-1.208	± 0.186
SUGARS AND SUGAR ALCOHOLS	**x-fold**	**sem**	**x-fold**	**sem**
Arabinose	1.000	± 0.242	1.201	± 0.306
Arabitol	1.000	± 0.125	1.260	± 0.075
Erythritol	1.000	± 0.159	1.252	± 0.087
Fructose	1.000	± 0.080	-1.004	± 0.168
Fructose-6-P	1.000	± 0.333	-1.151	± 0.117
Fucose	1.000	± 0.092	-1.262	± 0.202
Galactonate	1.000	± 0.145	-1.025	± 0.062
Galactose	1.000	± 0.177	-1.054	± 0.172

Glucose	1.000 ± 0.088	-1.014 ± 0.166
Glucose-6-P	1.000 ± 0.340	-2.652 ± 0.254
Glycerol	1.000 ± 0.160	-1.282 ± 0.107
Glycerol-3-P	1.000 ± 0.198	**-2.282 ± 0.254**
Inosito-1-P	1.000 ± 0.253	**-2.174 ± 0.170**
Inositol	1.000 ± 0.128	-1.022 ± 0.128
Maltose	1.000 ± 0.060	-1.259 ± 0.405
Ribitol	1.000 ± 0.125	1.291 ± 0.081
Ribonate	1.000 ± 0.159	1.120 ± 0.125
Ribose	1.000 ± 0.298	2.496 ± 0.295
Sucrose	1.000 ± 0.147	1.151 ± 0.090
Threitol	1.000 ± 0.157	**1.768 ± 0.118**
Trehalose	1.000 ± 0.068	-1.647 ± 0.310
Xylitol	1.000 ± 0.167	1.693 ± 0.205
Xylose	1.000 ± 0.113	1.286 ± 0.248
OTHERS	**x-fold sem**	**x-fold sem**
Butyro-1,4- lactam	1.000 ± 0.062	-2.173 ± 0.386
Cytosine	1.000 ± 0.060	-1.180 ± 0.068
Diethyleneglycol	1.000 ± 0.036	1.017 ± 0.025
Guanine	1.000 ± 0.141	-2.736 ± 0.527
Kaempferol	1.000 ± 0.189	**-3.004 ± 0.292**
Monomethylphosphate	1.000 ± 0.178	-1.391 ± 0.188
Phosphate	1.000 ± 0.345	-1.866 ± 0.112
Uracil	1.000 ± 0.227	**-3.371 ± 0.262**
AMINO ACIDS AND AMINES	**x-fold sem**	**x-fold sem**
2 - amino malonic acid	1.000 ± 0.226	-2.227 ± 0.298
Alanine	1.000 ± 0.251	-1.826 ± 0.267
Allantoin	1.000 ± 0.121	-1.218 ± 0.206
Arginine	1.000 ± 0.256	-1.158 ± 0.411
Asparagine	1.000 ± 0.298	-1.934 ± 0.295
Aspartate	1.000 ± 0.209	**-2.816 ± 0.272**
GABA	1.000 ± 0.078	**-1.809 ± 0.281**

Cysteine	1.000 ± 0.213	-1.647 ± 0.263
Ethanolamine	1.000 ± 0.129	1.296 ± 0.055
GABA	1.000 ± 0.156	-1.797 ± 0.283
Glutamate	1.000 ± 0.354	1.291 ± 0.280
Glutamine	1.000 ± 0.295	6.980 ± 0.569
Glycine	1.000 ± 0.240	-2.322 ± 0.310
Histidine	1.000 ± 0.269	-1.319 ± 0.404
Isoleucine	1.000 ± 0.262	-2.085 ± 0.358
Lysine	1.000 ± 0.291	-2.000 ± 0.403
Methionine	1.000 ± 0.247	-1.933 ± 0.479
Ornithine	1.000 ± 0.158	2.191 ± 0.516
Phenylalanine	1.000 ± 0.266	-2.036 ± 0.378
Proline	1.000 ± 0.080	-1.419 ± 0.215
Pyroglutamate	1.000 ± 0.239	1.181 ± 0.410
Serine	1.000 ± 0.195	1.099 ± 0.229
Threonine	1.000 ± 0.265	-1.746 ± 0.267
Tryptophan	1.000 ± 0.288	-2.742 ± 0.557
Tyrosine	1.000 ± 0.314	-2.179 ± 0.427
Valine	1.000 ± 0.239	-2.013 ± 0.306

UNKNOWNS	x-fold	sem	x-fold	sem
UN_14_275_20.752	1.000	± 0.075	-1.281	± 0.139
UN_16_361_21.963	1.000	± 0.095	-1.357	± 0.337
UN_17_174_23.147	1.000	± 0.260	-3.078	± 0.648
UN_18_319_23.921	1.000	± 0.189	1.421	± 0.121
UN_19_445_25.068	1.000	± 0.133	-1.067	± 0.196
UN_22_318_27.667	1.000	± 0.250	**-2.179**	**± 0.164**
UN_23_321_28.613	1.000	± 0.211	1.588	± 0.183
UN_24_191_29.266	1.000	± 0.262	-1.297	± 0.134
UN_33_647_35.483	1.000	± 0.276	**-3.182**	**± 0.278**
UN_6_306_16.021	1.000	± 0.059	1.087	± 0.089
Unknown_13.984_243	1.000	± 0.255	-1.242	± 0.375
Unknown_16.327_219	1.000	± 0.154	1.693	± 0.194
Unknown_16.430_116	1.000	± 0.237	-1.441	± 0.320
Unknown_16.633_142	1.000	± 0.297	-1.200	± 0.398
Unknown_17.096_201	1.000	± 0.249	1.025	± 0.167
Unknown_18.233_242	1.000	± 0.063	1.049	± 0.050
Unknown_19.173_245	1.000	± 0.359	1.913	± 0.442
Unknown_24.885_357	1.000	± 0.126	-1.010	± 0.202
Unknown_27.040_375	1.000	± 0.169	-2.132	± 0.369
Unknown_27.270_258	1.000	± 0.165	**-3.501**	**± 0.714**
Unknown_8.082_188	1.000	± 0.031	1.025	± 0.057
Unknown_8.699_282	1.000	± 0.350	-1.298	± 0.350
Unknown_8.919_86	1.000	± 0.264	**-2.118**	**± 0.100**
Unknown_9.956_248	1.000	± 0.163	**-3.197**	**± 0.313**

OTHERS	x-fold		sem	x-fold		sem
Monomethylphosphate	1.000	±	0.259	1.017	±	0.240
Diethylene_glycol	1.000	±	0.313	-1.453	±	0.266
Glycerate	1.000	±	0.097	1.549	±	0.243
Threonate-1,4-lactone	1.000	±	0.178	-1.039	±	0.202
Cytosine	1.000	±	0.177	-1.267	±	0.100
Glycerol-3-P	1.000	±	0.139	1.161	±	0.122
Pantothenic acid	1.000	±	0.134	-1.172	±	0.108
Phosphate	1.000	±	0.199	1.729	±	0.174
AMINO ACIDS AND AMINES	**x-fold**		**sem**	**x-fold**		**sem**
Aspartate	1.000	±	0.154	1.239	±	0.161
Ethanolamine	1.000	±	0.212	1.014	±	0.186
GABA	1.000	±	0.378	1.239	±	0.272
Glutamate	1.000	±	0.226	1.200	±	0.216
Glycine	1.000	±	0.117	1.119	±	0.124
Isoleucine	1.000	±	0.295	-1.376	±	0.279
Phenylalanine	1.000	±	0.329	-1.137	±	0.267
Proline	1.000	±	0.261	-1.038	±	0.177
Serine	1.000	±	0.160	1.390	±	0.154
Threonine	1.000	±	0.322	-1.182	±	0.245
Tyrosine	1.000	±	0.433	1.186	±	0.341
Valine	1.000	±	0.239	-1.105	±	0.170

UNKNOWNS	x-fold		sem	x-fold		sem
UN_2_276_13.279	1.000	±	0.229	1.275	±	0.185
UN_3_205_13.816	1.000	±	0.382	1.107	±	0.297
UN_4_262_14.466	1.000	±	0.050	**-1.244**	**±**	**0.025**
UN_6_306_16.105	1.000	±	0.095	-1.067	±	0.039
UN_7_306_16.255	1.000	±	0.092	-1.152	±	0.034
UN_8_292_16.499?	1.000	±	0.151	-1.299	±	0.075
UN_9_204_18.259	1.000	±	0.136	-1.084	±	0.156
UN_10_217_18.860	1.000	±	0.403	-1.346	±	0.153
UN_11_292_19.232	1.000	±	0.125	-1.003	±	0.100
UN_12_275_20.337	1.000	±	0.086	1.011	±	0.069
UN_13_285_20.524	1.000	±	0.367	-1.605	±	0.364
UN_14_275_20.752	1.000	±	0.161	-1.189	±	0.077
UN_15_273_21.216	1.000	±	0.095	-1.406	±	0.209
UN_16_361_21.963	1.000	±	0.433	-1.374	±	0.240
UN_17_174_23.147	1.000	±	0.181	-1.705	±	0.142
UN_18_319_23.921	1.000	±	0.074	-1.091	±	0.115
UN_19_445_25.068	1.000	±	0.166	-1.072	±	0.143
UN_20_204_25.590	1.000	±	0.214	1.049	±	0.167
UN_21_290_26.044	1.000	±	0.088	1.010	±	0.124
UN_22_318_27.667	1.000	±	0.174	1.488	±	0.211
UN_23_321_28.613	1.000	±	0.073	-1.101	±	0.064
UN_24_191_29.266	1.000	±	0.211	1.075	±	0.089
UN_25_204_30.286	1.000	±	0.056	-1.041	±	0.059
UN_26_328_31.254	1.000	±	0.122	-1.195	±	0.129
UN_27_318_31.709	1.000	±	0.159	1.025	±	0.102
UN_31_297_33.138	1.000	±	0.158	-1.083	±	0.129
UN_32_327_33.739	1.000	±	0.197	-1.514	±	0.186
UN_33_647_35.483	1.000	±	0.284	-1.308	±	0.385
UN_154_7.967	1.000	±	0.418	-1.584	±	0.440
UN_14_275_20.752	1.000	±	0.134	-1.124	±	0.045
UN_18.033	1.000	±	0.118	-1.061	±	0.094

Suppl. Table S2.3 Geometrical consideration and cell volume to surface ratio for cells of different size in the context of carbon cost efficiency associated with cell wall formation. The bigger is the cell diameter, the less carbon is required per volume unit.

Cell diameter, μm	Cell volume, μm^3	Surface area, μm^2	Volume to surface ratio
20	4186	1256	3.33
40	33493	5024	6.66
60	113040	11304	10
100	523333	31400	16.66
150	1766250	70650	25
200	4186667	125600	33.33
300	14130000	282600	50
400	33493333	502400	66.66
500	65416667	785000	83.33
600	1.13E+08	1130400	100

Suppl. Table S4.1 Mean values of fresh weight, dry weight, and bladder-related characteristics under non-saline and saline conditions with corresponding relative values

Accession		FW	DW	BD	BDM	BV	BI
127	Ctrl	4.3±0.13	0.35±0.014	16.4±0.9	82.7±4.8	0.005±0.001	0.052±0.005
	Salt	1.2±0.01	0.15±0.003	26.1±1.5	89.9±3.2	0.009±0.001	0.058±0.008
	Rel	27.7±1.1	42.56±2.126	165±15.4	110.2±7.5	201.8±29.5	113.8±15.314
132	Ctrl	3.6±0.37	0.35±0.028	17.9±1.3	110.5±7.6	0.013±0.002	0.063±0.01
	Salt	1.4±0.11	0.14±0.014	32.1±1.3	82.5±4.6	0.01±0.001	0.072±0.018
	Rel	39.3±5.73	39.82±2.721	190.6±18.7	76.4±8.1	72.3±3.605	113.39±19.981
133	Ctrl	2±0.11	0.22±0.012	30.8±3.7	103.5±5.5	0.017±0.001	0.047±0.007
	Salt	1.3±0.17	0.13±0.008	39.9±1.7	83.5±3.9	0.012±0.001	0.065±0.006
	Rel	62.3±9.6	58.26±6.221	143.5±15.1	80.9±2.3	75.429±5.361	153.12±27.111
134	Ctrl	3.4±0.1	0.35±0.005	22.4±1.6	98.7±3.5	0.011±0.001	0.061±0.009
	Salt	1±0.05	0.12±0.005	36.7±2.2	80.1±4.8	0.011±0.001	0.083±0.006
	Rel	30.2±1.51	33.26±1.247	170.7±15.5	82.1±7.6	107.4±9.194	146.43±16.624
135	Ctrl	5.1±0.18	0.44±0.019	17±0.9	100.3±3.6	0.009±0.001	0.042±0.005
	Salt	1.4±0.13	0.16±0.014	33.9±5.1	91±1.8	0.013±0.001	0.041±0.004
	Rel	26.4±2.41	35.74±2.789	191.3±32.1	91.4±4.7	124.2±1.7	106.05±18.773
136	Ctrl	2.4±0.22	0.22±0.026	13.6±1.3	103.2±2.8	0.008±0.001	0.04±0.006
	Salt	0.7±0.04	0.07±0.003	22.9±2.1	84.7±5.5	0.009±0.001	0.038±0.006
	Rel	30.5±3.64	34.69±3.643	172.4±13	82.4±6	104.9±11.9	107.7±26.4
137	Ctrl	2.6±0.18	0.26±0.008	34.9±4.6	95.5±6.8	0.014±0.001	0.065±0.007
	Salt	0.7±0.04	0.08±0.005	31.7±2	87.5±1.8	0.011±0.001	0.065±0.004
	Rel	29.2±3.16	31.61±2.014	102.2±12.5	93.8±7.9	72.3±5.9	104.5±10
138	Ctrl	2.8±0.21	0.25±0.022	17±1	110.6±4.4	0.012±0.002	0.05±0.002
	Salt	1.1±0.19	0.11±0.023	26.9±1.6	102.5±2.9	0.014±0.001	0.044±0.005
	Rel	38.8±4.01	41.59±8.609	166.3±16.9	93.4±5.4	100.1±7.3	87.5±8.1
140	Ctrl	4±0.44	0.44±0.054	21.6±1.3	97.4±4.6	0.011±0.001	0.038±0.003
	Salt	1.7±0.27	0.18±0.024	40.5±2.4	90.4±4.3	0.017±0.001	0.046±0.008
	Rel	43.7±12.02	41.74±10.721	188.8±5.5	94±7.5	170.4±22.1	124.3±26.3
141	Ctrl	4.6±0.13	0.38±0.012	19.4±1.5	96.3±7.9	0.009±0.002	0.065±0.011
	Salt	1±0.05	0.11±0.005	35.4±3.5	91.8±5.3	0.015±0.003	0.082±0.007
	Rel	22.8±1.26	28.02±0.942	192.5±23.7	96.6±6.3	131.1±12.7	147.5±35.5
144	Ctrl	4.2±0.21	0.47±0.034	24.6±2.9	117.7±1.7	0.019±0.002	0.048±0.007
	Salt	1±0.09	0.11±0.009	35.6±2.4	87.7±3.6	0.013±0.002	0.076±0.007

	Rel	23.9±3.06	23.41±3.358	161.1±21.4	74.5±3.2	59.2±5.9	173.1±30.1
	Ctrl	4.3±0.22	0.4±0.024	28.7±1.3	97.5±2.3	0.014±0.001	0.056±0.002
146	Salt	1.4±0.06	0.15±0.01	32.3±1.8	81.4±2.3	0.009±0.001	0.082±0.005
	Rel	31.1±2.96	38.81±5.965	115.3±9.1	83.8±3.4	65.5±7.6	146.2±5.4
	Ctrl	2.4±0.18	0.24±0.016	28±1.5	105.2±4.9	0.017±0.001	0.06±0.002
147	Salt	1.3±0.05	0.14±0.005	43.3±2.6	89.3±2.8	0.016±0.002	0.1±0.009
	Rel	54.8±5.84	60.64±3.232	160±14.5	85.9±6	108.2±10.3	166.4±13.9
	Ctrl	3.7±0.21	0.4±0.033	21.3±1.3	95.8±6.3	0.011±0.001	0.049±0.005
148	Salt	2.2±0.16	0.25±0.015	40.5±2.2	83±1.3	0.012±0.001	0.057±0.003
	Rel	58.5±3.76	63.99±5.184	197.2±16.2	88.2±6	135.8±17.1	125.4±19.9
	Ctrl	1.6±0.08	0.17±0.007	31.7±1.8	103±5.5	0.018±0.003	0.063±0.008
149	Salt	1±0.09	0.11±0.009	48.3±3.6	96.1±5.6	0.025±0.002	0.078±0.015
	Rel	62.1±2.81	67.47±6.995	152.8±8	94.8±9.3	141.6±19.8	123.8±17.3
	Ctrl	2.6±0.23	0.27±0.028	22.2±1.1	98.8±5.7	0.011±0.002	0.05±0.003
150	Salt	1.3±0.11	0.15±0.016	41.4±3.7	92.1±3	0.017±0.002	0.055±0.007
	Rel	53.1±5.69	57.53±7.001	187.3±14.4	94.5±6.2	158.8±9.4	110.5±11.1
	Ctrl	3.1±0.21	0.28±0.02	23.7±1.7	107.4±11.9	0.012±0.001	0.064±0.013
151	Salt	1.2±0.1	0.12±0.011	37.3±3.8	90.8±7	0.016±0.001	0.067±0.005
	Rel	37.6±4	44.49±4.959	168.1±25.8	88±11	108.3±11.1	137.3±43.6
	Ctrl	4.1±0.18	0.31±0.036	21.6±1.1	91.6±2.5	0.009±0.001	0.044±0.007
153	Salt	0.9±0.08	0.1±0.01	35.8±1.8	88.8±4.8	0.011±0.001	0.063±0.005
	Rel	22.6±1.82	33.33±2.293	168.5±8.7	97.2±5.8	148.4±15.9	154.7±17.7
	Ctrl	2±0.1	0.21±0.014	30.6±3	108.5±5.9	0.024±0.003	0.069±0.008
154	Salt	1.2±0.06	0.14±0.009	34±0.9	92.2±12.2	0.013±0.001	0.06±0.006
	Rel	59.7±5.07	71.32±5.288	121.5±12.8	85.7±12.8	85.3±11.6	91±13
	Ctrl	2.6±0.17	0.28±0.018	34.3±3.3	86.4±3.3	0.011±0.001	0.074±0.014
155	Salt	0.9±0.12	0.1±0.017	34.2±1.6	84±2	0.011±0.001	0.086±0.01
	Rel	35.8±6.52	33.02±5.798	116.5±21.2	98.1±5.6	97.9±10.3	139.5±33.3
	Ctrl	3.9±0.11	0.29±0.006	28.5±2.1	103.9±2.6	0.017±0.002	0.071±0.005
157	Salt	0.7±0.08	0.08±0.008	13.5±1	92.2±12.2	0.007±0.001	0.047±0.011
	Rel	16.7±1.67	25.43±2.515	45.8±5.3	88.8±12.1	40.8±10	66.8±17.7
	Ctrl	2.6±0.15	0.26±0.015	23.3±1.8	131.2±13.2	0.034±0.009	0.043±0.003
158	Salt	1.5±0.13	0.18±0.016	64.2±8.1	109.2±17.4	0.043±0.017	0.047±0.002
	Rel	58±2.99	71.52±8.06	303.8±55.6	91.2±20.6	126±12	112.6±10.9
159	Ctrl	2.9±0.3	0.31±0.027	27.6±3.1	91.9±4.4	0.011±0.001	0.064±0.008

	Salt	1.4±0.04	0.16±0.006	35.1±1.8	84±2	0.011±0.001	0.067±0.006
	Rel	50±6.03	52.44±3.242	142.7±19.9	92±4.1	112.8±7	113.7±19.9
	Ctrl	2.2±0.24	0.24±0.021	34.3±2.2	85.7±3.5	0.011±0.001	0.075±0.007
161	Salt	1.2±0.09	0.14±0.01	47.5±3.5	92.4±3	0.02±0.002	0.079±0.004
	Rel	59±9.81	59.12±6.979	145.4±16.2	108.4±5.3	199.7±22	109.6±12.9
	Ctrl	1.4±0.08	0.14±0.016	17.7±1.8	106.1±6.4	0.012±0.001	0.034±0.003
168	Salt	0.7±0.04	0.07±0.007	17.9±2.1	86.2±11.6	0.009±0.001	0.036±0.004
	Rel	50.4±1.45	53.28±2.348	108.9±13.7	84.1±14.4	89.8±15.2	105.5±5.4
	Ctrl	4.7±0.47	0.42±0.045	20.7±2.4	90.9±7.7	0.008±0.001	0.059±0.01
169	Salt	0.7±0.05	0.09±0.006	26.7±2.6	90.7±2	0.011±0.001	0.052±0.008
	Rel	15.7±1.22	21.95±2.333	127.7±13.2	103.8±11.9	137.5±10.6	98.1±19.4
	Ctrl	2.6±0.11	0.21±0.012	22.4±1.8	105.9±5.9	0.015±0.002	0.052±0.007
171	Salt	0.9±0.11	0.1±0.007	24.4±1.8	101±2.4	0.013±0.001	0.064±0.003
	Rel	34.9±5.1	46.84±4.108	113.5±10.8	96.7±6.1	99.6±8.2	133.3±19
	Ctrl	2.2±0.09	0.18±0.009	18.8±1.4	114.1±1.8	0.015±0.001	0.05±0.008
172	Salt	1.2±0.1	0.13±0.006	36.1±3.8	96±3.9	0.016±0.001	0.047±0.003
	Rel	54.1±6.45	75.58±4.674	199.3±20.3	84.1±2.2	112.8±6.5	103.4±14.8
	Ctrl	2.5±0.09	0.18±0.008	9.3±0.6	129.2±3.9	0.011±0.001	0.029±0.003
173	Salt	1±0.06	0.12±0.01	29.4±2	86±6.3	0.012±0.001	0.039±0.004
	Rel	39.7±3.08	64.75±6.458	354±48.1	67.1±6	119.2±4.3	151.8±35.8
	Ctrl	2.2±0.14	0.21±0.018	15.1±1.9	111.1±5	0.011±0.001	0.036±0.012
176	Salt	0.6±0.04	0.07±0.006	22.1±1.4	88.1±5.9	0.006±0.001	0.031±0.011
	Rel	29.3±1.41	37.66±6.188	163.5±20	78.9±2.4	71.2±7.6	190±145.4
	Ctrl	3.8±0.2	0.4±0.033	30.2±1.9	87.9±2.6	0.011±0.001	0.05±0.005
177	Salt	1.8±0.11	0.2±0.014	51.3±3.8	86.6±1.9	0.018±0.001	0.069±0.007
	Rel	48.1±6.27	52.04±6.121	175.5±15.3	99±4.2	160±12.3	145±20.2
	Ctrl	3.4±0.3	0.4±0.036	40.3±2.3	83.3±3.8	0.013±0.001	0.069±0.011
178	Salt	1.8±0.11	0.2±0.015	41±2.3	84.6±3.4	0.015±0.001	0.07±0.005
	Rel	54.4±3.12	52.76±5.299	105.2±9.1	102.1±4.9	122.4±17.2	114.7±21.1
	Ctrl	4.2±0.18	0.35±0.012	20.3±0.7	91.6±8.8	0.009±0.001	0.052±0.006
179	Salt	0.6±0.07	0.08±0.016	25.6±1.4	90±1.3	0.01±0.001	0.048±0.004
	Rel	15.3±1.41	23.52±4.077	128±8.6	103.1±12.7	119±20.4	95.1±8.1
	Ctrl	3.9±0.13	0.31±0.01	35.6±1.3	85.7±3.5	0.011±0.001	0.075±0.007
183	Salt	0.8±0.03	0.09±0.003	23.1±1.2	102.3±1.7	0.013±0.001	0.061±0.008
	Rel	20.4±0.9	28.95±0.986	65.5±4.1	120.4±6.7	113.8±12.9	83.9±14.4

187	Ctrl	5.3±0.35	0.48±0.021	30.2±2.1	90±11.5	0.012±0.001	0.067±0.014
	Salt	1.1±0.03	0.12±0.006	32.3±2.7	90±4.5	0.013±0.001	0.059±0.009
	Rel	20.1±0.84	24.53±1.88	106.4±10.5	106.9±14.5	106.8±13	97.4±16
188	Ctrl	3.9±0.29	0.4±0.031	33±2.1	99.7±3.6	0.017±0.001	0.048±0.006
	Salt	1.2±0.12	0.12±0.012	29.3±2.9	92.3±4.8	0.013±0.001	0.064±0.005
	Rel	31±3.51	30.8±3.561	96.7±15.6	93.1±6.1	70.7±8.8	145.1±24
189	Ctrl	3±0.18	0.34±0.02	37.9±1.7	79.8±4.4	0.011±0.001	0.061±0.003
	Salt	1.9±0.05	0.2±0.006	49.9±3.1	85.4±1.5	0.016±0.001	0.066±0.007
	Rel	65±3.44	59.61±3.887	130.7±12.6	108.6±7.2	153.4±19	109.8±11.2
190	Ctrl	4.6±0.11	0.46±0.022	29.8±2	106.6±3.5	0.019±0.002	0.06±0.005
	Salt	0.7±0.08	0.08±0.007	41.4±2.9	97.6±1.2	0.02±0.002	0.06±0.004
	Rel	15.6±1.4	16.28±1.311	146.4±16.2	92±3.5	116.1±9.7	103.8±12.9
191	Ctrl	1.9±0.1	0.19±0.012	17±1.7	121.1±2.9	0.017±0.001	0.032±0.003
	Salt	1±0.04	0.13±0.006	37±2.7	94.5±2.6	0.018±0.001	0.049±0.006
	Rel	55.8±4.11	70.8±2.072	268.2±57.3	78.1±1.7	110.3±6.5	159.2±22.6
192	Ctrl	4.5±0.33	0.46±0.038	30.6±1.9	103.6±3.8	0.021±0.001	0.069±0.008
	Salt	1.3±0.06	0.16±0.008	43.5±2.6	96.3±3	0.02±0.002	0.058±0.006
	Rel	30.3±2.99	34.87±2.79	146.7±12	93.7±5.6	116.6±13.3	88.3±13.1
193	Ctrl	4.7±0.33	0.48±0.035	19.6±2	84.2±3.3	0.005±0.001	0.048±0.007
	Salt	1.9±0.2	0.21±0.022	46.4±3.1	82.2±2.5	0.013±0.001	0.061±0.004
	Rel	42.3±7.39	43.82±1.66	251.2±21.2	98.5±6.2	255±32.7	135.9±18.4
194	Ctrl	3.2±0.2	0.37±0.028	37.7±3.8	105.3±3.3	0.025±0.002	0.065±0.01
	Salt	1.6±0.06	0.19±0.01	89.2±7.6	87.8±4.4	0.029±0.002	0.085±0.005
	Rel	51±3.84	52.48±6.105	252.2±23.1	83.4±3	133.9±13.3	148.1±26
195	Ctrl	4.2±0.23	0.49±0.028	39.9±2.1	76.2±2.2	0.009±0.001	0.057±0.005
	Salt	1.5±0.16	0.16±0.015	82.4±8.6	84.6±2.3	0.028±0.002	0.082±0.005
	Rel	37.3±5.94	34.39±4.819	201.7±23.5	111.4±4.4	321±46	145.5±11
196	Ctrl	3.1±0.42	0.39±0.052	23.7±2	90.3±3	0.009±0.001	0.051±0.006
	Salt	1.4±0.09	0.15±0.008	48.7±3.4	73±4.5	0.011±0.001	0.066±0.004
	Rel	47.6±7.35	40.56±5.143	246±59.1	80.6±3	130±15.6	136.3±18.7
197	Ctrl	8.3±0.5	0.75±0.074	18.8±1.3	110.5±4.6	0.012±0.001	0.036±0.009
	Salt	1.7±0.15	0.21±0.017	47.2±3.6	89.6±3.3	0.016±0.001	0.057±0.005
	Rel	21.5±2.08	28.71±2.483	265.9±29.3	81.7±4.6	157.7±1.1	261.3±131.6
199	Ctrl	2.6±0.05	0.28±0.009	39.9±3.6	99.7±5.7	0.021±0.002	0.072±0.01
	Salt	1.2±0.04	0.14±0.005	61.4±3.9	92.6±3	0.026±0.002	0.078±0.006

	Rel	46.3±1.4	48.12±1.757	175.6±21.4	95.4±8.2	177.6±9.4	115.2±14.6
	Ctrl	4.5±0.44	0.32±0.048	23.5±1.6	102.7±5.5	0.012±0.001	0.061±0.005
203	Salt	0.7±0.04	0.08±0.004	21.3±2.2	101.7±4.4	0.013±0.001	0.046±0.009
	Rel	16.5±1.16	27.28±4.858	99.9±10.2	99.4±3.1	123.5±10	80.8±20.9
	Ctrl	5.1±0.46	0.41±0.046	36.2±1.9	97.2±5	0.017±0.001	0.056±0.005
205	Salt	1.2±0.21	0.15±0.023	52.4±4.1	90.7±3.7	0.02±0.002	0.062±0.006
	Rel	24.9±3.82	37.14±5.998	145.8±10.5	93.6±2.8	114.8±7.6	109.9±7.6
	Ctrl	4.8±0.3	0.4±0.028	24.4±2	94.9±4.6	0.01±0.001	0.048±0.004
208	Salt	1±0.06	0.11±0.009	54.7±3.9	79.7±0.6	0.014±0.001	0.059±0.004
	Rel	21.2±2.39	26.75±1.201	228.8±26.8	84.9±4.7	144.9±15.6	127.4±18.5
	Ctrl	5.3±0.53	0.49±0.047	46.6±2.5	87.1±3.7	0.017±0.001	0.07±0.006
209	Salt	1.4±0.15	0.15±0.018	57±2.4	83.6±3.6	0.016±0.001	0.065±0.011
	Rel	26±2.54	31.69±3.104	130.8±6.5	96.9±6.7	100±9.3	95.7±19.7
	Ctrl	3.1±0.19	0.27±0.013	25.7±2.3	109.6±8.7	0.017±0.002	0.059±0.007
211	Salt	0.6±0.07	0.08±0.007	26.9±2.2	92.1±4	0.011±0.001	0.048±0.008
	Rel	20.9±1.78	28.19±1.974	109.4±10.6	85.7±6.4	66.4±2.5	89.4±25
	Ctrl	2.8±0.54	0.24±0.038	25.7±2	91.3±6.7	0.012±0.001	0.058±0.007
213	Salt	0.9±0.1	0.1±0.009	28±2.3	87.1±1.7	0.01±0.001	0.037±0.003
	Rel	35.7±7.94	43.57±7.029	117.4±14.6	98.1±9.2	82.1±5.5	69±11.1
	Ctrl	3.1±0.25	0.25±0.011	26.3±1.5	97.9±3.8	0.011±0.001	0.047±0.005
214	Salt	1.1±0.07	0.14±0.009	52.4±3.1	92.1±3.8	0.021±0.002	0.05±0.005
	Rel	38.1±5.06	54.61±4.532	210.2±24.2	94.8±6.1	185.7±20.7	111.4±14.6
	Ctrl	4.9±0.52	0.42±0.045	22±2.2	93.4±6.8	0.009±0.001	0.051±0.004
215	Salt	1.1±0.03	0.14±0.013	35.1±1.2	81±1.5	0.01±0.001	0.052±0.004
	Rel	22.9±2.44	33.77±2.334	173.4±17.2	88.6±6.5	114±6.8	104.8±14.2
	Ctrl	3.7±0.23	0.3±0.019	24.1±1.6	104.9±10.4	0.015±0.001	0.036±0.007
216	Salt	1.2±0.04	0.14±0.005	31.9±2.1	90.8±4	0.013±0.001	0.057±0.005
	Rel	33.9±2.21	48.01±3.788	138.3±13.8	90.4±11.3	78.9±12.1	212.4±78.4
	Ctrl	2.8±0.15	0.23±0.018	24.1±1	98.3±3.2	0.012±0.001	0.056±0.004
217	Salt	1.1±0.08	0.13±0.007	49.6±3.7	87.3±3.1	0.021±0.001	0.067±0.003
	Rel	41.1±4.2	56.52±6.057	208±9.3	89.1±4.2	162.6±15.1	123.4±9.9
	Ctrl	4±0.95	0.36±0.097	30.4±3.6	101.5±8.3	0.015±0.001	0.049±0.006
218	Salt	1.1±0.13	0.12±0.014	39.2±3.3	86.8±3.9	0.013±0.001	0.052±0.007
	Rel	29.2±3.58	39.53±5.209	150.7±24.2	87.5±7.9	86.6±8.9	114.5±21
219	Ctrl	3.9±0.53	0.33±0.045	26.5±3.9	123.1±10.8	0.024±0.001	0.033±0.01

	Salt	1±0.02	0.13±0.002	41.6±4.3	98.3±3.8	0.021±0.001	0.053±0.007
	Rel	28.4±4.32	43.16±6.311	201.4±37.5	81.6±5.7	80.8±3.5	291.4±123.5
	Ctrl	2.5±0.35	0.21±0.019	25.9±1.7	101±2.5	0.013±0.001	0.057±0.01
220	Salt	0.8±0.05	0.1±0.005	51.7±2.4	88±2.3	0.018±0.001	0.058±0.007
	Rel	33.9±2.43	47.13±2.988	206±13.1	87.3±3.1	135.1±5.3	118.5±31.7
	Ctrl	2.2±0.19	0.19±0.013	32.6±2.7	86.6±7.3	0.01±0.001	0.052±0.007
221	Salt	1±0.09	0.12±0.008	26.3±3	89.1±3.6	0.009±0.001	0.047±0.007
	Rel	47.8±4.16	61.54±4.29	84.3±9.1	106.4±11.8	77.2±12.2	91.4±8.4
	Ctrl	4.1±0.29	0.36±0.026	31.3±2.5	94.7±2.9	0.013±0.001	0.06±0.003
222	Salt	0.9±0.03	0.1±0.004	46.4±3.6	93.7±2.5	0.02±0.002	0.047±0.004
	Rel	21.2±1.59	27.26±2.422	135.4±10.8	99.2±2.8	163.6±3.7	80.3±10.8
	Ctrl	4.4±0.13	0.37±0.014	30.2±3.1	92±6.4	0.014±0.001	0.057±0.005
223	Salt	1.3±0.1	0.15±0.01	46.6±4	83±3.9	0.01±0.001	0.061±0.001
	Rel	29.6±2.51	40.66±3.828	180.5±19.3	92.5±9.1	90.1±12.5	109.9±8.8
	Ctrl	3.9±0.12	0.34±0.015	35.8±1.4	83.5±1.3	0.011±0.001	0.059±0.003
311	Salt	1.1±0.09	0.12±0.008	37.3±3.8	96.8±11.2	0.02±0.002	0.064±0.005
	Rel	27.4±2.92	34.51±2.522	109.1±12.9	116.9±15.8	198.7±18.3	110.4±11.8
	Ctrl	2.7±0.34	0.26±0.016	16.6±1.9	95.3±3.8	0.007±0.001	0.043±0.008
319	Salt	0.8±0.15	0.07±0.01	29.5±1.5	82.4±4.9	0.009±0.001	0.063±0.014
	Rel	25.9±3.69	26.54±5.56	194.9±18	87.5±7.4	139.4±23.3	151.7±26.4
	Ctrl	3.9±0.12	0.34±0.011	26.1±1.4	99.7±2.3	0.013±0.001	0.053±0.008
321	Salt	0.9±0.07	0.1±0.008	39±3.4	88.4±3.8	0.014±0.001	0.07±0.009
	Rel	22.5±2.17	28.86±2.619	153.9±16.1	89±4.9	102.3±7.5	141.4±21.8
	Ctrl	5.7±0.26	0.49±0.025	23.7±1.5	117.4±7	0.019±0.003	0.046±0.005
350	Salt	0.9±0.05	0.1±0.003	24±3.2	105.1±5	0.015±0.001	0.035±0.005
	Rel	16.7±1.14	21.52±1.498	103.5±12.1	91.1±7.8	80.13±9.526	78.18±13.264
	Ctrl	4.7±0.24	0.39±0.021	31±2.7	89.2±3	0.011±0.001	0.063±0.009
354	Salt	1±0.07	0.11±0.007	30.2±1.4	84.4±1.1	0.009±0.001	0.044±0.003
	Rel	21.2±1.67	28.86±1.648	103.3±9.6	95.2±4.1	85±2.7	76.3±12.7
	Ctrl	2.2±0.24	0.16±0.023	21.1±2.3	111.9±9.9	0.014±0.001	0.05±0.006
366	Salt	0.7±0.07	0.1±0.006	33.7±4.6	85.3±14.8	0.016±0.002	0.069±0.013
	Rel	35±5.41	65.04±8.415	187.7±28.7	76.3±12.9	122.6±12.4	141.3±26.2
	Ctrl	2.9±0.21	0.28±0.023	27.4±1.3	94±10.5	0.009±0.001	0.068±0.008
367	Salt	0.8±0.07	0.09±0.008	36.2±0.9	86.3±2.4	0.012±0.001	0.068±0.006
	Rel	26.8±3.07	31.4±2.224	135.9±9.2	95.1±7.8	121.1±14.6	111.5±26.2

Q3	Ctrl	2.6±0.22	0.24±0.016	25.2±1.3	118.1±4.2	0.022±0.002	0.052±0.006
	Salt	0.7±0.06	0.07±0.004	43.9±1.9	104.7±4.4	0.023±0.002	0.084±0.015
	Rel	28±2.64	31.57±2.594	173±14.5	89±4.3	131.9±7.7	178.7±47.5
Q4	Ctrl	3.2±0.38	0.28±0.032	35.1±2.5	105±3.5	0.021±0.001	0.072±0.007
	Salt	1.2±0.06	0.11±0.009	38±4.4	95.6±8.2	0.017±0.002	0.083±0.018
	Rel	39.9±4.36	41.41±8.547	121.5±17.8	90.8±6.6	78.2±4.9	129.2±40.9
Q5	Ctrl	3.5±0.18	0.32±0.014	31±1.5	109.4±2.9	0.021±0.002	0.071±0.002
	Salt	0.9±0.06	0.08±0.007	33.8±0.9	91.8±2.8	0.013±0.001	0.068±0.009
	Rel	27.1±2.61	24.81±2.581	109.5±6.8	84.3±4.5	60.8±7.7	96.5±14.5
Q6	Ctrl	4.5±0.27	0.41±0.031	39.5±2.3	109.6±1.5	0.027±0.001	0.064±0.007
	Salt	1.2±0.11	0.1±0.012	57.3±3.2	95.6±3.3	0.029±0.002	0.083±0.011
	Rel	28±3.24	27.84±4.752	152.4±15.1	87.3±3.6	126.5±10.2	139.5±27.5
Q7	Ctrl	5.3±0.45	0.49±0.042	34.1±2.1	104.7±3.5	0.02±0.001	0.076±0.005
	Salt	1.4±0.11	0.14±0.01	39.5±2.6	97.5±2.8	0.02±0.001	0.062±0.009
	Rel	27.8±3.02	29.19±3.78	117.9±8.4	93.6±4.6	99.5±7	86±18.3
Q11	Ctrl	3.9±0.45	0.31±0.034	35.1±1.1	105.1±3.2	0.022±0.002	0.077±0.007
	Salt	1.3±0.06	0.12±0.005	40.7±3.3	99.2±3.3	0.02±0.002	0.061±0.009
	Rel	35.4±3.98	41.18±4.119	117.2±10.3	94.5±2.7	107.1±7.5	79.5±9.2
Q14	Ctrl	4.4±0.37	0.35±0.037	17.7±2	111.2±3.9	0.012±0.001	0.035±0.005
	Salt	1±0.08	0.1±0.012	23.3±2.8	98.7±4.8	0.016±0.002	0.04±0.004
	Rel	23.3±4.44	31.77±7.347	143.1±20.5	90.4±6.8	128.8±7.9	126.9±27.9
Q20	Ctrl	5±0.33	0.43±0.029	22.2±1.5	122.1±7.1	0.021±0.002	0.038±0.003
	Salt	1.4±0.05	0.14±0.009	19.8±2.4	112.6±1.7	0.015±0.001	0.033±0.007
	Rel	29.6±2.83	32.77±3.918	89.1±7.9	93.4±5.2	83.36±8.835	89.99±19.546
Q21	Ctrl	2±0.08	0.16±0.009	11.6±0.9	131.5±21.1	0.01±0.003	0.019±0.002
	Salt	1.1±0.08	0.12±0.013	17.5±1.3	111.5±5.5	0.013±0.001	0.021±0.001
	Rel	54.1±5.35	77.79±11.805	159±20.4	94±14.4	145.2±7	115.1±13
Q22	Ctrl	3.8±0.31	0.33±0.028	36±2.5	95±8.1	0.014±0.001	0.065±0.008
	Salt	1±0.05	0.11±0.008	52±3.4	88.1±2.1	0.018±0.001	0.063±0.005
	Rel	26.4±3.22	36.69±6.022	148.3±11	95.4±8.1	136.9±15.5	101.2±13.3
Q24	Ctrl	2.8±0.06	0.21±0.012	18.3±1.4	95.7±3.9	0.008±0.001	0.048±0.007
	Salt	0.9±0.09	0.1±0.011	24.8±1.5	89.1±2.4	0.009±0.001	0.048±0.005
	Rel	30.7±3.55	47.17±5.947	143.4±15.2	93.9±5.2	113.8±12.1	105.7±11.7
Q26	Ctrl	3.8±0.24	0.31±0.033	32.8±1.3	83.7±2.9	0.01±0.001	0.074±0.004
	Salt	0.8±0.05	0.09±0.005	42±3.9	83.7±4.3	0.014±0.001	0.074±0.008

	Rel	21.5±2.03	31.71±3.852	125.2±14.4	100±4.1	134.3±13.8	100.1±9.2
	Ctrl	4.8±0.23	0.37±0.028	21.1±1.6	112.2±2.9	0.016±0.002	0.057±0.005
Q28	Salt	0.8±0.03	0.1±0.005	23.9±2	94.9±1.7	0.012±0.001	0.051±0.006
	Rel	17.5±0.44	26.43±1.085	115.3±9.5	84.7±3	76.8±5.7	94±16.5
	Ctrl	5.8±0.46	0.49±0.046	32.8±2	95.9±4.5	0.015±0.001	0.069±0.005
Q29	Salt	0.8±0.03	0.08±0.005	44.4±5.1	89.2±3	0.016±0.001	0.073±0.016
	Rel	13±0.48	17.32±1.227	138±16.1	93.8±4.6	105.8±8.2	110.3±26.9
	Ctrl	4.6±0.37	0.38±0.036	30.6±2.2	98.8±3	0.015±0.001	0.067±0.007
Q30	Salt	0.9±0.05	0.1±0.005	59.9±3.5	83.8±3.3	0.019±0.001	0.072±0.003
	Rel	19.1±1.66	26.93±2.033	208.6±22.2	85.1±4.1	118.1±7.3	112.8±12
	Ctrl	4.1±0.14	0.36±0.012	42.7±3.8	107.6±2	0.028±0.004	0.094±0.01
Q31	Salt	1.1±0.14	0.1±0.006	43.5±3.7	100.8±1.8	0.026±0.001	0.069±0.003
	Rel	26.7±3.38	27.08±0.855	105.4±7.1	93.9±3.1	88.3±6.9	76.9±9.6
	Ctrl	1.6±0.21	0.15±0.011	30.6±2	107.2±4.3	0.02±0.003	0.05±0.002
Q32	Salt	1.5±0.14	0.14±0.013	62±6.9	123.6±4.9	0.059±0.001	0.048±0.003
	Rel	96.2±10.53	93.33±9.252	219.5±32.2	116.2±7.4	339.4±32.8	98±6.4
	Ctrl	4.3±0.15	0.36±0.019	30.6±4.5	102.9±4.6	0.016±0.002	0.055±0.007
Q33	Salt	1.4±0.08	0.12±0.007	24.6±2.3	103±5.1	0.013±0.001	0.034±0.008
	Rel	31.8±1.38	34.95±2.73	105.2±22.6	104.4±5	78.4±9.3	71.3±20.3
	Ctrl	3.1±0.19	0.24±0.012	16.2±1.2	101.4±5.8	0.01±0.002	0.037±0.004
Q34	Salt	1±0.06	0.1±0.006	16.2±1.3	90.3±8.8	0.008±0.002	0.034±0.006
	Rel	33.7±2.2	40.85±3.509	105.7±12.9	84.6±9.7	90.1±5.4	92.5±14.9
	Ctrl	2±0.27	0.16±0.016	26.3±1.2	112.6±5.1	0.018±0.002	0.059±0.013
Q35	Salt	1.4±0.1	0.14±0.01	41.2±2	101.5±4.6	0.024±0.003	0.073±0.005
	Rel	75.6±10.12	87.74±13.669	162±14.6	90.7±4.8	145.9±15.2	154.4±37.4
	Ctrl	3±0.3	0.23±0.025	26.5±2.3	95.4±3.5	0.014±0.002	0.061±0.003
Q36	Salt	1.5±0.19	0.15±0.021	34.1±3	88.5±2.4	0.012±0.001	0.057±0.004
	Rel	54.8±10.68	68.52±12.507	140.4±20.4	93.4±4.8	99.1±6	93.8±7
	Ctrl	3.2±0.57	0.25±0.038	21.6±1.8	123.4±4.7	0.02±0.001	0.037±0.006
Q37	Salt	1.5±0.17	0.15±0.015	20.9±2.1	117.1±2.5	0.017±0.001	0.039±0.008
	Rel	52.6±10.41	68.62±13	108.3±18.3	95.3±3.2	86.7±11	126.4±39
	Ctrl	4.4±0.33	0.34±0.026	33.4±1.1	100.4±2.3	0.018±0.001	0.079±0.009
Q38	Salt	1.5±0.16	0.13±0.018	44.2±4.2	104.3±1.7	0.027±0.002	0.071±0.011
	Rel	34.5±5.19	39.14±7.948	135.4±16	104.1±3.1	162.8±29.7	100±22.3
Q40	Ctrl	6.6±0.46	0.64±0.061	46.8±2.4	106.3±3.9	0.029±0.002	0.078±0.011

	Salt	1.9±0.19	0.17±0.026	55.4±5.8	96.8±1.7	0.025±0.002	0.073±0.005
	Rel	30.3±4.81	29.88±5.838	123.3±14.9	91.6±3.8	93.2±11.2	103.7±19.7
	Ctrl	3±0.25	0.3±0.065	28.7±2.1	111.7±4.5	0.023±0.001	0.065±0.015
Q42	Salt	1.5±0.14	0.13±0.011	45.1±2.6	102.3±3.8	0.026±0.001	0.067±0.009
	Rel	50.3±2.37	51.04±8.611	164.9±14.7	91.7±2	119.6±12.6	118.6±20.9
	Ctrl	2.1±0.28	0.19±0.017	25.7±1.7	110.6±3.6	0.02±0.002	0.06±0.012
Q45	Salt	1.5±0.13	0.13±0.008	38.2±3	98.5±1	0.018±0.002	0.075±0.005
	Rel	75.3±12.32	73.91±8.89	153.5±13.7	89.4±3.2	106.9±11.9	153.3±40.7
	Ctrl	6.1±0.54	0.55±0.066	41.4±2.3	101.3±2.8	0.022±0.001	0.088±0.006
Q49	Salt	1.9±0.19	0.19±0.028	47.9±3.5	99.7±1.8	0.025±0.003	0.059±0.006
	Rel	31.5±4.46	36.96±7.219	117.1±7.9	98.9±4	115.6±10.3	69.5±10.4
	Ctrl	2.7±0.05	0.27±0.01	41.2±2.7	100±3	0.022±0.001	0.085±0.008
Q50	Salt	1.7±0.14	0.19±0.019	53±1.9	103.9±3.8	0.028±0.001	0.072±0.01
	Rel	63.6±4.64	70.68±6.478	133.6±12	104±3.6	134.7±4.8	88.9±17.6
	Ctrl	5.4±0.65	0.51±0.068	26.7±2.7	110.7±6.2	0.019±0.001	0.06±0.009
Q51	Salt	2.9±0.31	0.31±0.052	58.2±4.1	96.9±1.6	0.028±0.003	0.077±0.009
	Rel	54.4±8.64	61.46±11.88	246.3±41.2	88.9±6.2	159.9±17.1	152.2±43.8
	Ctrl	5.1±0.4	0.47±0.026	44.6±3.6	107.1±3.7	0.028±0.003	0.087±0.008
Q52	Salt	1.6±0.13	0.14±0.008	60.8±4.5	94.6±3.4	0.027±0.003	0.082±0.009
	Rel	32.4±5.28	29.79±1.256	142.6±11.9	88.5±2.6	104.2±12.6	99.4±16.2
	Ctrl	4.6±0.64	0.38±0.046	34.9±2.2	101.3±3.5	0.019±0.001	0.07±0.008
Q53	Salt	1.4±0.11	0.12±0.01	53.5±3.2	92.5±0.9	0.024±0.001	0.084±0.01
	Rel	35±5.23	36.83±8.321	155.6±9.8	91.9±4.2	121.8±15.3	127.3±21.7
	Ctrl	4.9±0.33	0.49±0.042	52.4±2.9	101.4±3.2	0.028±0.001	0.095±0.01
Q54	Salt	1.2±0.07	0.11±0.008	46.1±2.5	94.2±3.3	0.02±0.001	0.088±0.009
	Rel	25.5±2.3	23.62±3.012	89±3.9	93.4±4.9	73.6±9.7	97.2±16.7
	Ctrl	4.2±0.28	0.35±0.034	30.6±2	116.4±2.8	0.025±0.002	0.065±0.009
Q56	Salt	1.5±0.15	0.11±0.007	40.3±3.1	95.2±2.2	0.019±0.002	0.072±0.01
	Rel	37.7±3.98	31.71±3.684	135.4±11.2	82±2.7	76.6±8	118.9±25.9
	Ctrl	3.9±0.65	0.3±0.054	29.1±1.7	101.8±4.2	0.016±0.001	0.078±0.012
Q57	Salt	1.4±0.06	0.14±0.009	57.3±4	105.3±1.6	0.032±0.003	0.088±0.017
	Rel	40.1±6.8	54.63±10.277	205±21.5	106.5±6	219.5±11.5	119.2±26.7
	Ctrl	7±0.47	0.64±0.064	19.2±2.4	119.1±5.3	0.016±0.001	0.031±0.008
Q58	Salt	2.1±0.18	0.23±0.034	28.7±2.8	106.1±1.7	0.017±0.002	0.04±0.007
	Rel	31.8±4.85	38.2±8.539	179.9±29.2	90±5.3	111.9±8.2	148.6±30.6

Q59	Ctrl	5.1±0.58	0.41±0.054	23.3±2.6	119.3±9.2	0.023±0.001	0.061±0.011
	Salt	2.8±0.36	0.3±0.041	40.5±3.5	104.1±3.5	0.026±0.002	0.072±0.005
	Rel	56.3±4.7	76.83±12.585	193.5±25.8	88.7±5.4	117.3±11.6	136.2±25.7
Q64	Ctrl	3.8±0.33	0.31±0.023	25.4±2	107.3±2	0.017±0.001	0.054±0.007
	Salt	1.7±0.15	0.21±0.02	40.5±2.4	92.5±1.6	0.017±0.001	0.064±0.003
	Rel	48.2±6.65	67.98±9.942	167.2±14.1	86.3±2.6	100.5±8.1	127.7±18.4
Q65	Ctrl	3.7±0.22	0.29±0.031	42.5±2.2	117.4±3.9	0.034±0.001	0.087±0.003
	Salt	0.7±0.05	0.06±0.006	33.6±2.3	106.1±5.1	0.022±0.001	0.076±0.011
	Rel	19.6±1.7	21.82±3.495	83.3±9.7	70.6±17.8	59±2.6	86.3±11.7
Q68	Ctrl	2.3±0.16	0.18±0.011	12.9±0.6	203.2±16.6	0.045±0.006	0.019±0.003
	Salt	1.6±0.07	0.16±0.012	29.8±2.2	120.3±2.7	0.028±0.002	0.024±0.002
	Rel	71.5±6.8	91.72±8.732	234.5±20.3	60.9±5.3	64.3±4.2	146.5±28
Q75	Ctrl	6.5±0.26	0.51±0.029	8.8±1.2	121±5.7	0.008±0.001	0.032±0.006
	Salt	1.5±0.1	0.16±0.011	16.6±1.1	111.7±2.8	0.012±0.001	0.032±0.005
	Rel	23.1±1.52	32.87±2.478	297±93.5	93±4.2	169.8±14.1	122.6±33.5
Q76	Ctrl	6.3±0.41	0.52±0.036	10.8±1.3	132.9±4.6	0.015±0.001	0.034±0.008
	Salt	2±0.13	0.2±0.013	14.2±1.8	121.2±4.7	0.014±0.001	0.029±0.008
	Rel	32±2.95	39.03±4.72	162.3±35.3	90.6±8.2	97.7±0.1	158.2±41.2
Q77	Ctrl	6.7±0.41	0.64±0.033	19.8±1.4	135.1±7.2	0.025±0.002	0.036±0.007
	Salt	2±0.39	0.19±0.04	27.4±1.3	111.9±4.8	0.021±0.002	0.043±0.004
	Rel	31.3±8.75	31.68±8.72	149.1±18.8	83.9±6.3	85.4±6.2	170.8±69.8
Q78	Ctrl	6.2±0.42	0.5±0.035	9.7±0.8	130.9±5.5	0.01±0.001	0.038±0.008
	Salt	1.1±0.03	0.13±0.003	19.8±2	90.8±7.1	0.006±0.001	0.04±0.008
	Rel	18.8±1.03	25.39±1.168	216±25.4	69.3±8.1	92.1±9	183.5±104
Q79	Ctrl	5.4±0.22	0.44±0.024	16.4±0.6	141±5.2	0.022±0.001	0.036±0.007
	Salt	1.1±0.04	0.09±0.003	12.7±1.5	113.1±6.1	0.008±0.001	0.024±0.005
	Rel	20.1±1.27	20.11±1.228	77.5±8.4	81.5±2.5	43.8±4.2	63.5±15.5
Q80	Ctrl	5.7±0.37	0.44±0.027	11±0.9	115.1±5	0.008±0.001	0.031±0.006
	Salt	1.1±0.04	0.12±0.004	19.8±1	107.7±1.7	0.014±0.001	0.038±0.003
	Rel	19.8±1.42	28.84±2.121	193.5±20.4	95.5±6.2	177.3±13.5	140.1±20.3

Abbreviations:

DW: dry weight; FW: fresh weight; BD: bladder density; BDM: bladder diameter; BV: bladder volume; BI: bladder index

Suppl. Table S4.2 Mean values of stomatal characteristics and ionic contents under non-saline and saline conditions with corresponding relative values

Accession		SD	SL	SI	ECA	Na^+	K^+
127	Ctrl	64.2±3.6	29.4±1.3	0.16±0.005	2094±224	63±2	3049±301
	Salt	69.2±3.4	20.5±0.4	0.11±0.01	1410±169	887±105	3177±41
	Rel	112.6±10.1	70.4±3.9	68.75±6.733	73±15	1398±124	108±11
132	Ctrl	57.8±3.6	28.9±1.4	0.16±0.008	2290±240	30±6	2096±53
	Salt	71.1±6.8	18.7±0.6	0.13±0.007	1474±124	2029±370	2737±126
	Rel	128.2±13.9	65.2±3.4	83.69±5.903	67±7	7845±2357	131±8
133	Ctrl	91.2±6	24.6±1.1	0.13±0.01	1616±114	23±5	2263±315
	Salt	78.5±2.1	18.2±0.2	0.13±0.005	1338±59	1264±267	2843±217
	Rel	90±6.9	74.9±3.5	101.49±6.252	85±8	6143±1591	134±18
134	Ctrl	80±3.1	24.7±0.5	0.15±0.008	1559±48	27±4	1984±72
	Salt	69.4±2.1	20.5±0.3	0.15±0.008	1652±67	978±114	3050±68
	Rel	88.3±5	83±2.1	102.89±10.241	107±7	4035±697	154±5
135	Ctrl	72.4±3.1	28.8±1	0.17±0.019	1740±107	48±6	2137±103
	Salt	80.1±4.8	19.1±1.3	0.12±0.009	1469±101	1069±59	2960±87
	Rel	107±5.3	66.5±5	71.26±11.85	85±6	2345±294	140±8
136	Ctrl	80.4±4	27.3±0.8	0.15±0.012	2130±214	32±4	1905±46
	Salt	122.9±11.2	16.8±0.7	0.14±0.017	1241±158	1263±80	2539±198
	Rel	159.2±10.1	61.9±3.5	99.11±16.241	63±13	4224±513	134±12
137	Ctrl	108.9±2.9	24.7±1.1	0.15±0.005	1513±223	16±4	1811±192
	Salt	72.2±2.3	20.1±0.7	0.13±0.011	1508±91	1977±173	2771±227
	Rel	67.1±1.8	81.7±3.2	87.5±6.26	105±9	15123±3286	158±19
138	Ctrl	85.5±4.4	22.6±0.9	0.15±0.011	1729±141	43±13	1963±145
	Salt	81.9±5.6	17.6±0.8	0.13±0.007	1377±111	1847±301	3074±151
	Rel	96.9±12.5	78.7±5.3	87.78±5.885	83±10	6104±1805	161±18
140	Ctrl	80.6±3.1	24.6±0.6	0.15±0.012	1436±42	15±2	1700±87
	Salt	86±4.4	18.7±0.4	0.13±0.018	1112±168	1863±83	3074±151
	Rel	109.4±8.8	75.9±1.1	85.66±14.094	78±12	13384±1529	184±19
141	Ctrl	72.2±1.6	27.6±0.5	0.15±0.011	2043±49	13±2	2086±108
	Salt	56.9±2.5	18.4±0.7	0.12±0.01	1479±119	1684±159	2751±114
	Rel	79.1±3.7	66.9±2.9	81.44±9.982	73±7	14036±1998	134±12
144	Ctrl	79.8±4.3	26.8±1.3	0.18±0.008	1778±153	12±2	1859±52
	Salt	82.7±3.1	17.2±1	0.13±0.009	1352±228	2903±445	2561±68

	Rel	111.5±8.1	64.6±5	68.93±5.886	79±15	25493±4348	138±5
	Ctrl	95.5±3.4	23±0.3	0.16±0.008	1402±42	9±1	2240±83
146	Salt	65.1±2.2	20.4±0.4	0.15±0.009	1686±93	1845±127	2867±108
	Rel	69.1±3.7	89±1.9	95.14±9.778	120±7	20497±1395	129±8
	Ctrl	89.3±8.3	24.1±1.3	0.19±0.016	1950±268	10±0	2792±161
147	Salt	59.3±1.2	19.2±0.2	0.14±0.007	1615±62	1649±529	3574±146
	Rel	72.7±7.8	80.2±3.3	76.83±6.153	90±13	16163±4326	130±9
	Ctrl	92.7±3	24.8±0.2	0.18±0.008	1591±69	14±2	2043±100
148	Salt	105.4±3.5	18±0.6	0.14±0.006	1052±73	1348±365	2598±113
	Rel	114.3±3.8	72.6±2.3	79.08±4.828	67±6	10141±2068	128±6
	Ctrl	100.5±4	22.7±0.4	0.18±0.015	1363±108	20±3	1821±117
149	Salt	89.9±6.6	16.4±0.4	0.14±0.009	1200±84	1260±110	3178±119
	Rel	90.4±6.6	72.1±1.4	76.59±7.785	89±4	7106±1411	178±16
	Ctrl	84.5±2.2	24.8±0.4	0.18±0.011	1736±89	14±2	1782±57
150	Salt	97.7±2.6	17±0.7	0.15±0.008	1090±81	898±204	3699±416
	Rel	115.9±2.7	68.7±2.3	85.04±9.815	64±6	6955±2273	206±20
	Ctrl	90.1±5.2	24±0.5	0.19±0.01	1773±107	15±2	2379±102
151	Salt	74.8±4.6	18.8±1	0.16±0.012	1636±197	1605±197	2745±550
	Rel	84.7±6.4	78.4±3	86.42±6.95	92±8	11066±1098	119±27
	Ctrl	72±2.9	26.7±0.8	0.17±0.014	2094±189	21±4	2375±160
153	Salt	91.6±10.7	17.6±1	0.16±0.009	1166±96	1460±141	3316±394
	Rel	142.3±9	66.4±4.6	93.97±7.405	58±7	8079±1894	145±26
	Ctrl	85.8±4	25.4±1.4	0.16±0.007	1631±110	13±1	1855±28
154	Salt	79.5±5.6	16.5±0.5	0.16±0.01	1714±178	2350±281	2783±142
	Rel	98.9±8.9	65.9±4.5	100.1±4.49	109±16	20040±3474	150±7
	Ctrl	85.6±4.3	26.1±1.6	0.16±0.017	1456±182	7±0	2026±48
155	Salt	65.5±4.9	17.9±0.4	0.15±0.005	1661±204	2630±113	2775±53
	Rel	77.7±6	69.4±3.2	100.68±12.239	123±27	36366±2032	137±3
	Ctrl	105.9±5.8	26.8±0.6	0.22±0.012	1595±133	53±9	2649±296
157	Salt	67.9±3.7	19.1±0.4	0.16±0.018	1812±199	2709±459	2992±369
	Rel	66.6±8	71.5±3	71.01±5.301	118±19	5742±1337	126±31
	Ctrl	76.3±3.4	26.8±0.7	0.21±0.03	1994±71	6±1	2972±53
158	Salt	83.4±6.9	20.1±1	0.13±0.012	1152±159	1949±268	3122±375
	Rel	110±8.4	75.3±5	65.95±11.307	57±7	31331±4991	106±15
159	Ctrl	87.5±2.7	27±0.5	0.19±0.005	1618±89	25±2	1809±31

	Salt	85.4±6.1	18.5±0.2	0.14±0.005	1361±119	2048±223	3306±256
	Rel	99.5±9.1	68.5±1.4	72.04±2.425	86±10	8016±451	184±16
	Ctrl	90.1±3.4	22.8±0.5	0.16±0.006	1445±102	19±2	2031±103
161	Salt	78.7±4.7	18.6±0.8	0.14±0.006	1292±144	1796±36	3055±76
	Rel	89.4±8.1	81.7±3.7	91.98±5.872	92±13	9656±748	151±6
	Ctrl	94.6±2.8	24.3±1.1	0.19±0.01	1514±93	46±6	1906±166
168	Salt	90.3±3.5	16.6±0.6	0.15±0.005	1162±66	1655±98	2215±308
	Rel	96.4±3.8	69±4.8	82.21±5.61	79±8	3855±521	121±21
	Ctrl	89±2	24.9±1	0.17±0.007	1614±151	69±9	1998±171
169	Salt	91.2±3	17.6±0.4	0.12±0.015	1158±94	1673±180	2752±81
	Rel	102.5±2.9	71.1±3.3	74.77±9.461	74±8	2526±385	142±12
	Ctrl	95.9±2.6	24.4±0.6	0.24±0.018	1946±142	71±10	1986±233
171	Salt	77.6±3.9	18.5±0.2	0.17±0.007	1628±118	1490±92	2866±193
	Rel	80.9±3.2	76.1±2.5	74.03±4.01	86±10	2186±208	154±21
	Ctrl	83.2±2.3	23.8±1	0.17±0.009	1750±111	82±7	3000±144
172	Salt	91±3	17.5±0.7	0.13±0.012	1029±78	1127±26	2343±110
	Rel	110.5±5.8	74.1±4.7	75.95±10.846	60±7	1427±140	79±6
	Ctrl	78±4.5	27.7±0.5	0.21±0.013	2228±162	69±12	3078±221
173	Salt	96.4±5.3	16.8±0.6	0.12±0.011	888±53	1163±184	2378±92
	Rel	128.8±11.9	60.9±2.1	60.61±8.187	41±4	2028±621	79±5
	Ctrl	92.3±5.6	23.9±0.3	0.18±0.007	1551±83	37±10	1691±152
176	Salt	132.6±3.6	15.3±0.2	0.16±0.01	904±41	938±107	3182±214
	Rel	148.8±10.1	63.4±1.1	88.13±7.429	61±5	3638±1085	195±22
	Ctrl	76.3±3.8	23.8±0.5	0.17±0.017	1511±29	36±10	1881±153
177	Salt	88.6±2.7	17.5±0.8	0.14±0.007	1044±126	1670±171	2785±109
	Rel	117.9±5.2	73.8±4	81.2±6.31	69±7	6774±2411	151±12
	Ctrl	95.3±2.7	22.7±0.7	0.16±0.011	1207±51	20±3	1925±165
178	Salt	91.8±3.4	19.4±1	0.16±0.01	1161±102	1853±111	2714±162
	Rel	96.5±2.6	85.5±4.6	99.87±9.179	96±9	10249±1502	145±15
	Ctrl	91.8±4.7	24.2±0.9	0.2±0.016	1696±129	41±9	3145±224
179	Salt	87.1±5.4	18.5±0.5	0.13±0.008	1320±98	1806±190	2928±149
	Rel	99±11.2	76.6±2.5	67.4±4.422	79±5	5186±1037	96±11
	Ctrl	106.1±2.9	22.8±0.5	0.16±0.006	1445±102	28±4	2737±182
183	Salt	76.5±3.9	18.4±0.9	0.16±0.008	1629±152	1937±227	2825±92
	Rel	72.8±4.7	80.8±3.3	101.96±7.339	115±14	7018±511	105±8

187	Ctrl	78.3±2.9	24.8±0.7	0.19±0.011	1765±130	15±4	2285±38
	Salt	66.2±3.5	19.3±0.8	0.16±0.02	1570±194	1979±154	2484±195
	Rel	86.5±6.9	77.9±2.6	85.7±7.596	89±9	15227±2737	109±9
188	Ctrl	110.4±6.1	22.7±0.7	0.18±0.013	1289±125	18±4	1847±134
	Salt	77.6±4.6	16.8±0.3	0.16±0.01	1461±103	1524±265	2332±182
	Rel	72±5.3	74.4±2.3	89.4±4.598	119±15	10784±3869	128±11
189	Ctrl	105.2±4.3	23.5±0.4	0.17±0.012	1263±27	31±7	1838±111
	Salt	94±5.1	17.7±0.4	0.15±0.01	1005±92	2166±167	2521±118
	Rel	90.2±5.1	75.3±2.2	92.16±11.81	80±8	7837±1014	140±12
190	Ctrl	110±3.3	22.5±0.5	0.17±0.011	1389±67	34±7	1957±119
	Salt	81.3±5	17.3±0.6	0.15±0.014	1171±41	2036±133	2812±257
	Rel	75.1±6.2	77.1±3.6	89.55±10.174	85±6	7107±1343	136±10
191	Ctrl	97.9±4.3	27±0.9	0.17±0.007	1393±133	35±5	1707±82
	Salt	86.5±4.1	18.6±0.7	0.15±0.005	1294±127	1084±108	2725±155
	Rel	89.8±6.1	69.2±3.1	88.46±0.905	94±7	3389±642	160±5
192	Ctrl	95.9±4.6	24.3±0.8	0.19±0.015	1550±87	18±2	2098±177
	Salt	107.1±2	17.6±0.7	0.15±0.007	1030±26	843±172	2934±259
	Rel	114±6	72.8±2.7	79.35±5.647	67±4	5114±1186	144±18
193	Ctrl	71.1±3.5	25.4±0.8	0.14±0.006	1711±141	22±3	1777±65
	Salt	86.7±4.1	16.7±0.7	0.12±0.008	953±86	1582±273	3830±140
	Rel	123±5.4	66.1±3.4	82.76±4.914	56±3	7545±1130	217±13
194	Ctrl	102.6±7.7	22.9±0.7	0.18±0.012	1425±139	17±3	1358±140
	Salt	104.3±3.8	15.6±0.5	0.14±0.002	799±108	669±66	3509±129
	Rel	105.4±6.6	68.3±2.1	78.19±4.935	57±6	4480±1091	273±35
195	Ctrl	107.4±2.7	23.7±0.4	0.16±0.005	1243±66	26±4	2030±92
	Salt	99.4±3.1	17±1	0.15±0.015	872±139	2080±112	2473±95
	Rel	92.7±2.3	71.6±3.6	93.55±9.825	69±9	8552±1021	123±7
196	Ctrl	86.7±5.1	24.9±0.6	0.18±0.011	1694±112	24±5	2039±183
	Salt	101.1±4.7	16.9±1	0.14±0.003	1084±85	1812±179	2799±31
	Rel	122.1±11.4	67.9±4.5	79.16±4.27	66±8	9333±2494	142±13
197	Ctrl	102.8±3.8	25.2±0.6	0.2±0.008	1556±79	12±1	2058±22
	Salt	138.8±6.7	18.3±0.7	0.19±0.02	1023±112	823±102	2794±141
	Rel	138.3±11.2	72.6±3.7	93.32±12.228	67±10	7275±1344	136±8
199	Ctrl	102.8±1.6	22.1±0.6	0.18±0.008	1280±66	9±1	1575±98
	Salt	97±3.1	16±0.3	0.15±0.012	864±36	2169±260	2979±140

	Rel	94.7±3.9	72.8±2.1	83.44±5.8	68±2	25991±3933	191±13
	Ctrl	86.9±2.6	26.5±1	0.18±0.017	1886±243	43±4	2429±50
203	Salt	78.3±3.7	18.6±0.7	0.15±0.01	1432±155	1878±290	2446±100
	Rel	90.6±4.6	70.8±4.1	85.57±6.761	81±14	4591±858	101±4
	Ctrl	104.3±2.4	23.5±0.6	0.18±0.007	1415±42	37±5	2438±56
205	Salt	100.7±4.9	17±0.3	0.15±0.008	978±78	827±143	2869±148
	Rel	97±5.3	72.8±2.8	80.93±4.469	69±6	2213±205	118±5
	Ctrl	92.9±5.2	28.2±0.5	0.19±0.019	1616±171	37±8	2114±92
208	Salt	118.6±4	16±0.3	0.11±0.01	707±63	1935±203	3527±128
	Rel	131.8±9.5	56.9±1.3	63.93±11.669	45±4	9425±5330	170±10
	Ctrl	95.9±3.2	24.8±0.8	0.16±0.011	1265±101	48±6	2277±45
209	Salt	91±4.4	18.8±0.5	0.12±0.01	1259±189	1505±166	2720±114
	Rel	96±6.3	76.1±3.3	78.11±9.224	104±20	3508±927	120±5
	Ctrl	79.1±2.4	28.4±0.5	0.2±0.024	1894±83	22±4	2482±46
211	Salt	73.1±3.6	20±0.7	0.15±0.006	1507±160	1646±148	2490±232
	Rel	92.6±4.4	70.3±1.9	80.44±13.382	80±9	8376±1436	100±9
	Ctrl	73.7±3.5	28.2±1.3	0.17±0.013	1744±147	26±1	3379±218
213	Salt	67.9±2.9	19.2±0.5	0.12±0.009	1334±134	2202±76	2456±174
	Rel	93.1±4	68.7±3.6	75.3±9.117	79±10	8610±444	73±5
	Ctrl	94.9±3.7	26.1±0.5	0.19±0.012	1494±105	20±2	2832±125
214	Salt	120.7±4.1	16.9±0.5	0.12±0.009	835±46	1390±114	2873±101
	Rel	130.6±10.5	64.9±2.8	66.61±7.328	57±6	7501±1288	102±6
	Ctrl	76.5±3	27.9±0.9	0.18±0.016	1787±190	52±6	2453±71
215	Salt	85.2±2.5	18.5±0.7	0.11±0.005	1178±81	1344±66	2949±71
	Rel	112.8±5.3	66.4±2.2	67.56±7.426	68±7	2687±268	120±4
	Ctrl	91.8±5	25.5±1.6	0.17±0.014	1493±132	39±2	2623±101
216	Salt	78±4.1	19.7±0.6	0.12±0.013	1316±109	1431±129	2870±86
	Rel	86.3±5.5	78.2±4.6	73.42±10.904	90±7	3687±403	111±7
	Ctrl	78.5±2.6	28.3±0.6	0.19±0.014	1747±56	47±5	2594±37
217	Salt	88.2±3.1	17±0.4	0.1±0.006	892±62	2060±214	2657±163
	Rel	113.3±5	60±1.2	56.18±6.328	51±2	4426±407	103±7
	Ctrl	89.3±4.6	25.9±0.5	0.17±0.014	1482±122	72±4	2198±72
218	Salt	86±4.4	18.2±0.7	0.1±0.007	975±62	1224±85	2610±123
	Rel	98.9±9.3	70.6±4.2	62.9±5.521	68±9	1712±126	119±5
219	Ctrl	106.7±5	26.2±0.9	0.19±0.023	1548±158	32±4	2339±75

	Salt	97±4.8	17.5±0.4	0.11±0.011	957±133	1019±22	2995±185
	Rel	94.4±9.1	67±2.8	58.48±5.146	66±12	3559±701	129±11
	Ctrl	93.6±4.5	26.7±1.2	0.18±0.007	1544±158	24±2	2675±51
220	Salt	105.9±3	16.9±0.4	0.12±0.008	893±54	1737±263	2215±213
	Rel	114.7±4.2	63.9±3.8	65.93±5.956	59±4	7490±1224	83±7
	Ctrl	93.8±2.6	24.5±1	0.16±0.013	1300±87	71±5	2351±90
221	Salt	72.7±3.1	18.3±0.4	0.12±0.01	1336±51	2223±287	3499±85
	Rel	78.4±4.8	75.2±3.1	79.9±11.297	104±5	3118±361	149±3
	Ctrl	124±1.7	24.3±1.1	0.2±0.013	1348±124	44±4	2440±36
222	Salt	97.3±2.3	17.4±0.7	0.13±0.01	1179±311	1652±178	2659±68
	Rel	78.7±2.6	71.5±0.8	65±6.299	84±13	3809±440	109±3
	Ctrl	85.2±2.4	27.4±0.9	0.18±0.007	1640±90	37±5	2821±241
223	Salt	99.4±2.8	17.8±0.8	0.13±0.015	1102±209	1313±135	2624±180
	Rel	117.9±5.9	65.3±3.8	72.8±9.363	71±18	3881±692	95±9
	Ctrl	107.4±2.3	25.3±0.8	0.16±0.01	1240±90	38±2	2470±44
311	Salt	101.3±2.2	17.2±0.9	0.12±0.002	1164±211	1796±217	2579±108
	Rel	94.7±2.5	68±2.6	74.22±4.996	93±12	4782±677	104±4
	Ctrl	70.5±5	27.2±0.9	0.17±0.006	2285±272	94±13	1884±105
319	Salt	67±3.4	19.3±1	0.12±0.005	1549±179	3155±258	2680±252
	Rel	101.8±11.8	71.9±6	71.76±2.989	74±14	3790±822	141±8
	Ctrl	104.3±2.7	23.2±0.4	0.19±0.007	1488±65	61±5	2896±148
321	Salt	78.7±5.5	18.5±0.4	0.15±0.007	1312±92	1669±100	3170±283
	Rel	75.5±5	80.1±2.2	76.93±4.115	88±4	2851±352	109±8
	Ctrl	84.1±4.2	25.6±1.1	0.16±0.012	1449±106	37±4	2404±76
350	Salt	81.5±6.1	19.1±1.2	0.14±0.006	1406±270	1919±179	3321±216
	Rel	96.6±4.8	74.8±4.3	92.64±7.736	96±15	5299±592	139±10
	Ctrl	98.7±4.2	24.8±1	0.15±0.003	1324±33	53±10	2097±108
354	Salt	89±3.9	18.6±0.6	0.12±0.007	1144±91	1308±89	2523±107
	Rel	91.3±5.2	75.7±3.7	78.87±3.993	87±8	3028±836	121±8
	Ctrl	88.4±5.6	26.3±1.1	0.17±0.006	1655±243	22±4	2602±56
366	Salt	79.8±4.6	17.7±0.8	0.12±0.011	1202±176	1227±89	3017±195
	Rel	92.4±5.9	67.7±4.1	67.76±6.322	76±14	6709±1757	116±8
	Ctrl	74.2±2.6	27.4±1.1	0.19±0.014	1903±85	63±2	2703±101
367	Salt	74.4±3.2	19.2±0.7	0.14±0.004	1370±58	1616±359	2762±221
	Rel	100.8±4	70.4±3.5	76.34±5.883	72±4	2552±502	102±8

Q3	Ctrl	88.6±2.8	25.1±0.6	0.19±0.015	1706±24	31±9	2289±342
	Salt	86.9±2.7	17.2±0.5	0.14±0.024	1243±119	2298±109	3537±390
	Rel	98.8±4	69±2.9	71.21±10.636	73±8	12935±5134	168±30
Q4	Ctrl	92.9±2.4	25±0.8	0.19±0.003	1631±55	11±1	1990±42
	Salt	75.5±3.3	16.1±1.2	0.12±0.02	1372±176	1748±269	2227±150
	Rel	81.7±4.2	64.5±3.9	65.3±10.922	84±10	15390±1956	112±8
Q5	Ctrl	92.7±2	24.9±0.9	0.22±0.008	1631±86	9±1	1580±74
	Salt	85.2±4.6	17.1±0.8	0.14±0.006	1413±128	1504±84	3763±142
	Rel	92.1±5.2	69.1±4.9	66.83±4.891	88±9	17230±1375	241±17
Q6	Ctrl	110±2.6	22.6±0.7	0.18±0.019	1324±50	7±1	2060±40
	Salt	94.4±2.1	15.8±0.7	0.13±0.008	1091±53	2875±257	2938±112
	Rel	86.3±2.7	70.2±4.4	75.26±6.347	83±4	42153±6733	143±6
Q7	Ctrl	98.5±4.3	23.5±0.5	0.17±0.011	1438±60	6±0	1994±44
	Salt	86±4.1	18.5±1	0.13±0.007	1276±191	1215±119	2434±134
	Rel	89.9±7.4	78.8±3.7	78.05±4.739	89±12	22755±3388	123±9
Q11	Ctrl	88.6±3.1	25.3±0.3	0.2±0.012	1590±68	7±0	2286±60
	Salt	98.1±4.3	17.7±0.6	0.17±0.009	1195±95	1265±111	2641±34
	Rel	111.9±6.6	70.1±2.7	83.64±5.924	76±7	18398±1732	116±4
Q14	Ctrl	84.9±4.7	24.1±1	0.16±0.006	1575±138	16±1	2368±55
	Salt	105.9±7.9	16.5±1	0.15±0.009	1253±186	1345±179	3189±98
	Rel	125.3±13.3	68.7±3.3	92.34±5.923	82±13	8291±633	135±6
Q20	Ctrl	109.1±2.9	25.5±1	0.17±0.009	1261±73	24±2	2047±53
	Salt	100.3±5.3	19.6±0.6	0.15±0.012	1224±52	951±140	2585±123
	Rel	93±6.6	77.6±3.5	89.27±6.018	99±8	3886±421	127±6
Q21	Ctrl	67±2.8	28.6±0.3	0.15±0.014	2065±91	55±6	2265±75
	Salt	83±4.9	18.8±0.9	0.08±0.011	1419±163	1513±111	2428±62
	Rel	123.8±5.4	65.7±3.5	52.82±9.617	69±8	2929±404	108±5
Q22	Ctrl	83.4±3.6	25.2±1.4	0.17±0.015	1536±193	17±2	2593±87
	Salt	87.1±2.8	17.5±0.3	0.13±0.012	1025±76	1575±149	2781±147
	Rel	106.1±5.6	70.2±3.3	76.62±5.316	69±6	9825±1481	108±9
Q24	Ctrl	63.8±3.2	28.8±0.9	0.16±0.018	2190±95	50±7	2809±76
	Salt	69.4±3.9	20.3±0.4	0.13±0.011	1651±149	1630±161	2792±56
	Rel	112.5±10.4	70.7±3	87.28±12.173	76±8	3553±595	101±2
Q26	Ctrl	82.1±4.3	26.2±0.8	0.18±0.008	1713±98	39±10	2305±60
	Salt	77.8±7	18.7±1.2	0.12±0.01	1335±172	2556±133	1791±81

	Rel	98.1±12.1	72±6.7	66.98±6.784	81±13	8788±2344	77±5
	Ctrl	76.3±2.8	25.8±1.1	0.19±0.015	1945±124	64±14	1959±72
Q28	Salt	65.8±5.9	21.1±1.3	0.14±0.004	1822±226	1413±119	2773±240
	Rel	87±8	82.2±5.4	74.08±6.398	93±8	2971±877	144±19
	Ctrl	89.5±5.8	26.5±0.7	0.18±0.009	1569±135	18±2	1891±280
Q29	Salt	85.5±5	17±1.1	0.12±0.018	1230±159	2020±160	2624±256
	Rel	97.6±6.8	64.2±3.9	67.34±8.904	82±14	12454±2561	157±31
	Ctrl	93.8±3.3	25.9±0.7	0.18±0.013	1563±102	55±4	1724±325
Q30	Salt	91.8±2.4	17.9±0.2	0.11±0.004	972±39	1287±159	3607±167
	Rel	99.2±5	69.4±1.5	62.07±3.185	63±5	2394±332	252±61
	Ctrl	95.7±3.1	22.3±1.3	0.19±0.016	1432±88	7±1	2378±50
Q31	Salt	78.3±3.5	17.9±0.6	0.12±0.007	1238±74	2992±272	2123±95
	Rel	82.2±4	80.9±3.1	62.7±6.487	87±3	42786±6055	90±5
	Ctrl	77.2±2.7	27.9±0.5	0.2±0.026	1977±40	11±1	2384±40
Q32	Salt	81.1±4.8	17.5±0.5	0.13±0.009	1411±165	1870±130	2816±60
	Rel	105.5±6.3	62.8±2.7	67.96±8.433	71±8	17958±1233	118±4
	Ctrl	101.1±2.6	23±1.4	0.17±0.007	1419±72	17±3	2356±80
Q33	Salt	103.3±6.3	17.8±0.8	0.15±0.009	1132±131	1254±61	2653±50
	Rel	103.5±8.2	81.2±3.1	89.14±6.632	84±11	8614±1684	113±3
	Ctrl	85.6±3.8	24.7±1.5	0.18±0.008	1657±80	14±2	2408±53
Q34	Salt	71.6±6.6	18.8±0.9	0.13±0.01	1514±228	2041±213	2837±296
	Rel	85.8±9.8	77.5±6.8	74±8.269	93±15	15666±2203	118±13
	Ctrl	72±4	26.2±1.3	0.17±0.01	1757±184	36±8	2702±55
Q35	Salt	83±1.2	18.5±0.4	0.14±0.012	1251±20	1935±128	2953±159
	Rel	116.4±6.2	71.2±2.8	81.45±8.495	75±9	6690±1550	109±6
	Ctrl	75.5±3.5	24.2±1.2	0.16±0.004	1617±101	27±3	2530±69
Q36	Salt	74.2±3.4	18.9±0.7	0.13±0.01	1417±153	2190±101	2820±80
	Rel	101.3±8.5	79.1±6	82.8±6.411	91±14	8578±1114	112±3
	Ctrl	107.1±4.2	26±0.7	0.2±0.013	1527±106	41±12	2359±89
Q37	Salt	105±3.5	20±0.4	0.15±0.013	1175±70	1765±69	2594±78
	Rel	99.1±4.6	77.3±2.6	74.55±5.912	78±7	5344±988	110±4
	Ctrl	93.1±4.1	24.7±0.4	0.19±0.01	1597±97	8±1	2634±93
Q38	Salt	80.2±2.1	19.6±1.8	0.13±0.004	1310±59	2148±323	2356±84
	Rel	88.1±5.7	79.6±7.9	70.72±4.439	82±2	27150±3104	90±4
Q40	Ctrl	97.7±2.8	22.6±0.6	0.16±0.01	1248±77	10±1	2411±66

	Salt	78.9±3.2	18.1±0.7	0.1±0.011	1149±110	1929±197	3222±96
	Rel	81.1±3	80.3±3.9	66.03±9.639	93±10	19264±3488	134±4
	Ctrl	86.9±4.8	26.1±0.7	0.19±0.007	1790±138	12±2	2299±99
Q42	Salt	72.4±4.1	17.3±0.4	0.15±0.008	1335±84	2885±290	1885±175
	Rel	85.4±6.2	66.7±2.9	77.63±3.439	76±7	27033±4612	82±7
	Ctrl	78.7±3.6	27.4±0.5	0.16±0.008	1845±107	10±1	2306±94
Q45	Salt	75.5±3	19.6±0.3	0.15±0.011	1470±95	1200±125	3221±117
	Rel	98.7±7.8	71.6±2.2	94.51±10.463	82±9	12257±1883	141±8
	Ctrl	90.3±2.1	23±0.7	0.16±0.01	1442±95	8±1	1977±77
Q49	Salt	103.1±4.5	16.9±1.1	0.16±0.008	1073±104	1485±261	2427±113
	Rel	114.5±5.2	73.5±4.3	98.21±9.809	76±9	20159±4534	124±10
	Ctrl	95.1±5.3	23.6±0.9	0.18±0.006	1561±122	17±4	1869±201
Q50	Salt	82.8±4.4	19.7±0.5	0.13±0.011	1298±91	1008±132	3028±111
	Rel	89.1±6.2	84.1±2.8	75.29±7.785	84±6	7228±1830	171±22
	Ctrl	96.2±6.6	24.9±0.9	0.18±0.015	1481±116	12±5	2202±82
Q51	Salt	99.2±3.6	17±0.6	0.12±0.01	1039±47	1956±292	2470±161
	Rel	106.4±6.9	68.9±4.5	72.1±7.863	72±8	26070±8950	120±5
	Ctrl	87.5±3.8	24.2±1.5	0.17±0.008	1479±109	11±2	2179±54
Q52	Salt	100.9±2.5	16.5±0.2	0.15±0.01	1100±35	1732±289	2655±150
	Rel	117.6±6.5	69.3±4.9	92.82±7.781	76±6	19722±4732	122±8
	Ctrl	105.2±7.2	23.5±1	0.19±0.02	1550±98	13±2	2354±86
Q53	Salt	109.1±2.3	16.8±0.4	0.14±0.007	1022±33	1813±126	2838±131
	Rel	109.4±9.5	71.8±3.6	72.27±6.172	67±3	15668±2753	121±7
	Ctrl	102.8±4.4	20.9±0.6	0.17±0.006	1249±72	11±1	2344±53
Q54	Salt	81.7±3.5	19±0.5	0.13±0.014	1367±81	1800±141	3169±72
	Rel	81±5.2	91.2±3.6	77.2±9.822	111±10	15810±1442	135±4
	Ctrl	94±4	25±0.6	0.18±0.005	1589±98	13±4	2837±145
Q56	Salt	73.9±3.9	20.5±1	0.13±0.01	1514±119	1966±216	2624±92
	Rel	79.3±4.5	81.9±3.4	75.84±6.633	96±9	19911±5282	94±7
	Ctrl	72.4±2.2	27.2±0.5	0.17±0.007	1951±61	11±2	2589±71
Q57	Salt	76.3±1.9	17.4±0.8	0.11±0.003	1228±58	1249±13	2088±60
	Rel	105.8±2.6	64.4±2.3	61.54±2.961	63±4	12641±2073	81±2
	Ctrl	108.2±5.8	25.1±1.3	0.17±0.013	1327±150	11±1	2000±96
Q58	Salt	99.4±6.3	23.1±3.7	0.17±0.018	1240±191	1251±23	2464±130
	Rel	93.8±6.8	94.6±18.5	103.09±17.17	97±17	11848±1580	125±11

Q59	Ctrl	92.5±5.1	25.3±0.9	0.21±0.015	1803±178	28±5	2320±51
	Salt	105.6±4.5	18.2±0.8	0.16±0.011	1228±125	2100±92	3330±208
	Rel	116±5.7	72.3±4.1	80.81±11.184	70±9	12280±6148	144±13
Q64	Ctrl	73.9±2.9	25.8±0.8	0.17±0.013	1821±109	10±2	2732±197
	Salt	75.7±3.8	17.8±0.3	0.13±0.005	1376±98	1465±268	2795±187
	Rel	103±4.7	68.9±1.1	74.65±6.318	76±4	16780±4393	103±4
Q65	Ctrl	93.6±4.5	20.9±0.6	0.17±0.003	1376±52	19±5	2425±22
	Salt	69.2±2.8	20.2±0.6	0.16±0.014	1577±67	1763±37	3061±105
	Rel	75.4±4.3	97.1±3.7	89.94±8.255	115±8	12136±2773	126±5
Q68	Ctrl	89.9±2.3	24.9±0.6	0.17±0.015	1758±102	23±4	2222±42
	Salt	111.9±3.7	15.7±0.6	0.1±0.014	926±76	1526±33	3977±79
	Rel	125.9±7.2	63.1±2.6	60.5±9.446	54±6	7925±1987	179±6
Q75	Ctrl	72.9±2.7	31.8±0.9	0.2±0.014	2177±121	50±17	3087±98
	Salt	75.7±1.9	21.1±0.7	0.13±0.008	1360±88	1368±175	2700±131
	Rel	105.2±4.9	66.7±3.7	64.8±5.774	63±5	5405±1996	88±6
Q76	Ctrl	110±3.5	25±0.7	0.18±0.008	1644±141	22±2	2052±39
	Salt	87.6±3.7	21.2±1.1	0.15±0.01	1666±313	1093±19	2454±52
	Rel	83.6±3.8	85±5	81.42±4.854	105±23	5321±661	120±5
Q77	Ctrl	120.5±4.2	24.4±0.6	0.2±0.024	1408±68	39±10	1911±83
	Salt	138.6±11.5	20±0.6	0.19±0.017	1159±83	1416±123	2659±88
	Rel	115.2±8.8	82±1.1	105.68±22.091	83±5	4416±894	140±7
Q78	Ctrl	90.3±3.2	29.7±0.5	0.24±0.019	2285±184	44±6	2253±359
	Salt	127.7±6.1	19.1±0.7	0.2±0.021	1291±198	1675±271	2667±145
	Rel	140.8±5.5	64.7±3.1	83.91±6.375	60±15	4381±1325	124±14
Q79	Ctrl	119.4±6.5	24.1±0.4	0.21±0.011	1477±33	54±6	1805±116
	Salt	128.5±7.1	20.5±0.8	0.24±0.018	1551±133	1957±97	2478±112
	Rel	109.7±7.2	85.1±2.9	118.28±13.399	105±9	3790±451	140±13
Q80	Ctrl	106.9±7.6	28.6±1.4	0.29±0.045	1998±194	42±11	2002±151
	Salt	103.3±6.3	19.6±0.5	0.16±0.013	1241±31	747±62	2897±43
	Rel	103.4±11.7	69.6±5	60.52±12.693	66±10	2255±575	147±8

Abbreviations:

SD: stomatal density; SL: stomatal length; ECA: epidermal cell area; Na^+: leaf Na^+ concentration; K^+: leaf K^+ concentration

Suppl. Table S5.1 The sequences of primers for real-time RT-qPCR

Primer name	Sequences
CqSOS1	Forward: TTACTTGCCTCGTCTTTA
	Reverse: TCATGAGCCATTATGTGA
CqNHX	Forward: GCATTTCTGTTGCTGTGA
	Reverse: TGTGCCCTGACCTCGTAA
CqSKOR	Forward: ACGCCGAAGAAAATGGTACG
	Reverse: TCAAACAATCCCTCCCGACA
CqGORK	Forward: ATCCGGTTCTATGCAC
	Reverse: AGAGATTGAGAAGACATTTG
CqEF-1a	Forward: GTACGCATGGGTGCTTGACAAACTC
	Reverse: ATCAGCCTGGGAGGTACCAGTAAT

Suppl. Table S6.1 Mean values of studied physiological characteristics of cultivated and wild barley genotypes grown under control and saline (300 mM NaCl for 5 weeks) conditions.

		FW	DW	SPAD	Osm	Na	K
Cultivated genotypes							
BRINDABELLA	Ctrl	16.4±0.8	2.2±0.09	30.3±1.1	412±18	18.9±0.6	214±12
	Salt	3±0.2	0.5±0.04	43.7±1.2	1173±10	296±7	298±4
	Rel	18±2.5	23.2±2.2	144±9.2	285±15	1562±51	139±7
Dash	Ctrl	9±0.7	1.1±0.05	39.9±1.3	447±10	15.3±1	242±6
	Salt	1.7±0	0.3±0.02	51.3±1.5	1177±12	232±8	287±16
	Rel	19.5±2	28.8±2.4	128±5.6	263±5	1510±85	118±6
FRANKLIN	Ctrl	9.1±0.4	1.2±0.1	35.2±1	464±4	24.5±0.6	295±15
	Salt	1.6±0.1	0.3±0.01	42.4±0.9	1514±82	351±19	232±14
	Rel	17±0.9	25.6±1.6	120±5.5	326±19	1433±74	78.6±11
GAIRDNER	Ctrl	15.9±0.5	1.6±0.15	31.6±0.3	415±21	11.9±0.5	243±12
	Salt	2.5±0.2	0.4±0.04	46.8±0.4	1177±40	226±4	240±20
	Rel	15.5±1.2	27.1±5	148±2.7	284±19	1895±90	98.8±10
GEBEINA	Ctrl	8.9±0.6	1.2±0.04	30.8±0.6	528±6	15.3±0.5	336±12
	Salt	2.4±0.2	0.5±0.03	42.3±1.8	1147±41	306±10	324±5
	Rel	27±3.5	39.4±3.8	138±7.9	217±9	1995±205	97±3
MACQUARIE	Ctrl	10.2±0.7	1.3±0.08	34.1±1	475±8	15.9±0.6	253±8
	Salt	2.4±0.2	0.4±0.03	49.3±1.7	1144±28	284±11	236±17
	Rel	23±1.4	30.5±2	144±5.6	241±4	1790±93	93.3±8
MUNDA	Ctrl	11.1±0.4	1.5±0.12	32.3±1.1	456±24	19.2±0.3	231±8
	Salt	3±0.2	0.5±0.03	44.1±1.5	1084±12	185±11	311±11
	Rel	26.8±1.9	36.4±5	137±5	238±11	965±43	135±6
NUMAR	Ctrl	11.3±0.7	1.7±0.09	40.7±1.3	486±31	16.2±0.3	356±11
	Salt	2.9±0.2	0.6±0.02	44.6±1	999±48	285±11	351±19
	Rel	26±2.3	32.5±2.4	110±3.6	205±20	1762±70	98.6±6
YERONG	Ctrl	10.9±0.4	1.4±0.04	32.1±0.8	450±7	8.4±0.5	279±8
	Salt	2.8±0.1	0.4±0.04	47.3±1.4	1052±28	171±10	195±12
	Rel	26.1±1.5	31±2.5	147±6	234±9	2048±257	69±3
YF374	Ctrl	13.3±0.5	1.8±0.06	40.8±0.6	504±13	10.1±0.6	262±8
	Salt	2.6±0.2	0.5±0.03	46.2±1.1	1071±18	188±8	268±6
	Rel	19.3±1.8	27.3±2.2	113±4.1	212±6	1858±182	103±4

YSM1	Ctrl	8.5±0.5	1.3±0.07	38.8±1.4	560±11	11±0.4	255±7
	Salt	2.6±0.2	0.5±0.04	42.4±1.1	1083±5	294±18	340±14
	Rel	32.4±0.9	41.3±2.2	109±2.4	227±5	2685±172	133±6
ZUG293	Ctrl	9.4±0.5	1.1±0.08	37.9±1.4	411±10	15.4±0.4	211±10
	Salt	2.1±0.2	0.4±0.02	41.7±0.8	1061±42	158±9	292±14
	Rel	22.2±1.7	34.8±1.2	110±3.6	258±9	1026±67	139±8
ZUG95	Ctrl	13.5±0.5	1.7±0.1	35.3±1	473±20	14.3±0.4	278±8
	Salt	2.7±0.3	0.5±0.01	42.5±1.6	972±28	152±6	304±19
	Rel	19.7±1.7	31.5±2	120±3.9	206±9	1060±119	111±20
LSD (5%) Salt & Ctrl		9.1	7.7	9.7	352	124	45.6
LSD (5%) Rel		6.4	6.8	16.3	37.5	495	25.9
Wild genotypes							
CPI	Ctrl	9±0.3	1.1±0.1	33.6±1.5	528±19	22.3±0.7	231±8
	Salt	3.3±0.13	0.69±0.02	40.5±1.5	1007±26	159±5	268±41
	Rel	36.6±1.17	61.7±7.23	120±5.3	191±10	711±24	117±18
X115	Ctrl	11.6±0.6	1.4±0.1	35.1±1.1	422±7	16.6±1.2	245±4
	Salt	4.7±0.15	0.73±0.03	42.5±1.4	907±49	184±11	321±64
	Rel	40.1±2.42	52.6±3.57	121±6.3	215±9	1114±136	132±27
X117	Ctrl	12.4±0.7	1.5±0.1	30.4±0.6	405±12	9.2±1.4	215±9
	Salt	3.5±0.02	0.57±0.02	44.1±1.2	987±45	204±11	273±13
	Rel	28.6±1.42	39.3±2.04	145±5.7	244±8	2207±155	128±5
X118	Ctrl	11.8±0.6	1.6±0.1	32±1	409±10	8.4±0.8	227±4
	Salt	3.5±0.08	0.58±0.02	42.6±1.1	874±46	263±9	210±9
	Rel	30±2	37±4.47	133±6.5	214±15	3127±406	93±5
X120	Ctrl	11.5±0.8	1.3±0.1	28.2±0.4	388±6	35.1±1.6	196±6
	Salt	3.7±0.13	0.51±0.02	38.7±1.5	1126±49	471±21	99±8
	Rel	32±2.06	40.7±2.88	137±5.5	290±14	1340±123	50±4
X123	Ctrl	13.1±1.1	1.6±0.1	27.8±1	431±9	13±0.5	259±7
	Salt	4.4±0.1	0.77±0.03	36±1.1	896±55	154±3	383±78
	Rel	33.4±3.42	47.5±3.21	129±4	208±14	1185±147	149±32
X13	Ctrl	7.4±0.4	1.1±0.1	28.9±1.1	388±10	13±0.9	191±6
	Salt	3.8±0.19	0.59±0.04	40.3±0.5	1066±18	166±8	272±8
	Rel	50.7±4.19	54.5±1.64	139±4.5	275±11	1280±148	143±6
X133	Ctrl	11.4±0.8	1.2±0	28.1±1.2	421±16	9±1	274±13
	Salt	3.1±0.09	0.49±0.03	43.5±1.3	974±56	199±7	265±11

	Rel	27.3±1.38	39.9±2.71	155±7.7	231±24	2223±181	98±7
	Ctrl	8.9±0.4	1.2±0.1	28.7±0.8	439±12	13.5±1.2	235±12
X151	Salt	3.9±0.12	0.62±0.03	41.9±0.5	1025±56	230±8	237±12
	Rel	44.1±2.99	52.2±3.44	146±4.3	234±10	1703±156	102±8
	Ctrl	12.8±0.5	1.7±0.1	28.4±1.7	367±9	15.8±2.2	268±10
X192	Salt	3.9±0.08	0.52±0.02	37.6±0.9	1243±18	752±37	174±29
	Rel	30.7±1.14	30.1±1.55	132±8.9	338±12	4767±192	65±11
	Ctrl	10.3±0.3	1.4±0	27.5±0.6	463±16	18.4±1	281±15
X30	Salt	3.9±0.07	0.64±0.02	36.1±1.5	1247±32	264±12	341±15
	Rel	37.4±1.22	46.6±2.16	131±6.6	269±11	1439±109	123±8
	Ctrl	11.4±0.6	1.4±0.1	29.5±0.6	410±5	8.7±0.9	261±6
X51	Salt	3.4±0.16	0.52±0.02	41.9±1.2	790±24	154±5	184±12
	Rel	29.6±1.65	37±1.65	142±3.3	192±6	1769±125	71±5
	Ctrl	15.5±0.7	1.7±0.1	36.5±1.1	401±6	25.7±0.8	331±13
X97	Salt	5.6±0.17	0.83±0.03	41±0.7	837±87	169±9	299±47
	Rel	36.2±2.14	50±2.26	122±3.1	208±21	658±53	89±10
LSD (5%) Salt & Ctrl		8.9	7.7	9.7	314	172	59.8
LSD (5%) Rel		6.9	9.2	11.5	44.7	1149	32.0

Abbreviations: Ctrl - control conditions; Salt - 300 mM NaCl; Rel - relative value (% control); DW - dry weight (g plant^{-1}); FW - fresh weight (g plant^{-1}); SPAD – chlorophyll content (arb. values); Osm - leaf sap osmolality (mmol kg^{-1}); Na^+ - leaf Na^+ concentration (mmol l^{-1}); K^+ - leaf K^+ concentration (mmol l^{-1})

Suppl. Table S6.2 Mean values of studied anatomical characteristics under control and 300 mM NaCl conditions of cultivated and wild barley genotypes

		SD	SAL	SI	Gs
Cultivated genotypes					
BRINDABELLA	Ctrl	34.1±2.6	46.6±1.6	0.17±0.01	47.9±0.7
	Salt	34.1±1.4	45.8±1.2	0.18±0.01	12.2±1.6
	Rel	72.6±4.5	98.5±2.9	106±10	25.4±2.9
Dash	Ctrl	44.8±2.1	48.4±1.3	0.15±0.01	82.2±1.8
	Salt	44.8±2.5	47.1±0.8	0.17±0.01	20.5±1.5
	Rel	118.7±8.3	97.7±3.5	120±2	25±2.1
FRANKLIN	Ctrl	38.2±2.3	45.9±1.1	0.16±0.01	71.6±2.5
	Salt	38.2±2.6	43.5±0.6	0.14±0.01	18.5±1
	Rel	82±6.2	94.8±3	92±12	25.8±1.9
GAIRDNER	Ctrl	43.1±2.6	48.3±1.5	0.16±0.01	79.4±1.8
	Salt	43.1±1.5	43.4±1.4	0.17±0.01	12.6±1.3
	Rel	111.7±10.4	90.3±5.1	106±9	15.9±2
GEBEINA	Ctrl	40.3±2.3	48.1±0.8	0.17±0.01	51.8±2.7
	Salt	40.3±2.1	45.7±1.1	0.16±0.01	11.3±1.2
	Rel	76.3±6.7	95.2±3.5	94±1	21.8±2
MACQUARIE	Ctrl	39.7±1.8	45.9±1.7	0.17±0.01	47.1±3.7
	Salt	39.7±2.2	44±1.1	0.16±0.01	22.4±0.5
	Rel	98.9±8.1	96.3±4.5	92±3	47.6±3.7
MUNDA	Ctrl	34.7±2	48±1.2	0.16±0.01	59.9±1.6
	Salt	34.7±1.7	46.4±1.6	0.18±0.01	15.3±1
	Rel	71.2±4.6	97.2±5	111±8	25.5±1.1
NUMAR	Ctrl	31.3±2.8	46.6±1.5	0.18±0.01	56.4±2.7
	Salt	31.3±2.2	47.8±1.1	0.15±0.01	25.5±1.2
	Rel	65±5.2	102.8±3.3	88±8	45.2±2.2
YERONG	Ctrl	40.3±2.3	42.1±0.7	0.2±0.01	95.7±1.9
	Salt	40.3±1.8	43.3±1	0.17±0.01	18.5±1.5
	Rel	75.7±3.5	102.9±3.2	83±3	19.3±2
YF374	Ctrl	46.6±2.6	43.6±0.8	0.2±0.01	57.1±2.1
	Salt	46.6±2.2	41.8±1.4	0.18±0.01	18.6±0.6
	Rel	73±3.4	96.2±3.8	90±5	32.5±1.2

YSM1	Ctrl	36.4±2.7	51.1±1.4	0.14±0.01	64.3±3.1
	Salt	36.4±2.1	45.6±1	0.15±0.01	34.8±1
	Rel	89.9±13.5	89.6±3.6	104±10	54.1±4.1
ZUG293	Ctrl	39±2.5	47.1±1.5	0.18±0.01	77.8±3.7
	Salt	39±1.6	46.3±0.8	0.14±0.01	7.6±0.4
	Rel	94.8±6.7	92.6±5	81±6	9.7±0.7
ZUG95	Ctrl	34.9±2.7	50.5±2.4	0.18±0.01	80.1±4.3
	Salt	34.9±2.3	45.8±0.1	0.16±0.01	15.8±0.8
	Rel	61.8±5.3	97.7±3.5	93±5	19.8±1.2
LSD (5%) Salt & Ctrl		8.8	8.0	7.7	28.7
LSD (5%) Rel		18.7	5.8	12.5	14.1
Wild genotypes					
CPI	Ctrl	45.1±2.1	46.7±0.8	0.17±0.01	57.4±3.2
	Salt	40.3±2.1	43.8±0.8	0.15±0.01	24.3±1.1
	Rel	89.5±5.4	93.9±1.8	88±7	42.3±2.9
X115	Ctrl	47.2±2.1	46.7±0.5	0.18±0.01	75.2±2.9
	Salt	40.5±1.6	45.9±1.4	0.17±0.01	21.3±1.7
	Rel	85.8±5.1	98.5±4.1	96±7	28.4±1.7
X117	Ctrl	44.6±1.2	46.1±1.2	0.17±0.01	57.8±1.1
	Salt	42.7±1.8	44.1±0.8	0.17±0.01	12.9±0.7
	Rel	95.7±5.6	96±2.8	101±4	22.2±1.1
X118	Ctrl	49.4±2.4	44±1.4	0.16±0.01	46.2±3.7
	Salt	36.4±1.5	46.5±0.7	0.17±0.01	11.2±0.6
	Rel	73.7±4.9	106.2±3.8	102±8	24.3±3.4
X120	Ctrl	28.9±1.6	55.2±1.7	0.14±0.01	36.3±2.8
	Salt	32.3±1.7	47.5±0.9	0.14±0.01	18.1±0.7
	Rel	111.9±8.3	86.4±3.1	104±9	107.4±5.9
X123	Ctrl	52±2.7	43.1±0.9	0.17±0.01	61.3±3.2
	Salt	39.2±1.1	44.4±0.7	0.18±0.01	18.6±1.4
	Rel	75.5±3	103.2±3	106±11	30.4±1.3
X13	Ctrl	34.4±1.1	49.6±1	0.16±0.01	47.4±4.1
	Salt	34.9±1.1	46.2±1.4	0.17±0.01	14.2±1.5
	Rel	101.7±6.4	93.1±1.3	109±6	30±5.3
X133	Ctrl	32.6±1.3	52.6±0.9	0.16±0.01	31.7±3.7
	Salt	42.5±2.5	42.1±1.7	0.16±0.01	18.5±1.4

	Rel	130.5±12	80±2.4	100±4	58.5±5.1
X151	Ctrl	33.2±1.8	51.2±1.6	0.16±0.01	62.4±2.1
	Salt	40.5±2.5	47.1±1.4	0.16±0.01	20±1.5
	Rel	121.9±10.9	92.4±4.4	106±7	32±3.2
X192	Ctrl	31.3±2.1	53.6±1.9	0.16±0.01	52.1±0.9
	Salt	38.6±1.3	44.6±0.9	0.16±0.01	16±0.4
	Rel	123.3±10.6	83.6±2.8	101±4	30.7±0.7
X30	Ctrl	37.1±1.9	45.7±0.5	0.17±0.01	42.7±3.4
	Salt	39±2.2	43.5±1.2	0.16±0.01	21.1±0.6
	Rel	105.2±9.7	95.3±3.3	93±6	49.5±5.4
X51	Ctrl	36±1.5	45.5±0.9	0.17±0.01	41.1±1.2
	Salt	35.1±2.2	44.3±1	0.17±0.01	21±0.4
	Rel	97.6±7.6	97.4±2.6	100±7	51.1±1.6
X97	Ctrl	40.7±1.6	48.8±1.5	0.18±0.01	86.9±2.9
	Salt	47.7±2.3	43.9±1.6	0.16±0.01	24.7±2
	Rel	116.9±7.5	90.8±5.9	92±7	28.5±1.9
LSD (5%) Salt & Ctrl		9.7	8.4	7.7	22.5
LSD (5%) Rel		19.2	8.6	7.5	23.9

Abbreviations:

Ctrl: control conditions; Salt: 300 mM NaCl; Rel: relative value of characteristic; SD: stomatal density (cells mm^{-2}); SAL stomatal aperture length (µm); SI: stomatal index (number of stomata cells divided by number of epidermal cells); Gs: stomatal conductance (mmol m^{-2} s^{-1})